STUDY OF MECHANICAL AND TRIBOLOGICAL BEHAVIOUR OF AL BASED HYBRID MMCS FABRICATED BY STIR CASTING PROCESS

A thesis submitted to Delhi Technological University, Delhi for award of the Degree of

DOCTOR OF PHILOSOPHY

In

Mechanical Engineering

by

Ashish Kumar

(2K18/PHDME/26)

Under the guidance of

Dr. R.C Singh
(Professor)
Department of Mechanical Engineering
Delhi Technological University,
Delhi, 110042

Dr. Rajiv Chaudhary
(Professor)
Department of Mechanical Engineering
Delhi Technological University,
Delhi, 110042

DEPARTMENT OF MECHANICAL ENGINEERING
DELHI TECHNOLOGICAL UNIVERSITY,
DELHI, 110042

In heartfelt dedication to my beloved father,
Shri Jai Prakash Yadavendu

DECLARATION

I declare that,

a. The work contained in the thesis entitled **"Study of Mechanical And Tribological Behaviour of Al Based Hybrid MMCs Fabricated By Stir Casting Process"** is original and has been done by myself under the supervision of **Dr. R. C. Singh** and **Dr. Rajiv Chaudhary**, Professor, Department of Mechanical Engineering, Delhi Technological University, Delhi.

b. The work has not been submitted to any other Institute for award of any degree or diploma.

c. I have followed the guidelines provided by the Delhi Technological University, Delhi, in writing the thesis.

d. I have conformed to the norms and guidelines given in the Ethical Code of Conduct of Delhi Technological University, Delhi.

e. Whenever I have used materials (data, theoretical analysis, and text) from other sources, I have given due credit to them by citing them in the text of the thesis and giving their details in the references.

f. Whenever I have quoted written materials from other sources, I have put them under quotation marks and given due credit to the sources by citing them and giving the required details in the references.

Signature of the student

Ashish Kumar

Roll No. - 2K18/PHDME/26

CERTIFICATE

This is to certify that the work embodied in the thesis entitled **"Study of Mechanical And Tribological Behaviour of Al Based Hybrid MMCs Fabricated By Stir Casting Process"** by **Ashish Kumar**, (Roll No.**-2K18/PhDME/26**), in partial fulfilment of requirements for the award of Degree of **DOCTOR OF PHILOSOPHY** in Mechanical Engineering, is an authentic record of student's own work carried by his under our supervision.

This is also certified that this work has not been submitted to any other University or Institute for the award of any other diploma or degree.

Dr. R.C Singh
(Professor)
Department of Mechanical Engineering
Delhi Technological University,
Delhi, 110042

Dr. Rajiv Chaudhary
(Professor)
Department of Mechanical Engineering
Delhi Technological University,
Delhi, 110042

ACKNOWLEDGMENTS

I would like to express my deep gratitude, sincere thanks and appreciation to my supervisors Prof. R. C. Singh and Prof. Rajiv Chaudhary for their valuable guidance during this Ph.D. work. I am thankful from my heart for all the help, encouragement, and support you generously extended to me.

I would like to express, a sincere gratitude to Prof. R.S. Mishra, Chairman, DRC, Prof. Vijay Gautam, Member secretary, DRC, Mechanical Engineering Department and Prof. S K Garg, Head of the Department, Mechanical Engineering, Delhi Technological University, for their valuable help, motivation and extending all the necessary processing and experimental facilities during my research work.

I would also like to express, a sincere gratitude to Prof. R.K. Pandey, Prof. Sujit Angra, Prof. Ranganathan M. S. and Prof. Nao Kant Dev for serving my SRC committee members and many critical helps without which I would not be able to complete my thesis in time.

I am also grateful to Prof. Ranganathan M. S. (DTU) and Dr. N. Yuvaraj (DTU) for all the motivation and their teachings, without that I would not be able to finish my thesis work.

I gratefully acknowledge Institute Instrumentation Centre, IIT Kharagpur and CSIR – National Metallurgical Laboratory, Jamshedpur for the characterization facility.

I intend to accord my sincere appreciation to my friend and colleagues for their constant encouragement, help and cheer, especially Dr. Virendra Pratap Singh, Dr. Sudipta Mohapatra, Mr. Dhruv Singh, Dr. Biraj Kumar Sahoo, Dr. Akhileswar Nirala, Dr. Ashok Devangan, Dr. Gajendra Gaurav and Mr. Ranjit Prashad.

My sincere thanks to all the faculty and staff members of Department of Mechanical Engineering (DTU), who supported me during my entire course work and research work. I am grateful to Mr. Rajesh Bohra, and Mr. Manmohan for their technical and experimental support.

I am grateful to the management of at Galgotias College of Engineering and Technology, Greater Noida, particularly Mr. Sunil Galgotia, Founder Chairman, Dr. Dhruv Galgotia, CEO, Galgotias Educational Institute, Dr. Asim Qadri, Director and Dr. Pawan Kumar Arora, Head, Department of Mechanical Engineering, Galgotias College of Engineering and Technology, Greater Noida, for the timely help and support in every possible way to finish this work.

I am also grateful to the expert examiners for improving the overall quality of the thesis.

I am deeply indebted to my parents for teaching me the dedication and importance of education. I want to express my reverence and gratitude to my family members, who were a constant source of support for this work and during all my endeavors. I feel so proud to mention that the thesis would not have been possible without the support, and encouragement, of my Father, Mr. Jai Prakash Yadavendu and my elder brother Mr. Manish Kumar, to pursue my interest in the field of research.

Last but not least, I would like to thank my God, whose grace enables me to accomplish my research works.

ABSTRACT

Micro/nano reinforcements in aluminium matrix composites (AMCs) have recently gained attention for a number of applications due to their lightweight and better mechanical, tribological, thermal, and electrical properties. The incorporation of industrial and agricultural waste materials as reinforcements for the production of metal matrix composites (MMCs) is the utilization of waste and a reduction of pollution. A number of industries, including aerospace, automotive, and packaging, have demonstrated a keen interest in the development of innovative bio-waste particulate reinforced composite. The effect of reinforcements is investigated in the current research work. The two-stage stir casting method with Al_2O_3 and coconut shell ash (CSA) is reinforced with an aluminium matrix. Two sets of hybrid composites have been developed using

i) nano Al_2O_3,

ii) micro Al_2O_3 and

iii) coconut shell ash as reinforce material and AA7075 as the matrix.

The first hybrid composites contain 0.5% w/w of nano Al_2O_3 as reinforce material with varied 1-3% w/w of micro coconut shell ash in the AA7075 matrix. Second hybrid composites contain 5% w/w of micro Al_2O_3 with varied 3-9% w/w of micro coconut shell ash as reinforcements in AA7075 matrix.

The present study focuses on the investigation of mechanical, thermal, and wear behaviors of cast hybrid nano metal matrix composites (HnMMCs) of AA7075 with Al_2O_3 and coconut shell ash (CSA) nano and micro-sized particulates, respectively, as reinforcements. Microstructural analysis and various phase identifications were examined with the help of an optical microscope (OM), scanning electron microscope (SEM) equipped with EDX and Transmission electron microscope (TEM). Due to the two-stage stir casting process, the distribution of reinforcement in the aluminium matrix is ensured to be uniform. It was discovered that the addition of Al_2O_3 and CSA reinforced particles improved mechanical characteristics and tribological behaviour while decreasing impact strength marginally. SEM images of fractured specimens during impact and tensile testing revealed transgranular cleavage facets, micro-void coalescence, dimples, and a crack. The

tribological characteristics of the worn-out surfaces were examined extensively using SEM images. Overall, employing CSA in combination with Al_2O_3 in HMMCs may be an effective, smooth, and cleaner method for disposing of Al_2O_3 in terms of environmental pollution and waste contamination due to large-scale application in improving composite characteristics.

TABLE OF CONTENTS

LIST OF FIGURES

LIST OF TABLES

LIST OF ABBREVIATIONS

Al	Alumnium
AMC	Aluminium matrix composites
COF	Coefficient of friction
CSA	Coco nut shell ash
CTE	Coefficient of thermal expansion
CVD	Chemical vapor deposition
EDS	Energy Dispersive X-ray Spectroscopy
FES	Field emission scanning electron microscope
HAMC	Hybrid aluminum matrix composites
HMMC	Hybrid metal matrix composites
HEB	High energy ball mill
HV	Hardness Value
OM	Optical Microscope
MMC	Metal matrix composites
PRCL	Percentage of relative change in length
PM	Powder metallurgy
PMC	Polymer matrix composite
RD	Relative density
ROM	Rule of mixture
rpm	Revolution per minute
SEM	Scanning electron microscope
SPS	Spark plasma sintering
TCE	Thermal expansion coefficient
TEM	Transmission electron microscope
UTS	Ultimate tensile strength
Vol	Volume percentage
XRD	X-ray diffraction

LIST OF SYMBOLS

Symbols	
α	Coefficient of thermal expansion
σy	Yield strength
σi	Strength opposing the movement of the dislocation
D	Sliding distance
E	Elastic modulus
G	Shear Modulus
h	Hour
H	Hardness
HV	Vickers hardness
K	Bulk modulus
k	Thermal conductivity
σ	Stress
ε	Strain
T	Stiring temperature
t	Stiring time
ρ	Density
2D	Two dimensional
3D	Three dimensional
μ	Poisson ratio
τ	Shear stress
μm	Micrometer
μ	Coefficient of friction

CHAPTER 1
INTRODUCTION

In this chapter, a overview of lightweight materials and Advanced Metal Matrix Composites (AMHCs) has been furnished. The challenges linked with enhancing materials for AMCs, along with the benefits of utilizing the stir casting method for producing AMHCs, have been deliberated upon. Following that, the emphasis was placed on the processing factors and resultant response variables.

1.1 The prerequisite for lightweight materials

The competition between the aerospace and automobile sectors to develop vehicles that are more fuel-efficient and have reduced carbon dioxide (CO_2) emissions has grown more intense [1]. Consequently, governmental entities worldwide are actively promoting the advancement and creation of vehicles that are more efficient in terms of fuel consumption [2]. For instance, it's essential to highlight that a substantial 90% share of India's carbon dioxide emissions originating from transportation activities is linked to the road sector. The pursuit of decarbonization not only brings about notable environmental benefits but also leads to enhanced air quality, consequently positively influencing public health and well-being. Therefore, the formulation of a precise and measurable goal is imperative to propel India's comprehensive climate commitment forward. Consequently, a comprehensive meta-analysis has been conducted on the prominent energy and emissions models pertaining to India's road transport sector, specifically emphasising the Business as Usual (BAU) and High Ambition (HA) scenarios. Before the onset of the COVID-19 pandemic, projections indicated that the number of vehicles on Indian road networks would surpass 200 million by the year 2030. Presently, road transport heavily relies on petroleum as the primary energy source, a considerable portion of which is sourced through imports. In alignment with its commitment to the Paris Agreement's Nationally Determined Contribution (NDC), India aims to achieve a 33 to 35 percent reduction in the carbon intensity of its Gross Domestic Product (GDP) by 2030 compared to the 2005 levels. [3]. Although the government has implemented economy-wide emission reduction targets, it is noteworthy that there is

presently a lack of sector-specific objectives for industries with high emission levels, such as manufacturing and transport.

The fuel efficiency regulations vary across countries, with several nations implementing stricter standards compared to those in India. However, all nations share the common objectives of minimising CO_2 emissions and enhancing fuel efficiency. Manufacturing sectors have been engaging in extensive experimentation with diverse strategies, such as the utilisation of lighter vehicles, in order to effectively address customer demands and adhere to fuel economy regulations [4-8]. There are two potential approaches to address this issue: reducing the size of the vehicle or employing lighter materials. The reduction in the size of the vehicle may potentially compromise the safety and comfort of the passengers. Therefore, there is a widespread desire to reduce the weight of vehicles by utilising lighter materials, all while maintaining optimal vehicle performance. According to existing data, a 10% reduction in the weight of automobiles has demonstrated a notable enhancement in fuel economy, ranging from 8 to 10%. Moreover, a decrease in weight by 100 kg is associated with a reduction in CO_2 emissions by approximately 12.5 g/km. The adoption of aluminum alloys in the automotive sector, coupled with ongoing advancements in this crucial material, plays a pivotal role [9]. Additionally, lighter vehicles not only showcase improved performance but also ensure passenger safety. The aviation sector is also witnessing substantial growth in the utilization of lightweight materials [10-11]. The utilisation of epoxy-reinforced composites as a substitute for aluminium in the construction of the Boeing 787 aircraft results in a significant improvement in efficiency, with a reported increase of approximately 20% compared to conventional aircraft [12]. As a result, there was a rise in payload capacity, accompanied by a reduction in pollutants and fuel consumption. In aerospace and other transportation sectors responsible for managing CO_2 emissions and fuel efficiency, there is a pressing need for the development of high-performance lightweight multi-materials. There exists a significant demand for lightweight materials in order to achieve fuel efficiency goals through the production of lightweight vehicles [13-14], as depicted in **Fig. 1.1.**

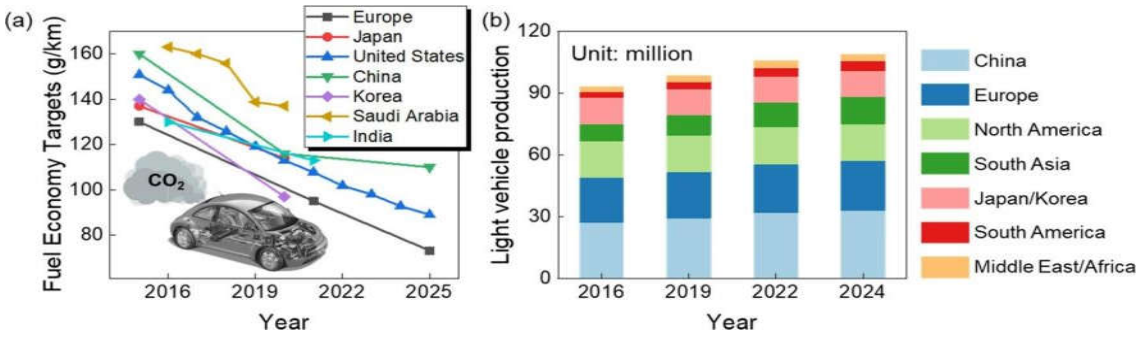

Fig. 1.1. Strong need for lightweight automotive materials. (a) Fuel efficiency targets in different nations (passenger vehicles) [13] (b) Light vehicle production in million units by the largest market [14].

1.2 The need for "Al matrix composites (AMCs)"

The automobile industry predominantly employed cast iron and low-carbon steel as the primary materials prior to the 1970s [15-16]. The engine block and cylinder head are considered crucial components in the context of a passenger vehicle [17]. Cast iron has been traditionally employed for various components due to its superior resistance to wear, high temperature strength, and ability to be cast. Nevertheless, due to its significantly high density of 7,870 kg/m3, the engine block assumes the role of the most substantial constituent within the automobile, accounting for approximately 3-4% of the vehicle's overall weight. In order to prioritise the reduction of vehicle weight and carbon dioxide emissions, modifications are made to the materials used in engine blocks to integrate alternative lightweight materials. The utilisation of natural and hybrid fibre composites as lightweight materials in diverse applications. In contemporary times, these composite materials have experienced a surge in popularity due to their cost-efficiency, enhanced strength, and positive environmental attributes. This paper aims to discuss the various classifications of natural and hybrid fibre composites, elucidate their inherent characteristics, and expound upon the diverse manufacturing techniques employed in their production. The article further examines the potential utilisation of these composites in the automotive, aerospace, and construction sectors. There is a requirement for additional research to enhance the performance and longevity of these composites, along with their potential for recycling and sustainability. In general, the progress made in the field of natural and hybrid fibre composites has shown promise in terms of their application as lightweight materials across diverse industries [18].

Aluminium alloys are considered as strong candidates for replacing cast iron and other types of steels in various applications. This is primarily due to their significantly lower density, which is approximately 35% of the density of cast iron, measuring at 2,700 kg/m3. The utilisation of aluminium alloys in lieu of cast iron has been found to enhance the probability of engine blocks achieving a weight reduction of up to 45% [19]. Aluminum-alloy engine blocks have been produced since the late 1970s, and in recent years, aluminum-alloy cylinder heads have completely supplanted cast iron counterparts [20]. The aerospace and automotive industries are expected to drive a substantial growth in aluminium production in the forthcoming decades, as indicated by the high demand observed in the sales market [21-23]. This paper discusses the scientific and technological significance of Metal Matrix Composites (MMCs) and the ongoing research endeavours aimed at enhancing their properties. The properties of strength, stiffness, and wear resistance in conventional metals can be enhanced by incorporating other materials such as ceramics or polymers into a metal matrix. Various methodologies are utilised in the production of Metal Matrix Composites (MMCs), including powder metallurgy, in-situ synthesis, and liquid metal infiltration. One of the primary obstacles encountered during the manufacturing of MMCs pertains effective management of the reinforcement material distribution and the attainment of a homogeneous dispersion of particles within the metal matrix [24]. Materials derived from high-performance aluminium alloys that demonstrate multifunctional characteristics, including improved wear resistance, mechanical properties, and superior electrical and thermal conductivity, while minimising any substantial increase in weight, are highly sought after in various industrial sectors due to the strict demands for weight reduction [24-26]. The proposed solution involves the production of aluminium-based matrix composites, as conventional aluminium alloys are unable to meet these requirements. **Fig.1.2.** demonstrates that aluminium is the predominant matrix material employed in metal matrix composites (MMCs).

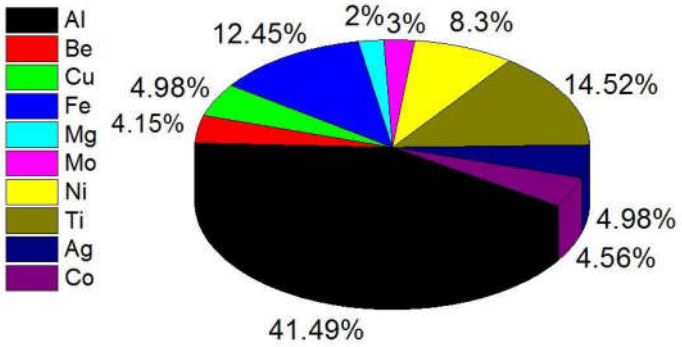

Fig. 1.2. Usage of Al matrix materials.

These composite materials exhibit a distinctive amalgamation of matrix and reinforcing characteristics, encompassing both ceramic and carbon-based alloys. Previous research has suggested that aluminium has the potential to be enhanced in terms of hardness, strength, and wear resistance through the addition of micron-sized ceramics, including titanium carbides (TiC), silicon carbides (SiC), boron carbide (B4C), and alumina (Al2O3). Several decades ago, synthetic ceramic reinforcements were utilised as substitutes for industrial and agricultural waste [27]. In contrast, composites that are strengthened with microparticles experience failure due to the initiation of fractures at the weak point of interbonding between the particles in the composites. To achieve the desired properties, a significant amount of reinforcement is necessary. It has been determined by researchers that the incorporation of nano-reinforcements into metal matrix alloys has the potential to enhance their strength and modulus, while concurrently reducing their ductility and toughness [28-30]. Furthermore, it is worth noting that the nano-reinforcements exhibit significantly higher strengthening efficiency compared to their micron-scale counterparts. The utilisation of nano-scale reinforcements, such as silicon carbide (SiC), aluminium oxide (Al2O3), carbon nanotubes (CNTs), and graphene, in the reinforcement of aluminium (Al) demonstrates potential in addressing the constraints associated with micro-scale reinforcements [31, 32]. Achieving uniform dispersion of nanoreinforcements in AMCs poses a challenge due to the influence of strong van der Waals forces and the inherent incompatibility between these reinforcements and the majority of MMCs alloys. As a result, the majority of aluminium matrix nano-composites (AMNCs) typically experience a restricted enhancement in strength as a consequence of the low concentration of nano-

reinforcements. This limitation hinders their potential for utilisation in engineering and biomedical applications. Numerous research endeavours have been conducted in order to address the bottleneck issue in the AMC.

The utilisation of heterogeneous grain structures, characterised by the presence of both soft and hard zones, such as bimodal, harmonic, gradient, and other variations, represents a highly effective approach. The exceptional mechanical properties of these materials can be attributed to hetero-deformation-induced (HDI) strengthening/hardening, which is widely recognised as the primary mechanism responsible for their outstanding characteristics. The incorporation of nano reinforcements into matrices featuring fine, ultra, and nanograined (FG/UFG/NG) architectures represents an additional approach to address the inherent tradeoff between strength and ductility. Hybrid micro/nano-reinforcements, referred to as micronano-hybridization, offer a highly efficient approach to address the widely recognised AMC issue. This study focuses on the fabrication process and characterization of composites, specifically examining the heterostructure approach and its potential to enhance the mechanical properties of metal matrix composites (MMCs) [33]. The incorporation of micro and nano-scale Al_2O_3 particles resulted in enhancements in the hardness, ultimate tensile strength, and wear resistance properties of the A356 aluminium alloy. The composite material also demonstrated favourable thermal stability and improved microstructural properties. According to the researchers, the compocasting method that has been developed demonstrates potential as a viable and efficient technique for the production of A356 composites reinforced with Al_2O_3 [34]. The dispersion and control of micro-level stress concentrations within hybrid composites can be significantly achieved. Despite significant advancements in the development of high-strength and ductile advanced metal composites (AMCs), the manufacturing process still poses considerable challenges in achieving durability and longevity.

1.3 Overview of hybrid aluminium matrix composites (HAMCs)

Typically, the production of HAMCs involves three main manufacturing techniques: solid state processing (SSP), liquid state processing (LSP), and in situ processing (ISP). SSP encompasses techniques such as diffusion bonding (DB), powder metallurgy (PM), and physical vapour deposition (PBD). LSP involves methods, like pressure, die casting,

infiltration process, and stir casting. Lastly, in situ, processing is another approach utilised in the production of HAMCs. Stir casting was determined by the researchers to be the most effective and auspicious technique among the aforementioned processes [35]. Several important factors, such as the melting temperature, stirring speed, stirring duration, holding time, stirrer positions, stirrer motion, design, die preheating, reinforcements, and others, should be considered before the production of composite materials [27, 36]. The characteristics of composite materials are determined by the optimal selection of these parameters.

The current study investigates the effect of reinforcements on the microstructural evaluation, mechanical, and wear characteristics of composites, with a specific emphasis on strength, toughness, and wear resistance. Moreover, there are several challenges intricated in the preparation of these composites, including the need to ensure a consistent dispersion of the reinforcement particles and to minimise the occurrence of defects. Over the course of the previous two decades, significant development has been made in the field of aluminium matrix composites (AMCs). Nevertheless, a significant portion of the existing research has focused on the advancement of individual reinforced AMCs, aiming to enhance their mechanical and tribological properties [35]. While single reinforced aluminium matrix composites (AMCs) possess satisfactory mechanical and wear properties, enhancing these characteristics necessitates the integration of multiple reinforcements within a singular aluminium matrix. The main categories of wear mechanisms encompass mild abrasive wear, oxidative wear, delaminating wear, and severe plastic deformation wear. The progress of hybrid aluminium matrix composites (HAMCs) has been undertaken with the objective of augmenting the properties of composites by integrating multiple reinforcement materials. In the context of an aluminium matrix, the matrix is augmented through the incorporation of multiple synthetic ceramics via mixing. Moreover, various technical applications, including aircraft, automotive, general optics, antennas, sophisticated electronic devices, and measuring instruments, necessitate both dimensional stability and appropriate mechanical strength [35, 37]. In electronic applications, there is a requirement for materials that possess high thermal conductivity and are lightweight [38]. This study investigates the various mechanisms responsible for enhancing the mechanical properties of these materials, encompassing load transfer, dislocation pinning, and Orowan strengthening. The materials

under consideration possess significant potential for utilisation across a range of industries, encompassing aerospace, automotive, and biomedical engineering, among others. Nevertheless, it has been observed that AMCs featuring only one reinforcement, particularly those with a limited amount of reinforcement, are unable to attain the desired optimal blend of characteristics. The application of higher levels of reinforcement has been found to enhance strength; however, it has been observed to have a detrimental effect on both ductility and fracture toughness [31, 39].

In recent decades, there has been an increasing inclination towards the utilisation of industrial and agricultural by-products for the production of composite materials, while preserving their intrinsic properties, as an alternative to the utilisation of synthetic ceramics. Fascinating findings have been documented from studies conducted on various industrial wastes, such as graphite, fly ash, and red mud, as well as agricultural wastes, including bamboo leaf ash (BLA), rice husk ash (RHA), palm kernel shell ash (PKSA), and coconut shell ash (CSA), among others [40]. One of the primary drawbacks associated with the utilisation of dual synthetic ceramics within the matrix is the reduction in ductility and increased brittleness exhibited by the composite materials. The surface roughness is influenced by the progressive decline in the material's machining properties, leading to increased brittleness. Additionally, the mass of composite rises due to the disparity in densities among the reinforced particles and matrices. The synthetic ceramics are commonly characterised by their high hardness and are frequently employed as abrasives in costly industrial applications. Agro-wastes present themselves as a viable solution to tackle the aforementioned challenges, while concurrently mitigating environmental pollution [27].

The reinforcement is provided to the liquid metal from the outside in the ex-situ technique. It is widely expected that challenges related to wettability and particle agglomeration would arise. The research results indicated that the inclusion of reinforcement resulted in a significant improvement in the mechanical properties of the material, in comparison to its original state as-cast. Nevertheless, beyond a specific threshold, the reinforced composite displayed diminished mechanical properties as a result of the significant aggregation of particles. The conventional technique of stir casting frequently leads to the agglomeration of reinforcement particles, presenting a notable drawback. In order to mitigate the problem at hand, ultrasonic waves were employed on the composite melt subsequent to mechanical

stirring, with the aim of reducing the aggregation of said particles. Consequently, the particles exhibit inadequate dispersion within the matrix, leading to an uneven distribution of reinforcement. The aforementioned issues were successfully resolved by employing the insitu method, which involved the production of reinforcing particles through a chemical reaction within the matrix melt. When choosing reinforcement for a precise application, it is essential to take into account the aforementioned criteria, as well as the influence of operating parameters on wear and mechanical properties. The durability of aluminium matrix composites is primarily influenced by several parameters, including the magnitude of applied force, the temperature, the concentration of reinforcing particles, the velocity and distance of sliding, and the hardness of the opposing surface of the disc [41]. The analysis of the aforementioned factors' influence on the composition and deterioration of composites facilitates the evaluation of the abrasion characteristics exhibited by aluminium composites with metal matrix compositions. The main objective of this review is to examine the production techniques employed for aluminium metal matrix composites (MMCs) and evaluate their influence on the wear and mechanical characteristics of various reinforcement materials incorporated within the aluminium matrix. This review offers a thorough examination of the microstructure of various composites, with a specific focus on the phenomenon of grain refinement. The present review also underscores the intricate applications and manifold challenges associated with aluminium metal matrix composites (MMCs), along with a proposed resolution to address these concerns. The review article will provide researchers with a comprehensive overview of the processing of Al MMCs, as well as a concise summary of the enhancements made to their mechanical and tribological properties. In summary, this review exhibits a comprehensive and well-organized approach, facilitating readers' ability to evaluate its content effectively.

In **Fig.1.3.** fishbone structure, also known as a cause-and-effect diagram, is employed to provide a general representation of the framework of the review.

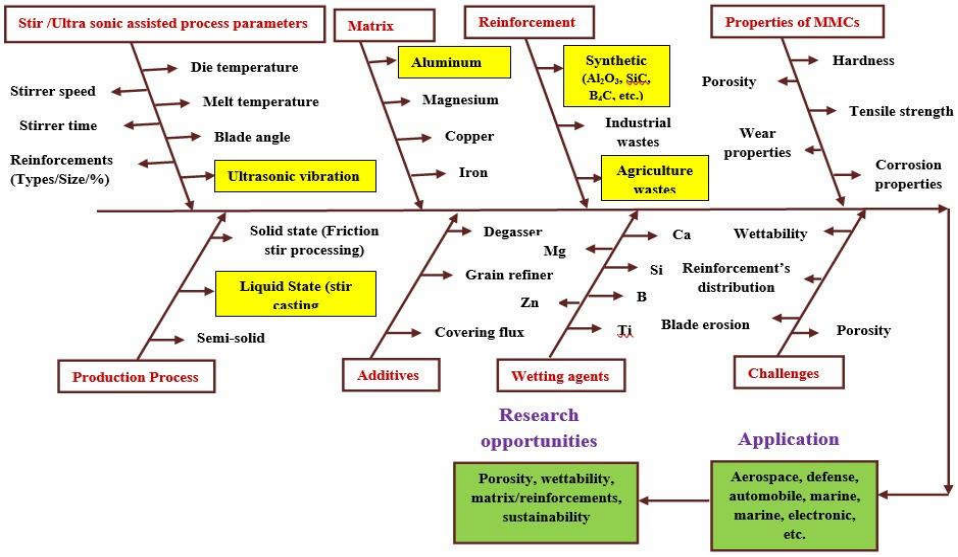

Fig. 1.3. A framework for creating high-quality AMMCs**.**

This diagram is particularly noteworthy as it adeptly encapsulates the variables that influence the superiority of MMCs. By adhering to the recommendations, several obstacles can be overcome, such as the incorporation of various reinforcements, both synthetic and natural, which will enhance the versatility of AMMCs for diverse applications.

CHAPTER 2
LITERATURE REVIEW

The literature on history of composites materials, numerous types, advantages, disadvantages, and applications of metal matrix composites (MMCs), in particular AMCs, is reviewed in this chapter. The various AMHCs based on the reinforcement used advantages, disadvantages, and applications were studied. The motivation for developing novel AMHCs with mechanical and tribological properties is also discussed in detail.

2.1 History and background of composites

The advancement of metal refining technology has been instrumental in enabling human advancement and shaping significant historical occurrences [42]. **Fig. 2.1.** The provided text visually represents the chronological development of material evolution.

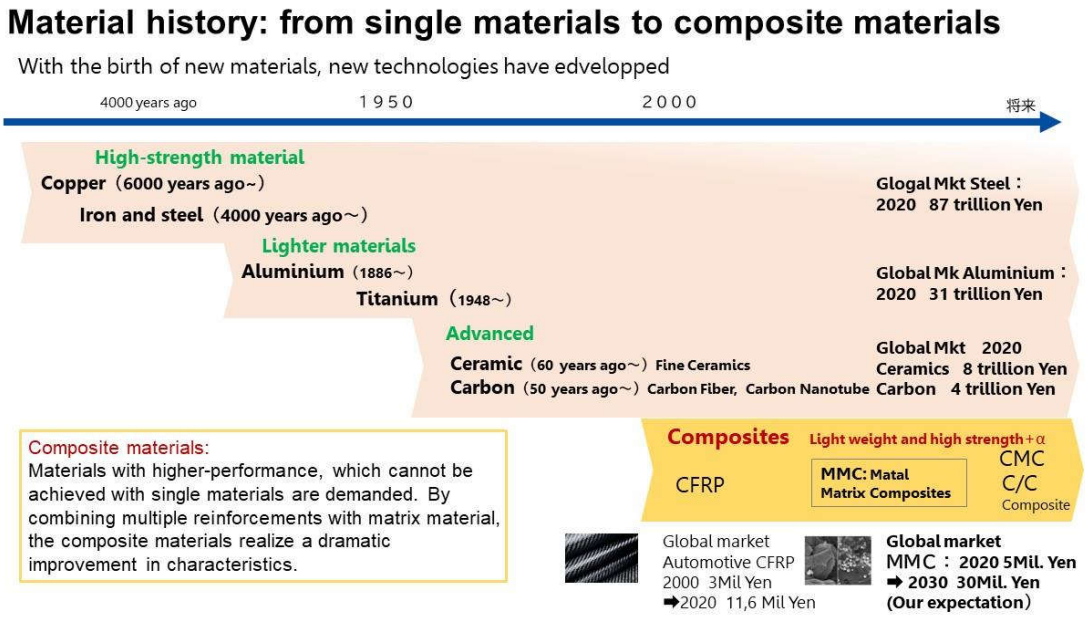

Fig. 2.1. Evolution of materials with time [42]

Iron, a material characterised by its superior strength in comparison to previous materials such as pottery and porcelain, was initially introduced approximately 6,000 years ago. In contrast, aluminium, a material that has had a notable impact on weight reduction, was first discovered approximately 150 years ago. Around six decades ago, a number of advanced materials with exceptional performance attributes, such as fine ceramics and carbon fibre,

were successfully developed (42). Composite materials that possess enhanced properties have been created by combining various materials in this manner.

As per the Farlex Free Dictionary, a metal matrix composite (MMC) is a material characterised by the presence of a continuous metallic phase, known as the matrix, that is blended with an additional phase, commonly referred to as reinforcement. The aforementioned combination functions to augment the mechanical robustness of the metal and enhance its thermal stability under elevated temperatures [43]. The metal matrix composite may be mistakenly classified as an alloy. According to the provided definition, it is crucial that the second element, referred to as reinforcement, is present in significant quantities and exists as a distinct phase. Furthermore, it is crucial to acknowledge that dispersion strengthening and precipitation strengthening may occasionally be mistakenly classified as metals reinforced by particles. The improvement of mechanical characteristics in MMC is achieved through the transmission of load from the matrix to the reinforced particles. To provide further clarification, the reinforcements function as the primary components responsible for bearing the load. Dispersion strengthening mechanisms function by impeding the motion of dislocations, thereby leading to the induction of strengthening effects. Palucka and Bensaude-Vincent have classified the progression of composite materials into four discrete generations, which include polymer, ceramic, and metal matrix composites [44, 45]. The main difficulties in the domain of composites revolve around addressing concerns associated with the determination of the elastic field surrounding a spherical inclusion and the computation of the effective elastic moduli of composite materials containing ellipsoidal inclusions. This paper presents mathematical equations and analytical solutions for the aforementioned issues, accompanied by numerical findings and graphical illustrations of the elastic fields. The aforementioned subjects within the field of solid mechanics hold considerable importance across multiple disciplines, including materials science, geology, and engineering. **Fig. 2.2.** The presentation showcases the sequential order of selected actions undertaken in the historical progression of Metal Matrix Composites (MMCs).

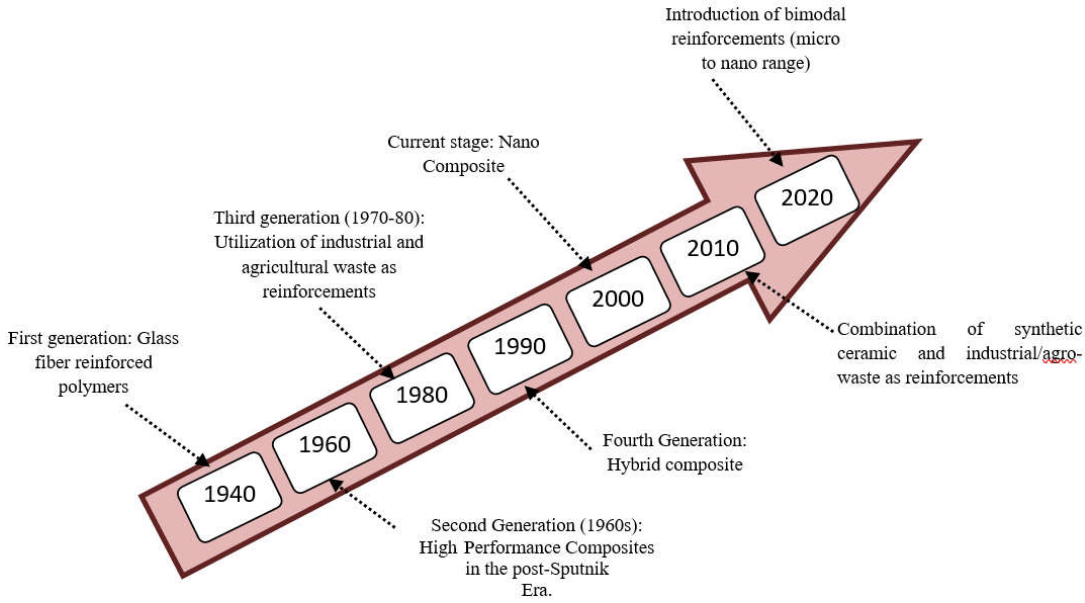

Fig. 2.2. Selected chronological events of MMCs in the past

The classification clearly indicates that the initial generation of composites did not yield a substantial improvement in the metal matrix. Composite materials possess superior properties compared to steel. Composite materials have been extensively utilised in diverse sectors, including aerospace, automotive, marine, sports goods, and consumer goods industries [46-48]. The demand for composite materials has experienced a substantial increase in the global market in recent decades. As a result, there has been a notable shift in the attention of material scientists towards the advancement of composite materials in contrast to monolithic materials. As illustrated in **Fig. 2.3** composite materials can be categorised into four distinct groups based on the composition of their matrix.

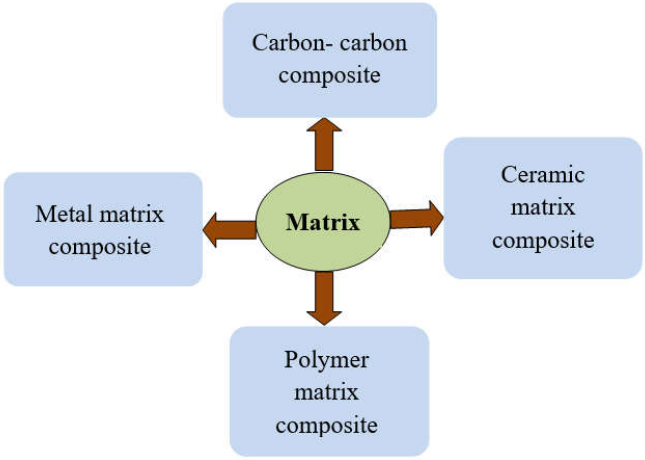

Fig. 2.3. Composite material classifications

The aforementioned classifications encompass ceramic matrix composites (CMCs), metal matrix composites (MMCs), polymer matrix composites (PMCs), and carbon-carbon composites (CCCs). In the realm of contemporary engineering applications, MMC offers multitude benefits when compared to alternative composite materials, as well as traditional monolithic metals and alloys [27].

2.2. Metal matrix composites (MMCs)

The Metal Matrix Composite (MMC) exhibits superior properties when compared to its individual constituent elements due to its unique combination of ductile metal and nonmetallic ceramic materials. As illustrated in **Fig. 2.4** MMCs often employ soft metals such as aluminium (Al), magnesium (Mg), copper (Cu), and titanium (Ti), along with their corresponding alloys, as the matrix material.

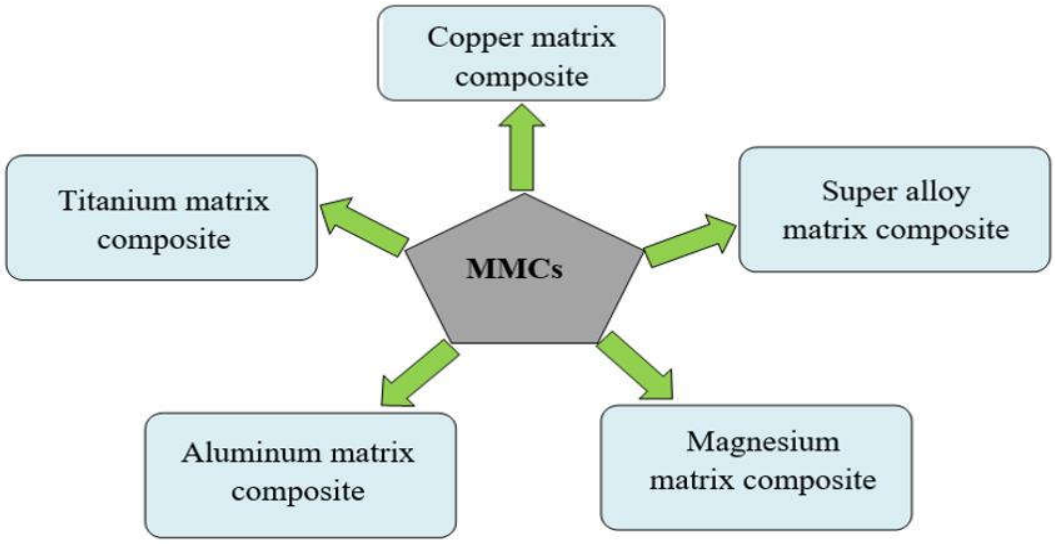

Fig. 2.4. Types of MMCs on the basis of matrix

The classification of MMCs is based on the presence of reinforcement particles and can be divided into three categories:

(i) MMCs that consist of reinforcement particles,

(ii) MMCs that include short fibres or whiskers, and

(iii) MMCs that contain continuous fibres.

The properties of MMC significantly influenced by remarkable compatibility observed between the matrix and reinforcement materials. The effective implementation of Metal Matrix Composites (MMCs) relies on the meticulous evaluation and choice of the reinforcing material, along with its dimensions, morphology, and quantity. The study examined the effectiveness of microwave sintering (MS) and hot extrusion techniques in achieving a regular dispersion of silicon carbide (SiC) particulates within the aluminium matrix. The outcomes suggest that the use of these nanocomposites shows potential for various engineering applications that require high durability and resistance to wear. The choice of reinforcement is influenced by the mechanical and thermal properties of the alloy, such as its tensile strength, elastic modulus, ductility, coefficient of thermal expansion (CTE), thermal stability, compatibility with the matrix, and cost [49]. In recent decades, numerous material scientists and researchers have made significant advancements in the development of MMCs by integrating various ceramic reinforcements, as shown in **Fig. 2.5.** [27].

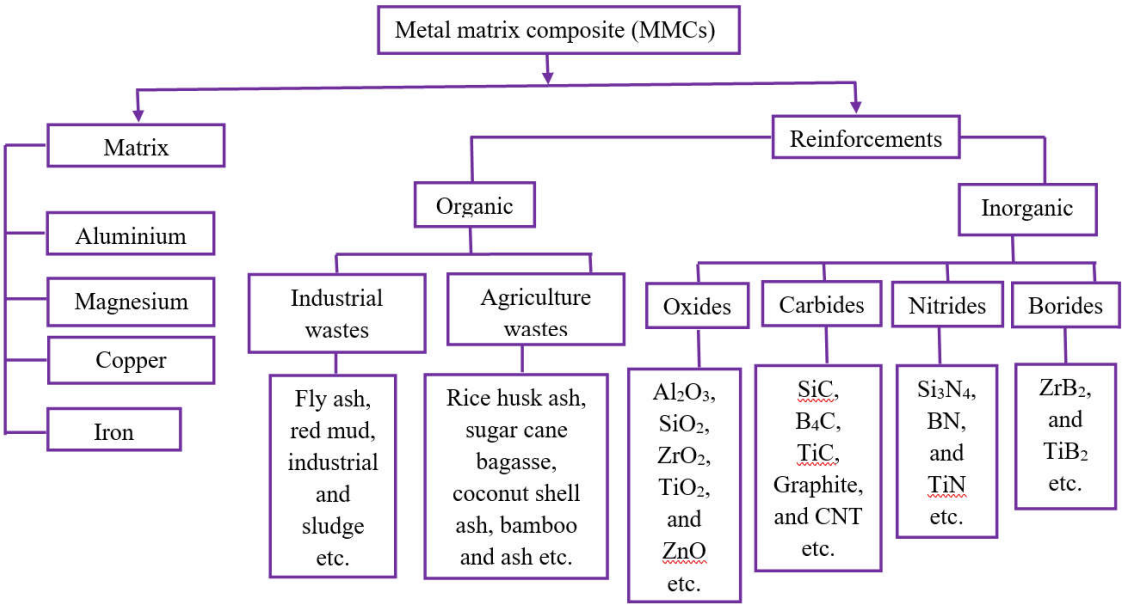

Fig. 2.5. Different types of matrixes and reinforcement employed for MMCs [27].

MMC materials are widely acknowledged for their high level of advancement and are commonly employed as both functional and structural materials in a variety of structural applications, as opposed to monolithic metal and alloy materials. The main aim of this research is to examine particle-reinforced composites, as they are widely accessible, economically viable, and readily dispersible in the matrix. Furthermore, these entities

exhibit a consistent distribution pattern throughout the matrix. The choice of reinforcing materials is contingent upon the specific goals and intended uses of the composite material. The potential for weight reduction in applications can be enhanced through the utilisation of reinforced lightweight metals (35, 50).

2.3. Aluminum matrix composites (AMCs)

As a result, a considerable percentage of engineers have chosen to employ aluminium matrix composites (AMCs) in a wide array of applications, including drive shafts, brake rotors, pistons, and cylinder liners [51-53]. The central objective in the fabrication of composites lies in the preservation of a robust interfacial bond between the matrix and the underlying metal substrate. The attainment of desired properties in advanced composites can present significant challenges when there is insufficient compatibility between the matrix and reinforcing constituents. The progress of magnesium-based metallic composites has been hindered by various unfavourable attributes, including increased vulnerability to oxidation and decreased ductility at high temperatures. To address this concern, it is crucial to create a controlled environment that is chemically inert, ensuring non-reactivity, throughout the manufacturing procedure [54-56]. Copper metal composites are commonly utilised in scenarios where the electrical and thermal characteristics hold importance. Nevertheless, the intrinsic mechanical properties of pure copper metal are relatively subpar, rendering it less notable as a matrix [57, 58]. Advanced Metal Composites (AMCs) effectively mitigate these limitations to a considerable extent and are widely utilised due to their favourable characteristics, such as remarkable resistance to abrasion, a high ratio of strength to weight, enhanced corrosion resistance, as well as convenience and practicality in processing through various techniques in a cost-efficient manner [59-61]. Moreover, the remarkable blend of properties exhibited by aluminum and its alloys renders them exceptionally well-suited for composite production. Aluminum alloys can be classified into two distinct groups based on their response to precipitation hardening: heat treatable and non-heat-treatable. Heat treatable alloys primarily benefit from age hardening, which imparts advantageous characteristics, while non-heat-treatable alloys acquire these properties through the process of work hardening, commonly known as cold working, as

illustrated in **Fig. 2.6**. This inquiry pertains to the suitable wrought aluminium alloys that are commonly often utilised in the fabrication of MMCs.

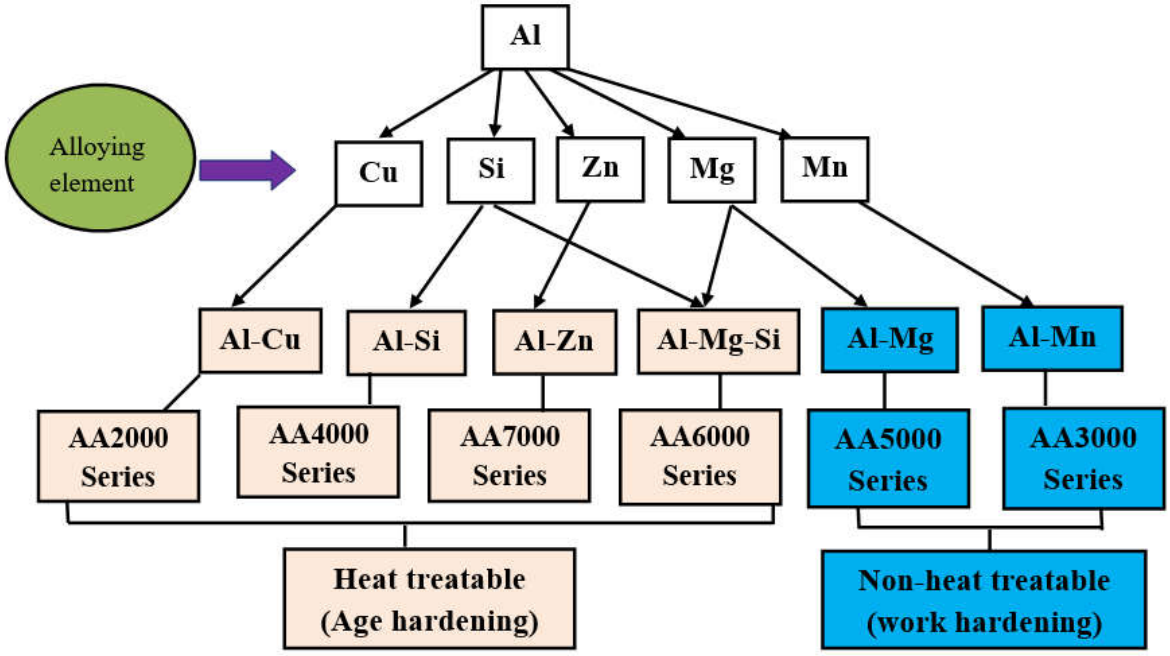

Fig. 2.6. List of commonly used wrought aluminum alloy [62].

In addition, the 1000 series of aluminium alloys is primarily comprised of alloys with a predominant composition of 99% pure aluminium. In contrast, the 8000 series of aluminium alloys is distinguished by the inclusion of supplementary elements, such as lithium, which gives rise to alloys such as the Al-Li alloy. Cast aluminium alloys, specifically those identified as A356.0, are employed in the production of composite materials, resembling the use of wrought alloys [62, 63]. There has been a significant rise in the quantity of research carried out on aluminium metal matrix composites (MMCs) in the past decade. **Table 2.1** displays a comprehensive collection of commercially accessible and frequently employed aluminium alloys that function as matrix materials in the advancement of Aluminium Matrix Composites (AMCs).

Table 2.1. A common aluminium alloy is used as the manufacturing matrix for AMCs.

Al alloy as matrix	Salient properties	Major applications	Ref.

A199/AA1100	High thermal and electrical conductivity, greater workability, corrosion resistance and ductility	Complex decorative foil, transmission power grids, packaging dishes and metal spinning	[65]
A356/LM25	High strength, excellent castability, corrosion resistance, heat treatability, machinability	Pistons, refractories, thermal protection	[66-68]
AA2024	Better strength to weight ratio, machinability, heat treatable	Aircraft body, rivets, thin sheets, sporting goods orthopedic braces,	[69, 70]
AA 6061	Better beat treatability, moderate strength, machinability, workability	Structural and architectural applications, marine frames, trucks, pipelines, rail road cars	[61,71, 72]
A413/LM6	Excellent fluidity, ductility, heat treatable, high strength, higher corrosion resistance, and high resistance to hot cracking,	Automobiles, pressure vessels and hydraulic cylinders	[73, 74]
AA 7075	Better tensile strength, wear resistance, and heat treatability	Components in automotive, aerospace, rock climbing, hang gliding, skating frames airframes	[75-78]

The aluminium alloy 7075 (AA7075) is highly recognised for its remarkable tensile strength and is extensively utilised in diverse industries including aerospace (e.g., wings, fuselage), automotive (e.g., brake disc, drum, piston), sporting goods, and electrical components [52, 64].

2.4 Reinforcements in MMCs

In **Fi. 2.5.** The study provides evidence that the Metal Matrix Composites (MMCs) can be improved by incorporating different reinforcing agents. These agents include organic

components such as red mud, bamboo leaf, and fly ash, as well as inorganic components like oxides, nitrides, carbides, borides, and other substances. Various types of reinforcements can be utilised, including particles, fibres, layers, and interpenetrating materials. The categorization of AMCs can be determined by the specific type of reinforcement utilised, such as laminar, fibre-reinforced, filled, flake, and particle-reinforced composites, as depicted in **Fig. 2.7.**

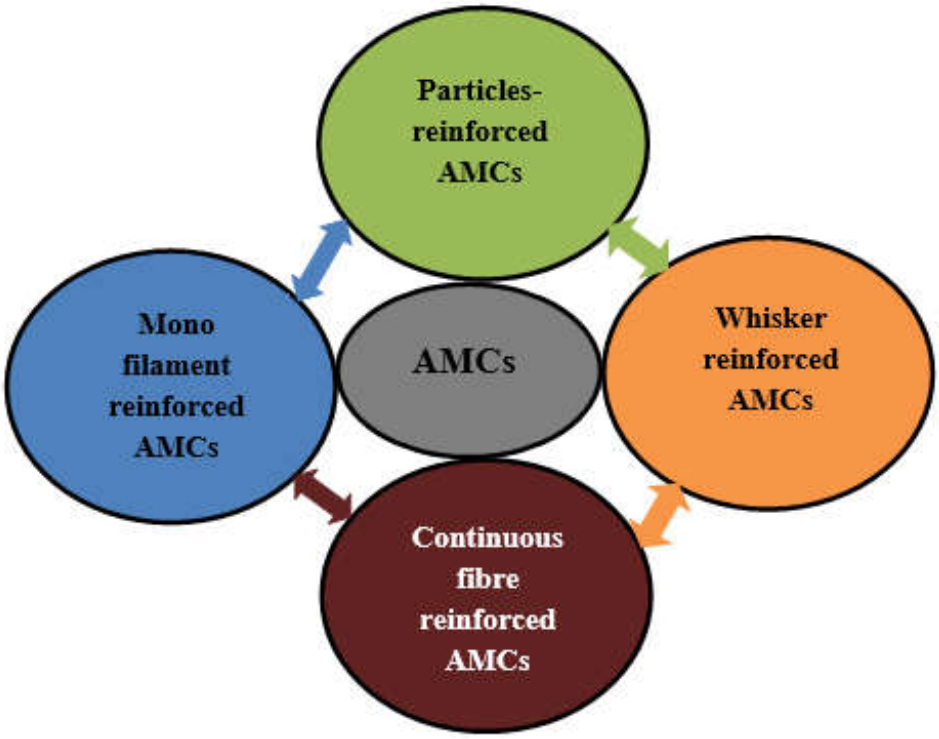

Fig. 2.7 Types of AMCs are shown in a schematic.

The main emphasis of this review centres on particle-reinforced composites, as they are widely accessible, economically viable, and easily dispersed throughout the matrix. The choice of reinforcing materials is contingent upon the specific objectives and intended applications of the composite material. The enhancement of lightweight metals facilitates the feasibility of applications that prioritise weight reduction. Aluminium (Al) is commonly utilised as a matrix material in metal matrix composites (MMCs) due to its advantageous mechanical properties and cost-effectiveness. These properties are further enhanced by reinforcing the aluminium matrix with materials such as silicon carbide (SiC), alumina (Al_2O_3), boron carbide (B_4C), and other similar substances. Multiple researchers have

employed diverse reinforcements in order to fabricate Metal Matrix Composites (MMCs), as demonstrated in **Table 2.2.**

Table 2.2. The most prevalent reinforcements in the creation of metal matrix composites.

S. No.	Reinforcement	Important properties	Industrial uses	Ref.
1	SiC	Good hardness, stiffness, specific strength, and thermal properties.	Brake rotors, pistons, calipers, propeller shaft liners, connecting rod, and drive shaft.	[51, 61]
2	Al_2O_3	Better strength and hardness.	Pistons, brake discs, connecting rods and cylinder heads	[79]
3	B_4C	Low density, high strength, high hardness, outstanding chemical stability.	Automotive applications.	[61]
4	SiO_2	Greater tribological and mechanical behavior	Wear-resistant applications	[80]
5	TiO_2	Robust bonding, better impact and tensile strength, hardness	Automotive applications	[81]
6	ZrO_2	Greater wear resistance and hardness	connecting rods, pistons, and cylinder liners	[82]
7	TiN	Greater wear resistance and strength	Solar (control films), cutting tools, and microelectronic uses.	[83]
8	Si_3N_4	Tensile strength and high hardness	Automobile parts	[84]
9	BN	Exceptional hardness, high strength at high temperature and low density	-	[85]
10	TiC	High hardness at elevated temperatures and excellent wear resistance	Connecting rods and pistons for automobile industry	[86]
11	CNT	Better strength, hardness, ductility and low density	Cylinder liners, aircraft landing gears and brake shoes	[87]

12	Fly ash	Better tensile strength, lower cost, impact strength and compressive strength	Casings, covers, pans, pulleys, valve covers, manifolds, engine blocks, brake rotors	[88, 89]
13	Red mud	Tensile strength, low cost, high hardness, compression strength, light-weight	Marine components, aircraft industry, drive shafts, bicycle industry, electrical parts	[90]
14	Graphite	Good thermal conductivity, low density and the coefficient of thermal expansion	Pistons, current collectors' cylinders, heat sinks, base plates and coolers, discs, rings and heat spreaders	[91]
15	TiB_2	Good abrasion resistance, excellent hardness and high strength	Super functional structures in the automotive, aeronotical, and defence sector	[92]
16	Tungsten disulfide	Self-lubrication and enhanced wear	Rotating vehicle parts	[93]
17	Rice husk	Superior mechanical and tribological properties	-	[94]
18	Coconut shell ash	High wear resistance and hardness	Automotive sector	[95]
19	Diamond	Good thermal conductivity	Microwave transistors, fins, and water-cooled blocks	[96]

Fig. 2.8. The variable "AMMCs" denotes the aggregate number of scholarly articles that have been published in the last ten years, specifically addressing the reinforcement of diverse particles. The data is displayed in **Table 2.2.**

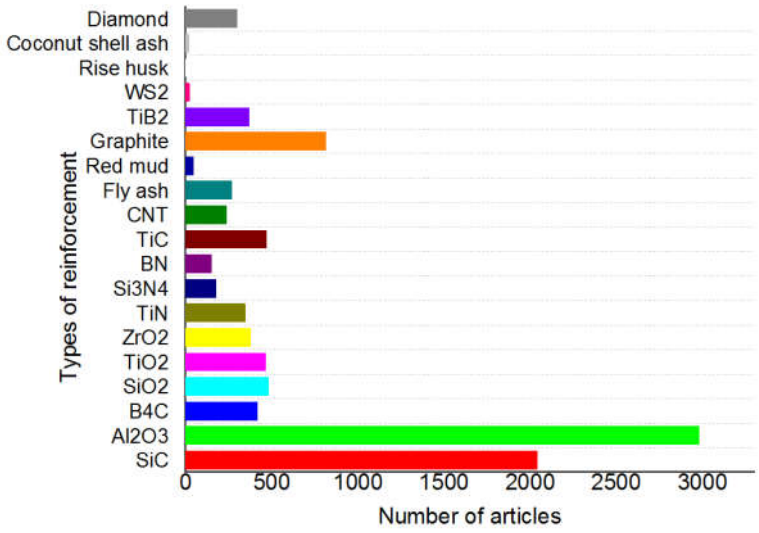

Fig. 2.8. The overall number of research papers that were available in the SCOPUS database each year between 2013 and 2023.

Various agricultural and industrial waste materials, including red mud, fly ash, rice-hull ash (RHA), and coconut shell ash (CSA), are frequently encountered and possess notable physical and mechanical properties that make them highly suitable for the prospective fabrication of new materials. MMCs serve as a notable reference point in this regard. The application of MMCs has evolved significantly since their initial implementation, encompassing a wide range of directions that extend beyond their original emphasis on structural and mechanical functionalities. This evolution has introduced novel concepts and expanded the very definition of MMCs. The following are the primary factors contributing to the limited progress in utilising agro-industrial waste constituents for the production of MMCs over the past few decades [40]:

i. A few decades ago, there were no legal regulations to prevent the disposal of industrial waste materials, such as waste glassware and metallurgical slags, through landfilling. Likewise, the combustion of agricultural waste materials, including rice husk and coconut shell ash, was not bound by any legal restrictions during that period.

ii. In contrast to concrete and polymer matrix composites, the manufacturing process of metal matrix composites (MMCs) necessitates the application of elevated temperatures. Addressing the aforementioned challenges is crucial to accelerate the utilization of agro-industrial waste constituents in MMCs.

a) Determining the optimal calcination temperature for the dissolution of organic materials while preserving the essential chemical components necessary for reinforcing the matrix.
b) The objective is to determine suitable reactants for chemical processing in order to remove undesirable chemical constituents.
c) The task at hand involves the identification of a manufacturing technique capable of producing Metal Matrix Composites (MMCs) while simultaneously preserving the essential characteristics of the waste materials. These characteristics include process time, temperature, pressure, matrix chemical composition of the matrix, and reinforcing percentage, among others.

iii. The potential risks associated with the calcination of agricultural waste have been a topic of extensive discourse over an extended period. According to a study conducted by Hall and Scrase in 1998, it has been observed that the calcination process applied to agricultural waste products does not consistently contribute additional carbon dioxide (CO_2) emissions to the environment.

iv. The absence of comprehension regarding the distinct characteristic of agricultural and industrial scrap materials results in a deficiency of confidence among clients. While composites derived from waste materials generally exhibit comparable or superior performance to conventional composite materials, consumers frequently express apprehension regarding their quality and efficacy.

v. The aforementioned issues necessitate a period of incubation for critical scientific investigation and technological progress, subsequently leading to the expansion of operations to a pilot plant and ultimately to an industrial scale.

The experimental investigations have revealed that the properties of the chosen matrix and reinforcement alloy have the greatest impact on the behaviour of the composites. Secondary variables encompass a range of factors, specifically the dimensions and morphology of the reinforced ceramic particle, the method employed for processing, and the associated variables related to these factors [97, 98]. Consequently, the extensive utilisation of these items was impeded.

Recent studies have demonstrated that metal matrix composites (MMCs) that incorporate nanoparticles as reinforcements exhibit enhanced tribological and mechanical characteristics in comparison to MMCs that employ micron-sized reinforcements. In comparison to particles that are on the micron scale, the introduction of a relatively small proportion of particles on the nanoscale significantly enhanced strength, while maintaining fatigue and creep properties at the same level [99]. The inclusion of SiC nanoparticles at a concentration of 2.0 wt.% in AA356 alloy resulted in a notable enhancement of the material's yield strength, exhibiting a 50% increase as reported in reference [100]. According to the investigation done by Du et al. [101], the incorporation of 2.0 wt.% nano-SiCp into the AA356 alloy matrix composite led to a notable enhancement of 22% in ultimate tensile strength. Despite the superior properties exhibited by nanoparticle-reinforced composites, the existing manufacturing techniques employed to produce bulk composites with intricate geometries and precise shapes are currently lacking in both profitability and reliability.

2.5 Research behind the development of hybrid aluminium matrix composites (HAMC)

AMCs are commonly employed in diverse technical applications owing to their advantageous mechanical properties. In order to enhance the existing frictional and wear resistance of singly reinforced Aluminium Matrix Composites (AMCs), it becomes imperative to incorporate two or more reinforcements within a single Aluminium matrix. AMCs are employed in diverse specialised applications within the discipline of structural engineering, including the areas of general optics, aircraft, and electronics packaging. The choice of these materials is grounded in their capacity to offer precise temperature control and demonstrate exceptional mechanical durability. Moreover, it has been noted that single-reinforced anisotropic matrix composites (AMCs) are insufficient in fulfilling the growing service demands in various advanced technical sectors, including transportation, aerospace, marine, electron packaging, and automotive industries. As a result, a multitude of scholars have diligently strived to put forth various solutions to the aforementioned problem. Several researchers have developed a strategy to increase the characteristics of AMC by utilising waste as reinforcement materials. The second methodology entails incorporating particles that possess dimensions within the nano- and micron-scale range (≤ 50 μm ≤ 100

nm) in order to enhance the characteristics of AMCs. Furthermore, these advanced metallic composites (AMCs) exhibit enhanced ductility and fracture toughness, in addition to their heightened strength. However, there are several key limitations that need to be addressed. These include the limited accessibility to nanoparticle reinforcements, their limited ability to withstand wear, and the inherent inefficiency of the production process. The third strategy involved the implementation of Hybrid Anisotropic Material Composites (HAMCs), which were created by researchers in the field of materials science and fortified with various reinforcements. The Advanced Metal Matrix Composites (AMMCs) represent a new class of composites that possess a unique combination of micro- and nanoparticle properties. Moreover, these composites are more economically viable to produce in comparison to single-reinforced AMMCs. Moreover, the utilisation of industrial and agricultural wastes as a replacement for synthetic ceramic reinforcements is being implemented as a strategy to address both economic costs and environmental pollution. The investigation of Additive Manufacturing and Hybrid Composite materials has been examined as a prospective resolution for meeting the demands of sophisticated engineering applications. The uniform distribution of reinforcement particles within the aluminium matrix is of paramount importance in the advancement of Aluminium Matrix Composites (AMCs) with tailored properties. The attainment of the desired attributes of manufactured AMCs can be achieved by meticulously choosing an appropriate fabrication technique and ensuring the maintenance of optimal process parameters.

2.6. Fabrication process of AMCs

The placement of reinforcement has a significant influence on the size, homogenous distribution, and tribological characteristics of aluminium matrix composites (AMCs). The customization of AMHC materials can be achieved through the deliberate selection of suitable reinforcement and the implementation of appropriate synthesis techniques. Various synthesis techniques are utilised in the fabrication of AMHCs, including solid-state, liquid-state, semi-solid approach, and deposition route [35]. **Fig. 2.9.** This text demonstrates the current methodologies utilised in the fabrication of advanced manufacturing composites (AMCs). The values depicted in **Fig. 2.9.** The sources cited in this context are derived from existing literature [27, 53].

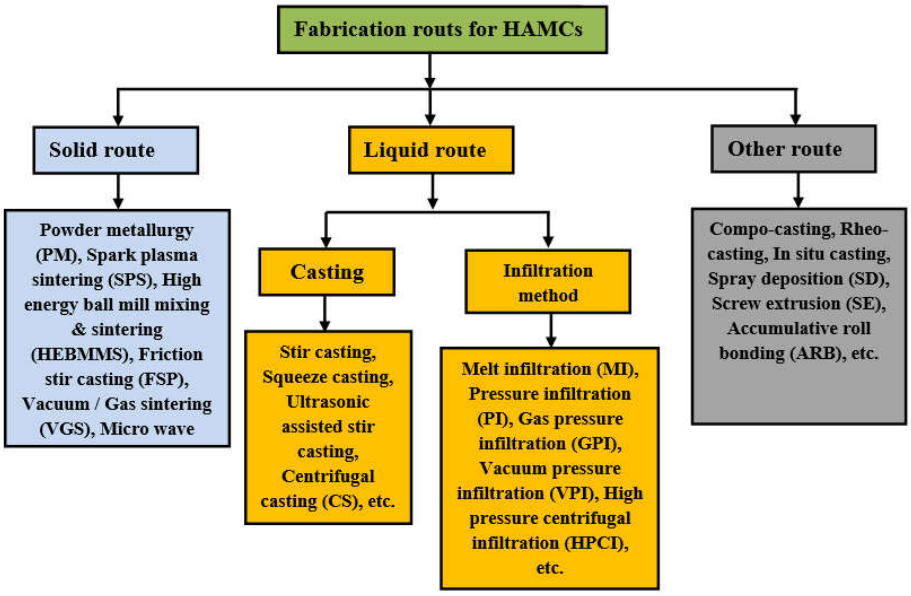

Fig. 2.9. Fabrication routes for HAMCs.

To determine the optimal approach for the advancement of AMCs, it is crucial to possess a thorough comprehension of the essential characteristics associated with them. Each approach possesses its own set of advantages and disadvantages. Academic researchers have made efforts to enhance traditional approaches in order to improve the effectiveness of AMCs. An exemplary demonstration can be observed in the stir casting technique, which involves the vigorous agitation of the molten liquid to promote the comprehensive integration of the reinforcement material into the aluminium matrix. The following sections of this study are devoted to analysing the prevailing production methods employed by AMCs. **Table 2.3** provides a comprehensive compilation of the diverse production processes utilised in the manufacturing of Metal Matrix Composites (MMCs).

Table 2.3. Production processes and properties of various MMCs.

Process	MMC	Properties	Advantages	Disadvantages	Applications	Ref.
Spark plasma sintering (SPS)	Al/Al2O3 & SiC/Al	Hardness (324.6HV)	Homogeneous sintering and compaction levels are collected in a single process	Individual modest symmetrical forms are permissible, A costly pulsed DC generator	Nozzle, armor	[102]

				is necessary.		
High-energy ball-milling (HEBMS)	Al-Al2O3	93.9 HV Hardness	Consistent reinforcement dispersal, dispersal, Decent flowability	Costly	Refractory structure	[103]
Rapid Vacuum Sintering	MgO-doped Al2O3	Superior hardness	Mass production, least porosity,	Expensive	Hard metal tools, microdrills	[104]
Micro-wave Sintering (MS)	Al5%, SiC Ti0.5%	Tensile strength (183.9 MPa), and hardness 65.46±0.58 HR15T	Enhanced mechanical behavior,	Appropriate for particular dielectric material and not appropriate for alumina and Silicon nitride	Bio- medical applications	[105]
Melt infiltration (MI)	Al/ Ti_3SiC_2	Hardness 751HV, compressive strength 750MPa	Enhanced wear behavior, Lucrative High temperature ability	Inadequate temperature and depth cause obstruction in infiltration	aerospace industries	[106]
Pressure infiltration	Al/GNPs	250 Mpa Tensile	Enhanced tribological aspects, cost-effective for mass production	High porosity, high cost, not appropriate for bulky casting	Engines, wheels, and piston	[107]
Gas pressure infiltration (GPI)	Aluminum alloyAl Si_{12}/Metallic glass Ni60Nb20Ta20 flakes		Enhanced thermal conductivity, Accomplished for high temperature,	Manufacturing rate lesser than stir squeeze casting, Sluggish solidification method	Brake calipers, hydraulic components	[108]

Vacuum pressure infiltration (VPI)	2D-Cf/Al	Tensile 281.2MPa	Condensed porosity, enhanced UTS, close shaped composite can be attained	Sluggish solidification method, Deficiency of wettability, crack development	Electronic packaging	[109]
Stir casting	A356/10 wt. % fly ash	Tensile strength (Max 62) Mpa	Mass production, automated casting	Heat treatment required	Manifolds, Pump housings, cylinder heads	[113]
Centrifugal casting	Al–B–Mg	Hardness values of 80–90Hv	Well mould filling, Almost free from porosity, Dense grain structure, Better strength, and High wear resistance	Deprived casting at inner surfaces	Liners for IC engines, Sewage pipes, Automotive piston, Rotors for brake, mill rolls for textile and paper, Nozzles,	[114]
Squeeze casting	AA7050/0.3 wt. % graphene	Ultimate tensile strength 255 Mpa	Evenly reinforcement dispersal, Particulates at 0.3 wt. % graphene	Further setup required and therefore rises the Manufacturing cost	Automotive and aerospace	[115]
Vacuum casting	B4C/ Al6061	UTS 340MPa	B_4C particles are evenly distributed inside the metal matrix	Higher cost	Aerospace, automotive, and nuclear field	[116]
Compo-casting	AA7075 /Gr/fly ash	Tensile Strength (213MPa) and hardness(62 HRB)	Consistent reinforcement dispersal, Particulates is attained, Enhanced reinforcement wettability	Semi-solid route smarts from porosity and processing problems	Production aerospace part	[117]

Rheo-casting	AA356/ SiC	Hardness (70 – 95) HRB	Negligible porosity, Intricate shapes, condensed shrinkage, outstanding mechanical surface finish	Costly process	High wear-resistant parts	[118]
In-situ	A380/TiB2	Tensile strength 160 Mpa	Greater bonding between the matrix	With the rise in reinforcement content the ductility decreases	Automobile and aerospace industries	[119]
Spray atomization and Deposition processing	LM13/ Zircon	Hardness (80HV)		Costly and porosity issue	Automotive sector	[120]
Metal Injection moulding	AA6016 (AlMg1SiCu)/graphite	Hardness 46.6HV, Compression strength 248MPa	Better dispersal,and hardness, Mass production of minor and complex parts	For small components	Electronic industry, base plates, coolers, disc sand rings	[121]
Roll bonding	Al1050/ NaTiC	Ultimate tensile strength 58 Mpa	High strength and corrosion resistance	Needs huge load abilities, Costly dies, Low production rate	Structural, automotive applications	[122]

2.6.1 Powder metallurgy

Powder metallurgy (PM) is widely acknowledged as a manufacturing method that enables the production of near-net shape components, thereby eliminating the need for additional product processing. The approach is regarded as expensive because it relies on the use of powdered raw materials, which result in higher costs compared to their solid counterparts. **Fig. 2.10.**

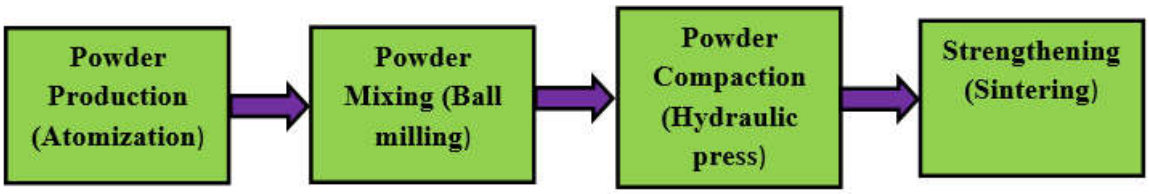

Fig. 2.10. Processing route of Powder Metallurgy.

This study demonstrates the application of four distinct processes to achieve the specified objective. The raw material undergoes a series of processes, including atomization, which leads to its transformation into a powdered state. The powdered parent matrix is blended with reinforcing elements through a range of milling techniques, including ball milling, planetary milling, and high energy milling [123]. The powder mixture is then compressed at high pressures using sturdy hydraulic presses. The dies used for compacting the powder take on the shape of the dies themselves. The consolidation of the green compact is subsequently enhanced through the process of sintering in a specifically designated sintering furnace [123, 124].

The production of AGNCs via PM-based methods involves three primary steps: (i) the integration of graphene into the Al-matrix powder, (ii) the creation of AGNC powder, and (iii) the subsequent secondary treatment of AGNCs, which may include extrusion, rolling, and other methodologies. In continuation of the preceding discourse, Yu et al. (2012) undertook a research endeavour aimed at investigating the influence of varying milling durations on several aspects, namely the dispersion of graphene nanosheets (GNS), the occurrence of defects in GNS, the generation of Al4C3, and the electrical and mechanical characteristics of an Al6063-0.3 wt.% GNS composite. The enhancement of GNS dispersion was observed to be dependent on the duration of milling, resulting in a uniform distribution after a milling time of 3 hours. **Fig. 2.11(a)** illustrates the presence of a slender Al2O3 layer at the interface between aluminium (Al) and graphene nanosheets (GNS) subsequent to a one-hour milling procedure. **Fig. 2.11(b)** illustrates the composite that underwent a milling process lasting for a period of three hours. **Fig. 2.11(a). 2.11(b).**

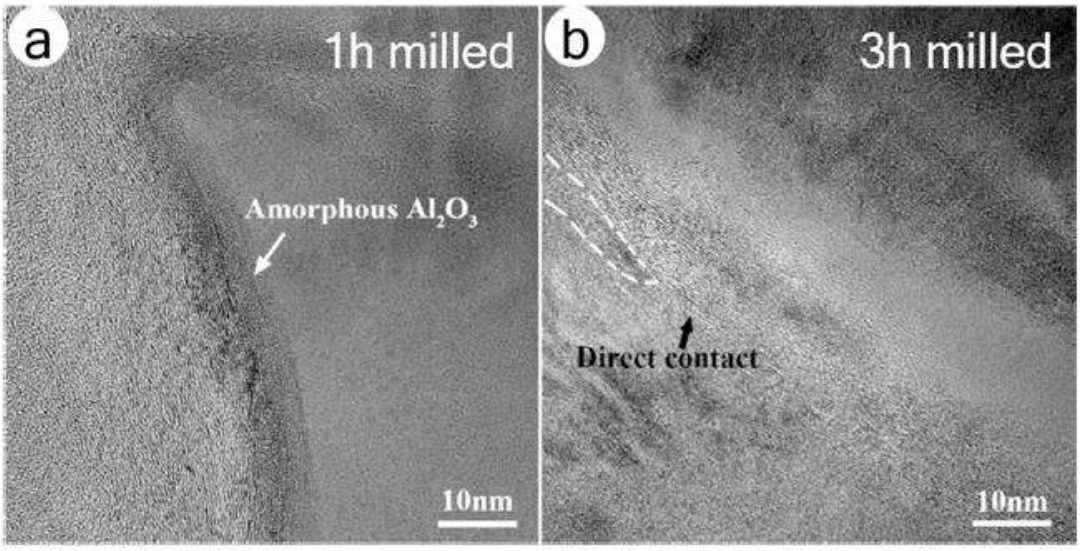

Fig. 2.11. HR-TEM images of AA6063 (0.3 vol.% GNS) after milling for (a) 1 h and (b) 3 h, respectively, demonstrate the thin layer of amorphous Al2O3 between the metal and the GNS, as well as their direct contact [125].

The fracture of the aluminium oxide (Al_2O_3) layer on the surface of gas-atomized aluminium (Al) particles occurred during the milling process, primarily due to the impact exerted by the milling balls. Following this, the Al_2O_3 layer underwent complete disappearance subsequent to a milling period of 3 hours. The production of Al_4C_3 was not observed within a milling duration of 1 or 2 hours. Furthermore, it was observed that the dimensions of Al_4C_3 exhibited an increase from 10 to 20 nm to 50 nm as the duration of the milling process was extended from 3 hours to 4 hours. The increased dimensions of Al_4C_3 can be primarily ascribed to an augmentation in the occurrence of defects during the milling procedure. Furthermore, with an increase in the milling duration from 0 to 4 hours, there was observed a corresponding increase in the ratio of the intensity of the D-band to the intensity of the G-band (ID/IG) of the powders. This increase in the ID/IG ratio suggests that there was an enlargement in the diameter of the graphene nanosheets (GNS). Furthermore, it was observed that the grain size of the compacted materials exhibited a decrease as the duration of milling increased. The grain size reached its minimum value after a milling duration of 3 hours. The composites that were subjected to a milling process for a duration of 3 hours demonstrated the most elevated levels of electrical conductivity and tensile strength. The composite, after undergoing a 4-hour milling process, exhibited a notable increase in the concentration of Al_4C_3, which subsequently led to a reduction in the

properties of the underlying base metal. In their research, Issa et al. [126] utilised the powder metallurgy technique to produce composites consisting of SiO_2/Al. The powder mixture was subjected to a processing period lasting two hours in an argon atmosphere to ensure uniform blending. Following that, the milled mixture was subjected to compression using circular dies at a pressure of 200 MPa. The sintered specimen was subjected to extrusion using an extrusion ratio of 8:1 (ball/powder), incorporating graphene oxide (GO) as a reinforcing agent [127]. The fabrication process of the $AlMg_5$ composite involved the utilisation of a powder metallurgy technique, which encompassed the procedures of ball milling and hot pressing. The experiment involved the use of powder samples, specifically GO (graphene oxide) with dimensions measuring 1 mm in length and ranging from 5 to 20 nm in thickness, as well as $AlMg_5$ powder with a purity level of 99.5% and particle size of 63 μm. These samples were subjected to a ball milling process lasting a total of 20 hours. The milling procedure was carried out under an argon atmosphere at a ratio of 8:1. The powder mixture was inserted into a preheated steel mould and then exposed to a uniaxial pressure of 570 MPa. The final sample was produced, yielding a specimen with dimensions of 30 mm in diameter and 5 mm in thickness. The microstructural analysis demonstrated that the dispersion of graphene oxide (GO) was uniformly distributed at a concentration of 1% by volume. The fabrication of aluminium matrix composites (AMCs) with improved mechanical properties was achieved through the successful utilisation of the powder metallurgy (PM) technique [101, 102]. **Table 2.4** presents a comprehensive overview of diverse research efforts related to the evolution and progress of Asset Management Companies (AMCs).

Table 2.4. AMCs and their corresponding properties of PM manufactured AMMCs.

S. No.	Matrix	Reinforcements	Process parameters	Finding	Ref.
1	Al	TiO_2 (nm size)	Pressure- 1.04 MPa, Sintering temperature- 450 °C (Atmosphere- argon)	Enhanced hardness and wear resistance	[124]
2	Al	B_4C and SiC	Pressure-150 MPa Sintering temperature- 610 °C	Improved in hardness	[123]
3	Al (99.5 %)	SiO_2	Sintering temperature- 610 °C, Milling time-2	Improved hardness and strength by 41.8	[126]

			hours,	% and 24.8 % respectively.	
4	Al (99.05 %)	Graphene	Sintering time (60, 120, 180, 300) minutes and Sintering temperature (550, 600 and 630 °C)	Density and hardness reduced due to increment in sintering time	[128]
5	$AlMg_5$	GO	Pressure - 570 MPa, Milling time - 20 hrs	Enhanced properties with uniform dispersal of GO.	[127]
6	Al (98 %)	Graphene	Sintering Temperature-560 °C, Milling speed - 300 rpm, Sintering time-4 hours	Hardness and tensile strength improved	[129]
7	Al (99.9 %)	Graphene	Sintering time (1, 2, 3, 4, 5) hrs, Milling time (1, 2.5 and 5 hrs.), Sintering Temperature 510 °C, And (Atmosphere - Argon)	High hardness achieved	[130]

The ultimate tensile strength, yield strength, hardness (HV), and percentage elongation values of AMCs and the aluminium matrix. **Fig. 2.12-2.15.** Composites incorporating graphene **Fig. 2.14** have demonstrated superior performance in comparison to their alternatives. However, the existence of high-strength graphene imposes notable limitations on indentation.

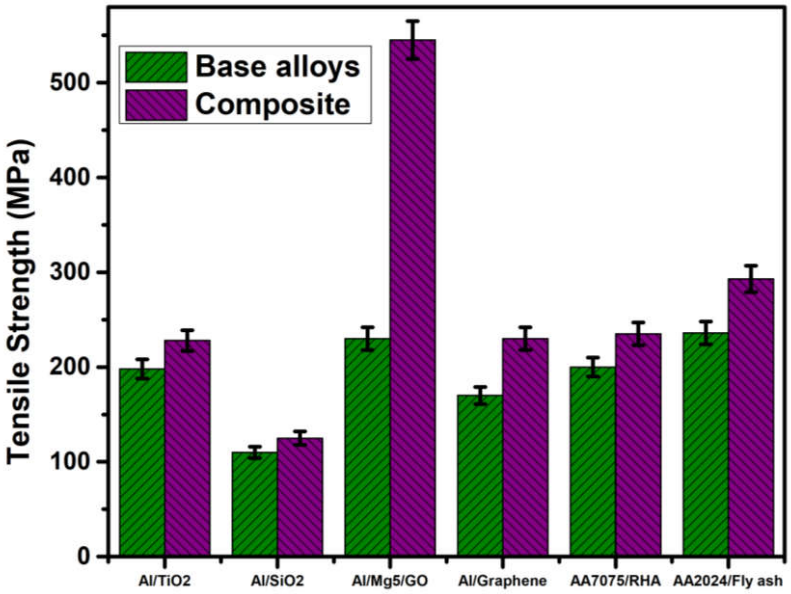

Fig. 2.12. Tensile strength of composites and parent metal developed by PM [35].

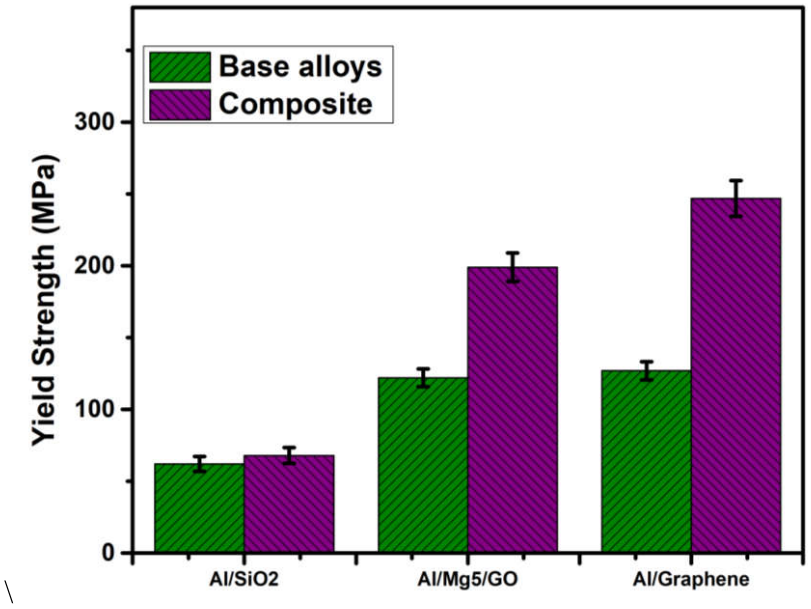

Fig. 2.13. Yield strength of composites and base metal developed by PM [35].

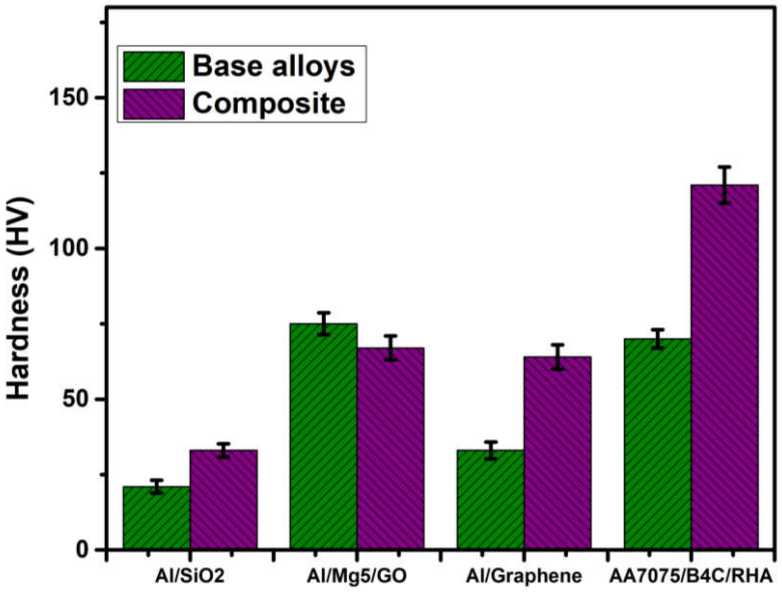

Fig. 2 14. Hardness (HV) of composites and base metal developed by PM [35].

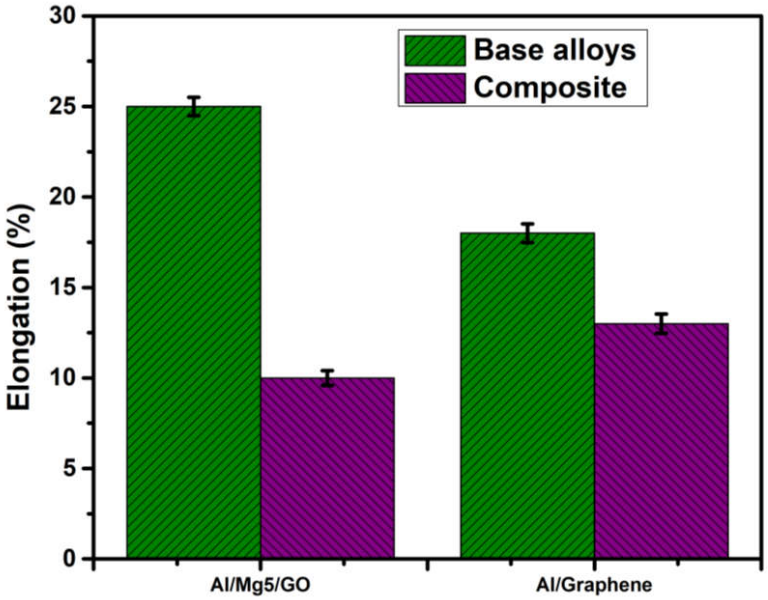

Fig. 2.15. Percentage elongation of composites and base metal developed by PM [35].

In their study, Sun et al. [33] developed a composite material known as B4Cp/6061Al. This approach involves the incorporation of small-scale strengthening materials, such as micro and nanoparticles, into matrices characterised by fine, rough textures. These particles are distributed either within or outside the matrix structure. The aforementioned composite material exhibits a remarkable amalgamation of strength and ductility. The integration of micro and nanoparticles allows for the redistribution and subsequent suppression of stress concentration at the micro-scale within the hybrid composite. The electron backscatter diffraction (EBSD) image presented in **Fig.2.16** demonstrates the presence of a bimodal microstructure within the aluminium alloy matrix of the composite specimen. **Fig. 2.16(a).** The bimodality of the grain size distribution is supported by the presence of two distinct grain populations: ultrafine coarse-grained (UFG) grains measuring approximately 430 μm and coarse-grained (CG) grains measuring approximately 2.5 μm. **Fig. 2.16(b)** depicts a particulate of B4Cp within the ultrafine-grained (UFG) matrix, as observed in the transmission electron microscopy (TEM) image. Additionally, **Fig. 2.6.(c).** displays the energy-dispersive X-ray spectroscopy (EDS) mapping of the designated interface.

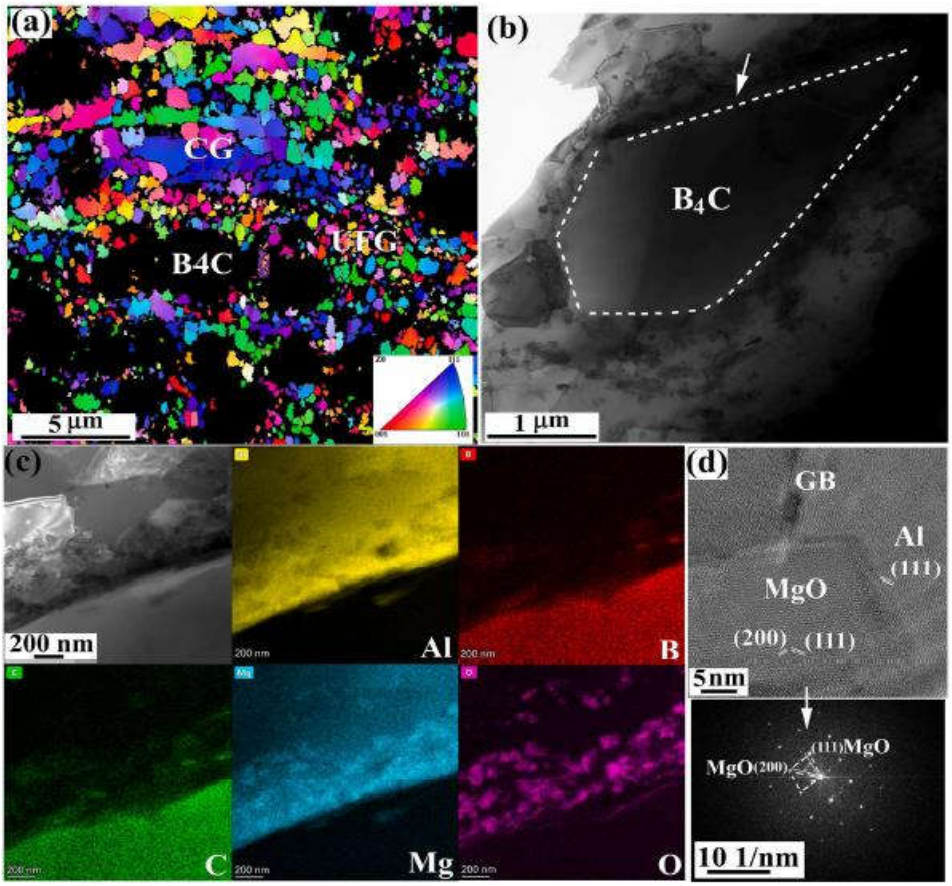

Fig. 2.16. (a) EBSD pictures illustrating the B_4Cp dispersed in the bimodal matrix, (b) A STEM image demonstrating a B_4Cp particle within the UFG matrix, accompanied by EDS mapping analysis (c) of the designated interface and (d) A high-resolution TEM image along with a SAED pattern, which confirms the formation of MgO [33].

The cartographic representations illustrating the spatial arrangement of magnesium and oxygen substantiate the formation of magnesium oxide nanoparticles in situ, exhibiting an approximate mean diameter of 60 nanometers surrounding the B4Cp. 1 displays a detailed view of the crystal structure of the material under investigation. The formation of magnesium oxide is further supported by the corresponding selected area electron diffraction (SAED) in **Fig 2.16(d).** The researchers demonstrated that this distinctive configuration possesses the capability to offer both intrinsic and extrinsic toughening mechanisms. The mechanisms encompassed in this study involve various processes that contribute to the overall behaviour of the material. These processes include the improved capacity to retain dislocations within regions of ultrafine-grained (UFG) structure, the occurrence of twinning within UFG regions, the strengthening effect resulting from hetero

deformation, the diversion and connection of cracks facilitated by nano dispersoids, and the reduction of crack sharpness at the boundaries between UFG and coarse-grained (CG) regions.

2.6.1.1 Challenges and future developments of the powder metallurgy route

Although some fundamental concerns and challenges regarding the utilisation of aluminium powder have been addressed, there is still a significant requirement for additional research to explore the impact of various aspects of the powder metallurgy (PM) process on the properties and functionality of materials. The relative significance of material characteristics and performance, as a result, is occasionally deemed less substantial, despite the substantial advancements achieved in enhancing and comprehending the reaction of powder metallurgy processing. The performance and material properties of contemporary aluminium PM alloys present significant challenges in meeting the increasingly stringent requirements of various applications, thereby impeding their widespread utilisation. The utilisation of powder metallurgy (PM) alloys containing aluminium may witness an increase due to advancements in their ductility, modulus, and performance in diverse conditions such as fatigue, corrosion, or high temperature. The powder metallurgy (PM) process encompasses several components that can be utilised to improve the properties and performance of materials. These components include the development of alloy systems, the production of powders, the implementation of alloying techniques, the utilisation of consolidation techniques, and the application of secondary processing.

The presence of iron impurities in aluminium powder metallurgy (PM) alloys has not received adequate attention. The investigation of iron correctors, such as manganese, has the potential to yield favourable outcomes in the reduction of iron compound formation that contributes to embrittlement, as well as in the improvement of ductility. The exploration of incorporating nano powder aluminium or ceramics into aluminium powder metallurgy (PM) alloys offers a compelling avenue for the development of alloys with enhanced microstructures, as long as the oxide content of the aluminium powder remains within acceptable limits. The incorporation of minor alloy elements into the base aluminium powder, akin to the approach observed with transition metals, may be regarded as a

prospective tactic for the advancement of novel and unconventional chemistries in powder metallurgy (PM) alloys. This methodology has the potential to result in improved material characteristics while minimally impacting the performance of the powder metallurgy (PM) process. The field of additive manufacturing of aluminium PM alloys is currently experiencing a noteworthy advancement, characterised by the expiration of prominent patents and the increasing compactness, efficiency, and cost-effectiveness of the technology. The chemical constraints that are commonly observed in traditional aluminium powder metallurgy (PM) alloys do not impose limitations on these specific alloys. The production of heat-resistant aluminium powder metallurgy (PM) alloys, such as aluminium-manganese or aluminium-magnesium alloys, is indeed a viable possibility. Moreover, it is feasible to cultivate novel alloys that are specifically customised for the purpose of additive manufacturing. The application of this technique demonstrates significant benefits in the development of advanced aluminium-transition metal alloys that possess improved properties suitable for high-temperature applications, resulting in a natural reduction of residual stresses. Nevertheless, there are specific apprehensions regarding the production of aluminium powder metallurgy (PM) alloys using additive manufacturing techniques. The investigation of traditional aluminium powder metallurgy (PM) alloys and the newer quick solidification processed aluminium PM alloys holds considerable promise for knowledge acquisition, even in light of the current inclination towards exploring guidance from alternative additive manufacturing materials.

Two potential consolidation techniques that merit further investigation in the context of aluminium powder metallurgy (PM) alloys are spark plasma sintering and powder forging. These methodologies possess the capacity to enhance the formation of complex microstructures that demonstrate enhanced ductility and strength. Another area of focus relates to the development of economically efficient secondary processing methods. The inclusion of a solution treatment in the sintering process prior to quenching has the potential to improve the strength of the material, thereby eliminating the need for additional and more expensive heat treatments.

2.6.2 Friction stir processing (FSP)

The application of intense plastic deformation is employed in the context of friction stir processing (FSP) to facilitate the fusion of materials. The technique being discussed pertains to the domain of solid-state joining methods and is grounded in the principles of friction stir welding (FSW) [131,132]. One potential advantage of utilising this approach lies in its capacity to maintain the inherent attributes of the matrix while enabling the augmentation of advanced materials with enhanced surface properties. **Fig. 2.17.** The diagram depicted in **Fig. 2.17.**

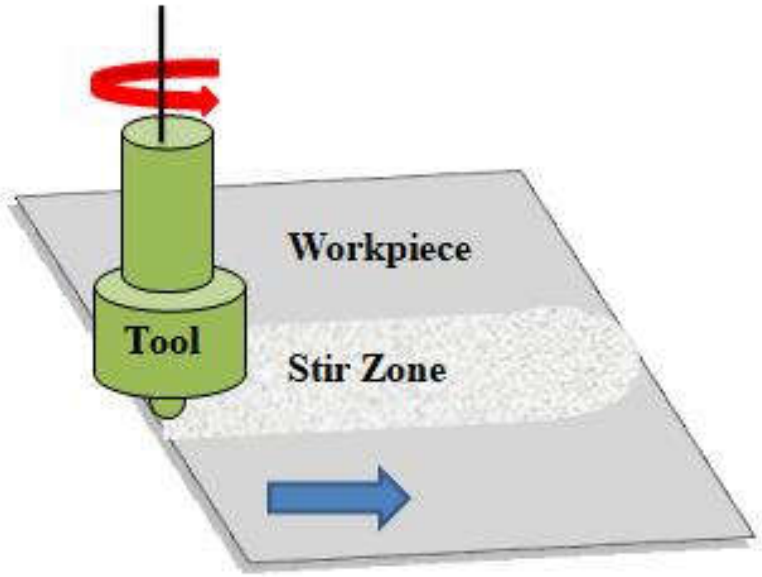

Fig. 2.17. Schematic diagram of FSP

This demonstrates the fundamental principles of the process. The rotational device generates a significant quantity of thermal energy due to the frictional interaction with aluminium. The reinforced material is incorporated into the plastic region, resulting in a significant rise in temperature for the designated metallic component in contact. The FSP technique was employed to fabricate B4C reinforced Al 7075 composites in a single study. The AMCs that were manufactured demonstrated enhanced grain structure and mechanical properties, as indicated by the characterization and mechanical tests carried out [133]. Several research studies have provided evidence of the advantages associated with performing multiple iterations of friction stir processing (FSP) when integrating gold nanoparticles (GNPs) into an aluminium 5052 matrix. According to the findings presented

in reference [132], the investigation revealed that the process of refining grains in AMCs led to a notable enhancement in both tensile strength and hardness.

Khodabakhshi et al. [132,134] conducted a research investigation wherein they utilised a multi-pass Friction Stir Processing (FSP) technique to manufacture a composite material. This composite material was composed of a reinforced Al-Mg alloy (AA5052) matrix combined with Graphene Nanoplatelets (GNPs). The objective of this research is to examine the effects of incorporating graphene nanoplatelets (GNPs) into AA5052 alloy on its microstructural properties and mechanical behaviour. The addition of graphene nanoplatelets (GNP) at a concentration of 3 volume percent to the base material led to a notable improvement in both hardness, with a 53% increase, and yield strength, which experienced a more than threefold increase. The primary factor that contributes to this phenomenon can be ascribed to the improvement of the microstructure through the application of friction stir processing (FSP), along with the even distribution of graphene nanoplatelets (GNPs). Grain size of aluminium-magnesium compounds experienced a decrease from an initial dimension of 10.7 nm to 9.7 nm as a result of the Friction Stir Processing (FSP) technique. Following that, the size of the grains was subsequently reduced to 2.1 nm through the incorporation of Graphene Nanoplatelets (GNPs) into the alloys. The researchers have attributed the significant reduction in grain size to a combination of Zener pinning and particle-induced nucleation mechanisms that take place during the recrystallization process. This reduction can be attributed to the inclusion of graphene nanoplatelets (GNPs). **Fig. 2.18 (a & b)** illustrates the changes in grain size as described in the citation [135].

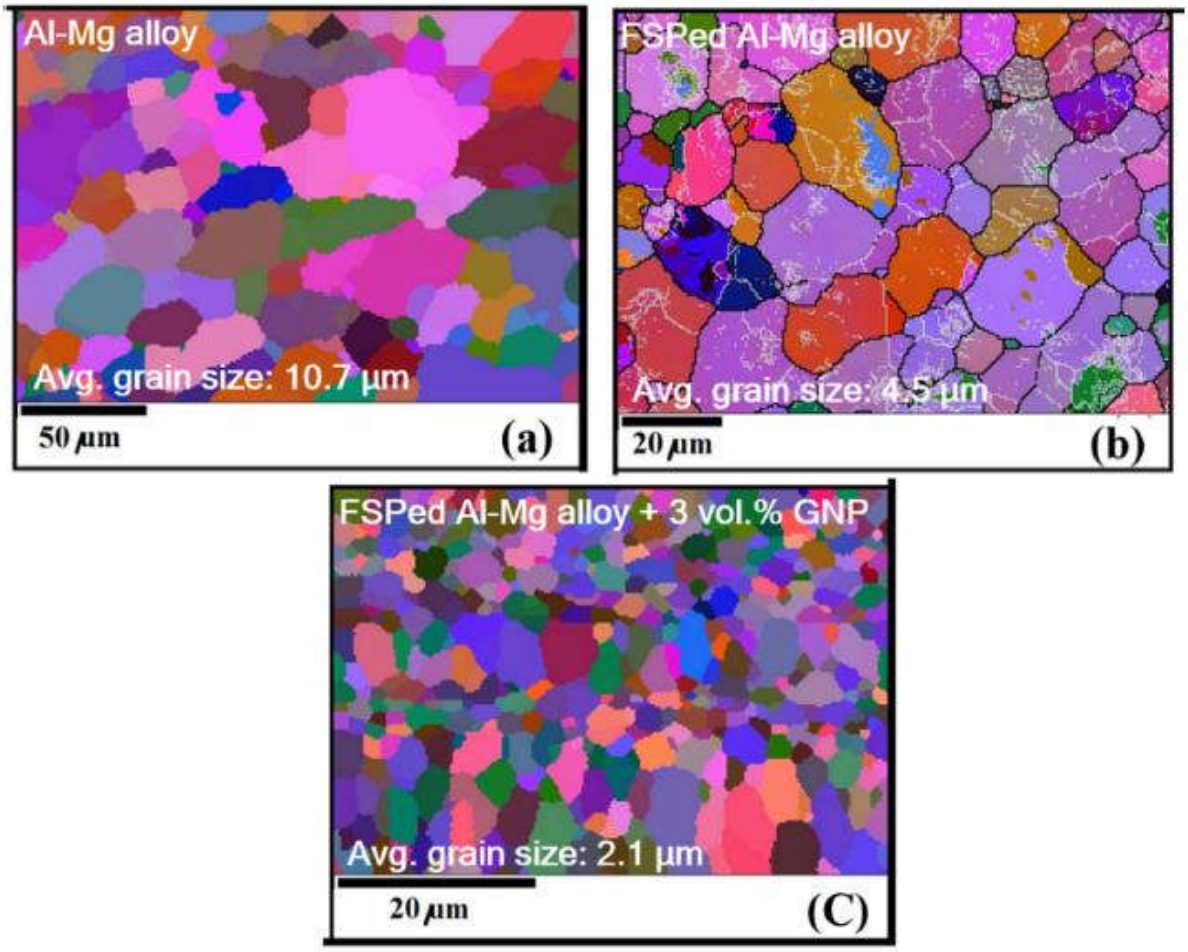

Fig. 2.18. Aluminum-Magnesium alloy, FSPed Aluminum-Magnesium alloy, and FSPed Aluminum-Magnesium alloy + 3 vol.% graphene grain boundary distribution analysis by EBSD [132].

The inhibitory effect of grain boundary nanoparticles (GNPs) on grain growth during recrystallization has led to improved mechanical properties.

Furthermore, a separate research investigation offered empirical evidence for the successful production of SiCp-reinforced Al5052 composites using Friction Stir Processing (FSP). The implementation of this manufacturing technique resulted in significant improvements in the ultimate tensile strength (UTS), yield strength (YS), and hardness of the composites, showing approximate enhancements of 60%, 75%, and up to 140%, respectively. [136]. Orowska et al. [137] utilised friction stir processing (FSP) as a methodology to produce nanocomposites comprising an aluminium matrix with both coarse-grained (CG) and ultrafine-grained (UFG) structures in their research investigation. The structural integrity of these entities was further enhanced through the incorporation of Al2O3 nanoparticles. The basic material had a normal

grain size of 1 µm, whereas the nanocomposite exhibited an aggregate grain size of roughly 4 µm. On other hand, the sample that underwent the friction stir processing (FSP) technique without any form of reinforcement exhibited an average grain size of 12 µm. The results obtained from the electron backscatter diffraction (EBSD) analysis, as depicted in **Fig. 2.19.**

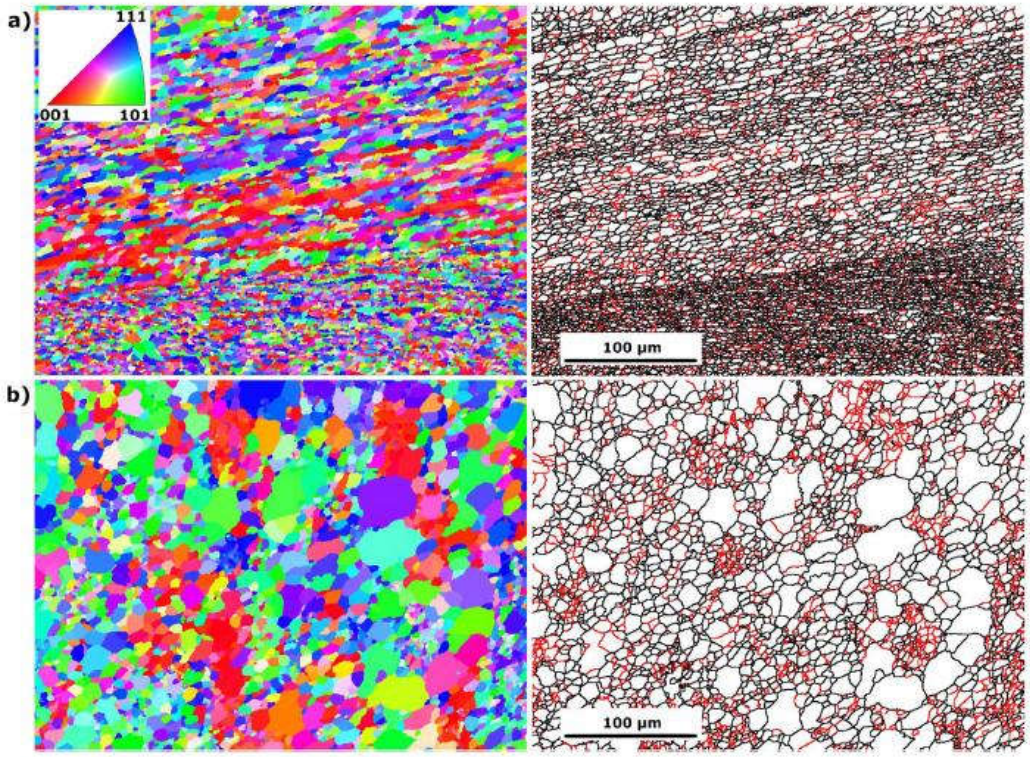

Fig. 2.19. OIMs and grain boundaries distribution of (HAGBs (black lines), LAGBs (red lines)) maps of the stir zone of the course grain single pass + Al_2O_3 specimen representing: (a) PDR, and (b) uneven grain dispersal [137].

The data obtained from the experiment conducted on **Fig. 2.19.** indicates the existence of two distinct regions, each exhibiting contrasting characteristics. One region is identified by the presence of nanoparticles, while the other region lacks these particles. The region displaying nanoparticles that are uniformly dispersed (situated in below the figure) exhibits a notably heightened grain boundaries' density, predominantly composed of HAGB. Specified geographical area, mean diameter of the grains is recorded as 3.9µm. The area referred to as the PDR, situated in the upper section of the visual representation, displays a greater grain size, which is distinguished by an average measurement of 9.6µm and a larger grain size surpassing 20µm. **Fig. 2.19(a).** The provided micrographs illustrate the solidification zone of the coarse grain single pass specimen. The nanoparticle exihibit a

tendency to aggregate, leading to the formation of piles with varying dimensions. The dispersion of reinforcing oxides exhibits homogeneity, occurring consistently at both the interfaces between grain boundaries and within the interiors of the grains. The decision to employ multiple passes for the ultrafine-grained (UFG) sample was made due to the inadequate dispersion of nanoparticles observed in the coarse-grained (CG) sample after a single run of the fluidized bed spray granulation process. The attainment of uniform nanoparticle dispersion was not accomplished in a singular iteration, leading to the creation of aggregates between particles and the emergence of regions with inadequate dispersion as well as large agglomerates. As a result, the presence of agglomerated regions resulted in the manifestation of brittle fractures. **Fig. 2.19(b).** The provided images depict the electron backscatter diffraction (EBSD) maps that correspond to the two pass sample regions.

The size of the grains varies noticeably between different zones. The heat impacted zone (HAZ) showed a noticeable increase in grain size, with an average value of 11.4 m. High-angle grain boundaries (HAGBs) make up the majority of the grains in question, and these grains have a morphology that is almost equiaxial. Following the heat-affected zone (HAZ), there is an abrupt increase in the density of grain boundaries. The presence of nanoparticles in both the stir zone (SZ) and the thermo-mechanically affected zone (TMAZ) of this phenomenon is what caused the drop in grain size. In comparison to the heat-affected zone (HAZ), the average grain size in both zones was found to be smaller, measuring 4.5 m and 4.1 m, respectively. **Fig. 2.20(a, b).** the ultrafine-grained (UFG) 1FSP + Al2O3 sample is shown in transmission electron microscopy (TEM) pictures showing the thermo-mechanically impacted zone (TMAZ) and the surrounding unaffected zone (SZ).

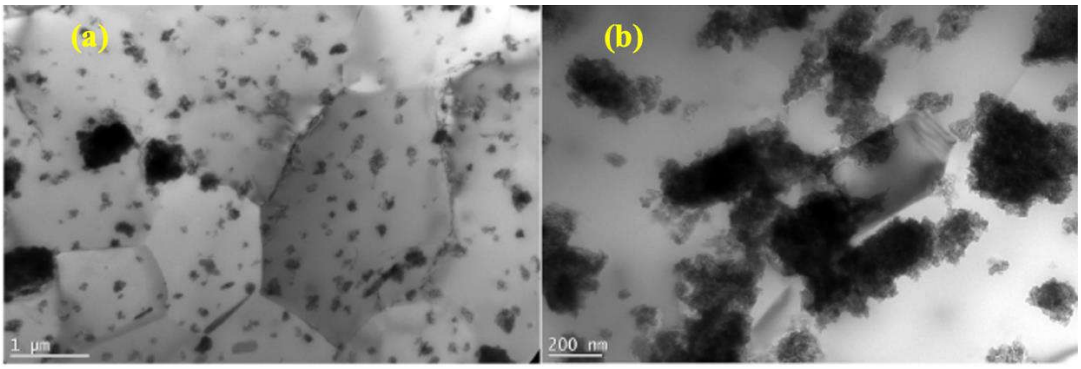

Fig. 2.20. (a) TEM micrographs of TMAZ of CG-2FSP + Al2O3 and (b) TEM micrographs of SZ of CG-2FSP + Al2O3 [137].

While the grains in the unaffected zone (SZ) have a mostly equiaxial shape, those in the thermo-mechanically impacted zone (TMAZ) have an extended morphology. Unevenly shaped particles that are randomly dispersed are present in both zones. The triple junctions, grain borders, and the interiors of the grains all include these particles. The key to obtaining the smaller size was the use of precise stirring parameters, which permissible for a even dispersal of reinforced particles and required multiple FSP passes. **Fig. 2.21** depicts the heat-affected zone (HAZ), the thermos-mechanically affected zone (TMAZ), and the unaffected base material (SZ) areas' electron backscatter diffraction (EBSD) patterns. The size of the grains varies significantly amongst the various zones.

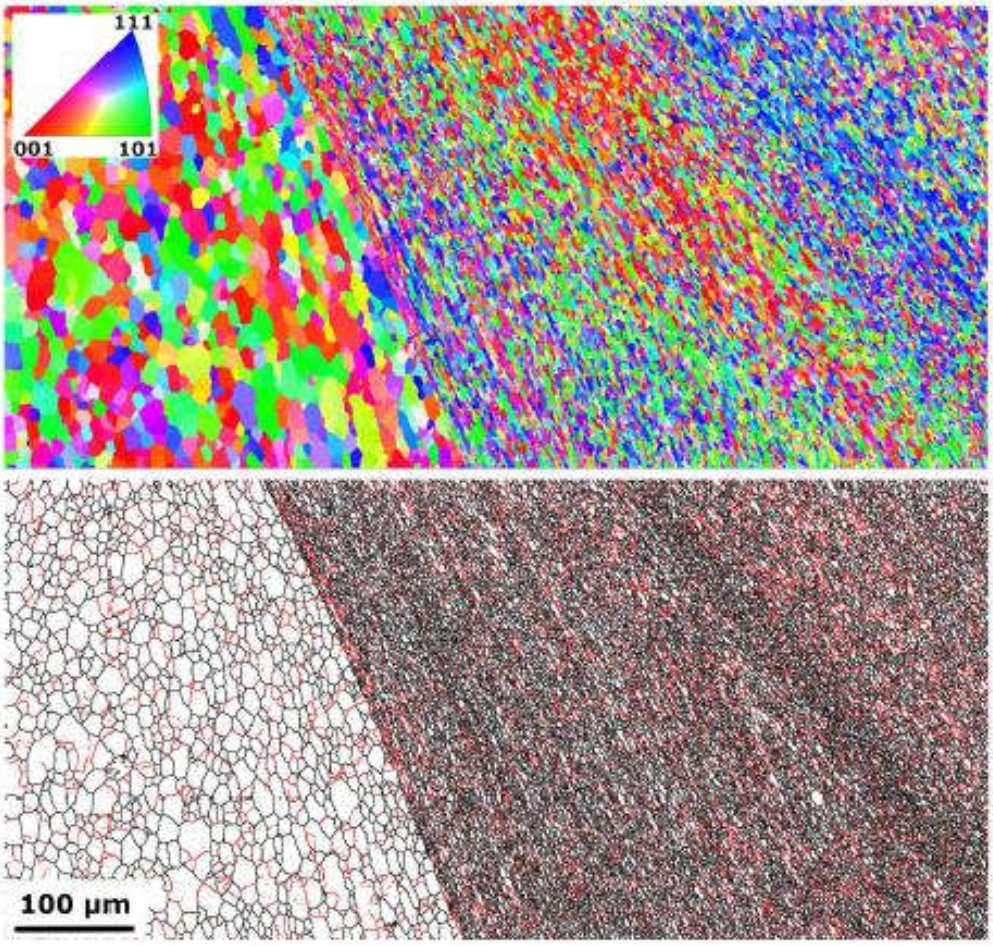

Fig. 2.21. UFG-2FSP + Al2O3 sample's OIM and grain boundary distribution map in the SZ, HAZ, and TMAZ are shown in [137].

The heat affected zone (HAZ) showed a considerable increase in grain size, with an mean value of 11.4 m. The grains themselves have a nearly equiaxial shape, although a sizeable

part of the grains have high-angle grain borders (HAGBs). According to the Hall-Petch effect, there is a noticeable rise in the density of grain boundaries. Both SZ and the thermos-mechanically impacted zone (TMAZ) include nanoparticles, which is the cause of the observed grain refinement. With values of 4.5 m and 4.1 m, respectively, the normal grain size in both areas is noticeably less than that found in the HAZ. **Fig. 2.22** shows the TMAZ and SZ of the TEM microstructure of the UFG-2FSP + Al2O3 sample.

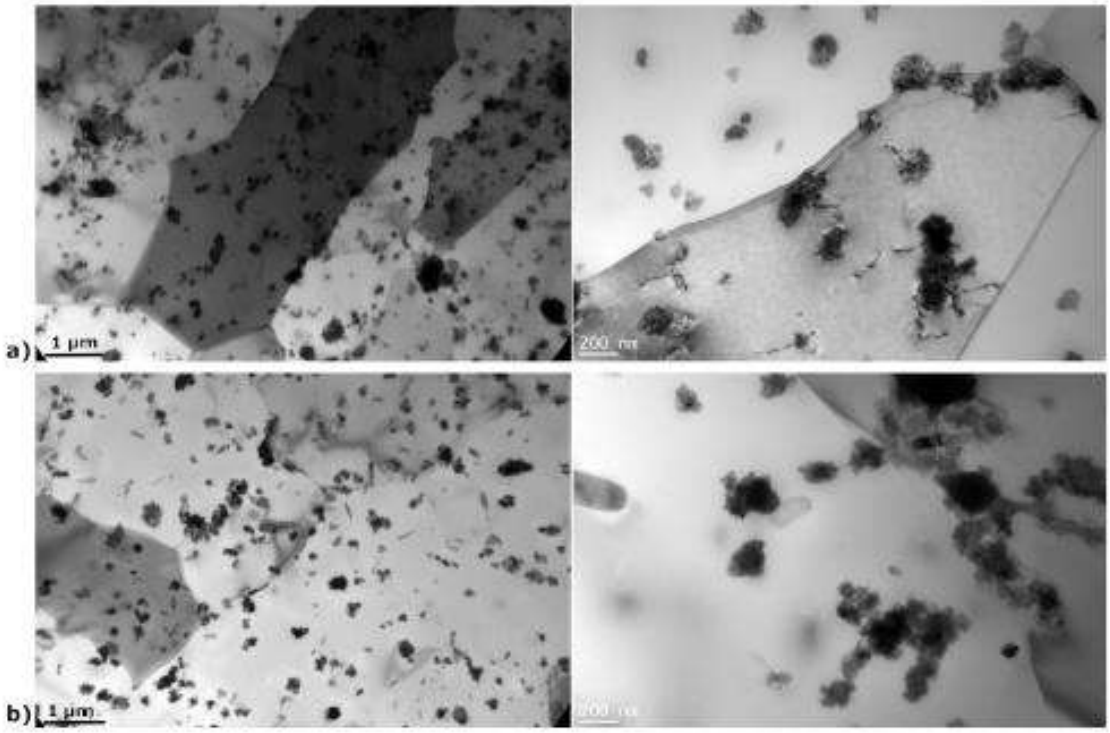

Fig. 2.22. TMAZ and SZ are examples of the TEM microstructure of the UFG-2FSP + Al_2O_3 sample, respectively [111].

UFG-2FSP (Ultrafine Grained-2 Friction Stir Processed) + Al2O3 sample, the TEM images of the TMAZ and SZ show that the grains in the TMAZ exhibit elongated morphology, but the grains in the SZ display approximately equiaxial shape. Within the grains as well as at the intersections of three grains and the boundaries between them, one can see randomly dispersed particles with uneven forms in both locations. Agglomerates in the SZ are typically about 170 nm in size, which is roughly 2.2 times larger than the typical diameter of nanoparticles. Additionally, the size of these agglomerates is less than the agglomerates seen in the CG-1FSP + Al2O3 sample. The particular FSP settings that were chosen are to blame for the mounds' small size. This has to do with the ability to distribute reinforcement

uniformly utilising just two FSP passes.The effect of inter-cavity spacing on the production of aluminium 5083 matrix composites (AMCs) reinforced with boron carbide (B_4C) and multi-walled carbon nanotubes (MWCNTs) was studied by Khan et al. (2013). It was found that composites with an inter-cavity spacing of 10 mm exhibit high tensile strength and hardness values. The effect of B_4C particle size on the characteristics of aluminium matrix composites (AMCs) was also investigated by the researchers. The researchers used the best FSP process parameters to add ceramic particles like TiC, SiC, B_4C, Al_2O_3, and WC to an Al 6082 matrix to improve its mechanical properties. According to reference [139], the TiC/Al 6082 composites demonstrated outstanding hardness and wear resistance. Al_2O_3 has a smaller size than other reinforcements like WC, SiC, B4C, and TiC, which results in comparatively lower levels of fracture and a stronger resistance to plastic deformation. In another work used the Flame Spray Pyrolysis method to disperse rice husk ash (RHA) in the AA6061 alloy at a volume fraction of 18%. The structural changes brought about by stirring were found to have raised the tensile strength of the 18 vol.% RHA composites to 285 MPa. **Table 2.5** summarises the research done on the use of FSP in the production of AMCs.

Table 2.5. The summary of studies on AMC fabrication using FSP.

S. No.	Matrix	Reinforcements	Process parameters	Findings	Ref.
1	Al 5052	GNPs	TRS-1250 rpm, TTA-3°, TTS-25 mm/minute.	Intense grain refinement.	[132]
2	Al 7075	B4C	Various TRS	Intense grain refinement.	[133]
3	Al6061	Graphite, Graphene, and CNT	TRS-1100 rpm, PD-1.2 mm and TTS-0.2 mm/minute	The number of FSP passes had an impact on the tribological properties.	[141]
4	Al5052	Silicon carbide (SiC)	TRS-1075 RPM, TTA-2.5 °, TTS-30 mm/minute	UTS, YS, and hardness showed an increase of 60%, 75%, and 140%, respectively.	[136]

5	AA7075	Silicon carbide (SiC)	Multiple passes	In double pass consistent dispersal of grain found	[142]
6	Al5083	MWCNT and B4C	Single pass FSP	There was a 20% rise in hardness and a 40% rise in tensile strength.	[138]
7	Al 7075	TiC	TRS-1000 rpm, TTS- 300 mm/min, AND PD-2.8 mm	Micro hardness value decreased.	[143]
8	Al 5083	Micro and nano B_4C	TRS-1000 rpm, AND TTS- 25 mm/min.	The homogeneous blending of nano B_4C led to a rise in both tensile strength and hardness.	[144]
9	Al5052	SiO_2 (nm size)	TRS-1200 rpm, TTS-20 mm/min	A uniform distribution of SiO_2 was attained.	[145]
10	Al	WC	TRS-1600 rpm, TTS- 60 mm/min, Axial force −10 kN, TTA-2°, PD-0.2mm	Composite materials were created that had finer grains and higher levels of hardness and strength.	[146]
11	Al 7075	TiC	TRS-1000 rpm, TTS 300 mm/min, PD-2.8 mm	Micro hardness value decreased.	[147]
12	Al 6082	TiC	1200/60 (TRS/TTS) Load-10 kN	Examined the effect on the wear characteristics	[148]
13	AA1100	E & S-glass fibers	1000/25 (TRS/TTS) TTA-3°	Improved mechanical characteristics.	[149]
14	Al 6061	RHA	TRS-1600 rpm, TTS-60 mm/minute, Load-10 kN	Improvement in UTS.	[140]

Figs. 2.23 and 2.26. Studies that were done between dates of **Figs. 2.23 and 2.26.** are graphical representations that show them.

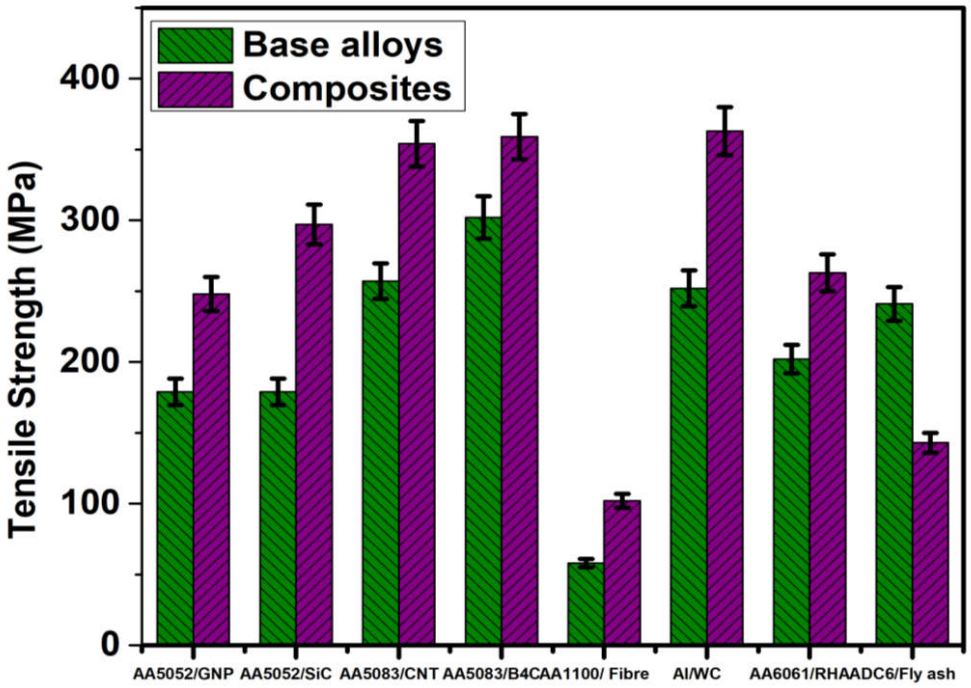

Fig. 2.23. Tensile strength of the AMCs created by FSP as well as the parent matrix [35].

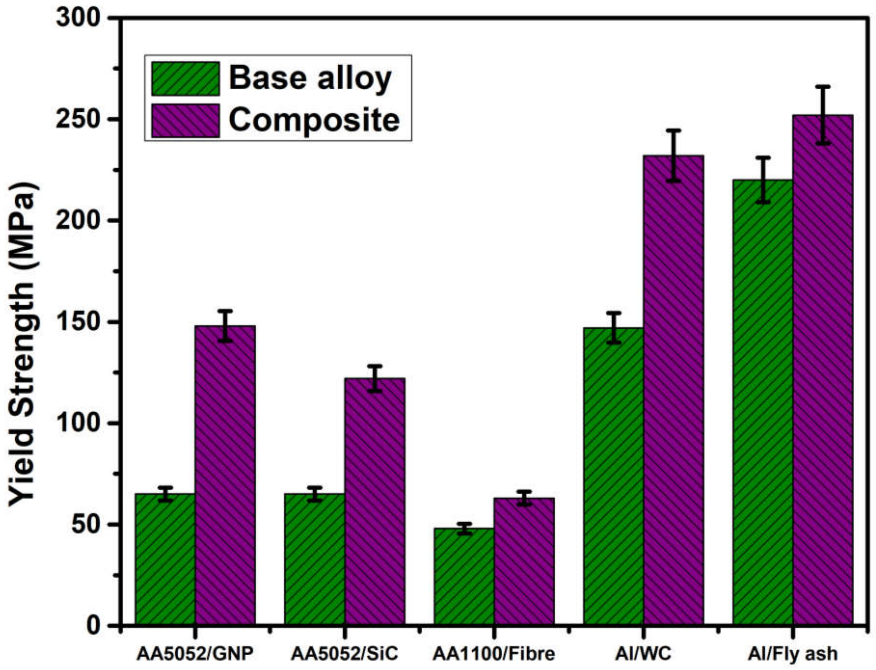

Fig. 2.24. The yield strength (YS) of the parent matrix and AMCs produced through FSP [35].

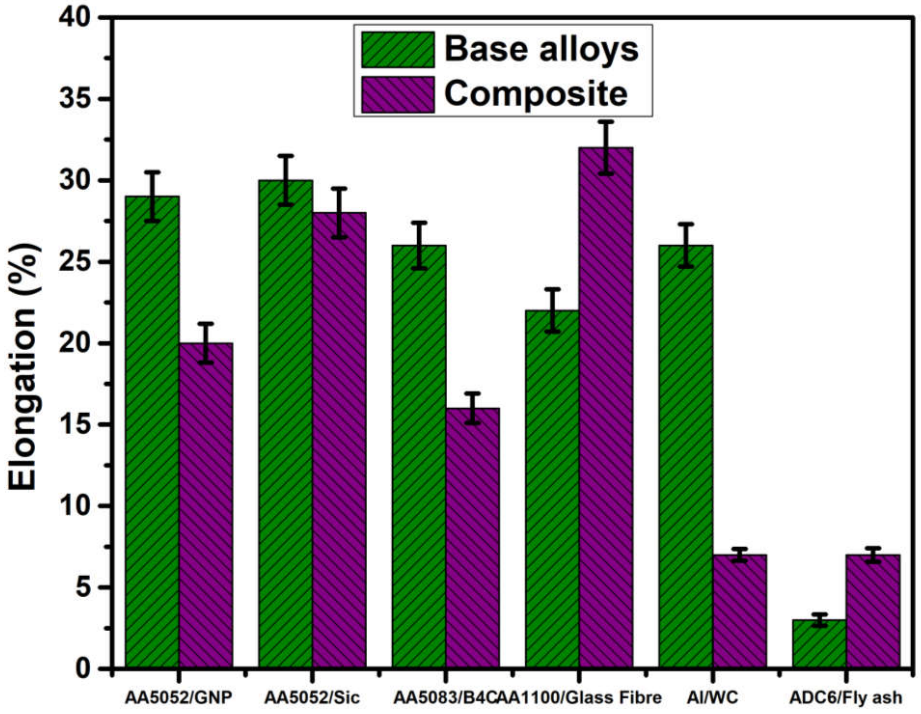

Fig. 2.25. The % elongation of the parent matrix and AMCs produced using FSP [35].

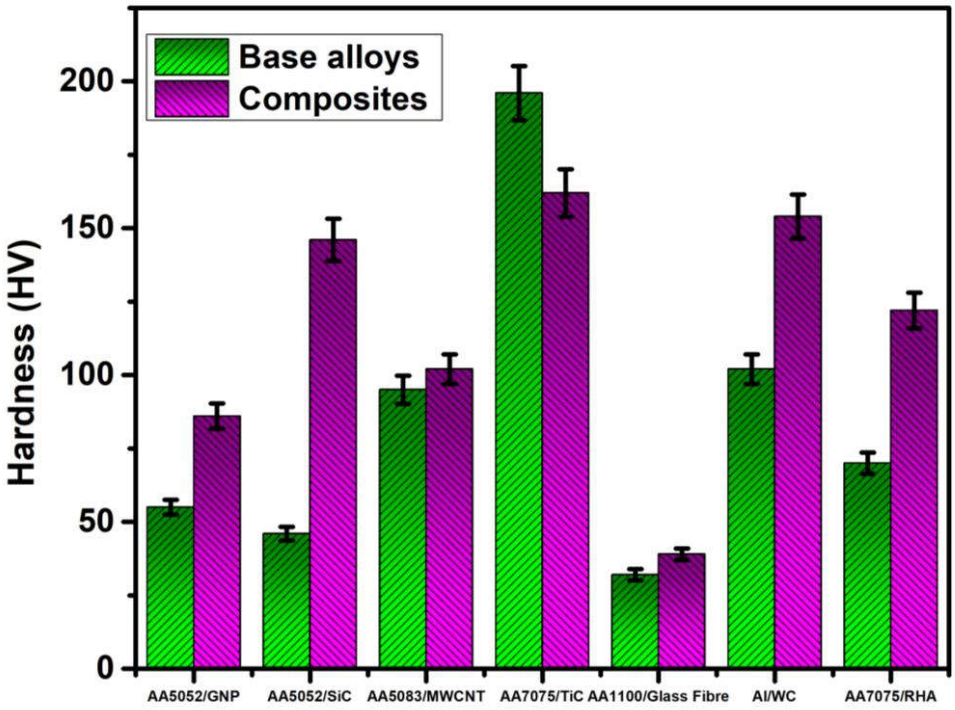

Fig. 2.26. The hardness of both the base matrix and AMCs produced through FSP [35].

The aforementioned study AMCs [146] demonstrates a decrease in the percentage elongation, as depicted in Fig. 2.23. As the weight percentage (WC) dose in the aluminium Al matrix increases, the observed effect is a corresponding change in the measured value of Fig. 2.23. The observed reduction in percentage elongation can be attributed to the initiation of cracks at processed lines, a decrease in strength, and the consequential impact on toughness. Based on the information presented in Fig. 2.26., According to the study conducted by [147], it was found that the TiC/Al 7075 composite exhibits the lowest level of hardness among all the analysed advanced metal matrix composites (AMCs), with a value of Fig. 2.23.The hardness of the produced composites was observed to decrease as a result of the stirring action of the FSP, which caused a modification in the initial condition of the base matrix, specifically T651. The WC/Al composites exhibited superior hardness due to the process of grain refinement and a decrease in dislocation density [146].

2.6.2.1 The effects of process parameters on AMCs produced through FSP

The final quality of the product is influenced by various components within the FSP. Previous studies have established that the quality of aluminium matrix composites (AMCs) is influenced by various factors, including the choice of reinforcing material, the technique employed for incorporating reinforcement into the samples, the parameters of FSP, the number of passes, and the FSP process method. In order to achieve improved manufacturing processes and maximise the efficient use of materials, it is imperative to establish a comprehensive understanding of the relationships between process variables and the structural properties of composites.

Influence of reinforcement composition

Hybrid aluminium matrix composites (HAMCs) have been established in recent times to enhance their overall properties. This is achieved by incorporating two or more distinct types of reinforcement particles into the aluminium matrix. Nazari et al. [150] employed graphene and T_iB_2 as hybrid reinforcements in order to fabricate hybrid aluminium matrix composites (AMCs) through the process of friction stir processing (FSP). The composite material consisting of 20wt. % T_iB_2 and 1wt. % graphene successfully addressed the trade-off between wear resistance and strength. In contrast to the uniform distribution of T_iB_2, which functions as the load-bearing component within the Aluminium matrix, the

incorporation of graphene as a lubricant during the friction process resulted in a reduction in friction between T_iB_2 particles. Additionally, this inclusion of graphene led to an enhancement in the wear resistance of the composite materials, as reported in a study [150]. In general, the research findings indicate that the hybrid composites exhibited superior characteristics compared to the mono composites, thus presenting a promising avenue for future investigation.

Influence of FSP parameters

The reinforcement dispersal and structural performance of the reinfored particles in the Al-matrix are determined by the FSP parameters, which significantly affect the material characteristics. These parameters include tool rotational speed (TRS), tool tilt angle (TTA), and plunge depth (PD). The TRS and TTA have a substantial impact on the reinforcement clustering and its distribution. In general, at higher TRS, the further vigorous stirring accomplishment leads to reduce the clustering size and also leads to even dispersal of particles in the metal matrix, which is crucial to producing AMCs with superior tribological and mechanical characteristics [151]. There is a crucial TRS where the distribution of reinforcing particles is better, as evidenced by a variety of aluminium alloys. Beyond a certain critical speed, a rise in temperature can reduce the resistance of reinforcing particles to the surrounding matrix, leading to softening of the matrix. This can help disperse the particles more uniformly and decrease the chances of them clumping together [152]. For various materials and welding situations, this critical speed varies [153].

- The TTS influences the amount of heat input, material mixing, and metallurgical bonding. High TTS can result in poor graphene dispersion, which affects the entire spectrum of composite properties. When Kalyanamanohar et al. [154] utilized FSP to manufacture a nanographene-reinforced 6060 Al surface composite, they noticed that faster welding speeds not only generated specific tunnel defects and voids, but also had a detrimental effect on the reinforcement dispersion in the treated region. Hence, the micro hardness levels of AMCs reduced. According to Lim et al. [155], higher plunging depth increased the homogeneity of nanotube dispersion in the Al-matrix. TTA effects the dispersion and homogeneity reinforcement of the metal matrix and facilitates the smooth movement of the tool during FSP [156]. The

impact of plunging depth and TTA on the structural characteristics of graphene-reinforced AMCs require further investigation.

Influence of multiple FSP passes

The mechanical and thermal impacts applied to the treated materials are significantly influenced by the FSP pass and route. Montazerian et al. [157] established a correlation between the number of FSP passes and the mechanical characteristics, graphene distribution, and structural integrity of Al-Cu-graphene composites. With an increase in the FSP passes, the graphene clusters gradually decreased in size, leading to a significant improvement in graphene dispersion. Consequently, augmenting the number of FSP passes has the potential to enhance the tensilee characteristics of the composites [157]. The strength of composites may be reduced by excessive FSP passes or even the destruction of reinforcement. Such as, Izadi et al. [158] demonstrated that the production of turbostratic and polyaromatic carbon structures together with Al_4C_3 during the three FSP passes damaged the tubular CNTs structure. When producing particle-reinforced matrix composites using various materials, FSP path defines the location of the tool pin axis in relation to the interface that has to be welded. Aluminum and copper alloys were dissimilarly welded with the inclusion of graphene by Jayabalakrishnan et al. [159] who also looked at how the welding route affected the weld characteristics.

2.6.2.2 Challenges and future developments of the FSP route

Future avenues for relevant research can be explored from multiple perspectives, including modifying the approach for incorporating bimodal reinforcements of nano and micro sizes, improving the parameters of Friction Stir Processing (FSP) such as tool tilt angle and plunging depth, utilising different types of tools, and adjusting the tool pattern. These endeavours aim to mitigate the constraints associated with surface processing and enhance the performance of processed materials. Despite some positive outcomes, the use of FSP in industrial settings continues to be restricted. Moreover, the application of FSP extends beyond its existing uses. The field of Functional Solid-State Physics (FSP) exhibits considerable promise in the development of functional materials characterised by improved properties. The realisation of this potential can be achieved through the integration of

Friction Stir Processing (FSP) with modern manufacturing techniques, including Friction Stir Additive Manufacturing (FSAM) and Ultrasonic-Assisted Friction Stir Processing (UAFSP). The aforementioned advancements, when combined with FSP, constitute notable accomplishments in the progress of innovative and contemporary engineering applications within the manufacturing industry. The utilisation of friction stir additive manufacturing has proven to be an effective method for the production of structural metals. Additionally, the application of ultrasonic-assisted friction stir processing has demonstrated the ability to increase the speed of friction stir processing without any adverse effects on the microstructure and properties of solid components. Moreover, the utilisation of FSP (Friction Stir Processing) as a technique for surface modification can be effectively employed in the process of mechanical alloying. The comprehensive understanding of the fundamental challenges related to this nascent technology, including the comprehension of material flow, remains incomplete. In order to attain commercial success in the field of FSP, it is imperative for researchers to delve deeper into these matters, thereby enhancing their comprehension of the intricate complexities associated with them. Prioritising comprehensive investigations of these issues is imperative prior to the industry's complete commercial adoption of this process. Further research is necessary to thoroughly examine the effects of bimodal reinforcements on the microstructures and characteristics of friction stir welded joints involving dissimilar metals. This investigation aims to broaden the potential applications of this welding technique.

2.6.3 Stir Casting

To achieve successful casting of MMCs, it is imperative to establish initial intimate contact and bonding between the ceramic phase and the molten alloy. The process involves either combining ceramic dispersoids with molten alloys or infusing molten alloys into preforms made of the ceramic phase under pressure, followed by whirling the resulting composite in melts is required to accomplish this [21, 160]. Due to the low wettability of the majority of ceramics, promoting intimate contact between the fibre and alloy often requires artificially boosting wettability or applying external forces to overcome the viscous drag and thermodynamic surface energy barrier. The most common mixing methods for introducing and uniformly distributing a discontinuous phase in a melt include:

- Adding particles to a forcefully stirred, completely or moderately molten alloy.
- Using injection cannon to inject the discontinuous phase into the melt.
- Dispersion of discontinuous phase pellets or briquettes.

In all the methods mentioned above, an external force is employed to introduce a non-wettable ceramic phase into a melt and create a homogeneous suspension of the ceramic within the melt. The uniformity of particle dispersion in the metal before solidification is influenced by the early clustering of particles in the loose powder stage and the kinetics of particle mobility in agitated liquids. The resulting melt-particle slurry can be cast using various techniques, including centrifugal casting, gravity casting, traditional foundry methods like pressure-die casting, as well as more modern approaches like melt spinning, spray code position, or squeeze casting (liquid forging). This is because the particles within the liquid metal move due to buoyancy as the metal solidifies, and they become enclosed within the solid structure through crystallization. The spatial organisation of ceramic particles inside the casting has significant importance as it directly influences the characteristics of the composite material that is produced [21]. The distribution of phases is influenced by the quality of the melt-particle slurry before casting, as well as the following additional variables:

- Particle and melt-specific gravities.
- The viscosity of solidifying.
- Particle size, shape, and volume percent.
- The particles' and matrix alloy's thermal characteristics.
- In addition to understanding the morphology and chemistry of crystallizing phases, it is also important to understand their interactions with particles. For example, during the solidification of a ceramic material, particles may become trapped within the growing solid. These particles can affect the final properties of the material, and so it is important to understand how they become trapped and how they affect the solidification process.
- Particle flocculation,
- The existence of any external pressures during primary phase solidification on ceramics, and particle trapping or forceful by solidifying surfaces.

The use of this processing method is widespread for advanced manufacturing composites due to its ability to facilitate mass production, provide superior control and handling, offer cost-effectiveness, and enable nearly net shaping [161, 162]. The process flow diagram in **Fig. 2.27** illustrates the key stages in this approach.

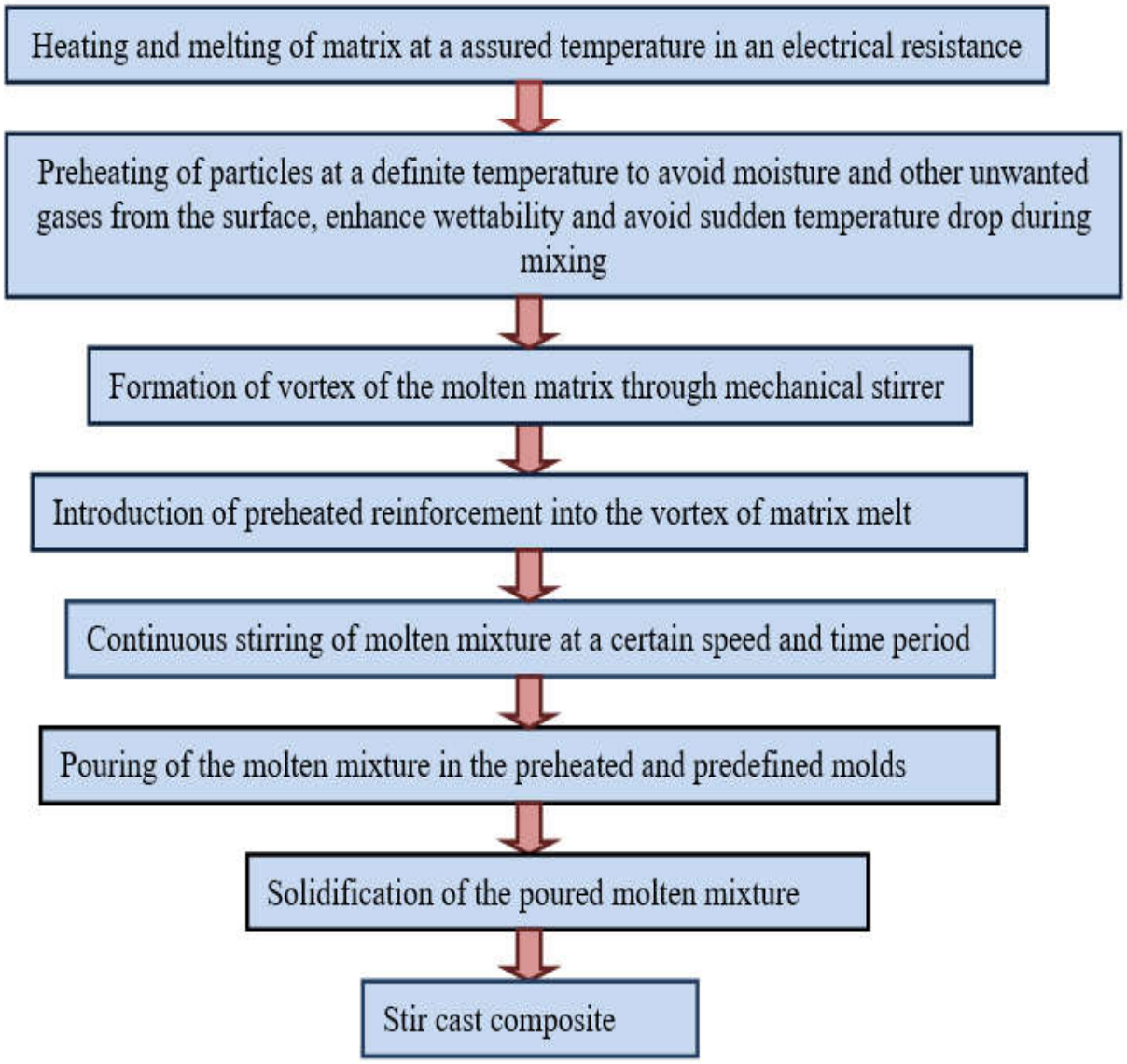

Fig. 2.27. Process flow diagram of key stages in stir casting technique.

Fig. 2.28 depicts the sketch diagram of a conventional stir casting setup. A melt of the matrix material is formed in this setup, and reinforcing phases are fed into it via a feeder in an electrical resistance furnace.

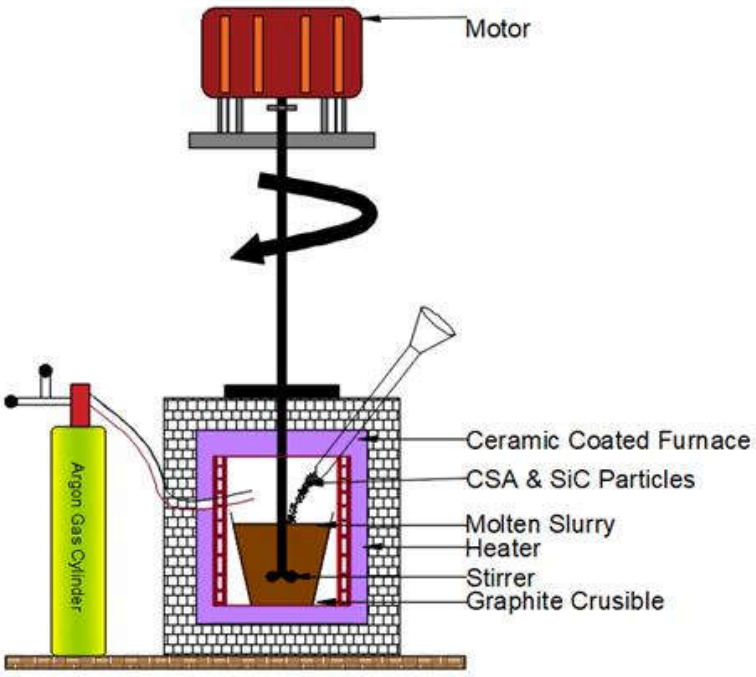

Fig. 2.28. Sketch diagram of stir casting set up.

In 1965, Badia and Rohatgi developed an Al/Graphite composite using gas injection and stir casting, and they found that it had better mechanical properties than a monolithic alloy [21]. SiC/Al composites were created using the stir casting by Rahman et al. [163]. AMCs' tensile strength and hardness increased as a result of the high SiC content. In a different study, simulation and numerical methods were used to forecast the mechanical properties of AMCs produced using the stir-casting process [164]. It was found that analytical and numerical modelling was probably used to examine the impacts of factors when combined and determine the best configuration. During stir casting, a zirconia-coated steel impeller has been utilized to stir the molten mixture of Al_2O_3 and Al 6061. AMCs that had been created had improved tensile, yield, and hardness properties up to a particular wt.% of Al_2O_3 [165]. Al/TiB_2 composite was developed by Tee et al. [166] using a stir-casting procedure in an argon environment. Metallurgical analyses of the Al matrix indicated evenly scattered particles. During the creation of AMCs, the impact of stirring speed was investigated [167]. According to a report, a constant stirrer speed should be used to manufacture cast composite with no defects. Another attempt involved the development of stir-cast TiC reinforced AA6061 composites [168]. The UTS were seen to rise at stirrer

speeds up to 300 rpm. Using a stir casting method, bamboo leaf ash (BLA) from left-over agricultural by-products have been reinforced in an Al-4.5%Cu [169]. The incorporation of bamboo leaf ash into the base matrix resulted in a notable improvement of 4% in both the tensile strength and hardness of the composite. The influence of SiC on the properties of SiC/Al 6061AMCs was studied in a study conducted by Moseset et al. [170]. The stir-casting process was employed to generate the AMCs. The ultimate tensile strength of the composite containing 15 wt.% SiC (silicon carbide) is improved by 65.2% in comparison to the base matrix. Additionally, the microhardness value of the composite is increased by 133.3%. It should be noted that these improvements were achieved without the use of any plagiarized content. Computational modelling and simulation were used to correlate the effects of several process factors, including the number of blades, stirring speed, etc., in the stir casting method [171]. To investigate the effects of this technique's parameters, a precise computer model was developed. Researchers investigated how the feeder design impacted the behavior of the resulting AMC [172]. The reinforcing particles were sprayed into the molten base metal using a feeder of the funnel design. The reinforcement particles are sprayed into the main matrix uniformly thanks to improved stirring and feeding mechanisms. Stir casting was used to generate AMCs with reinforcement made of Fly-ash (2, 4 and 6 wt.%). When the wear characteristics of produced composite specimens have been examined, it was discovered that AMCs with fly ash (6 wt. %) displayed reduced wear however AMCs with fly ash (4 wt. %) showed a low coefficient of friction [173]. A thorough analysis of pure Al and TiB_2 composites produced by stir casting revealed that stirring intensity and duration had a significant impact on agglomeration, inclusions, and oxidation [174]. SiCp addition caused a decrease in the length of the dendritic and an accelerated nucleation frequency. It was noted that the AMCs had increased tensile strength. Vacuum moulding-aided stir casting was utilized by Singh et al. to create SiC/Al 6063 composites. The process parameters were optimized, which improved the wear characteristics [175].

Squeeze operation is further used in combination with stir casting to obtain a better surface quality and reduced porosity. This technique offers a blend of the benefits of casting and forging. The resulting product has outstanding mechanical properties due to the combination of elevated pressure and fast cooling during the manufacturing process [176-

178]. Kannan et al. [179] used stir and squeeze casting to create SiC/Al7075 and SiC/Al2O3/Al7075 composites. The composites properties that were created were compared and deliberated. Squeeze casting was used to create Al6101/A356 bimetal [180]. The bimetal was heat treated, and the effect on mechanical characteristics was investigated. The metallurgical connection between two aluminium alloys was strong as a result of squeeze casting. The yield strength, UTS, and elastic modulus were all enhanced, while elongation was decreased compared to Al. Another effort used squeeze casting to strengthen carbon fibres in A413 alloy. Increased carbon fibre content results in increased porosity and decreased density [181]. The inclusion of short carbon fibres with a coating, in amounts of up to 3 weight percent, led to significant improvements in both hardness and ultimate tensile strength (UTS). Specifically, the coated fibres were found to enhance the hardness of the material by 60% and increase its UTS by 100%. Hashem et al. [182] examined the mechanical characteristics and microstructure of squeeze-cast Ni/Al-Si composites. Research studies have shown that composites comprising 2% alumina and 5% nickel have exhibited the highest UTS and ductility. Further enhance the mechanical properties of these composites, researchers created aluminium matrix composites (AMCs) reinforced with nickel-coated polyacrylonitrile-based carbon fibres [183]. As a consequence, the AMCs exhibited higher tensile strength. The enhancement in ultimate tensile strength (UTS) was ascribed to two factors: the improved ability of the reinforcement to bond with the molten aluminium and the safeguarding of fibres through chemical means. Another study utilized a thermomechanical simulator to replicate isothermal compression on composites made from SiCw/Al6061 through squeeze casting [184]. Yang et al. [185] created $Al_{18}B_4O_{33}$ (aluminium borate) whiskers reinforced Al2024 composites using the squeeze casting process. When compared to the base matrix, the composite's compressive yield strength increased by 47% at 623 K. There was no evidence of fibre agglomeration or strong fibre matrix bonding. Hardness of the composite of more than 50% as compared to the Al6061 matrix has been attained at 7.4 vol.% carbon fibre [186]. Jojith et al. [187] conducted metallographic analysis, hardness tests, and reciprocating wear tests on both untreated and T6 treated samples. The findings indicated that the use of the T6 treatment resulted in enhanced hardness and wear resistance of the composite material. Furthermore, the T6 treated sample exhibited a microstructure

characterised by a more homogeneous dispersion of particles, hence leading to enhanced characteristics. Overall, the study highlights the potential of T6 treatment to enhance the properties of Al_2O_3/Al7Si0.3Mg functional composite materials and provides valuable insights into the material's behavior and characteristics. The EBSD analysis showed that the morphology of the α-Al grain structure had been altered, while the TEM analysis revealed the presence of intermetallic iron and nano-sized β-Mg_2Si precipitates in the material. The indexed orientation code triangle was used to represent the crystallographic orientations of the Al matrix grains, which were individually coloured based on their orientation. **Fig. 2.29(a)** and **(b)** display the EBSD grain boundary maps of the untreated treated (UT) and heat treated (HT) composites, respectively. One of the most significant advantages of the grain refinement method for enhancing mechanical properties was strain fields with higher dislocations. The refined and equiaxed grains in the Al-matrix are perceived in **Fig. 2.29 (b)**, with grain sizes ranging from 0 to 110 µm.

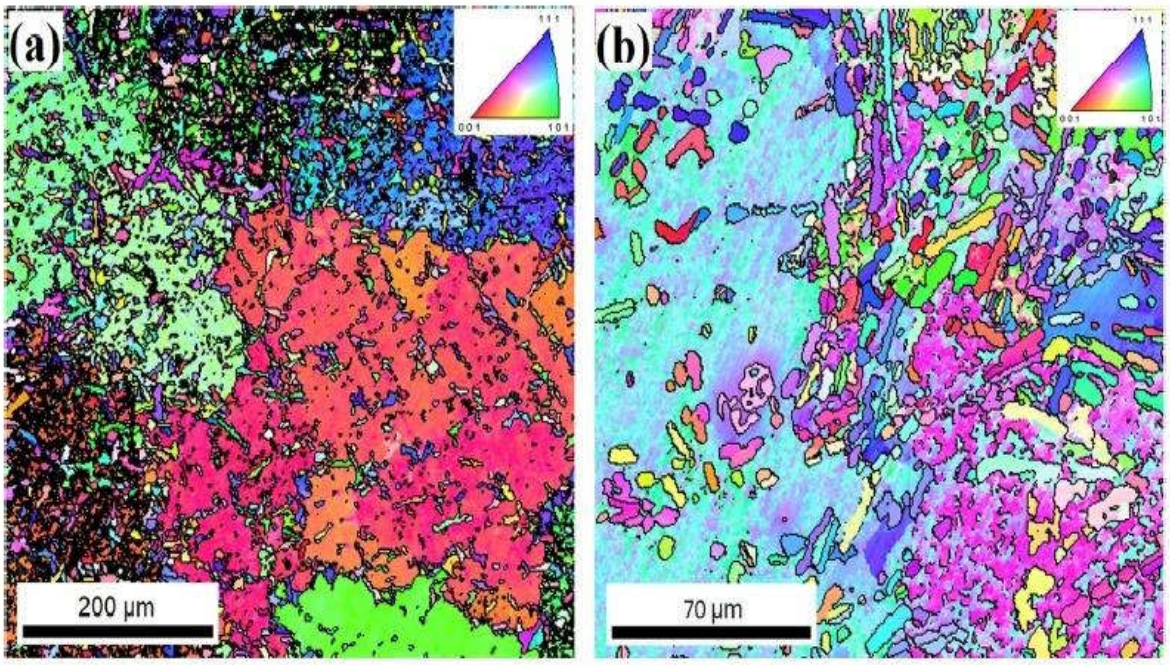

Fig. 2.29. Untreated and heat treated Al_2O_3/Al_7Si0.3Mg composite (in (a) and (b) respectively) outer layer EBSD investigation [187].

The outer layer of the 10 weight % Al_2O_3/$Al_7Si_{0.3}$Mg composite showed intermetallic phases, Mg_2Si precipitates, and dislocation lines that were confirmed by HRTEM images **Fig. 2.29**. The intermetallic phases α-Al, Si and $MgAl_2O_4$ are visible in bright-field TEM

picture **Fig. 2.30(a)**, and the appropriate SAED pattern is displayed in the inset as a striped pattern. The Mg_2Si intermetallic phase is shown in **Fig. 2.30(b)**, and neighbouring dislocation lines are indicated by red and blue arrows, respectively. The second phase and the intermetallic phases entangle with the dislocations, causing a effect of dislocation-pinning that reinforces the composite structure. In **Fig. 2.30(c)**, the dislocation lines are seen to become entangled with one another. The inset in the same figure, indicated by the blue arrow in the zoomed-in version of **Fig. 2.30(b)**, illustrates the needle-shaped Mg_2Si phase with its corresponding SAED pattern. The results of the unlubricated reciprocating wear experiment revealed that the wear resistance of both composites increased by 20-40% with an increase in reinforced particle content, nevertheless reduced with increment in wear parameters.

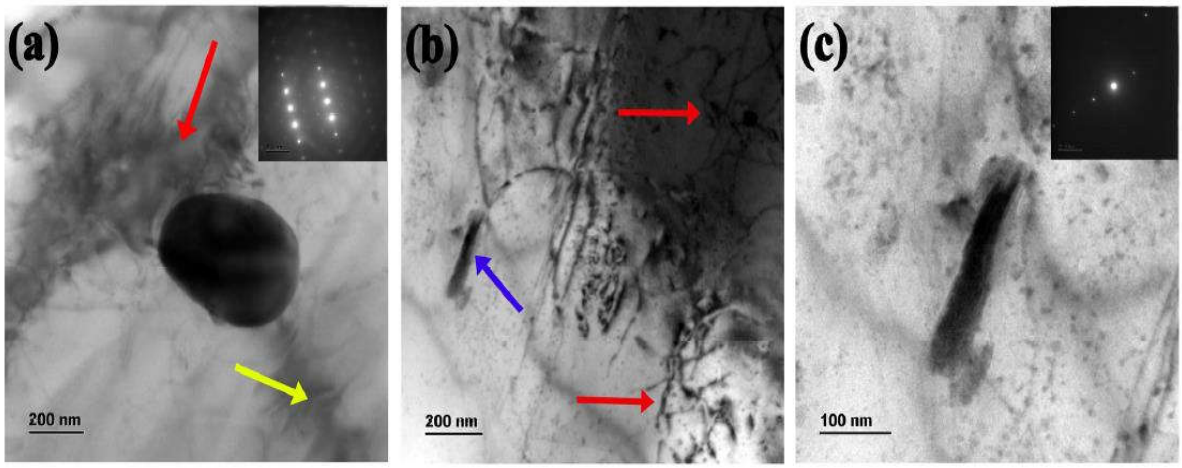

Fig. 2.30. HT Al_2O_3/Al7Si0.3Mg composite layer HR-TEM microstructure (a) Al(Mn, Fe)Si, (b) the dislocation lines (red arrow), and Mg_2Si IMC (blue arrow), and (c) Mg_2Si IMC [187].

In their study, Kumar et al. [188] employed a bottom-pouring kind stir-casting metod to fabricate a novel series of AMCs reinforced with varying weight fractions of ZrB_2 particles. The addition of ceramic particles has been shown to enhance the mechanical and corrosion properties of aluminum alloy. The material was subjected to several analyses, including corrosion potential, current, linear polarization resistance (LPR), the double layer capacitance, charge transfer resistance, and corrosion resistance evaluations.. It is imperative to ensure that the AAMCs are free from any form of plagiarism to maintain scientific integrity and avoid ethical concerns. The Tafel plots presented in **Fig. 2.31(a)**

demonstrate the effect of incorporating ZrB_2 particles on the corrosion resistance of AA7178 and its composites.

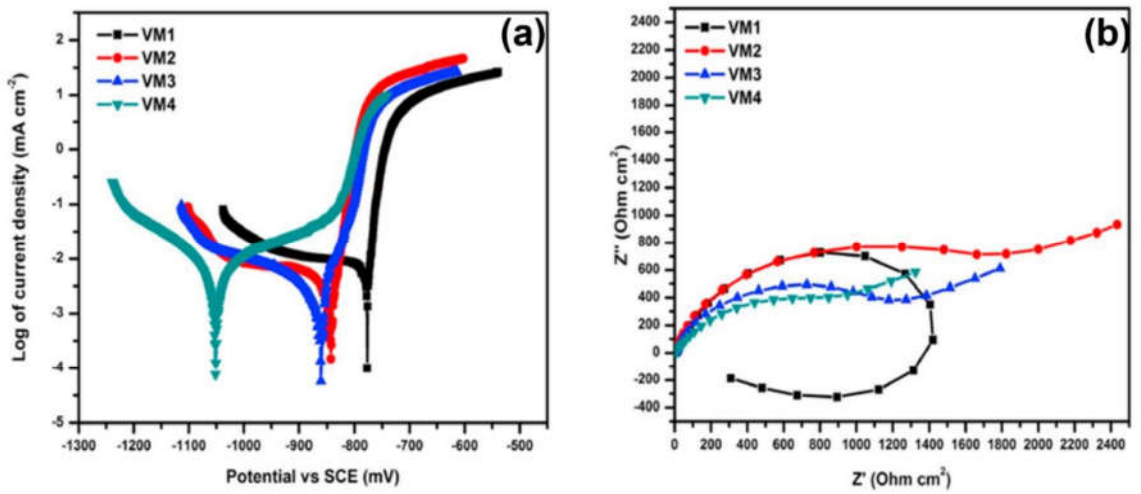

Fig. 2.31. (a) The potentiodynamic polarisation curve of the AA7178 alloy in a 3.5% NaCl solution with varied ZrB_2 weight percentages (b) A Nyquist plot of the Z′ vs. Z″ data obtained from electrochemical impedance spectrographs of the AA7178 alloy in 3.5% NaCl solution with varying ZrB_2 weight percentages [188].

The addition of ZrB_2 particles led to a decrease in potential and a reduction in current density, indicating an improvement in corrosion resistance. The electrochemical impedance spectrum has been used to further investigate the reaction of the corrosion mechanism of the composites. The Nyquist and Bode plots of the Al7178-ZrB_2 MMC after immersion in a 3.5% NaCl solution are depicted in **Fig. 2.31(b)** and **Fig. 2.32(b)**, respectively.

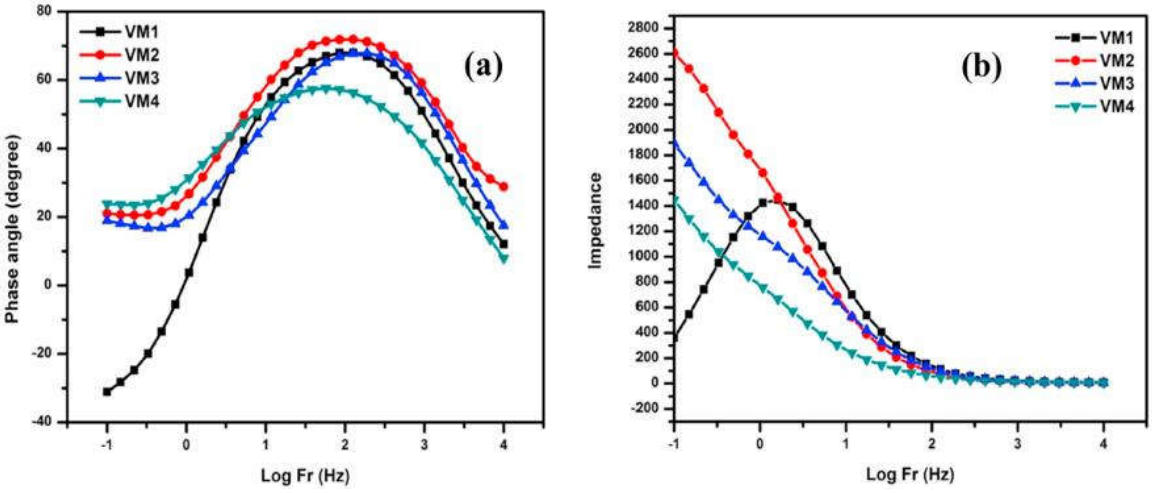

Fig. 2.32. (a) Logarithmic frequency vs. phase angle (degree) and (b) Logarithmic frequency vs. impedance Bode graphs of Al7178 matrix immersed in 3.5% sodium chloride solution [188].

The monolithic alloy exhibited an inductive loop in the impedance spectra, indicating resistance to charge transfer at low frequencies and surface depression on the electrode. The presence of capacitive half-circles in both the high and low-frequency ranges is a typical characteristic related with the aluminium oxide layer and electrolyte in the electrochemical impedance spectrum. The charge transfer resistance (Rct) increased, as observed in the polarization curves represented in Nyquist plots, confirming that incorporating 10% ZrB_2 into the composite improved corrosion resistance. This finding is consistent with the results obtained from polarization studies. According to the EIS results, an increase in charge transfer resistance (Rct) leads to the development of a protective layer on the metal's surface, while the capacitance of the double layer (Cdl) decreases.

Bembalge and Panigrahi [189] have developed bulk ultrafine grained (UFG) AA6063/4 wt.% SiC composite sheets using a unique hybrid technique that combines stir casting and cryo-severe plastic deformation. The composite sheets have varying sizes of SiC reinforcement, including 1 μm, 12 μm, and 45 nm.

In UFG (Ultrafine-grained) composites that have been included with fine, coarse, and nano-sized silicon carbide particles, the use of cryo rolling and the size of the silicon carbide particles has led to a notable microstructural refinement, with a size less than 350 nm in all ultrafine-grained composites. This refinement has resulted in the accumulation of a high density of dislocations, which has, in turn, led to significant improvements in tensile strength. Specifically, the tensile strength of the composites has increased by 88%, 108%, and 141% depending on the size of the SiC particles, in contrast to the base alloy without reinforcement. **Fig. 2.33** depicts the results of the TEM examination of cryo rolled samples that were done to investigate the microstructural changes. The TEM picture of the cryo rolled parent alloy reveals the microstructure exhibited in **Fig. 2.33(a)** reveals excessive dislocation density and dislocation cell structures highlighted by yellow arrows, while **Fig. 2.33(b)** displays a limited number of clearly established ultrafine grains with a mean grain size of 500 ± 20 nm. The matrix-particle interface zone has a pool of dislocations in the cry rolled coarse composite's TEM images **(Fig. 2.33c**), and there are UFG grains present that are not near the SiC particles **(Fig. 2.33d)**. In the matrix region of the cryo rolled fine grain composite, an evident polygonal cell structure is displayed adjacent to the fine silicon carbide particle depicted in **Fig. 2.33(e)** ,as denoted by a yellow arrow, alongside the

presence of ultrafine grains (UFG) (Fig. 2.33f). Conversely, in the scenario of the cryo rolled nanocomposite, fine cell structure is apparent, accompanied by grains at the nanoscale **(Fig. 2.33g and h)**.

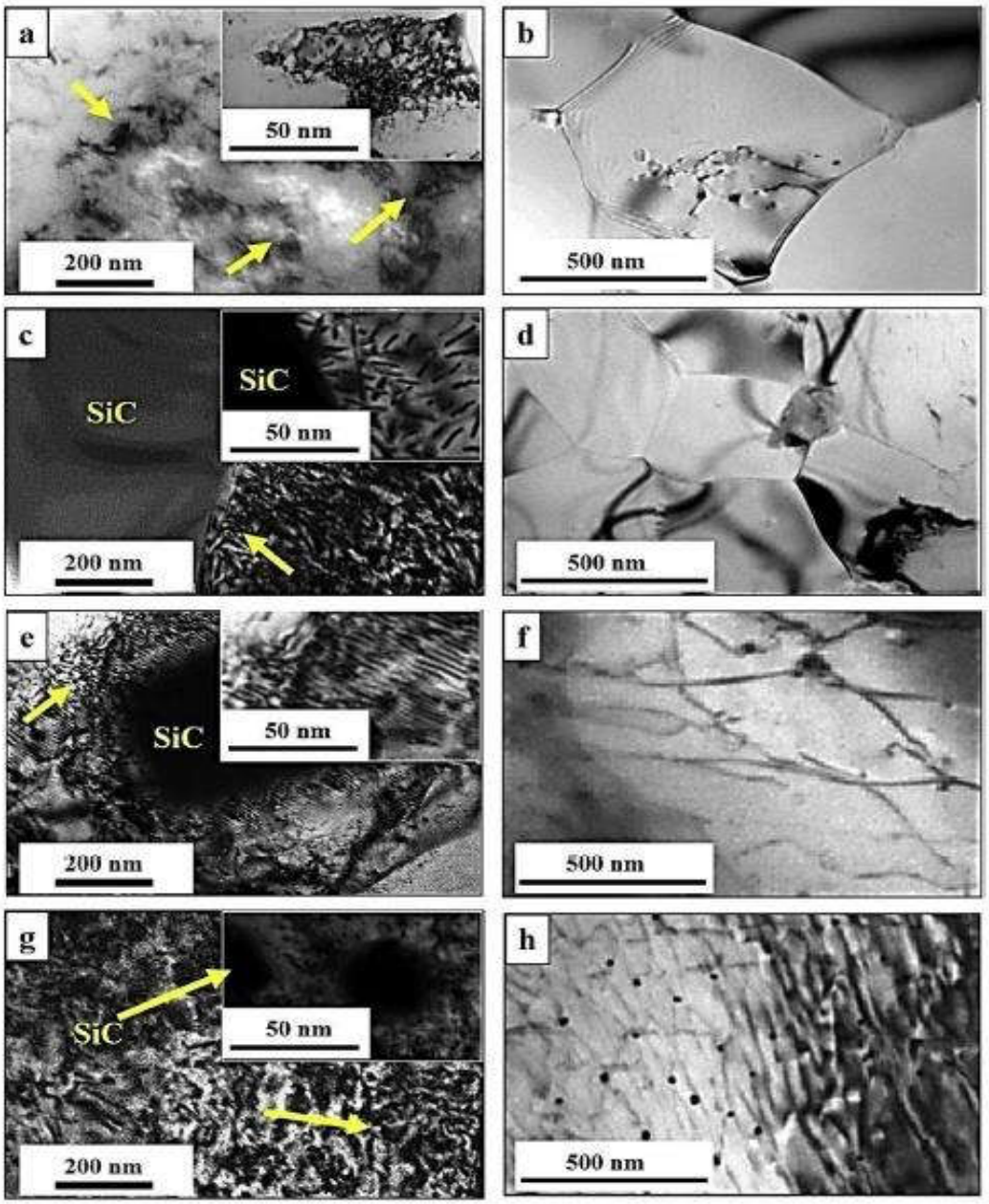

Fig. 2.33. The cell architectures (depicted by yellow arrows) and growth of ultrafine-grained (UFG) in the aluminium matrix are seen in TEM microstructure (a) and (b). SiC particles and the matrix interface in (c) and (d) show a buildup of dislocations and UFG in the composite specimen. In the matrix area distant from the silicon carbide particles in the fine composite, images (e-f) depict the dislocation cell structure around silicon carbide particles. In the UFG regime of the nanocomposite, (g) and (h) show significantly displaced cell architectures and grains [189].

Sambathkumar et al. [190] conducted research to assess the corrosion and mechanical characteristics of AA7075 hybrid composites containing varying volume fractions (0-15%) of TiC and SiC. The researchers employed a two-stage stir-casting process and implemented in pursuit of this objective. The melting process was executed within a furnace equipped with the fire-resisting motor and a speed regulator. The composite produced showed superior hardness and tensile strength compared to the parent metal. In another study by Radhika and Charan [191], a two-step stir-casting process was employed to fabricate LM 25 with 10% TiC particles. When an ideal 10% reinforcement is employed, particles are uniformly dispersed. Kumar et al. [192] used two stage casting to investigate nano alumina and micro coconut shell ash reinforced AA7075 HMMC and reported considerable improvements in mechanical properties. Pazhouhanfar and Eghbali [193] used a stir casting furnace to create an Al6061-3, 6, 7% TiB_2 composite and investigated its mechanical properties as well as microstructural characterization. The results of tensile tests indicated that the inclusion of 9 wt. % TiB_2 reinforcement particles in the composites led to a substantial enhancement in their ultimate tensile strength, which reached 257 MPa. This value represents an increase of 29.2% compared to the strength of the base alloy. In a similar study, Srivastava et al. [194] employed ultrasonic solidification to fabricate Al6061 alloy composites reinforced with 1% nano Al_2O_3 at different temperatures. The production process is illustrated in **Fig. 2.34** and involves the use of an ultrasonic unit, electric resistance furnace, controlled argon atmosphere and thermocouple. The results demonstrated that ultrasonic treatment resulted in outstanding reinforcing distribution in composite specimens. Meanwhile, because to the high melt viscosity, several particle agglomerates are observed in the composite.

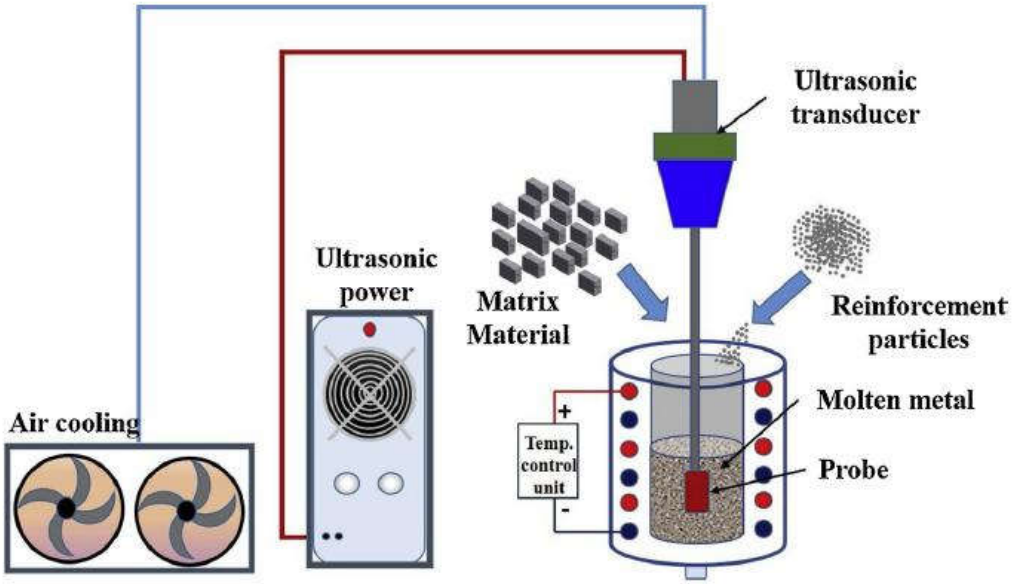

Fig. 2.34. Ultrasonic assisted stir casting setup schematic diagram [9].

Kumar et al. [195] focus on the preparation and characterization of a hybrid nano-composite material. The material is made up of AA7075 aluminium alloy, Al_2O_3 nanoparticles, and coconut shell ash (CSA) using ultrasonic-assisted stir casting. The study investigates the effects of varying amounts of CSA and Al_2O_3 nanoparticles on the mechanical and microstructural properties of the resulting hybrid nano-composite. The samples' microstructural examination revealed that the aluminium oxide and CSA atoms were evenly dispersed throughout the matrix. Additionally, the study found that the addition of CSA and Al_2O_3 nanoparticles enhanced the mechanical properties of the hybrid nano-composite, including hardness, tensile strength, and wear resistance. Overall, the study concludes that the AA7075/Al2O3/CSA hybrid nano-composite prepared through ultrasonic-assisted stir casting shows great potential for use in high-strength applications, such as the aerospace and automotive industries [195]. The literature on the production of AMCs by stir casting is included in **Table 2.6**. The various AMCs fabricated by reinforcing Al2O3, SiC and B_4C are listed in **Table 2.7, Table 2.8, and Table 2.9**, respectively.

Table 2.6. This summary provides an overview of fabrication of AMC (aluminum matrix composites) through stir casting.

S. No.	Monolithic alloys	Reinforced particles	Optimum parameters	Outcomes	Ref.
1	Aluminium	SiC	Speed-(450-550 rpm), Time-15 minutes.	Increased hardness	[162]
2	AA6061	TiB_2	Speed-350 rpm, Time-15 minute.	Enhanced tensile strength	[193]
3	AA6061	TiC	Speed-300 rpm, Time-15 minute, Blade angle-30°	Increased UTS	[168]
4	AA6061	Al_2O_3	Speed-200 rpm, Time-10 minute.	Improved hardness tensile, and yield strength	[165]
5	Al-4.5 wt. %Cu	Bamboo leaf ash	Speed-600 rpm, Time-10 minute.	Improved hardness	[169]
6	AA6063	SiC	Speed-500 rpm, Time-10 minute.	Enhanced tribological characteristics	[175]
7	A356	SiC	Speed-600 rpm, Time -7 minute.	The compressive and tensile strength of composites containing (1.5 wt%) nano SiC is higher.	[196]
8	LM6	SiC	Speed-600 rpm, Time- 10 minute	Hardness and elongation were improved by 31 and 34 % correspondingly	[172]
9	Al	TiB_2	Speed-60, 180 and 300 rpm, Time-60 minute.	The SR-CT characterization technique has verified that the particulates are evenly spread out.	[174]
10	$AlSi_{12}$	Al_2O_3	Squeeze Pressure 100 Mpa	Enhanced thermal conductivity, fracture toughness and hardness.	[112]
11	Al	Fly ash	Speed-100 rpm	Wear resistance improved.	[173]
12	A1060	Diamond particles	Squeeze pressure	Bending strength and thermal conductivity have been increased by 124% and 89% respectively.	[197]
13	Al	MWCNT	Squeeze Pressure (100 MPa)	Pore free distribution of reinforcement	[198]

Table 2.7. Characteristics of Al_2O_3-reinforced AMMCs.

S. No.	Matrix	Reinforcements	Weight fraction (%)	Casting method	Particle size	Porosity (%)	Hardness	Ultimate strength (MPa)	Ref.
1	AA2024	Al_2O_3	10, 20 and 30	Stir casting (SC)	66, 32 and 16, µm	5	135BHN	112(T)	[70]
2	AA356	Al_2O_3	1 to 7.5	SC	20µm	6	75BHN	450(C)	[79]
3	A356	Al_2O_3	1 to 4	SC	50nm	2	72BHN	630 (C)	[79]
4	Al–Cu alloy	Al_2O_3	1.5	SC	50nm	2	92HV	240 (C)	[199]
5	A356	Al_2O_3	1.5	SC	20nm	3.4	120BHN	265 (T)	[200]
6	AA2024	Al_2O_3	5	SC	50µm	8.4	82HV	224 (T)	[201]
7	A356	Al_2O_3	2.5	SC	50nm	–	96HR	182 (T)	[202]
8	AA2024	Al_2O_3	1	SC	65nm	Low	–	215 (T)	[203]
9	AA6061	Al_2O_3	20	SC	36µm	–	38BHN	–	[204]
10	A356	Al_2O_3	1	Stir + squeeze casting (SSC)	30	–	70HRB	220 (C)	[205]
11	A356	Al_2O_3	1.5	SC	20nm	2.7	–	190 (C) Yield	[206]
12	AA7075	Al_2O_3	6	SC	20µm	–	120HV	290 (T)	[207]

S. No.	Matrix	Reinforcements	Weight fraction (%)	Casting method	Particle size	Porosity (%)	Hardness	Ultimate strength (MPa)	Ref.
13	A206	Al_2O_3	5	SC	10μm	8	–	220(T)	[208]
14	A206	Al_2O_3	5	SC	100nm	12.2	–	270(T)	[208]
15	AA7075	Al_2O_3	1.2	SC	50nm	4.3	160HV	400 (T), 760 (C)	[209]
16	AA6061	Al_2O_3	2	SSC	–	Less	74HB	193 (T), 316 (C)	[210]

Table 2.8. Characteristics of AMMCs developed by incorporating SiC.

S. No.	Matrix	Reinforcements	Weight Fraction (%)	Casting technique	Particle size	Porosity (%)	Hardness	UTS (MPa)	Ref.
1	Al2024	SiC	5	SC	18μm	11.5	74HV	192(T)	[201]
2	Al7075	SiC	20	SC	36μm	–	50HB	–	[204]
3	Al6061	SiC	6	SC	20μm	–	90HV	160(T)	[211]
4	Al356	SiC	10	SSC	10μm	4	66HB	195(T)	[212]
5	Al356	SiC	10	SSC	40μm	–	89HB	245(T)	[213]
6	AA356	SiC	20	SSC	12.6μm	–	–	178(T)	[214]
7	AlSi7Mg2	SiC	15	SSC	23μm	10.5	98HB	165(T)	[215]
8	Al-Si alloy	SiC	3.5	SC	50nm	1.6	78HB	280(T)	[216]
9	A356	SiC	15	SC	–	Low	95HV	206(T)	[217]
10	AA6061	SiC	30	SSC	16μm	Low	84HB	200(T)	[218]
11	AA6061	SiC	6	SC	20μm	–	98HV	270 (T)	[219]

S. No.	Matrix	Reinforcements	Weight Fraction (%)	Casting technique	Particle size	Porosity (%)	Hardness	UTS (MPa)	Ref.
12	AA7075	SiC	6	SC	150μm	Low	118HB	269 (T)	[219]
13	Al-Mg-Mn alloy	SiC	5	SC	–	Low	63.6HB	–	[220]
14	AA356	SiC	10	SC	7μm, 33μm	–	141HB, 134 HB	430(T), 380 (T)	[221]
15	AlMg4.5Mn	SiC	10	SC	35μm	2	77HB	348(C)	[222]
16	Al	SiC	10	SC	40μm	High	67HB	205(T)	[223]
17	Al6061	SiC	15	SC	35μm	–	82HV	265(T)	[224]
18	Al356	SiC	3.5	SC	50nm	–	–	280(T), 292 (C)	[225]

Table 2.9. Characteristics of AMMCs developed by incorporating B_4C.

S. No.	Matrix	Reinforcements	Weight fraction (%)	Casting technique	Particle size	Porosity (%)	Hardness	UTS (MPa)	Ref.
1	Al	B_4C	8	SC	70μm	–	50HV	140(T)	[226]
2	Al	B_4C	8	SC	80nm	–	54HV	155(T)	[226]
3	A356	B_4C	10	SC	20μm	–	74BHN	265(T)	[227]
4	A356	B_4C	10	Squeeze casting	20μm	2	68BHN	270(T)	[227]
5	A356	B_4C	10	SC	1μm	1.8	77BHN	142(Y)	[227]
6	AA6061	B_4C	15	SC	60μm	–	80VHN	260(T)	[228]
7	AA2024	B_4C	30	Squeeze casting	33μm	3	120BHN	115(T)	[229]
8	AA2024	B_4C	20	SC	20μm	–	210BHN	305(T), 340	[229]
9	Al	B_4C	10	Squeeze casting	30μm	–	51HV	132(T)	[230]
10	Al	B_4C	15	SC		1.8	77BHN	210(T)	[230]
11	AA6061	B_4C	15	SC	30μm	–	97VHN	270(T)	[231]
12	A356	B_4C	15	Squeeze casting	10–21μm	2.6	69BHN	135(Y)	[232]
13	A356	B_4C	12.5	Squeeze casting	20μm	–	75BHN	–	[233]

Plots depict the comparative tensile strength **Fig. 2.35**, % elongation **Fig. 2.36**, Vickers's hardness **Fig. 2.37** and Brinell hardness **Fig. 2.38** of basic matrix and processed AMCs. TiB_2/AA6061 composites have demonstrated the maximum tensile strength out of all the experiments taken into consideration [163, 165, 169, 170, 172, 193]. For AMCs with SiC as reinforcement and LM6 (Al-Si) as the basis matrix, the largest percentage elongation is observed **Fig. 2.36**. The lowest tensile strength of AMCs was attributed to SiC clustering in the Al matrix **Fig. 2.35**.

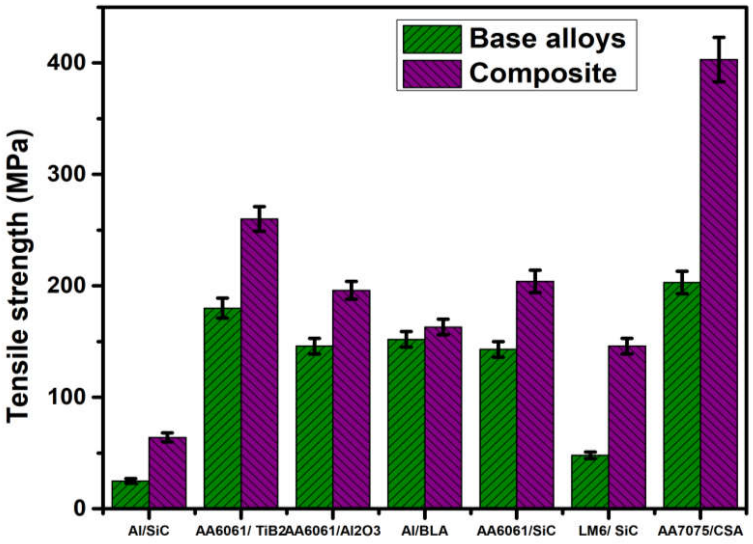

Fig. 2.35. Evaluation of the parent metal's and the AMCs' tensile strength after stir casting [35].

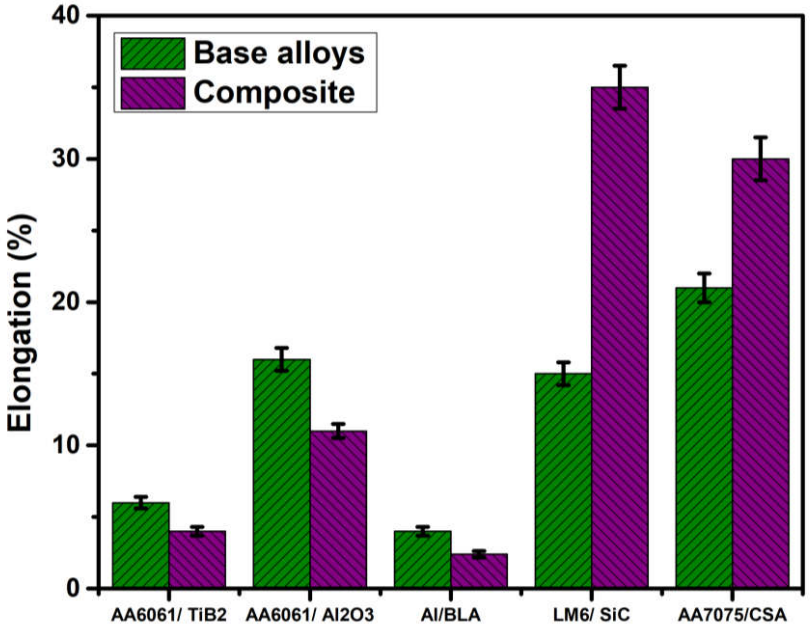

Fig. 2.36. Elongation in percent of the parent metal and AMCs after stir casting [35].

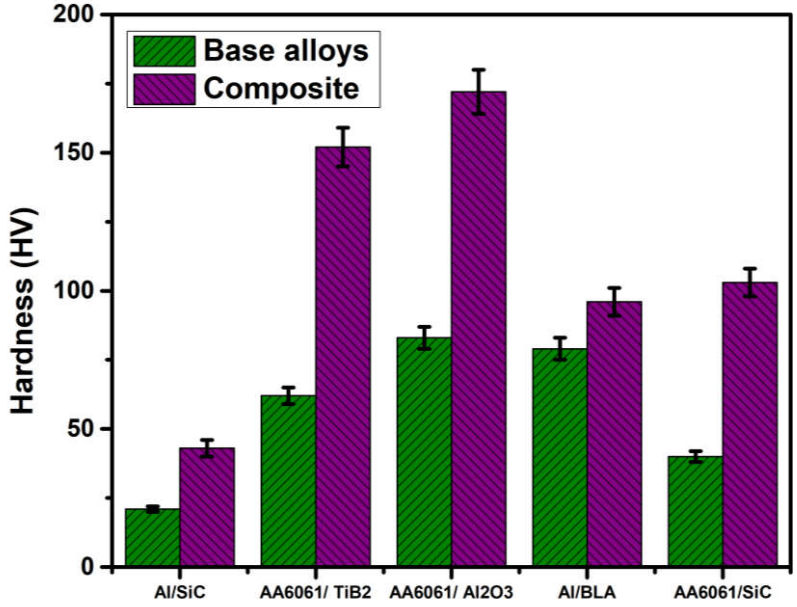

Fig. 2.37. Parent metal hardness and AMCs produced by stir casting [35].

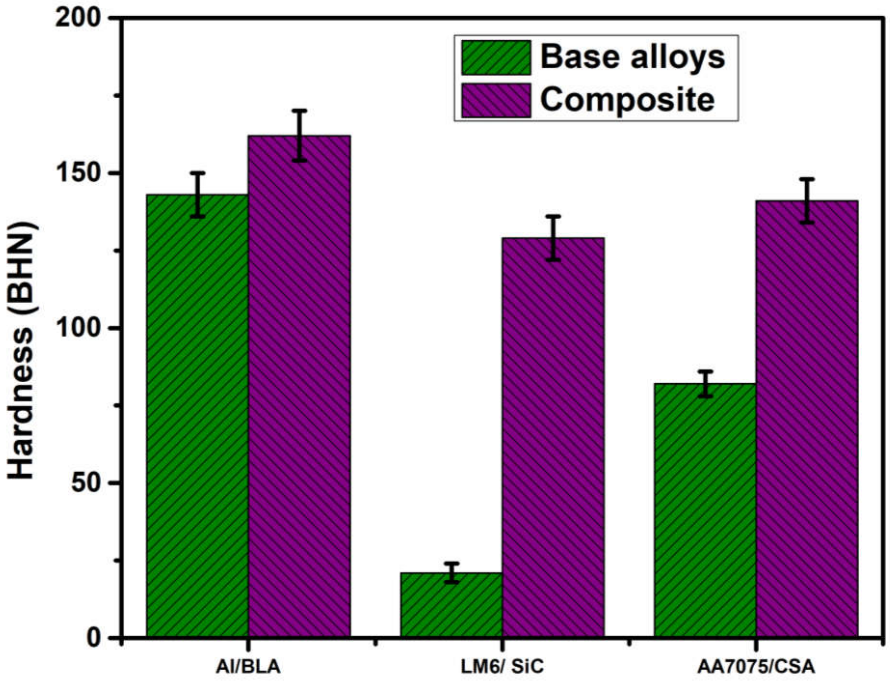

Fig. 2.38. Hardness of parent metal and AMCs processed by stir casting [35].

On the other hand, TiB_2/AA6061 composites achieved the maximum tensile strength. This rise was attributed to the Hall-Petch outcome, the Orowan strengthening process, and an increase in dislocation density. Clusters or agglomerations of reinforcement particles have been eliminated as a result of the better SiC feeding arrangement in the molten Al matrix. For SiC/LM6 composites, uniform SiC dispersion has eventually contributed to the highest percentage elongation **Fig. 2.36**. In comparison to AA6061 matrix, the inclusion of stiffer and harder Al2O3 has reduced the AMCs surface indentation and enhanced composite hardness **Fig. 2.37**.

2.6.3.1 Squeeze and stir casting process parameters prompting the mechanical behaviour of AMMCs

Numerous scholars have conducted investigations into the manufacturing of composites through the utilisation of squeeze casting. However, there exists a dearth of research specifically dedicated to the optimisation of parameters in the context of stir casting assisted with squeeze casting. The objective of this study is to develop composites and recognize the optimal parameters for improving the tribological, mechanical and corrosion properties of aluminium, thereby facilitating its utilisation in numerous applications. The

assessment of four tiers of parameters facilitated the identification of a particular amalgamation of input parameters that would augment the desired output, encompassing wear, hardness, ultimate tensile strength, and porosity of the prepared composites. Extensive research was conducted on these parameters.

- **Reinforcement size:** In the stir casting method, particle size has significance on the material's strength. The mechanical qualities improve with decreasing size.
- **Stirring speed:** The way in which reinforcement particles are spread throughout the matrix is precise by the molten aluminum's viscosity, which has to strike a balance between being too high and causing too much obstacle for movement of particles during stirring, and being too low and failing to suspend and carry the particles. By accelerating, the distance between particles grows. It is challenging to give a precise numerical number for the stirring speed since it relies on the profile of the stirrer blade.
- **Stirring time:** To enhance the mechanical characteristics, the particle dispersion should be homogenous. A longer stirring period results in an even dispersal and good separation of the reinforcement particles. It might not be advisable to be too specific because the stirring time also depends on the blade profile (shape).
- **Squeeze pressure:** It has the utmost impact on how to raise the standard MMCs. It enhances the interfacial and wettability bonding of the reinforcement and matrix. By reducing gas bubble nucleation, the squeezing pressure lowers the percentage of porosity [234]. Additionally, the heat loss via dies accelerates cooling.
- **Melt temperature:** Although the wetting capability of the melt is improved by the high melt temperature, the viscosity of the melt is decreased, which may not be desired. When the melting temperature is low, the particle agglomeration occurs. Therefore, it is necessary to keep the melt at a suitable temperature.
- **Die preheating temperature:** This is also one of the most important parameters that has the potential to affect MMCs' characteristics. The size and form factor of the main Al particles in $AlSi_9Mg$ generated by the semisolid squeeze casting technique increases as the die temperature rises. The mechanical characteristics went up as a result, however at 300 °C, the form factor abruptly drops, leading to worse mechanical properties [235]. When the die temperature is too low, problems

with cold shut defects arise that have a negative impact on the mechanical qualities. The working environment is impacted and die life is decreased by excessive die temperature.

- **Stirrer blade design:** To prevent the interaction between stainless steel and Al alloys at higher temperatures, stirrer blades made of stainless steel are often coated with zirconia. To produce the vortex and accomplish the appropriate melting of the melt, the impeller/blade design is crucial.

2.6.3.2 Techniques to optimize the process parameters

These are various parameters for the stir casting method which are optimized using a variety of optimization techniques. The most well-known ones include multi objective, regression, and Taguchi approaches, as well as grey relational analysis. Analysis of variance (ANOVA), Taguchi method, genetic algorithm, swarm optimizer, and finite element approach are some examples of statistical techniques. A mathematical model was created by Vijian and Arunachalam [236] utilizing multiple variable linear regression analysis. The desired functions of the evolutionary algorithm are determined through the utilisation of the weighted sum method, which is based on the outcomes derived from the regression analysis. A genetic algorithm is employed as a tool to enhance the mechanical characterstics of hybrid composites. Senthil and Amirtha gadeswaran [237] performed experiments to optimise parameters in the squeeze casting technique using the Taguchi methodology. The validation test revealed that the created composites had enhanced mechanical characteristics. Regression analysis was used by Goyal et al. [238] to create a mathematical model and forecast the ideal procedure parameters. By means of ANOVA, the optimal parameter settings resulted in enhanced mechanical characteristics. Su et al. [239] used the finite element approach to examine the current behavior of particles throughout the process of mixing in the crucible and looked into factors including rotating speed, blade angle, impeller diameter, and stirrer shape. The author further recommended a parameter setting to achieve a consistent dispersion throughout the stir casting process.

2.6.3.3 Challenges and future developments of stir casting route

Although stir casting is a fairly common method for MMCs, it has some drawbacks that make production difficult. Based on an analysis of the literature and production experience with AMMCs, the subsequent statements review the difficulties encountered during the AMMCs production:

- Even with micron-sized reinforcement particles, uniform distribution is a significant problem that has a variety of effects, notably on the mechanical characteristics of MMCs. To achieve an even dispersion of the reinforcing particles, variables such the melt's viscosity, the stirrer's speed, the duration of the stir, and the particle size must be controlled. Due to the fact that the particles may either settle or float, a non-uniform dispersion can also be brought on by the matrix's and the reinforcement's different densities. Nano-sized reinforcements are not only pricey, but also pose a risk of agglomeration and need careful handling. One of the biggest factors preventing MMCs from being used commercially to the level that researchers had hoped is due to the dispersion of reinforcement particles.
- Wettability is an essential factor that impacts the grain bonding between the matrix and the reinforcement constituent part, and therefore the mechanical characteristics of the MMCs.
- Additional significant problem in the manufacture of MMCs is porosity, which has a significant impact on strength. The porosity in the cast product can be reduced in a variety of methods, as was addressed in the previous part and advised in the later section.
- Throughout the manufacturing of MMCs reinforced with Al_2O_3, SiC, or any other hard microparticles, erosion of stainless-steel stirrer blade. At 300 °C, a high-temperature lubricant was manually added to prevent the stirrer's metal from eroding and to keep the molten aluminium from adhering to the stirrer. Blade replacement on a regular basis would be difficult, especially in large production where it would slow down output and raise costs for consumables. Additionally, the material from the eroding stirrer blade may end up in the MMC and affect its characteristics.

- Another issue that has to be handled by the experts in the future of furnaces is reinforcement mixing rate, as most designs do not permit a constant rate of mixing.
- A problem with reinforcement is that it could interact with the matrix material and create undesired phases.

2.7. Recommendations

The review's novelty lies in the evaluation of several manufacturing techniques, which revealed that the stir casting method is cost-effective for mass production. According to the assessment, bimodal reinforcement (nano and micro size) is the best combination. The following suggestions are provided in light of the difficulties already covered.

2.7.1 Recommended matrix and reinforcement materials

Although recommending is completely arbitrary, it is feasible to do so generally if the AMMCs are used. Al7075 (ISO designation: AlZn5.5MgCu) is the best alloy for high strength applications may vary from 280-570 MPa reliant of the heat treatment condition. The strength of the MMC is additional increased by the addition of reinforcement. Both LM6 and LM25 have great corrosion resistance and outstanding fluidity, making it simpler to cast them into complex shapes. Contrary to Al alloys, there is a far wider choice of reinforcements available, however broad suggestions may be given based on how the MMC will be used. As was previously mentioned in the Introduction section, the majority of reinforcements are inorganic ceramic phases. Due to their higher hardness (applications requiring wear resistance) and specific strength, the carbide and oxide-based materials, specifically SiC and Al2O3, respectively, in micron size, are used the most commonly among these. Recently, it has been shown that Al matrix with nano size reinforcement has higher mechanical and tribological characteristics; nevertheless, it has also been shown that there are certain drawbacks, such as wettability and reinforcing cost. Therefore, a better approach to address these drawbacks is a bimodal (nano and micro size) combination. Graphite and WS_2 are advised for applications that require self-lubrication. MMC manufacture utilizing scrap aluminium as the matrix and suitable industrial waste byproducts (including agricultural waste) as the reinforcing material is still a vast topic that has potential for considerable independent research.

2.7.2 Suggested stir-squeeze parameters for the production of AMMCs

Fig. 2.39 provides the suggested parameter range for squeeze casting. These suggestions are based on the findings of the study presented in this section.

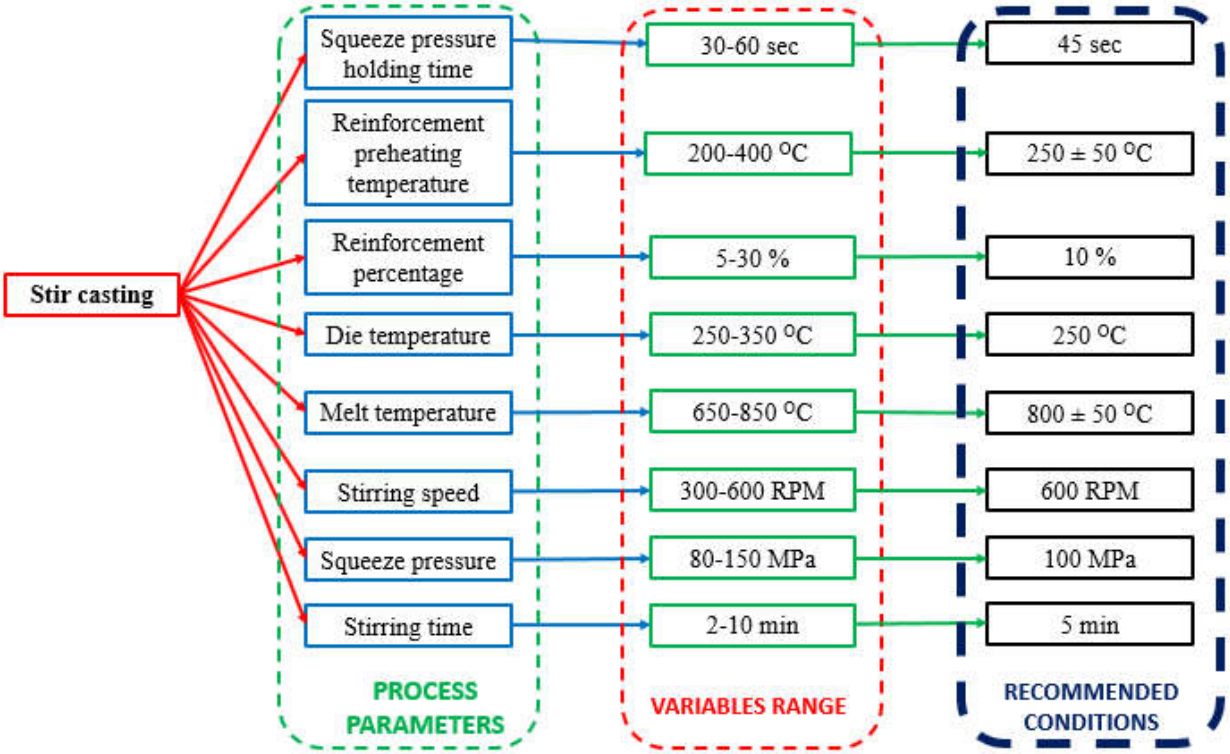

Fig. 2.39. Suggested process parameters for stir-squeeze casing method [27].

The parameter that has the greatest influencing power among all others is squeezing pressure. The majority of earlier studies indicated that a squeezing pressure of 100 MPa is appropriate for refining grains and reducing porosities. No extensive impacts were noticed over 100 MPa squeezing pressure [240].

The most important aspect for affecting the improvement of the product's qualities was found to be the squeeze pressure holding time. Therefore, it was advised to utilize a holding period of between 30 and 45 seconds since, after that, the rate of heat dissipation remained unaffected [237]. The suggested melt temperature for aluminium alloys for the squeeze casting process is 700 °C; however, when the melting temperature was lowered from 780-680 °C, gradually the macrostructures got finer [241]. The melt temperature needs to be higher than 600 °C to ensure efficient penetration of reinforcement. According to reports, the tensile production of the aluminium alloy (AlSi9Mg strength)'s and elongation when the

preheating via semi-solid squeeze casting [242]. The die's temperature is increased from 200°C to 250°C, however no discernible difference was seen between 250-300°C. At 350°C, the elongation and tensile strength abruptly reduced, and the microstructure contained many rosette particles [235]. To get a consistent mixture, the stirring time should be longer than 5 and less than 10 minutes. More than 10 minutes causes particle agglomeration, which lowers the composites' mechanical characteristics [243]. However, as stated previously, this is subjective because the vortex intensity is influenced by the stirrer's profile. Since it prevents direct contact with molten metal and the resulting problem of blade deterioration, therefore electromagnetic stirring is preferable. If an electromagnetic stirrer is unable to fit, the blades may be given strong coatings to stop erosive wear and need less frequent stirrer replacement. The surface of the reinforcement is cleaned of impurities, particularly gases that have been adsorbed, and the wetting is improved by preheating it before adding it to the melt [244]. In addition, moisture is removed. For the majority of reinforcing particles, preheating at a temperature of 250–300°C is recommended.

2.7.3 Suggested additives and wetting agent

Grain refiners are the best additive since they may significantly enhance the MMCs' strength with little work or energy required. When related to alternative methods of degassing the melt, adding tablets is the most convenient way to do it. Although it is not required, flux might be put into molten metal to aid in the removal of slag. The slag, which often floats at the top after the metal melts and before addition of reinforcement, might be detached by means of a scoop whereas wearing the appropriate particular protecting equipment. In order to reduce porosity BORAX can be used with reinforcement at 1:2 ratios when it is in powder form. The aluminium composite's tensile and yield strengths improved [245].

The reinforcement particles can be modified through the inclusion of alloying elements, applying coatings to them, subjecting them to heat treatment, or using ultrasonic cleaning techniques, and ultrasonic vibration are a few methods for enhancing wetting. The simplest method is to heat treat the reinforcing particles and alloy them. Magnesium is an effective surfactant that has been used to encourage wetting [246]. The interfacial bonding between

the reinforcement and matrix should be improved by 1 to 2%. The mechanical properties of metal matrix composites (MMCs) experience a decline when the magnesium (Mg) content surpasses 2% as a result of the formation of low melting constituents. [246]. While adding magnesium to the melt, appropriate safety measures should be implemented. The findings indicate that incorporating mono-synthesized particles into composite plates can enhance their tensile strength (by 13.9%), impact resistance (by 26.98%), and hardness (by 21.9%). Specifically, the AA6061/Al2TiO5 plate shows moderate improvements in these properties due to the inclusion of mono-synthesized oxide reinforcement particles [280]. Ultrasonic vibration can also be employed to promote wetting if the furnace has an ultrasonic stirrer setup. Even while coating the reinforcement constituent part with a wettable metal can improve wetting, doing so rises processing time and expense, particularly if the MMCs' MMCs are coated using a sophisticated and costly technique [247].

2.8. Current applications of AMMCs

Table 2.10 provides a list of the various AMMCs' present uses. This table makes it abundantly clear that AMMCs are of economic importance and that additional research into AMMC applications is essential. Research on hybrid AMMCs and those utilizing nanoscale reinforcements is ongoing, and several studies are constantly being published by researchers all over the world. As a result, the next generation of AMMCs will be hybrid composites with superior qualities.

Table 2.10. Several applications of AMMC's

S. No.	Matrix	Reinforcement	Application	Company	Ref.
1	Al	SiC	Disc brakes for high-speed trains	Temponik	[248]
2	Al	SiC	Pistons	Ztotecki	[249]
3	AA2009	SiC	Fan exit guide vanes, F-16 ventral fin sand fuel Access covers	DWA	[250]
4	AA6091/ AA6092	SiC	Electronic packing		

5	Al	SiC	Heatsinks, display equipment, semiconductor inspection parts	Ferro Tec	[251]
6	Al	Al_2O_3	Equipment for display device		
7	Al/Nextel610/45f		Pushrods	3M	[251]
8	Al	Al_2O_3	Cylinders leaves in engines, brake pad backing plates, piston-recess walls, bearings, brake discs	Ceram Tec	[252]
9	AA2024/ AA6061	SiC	Helicopter components, satellite structures, wheels, piston pins outlet guide vanes, hydraulic blocks fixed wing structure, pistons, cylinder liners pushrods, train chassis components of the rain, optical sensors	Materion	[253]
10	AA2024	Al_2O_3	Heat sink, turbo impeller, stator vane, and piston head	Elementum3D	[254]
11	Al	Al_2O_3/ B_4C	connecting rods, armour, brake rotors, optical housings, and pistons	MCubed Technologies	[255]
12	Al	Al_2O_3(nano)	Connecting rods, piston, and aeronautical armour	Gamma alloys	[256]

The possible uses of AMMCs in numerous sectors are depicted using a tree diagram in **Fig. 2.40**. The roots show the crucial elements that have an impact on those applications.

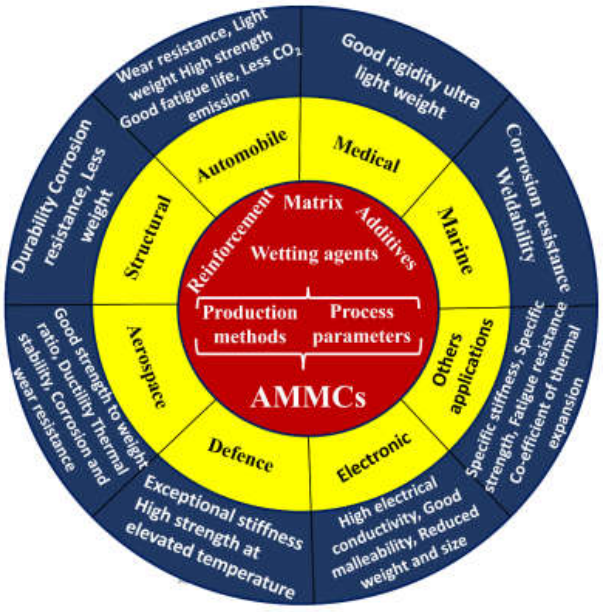

Fig. 2.40. The utilization of AMMCs in different sectors [27].

2.9. Research openings in the development of MMCS

As highlighted earlier, the production of Metal Matrix Composites (MMCs) presents numerous challenges. The characteristics of MMCs manufactured through diverse casting techniques exhibit significant variations, making the selection of an appropriate method for a specific application a complex task. Achieving optimal process parameters and conditions is essential for the manufacturing of diverse MMC compositions, and this necessitates a thorough optimization process. The existing or published literature proves insufficient in establishing comprehensive process parameters, particularly for a wide range of matrix and reinforcement materials, encompassing both traditional and recently introduced nanomaterials. Given that any casting process inherently introduces some degree of porosity, it becomes imperative to thoroughly address methods aimed at minimizing porosity, warranting adequate consideration in MMC production processes.

Another factor that significantly affects the mechanical characteristics is the even dispersal of the reinforcing particles. Similar to this, the bonding which is regulated by the wettability, has a substantial influence on the mechanical properties [257]. Except for Hashim et al. [246] and Razzaq et al. [257], there isn't much study on wettability. The

significance of recycling materials has grown in importance as society increasingly emphasizes the adoption of environmentally friendly practices; however, this aspect has unfortunately been somewhat overlooked, as noted in recent studies [258, 259]. Despite the limited attention, there remains substantial potential for conducting specialized research in the utilization of waste, scrap, and discarded materials for both the matrix and reinforcement components in the creation of Metal Matrix Composites (MMCs). This field offers ample opportunities for exploration and innovation in sustainable materials science. [259-280].

CHAPTER 3

EXPERIMENTAL PROCEDURE

Utilising a comprehensive examination of existing scholarly works, we employed a two-step stir casting methodology to fabricate an innovative hybrid composite material. This composite material consisted of AA7075 as the matrix, with Al2O3 and coconut shell ash serving as the reinforcing agents. Two distinct sets of hybrid composites, namely AA7075/Al2O3np/CSA and AA7075/Al2O3mp/CSA (as depicted in **Fig. 3.1(a-b).**), were fabricated using the stir casting method. Various characterization techniques were employed to assess the microstructure, mechanical properties, and wear behaviours of the developed composites. The experimental methodology has been explicated in the following sections. The composite material being examined in this study is AA7075, which is reinforced with Al2O3 particles. This composite is commonly known as CSA.

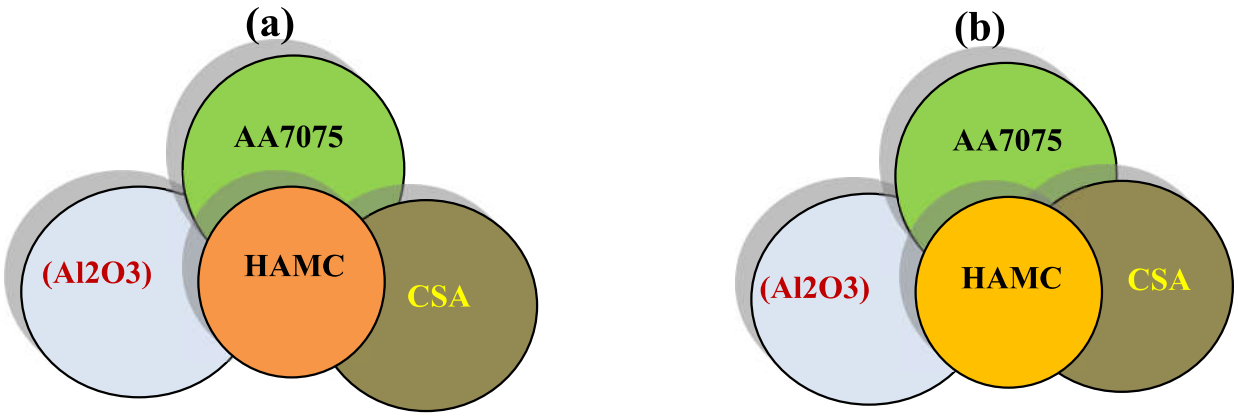

Fig. 3.1. Schematic of (a) AA7075/Al2O3$_{np}$/CSA and (b) AA7075/Al2O3$_{mp}$/CSA hybrid composites

3.1. Experimental details of AA7075/Al2O3$_{np}$/CSA hybrid composites

The experimental methodology employed in the development of Hidden Markov Model Classifiers (HMMCs) is illustrated in **Fig. 3.2.** The hybrid composites that have been developed were subjected to further investigation in order to conduct microstructural characterization, mechanical testing, and wear testing.

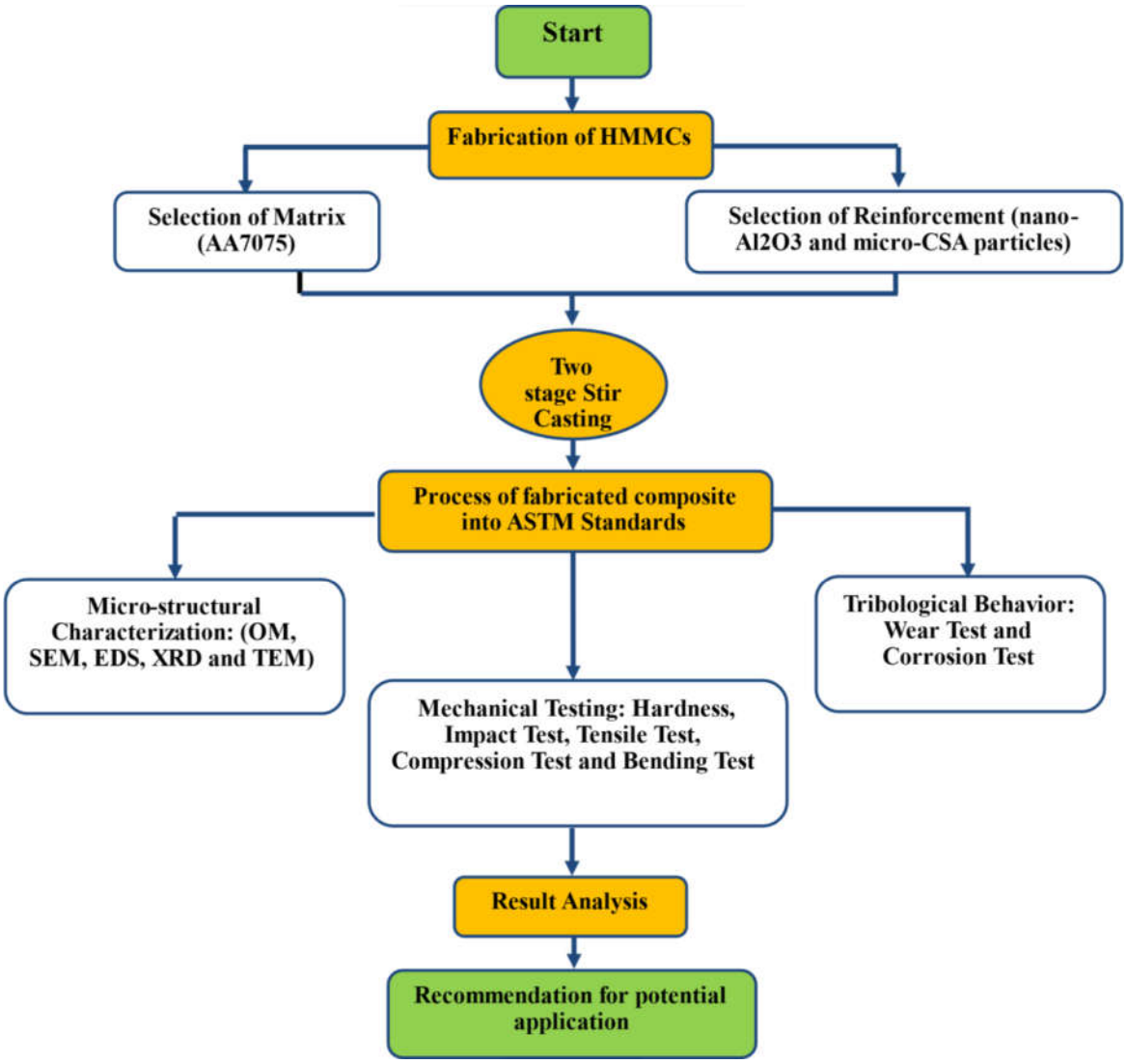

Fig. 3.2. Schematic synthesis representation of HMMCs

3.1.1 Materials

AA7075 is a material of significant importance for industrial applications, thus justifying its choice as the matrix material. The reinforcing materials selected for this investigation consisted of micro-sized CSA particles, measuring between 40 and 60µm, and nano-sized alumina elements, measuring between 40 and 90 nm in size. The coconut shell is placed within a designated receptacle and subjected to a controlled drying process under sunlight for a duration of four days, with the objective of eliminating any residual moisture content. The coconut shell undergoes a process of fragmentation into small particles prior to its combustion within an exposed furnace, resulting in the production of ash. In order to

remove carbonaceous particles present in CSA, the fine ash particle is gathered and subjected to a heating process lasting 3 hours at a temperature of 620 °C within a muffle furnace. The chemical constituents of the selected materials are shown in **Table 3.1-3.2.**

Table 3.1. Chemical make-up of AA 7075 alloy, expressed as a percentage.

Element	Zn	Cu	Mg	Si	Fe	Mn	Ti	Cr	Pb	Al
Percentage	5.31	1.13	2.12	0.41	0.52	0.29	0.22	0.18	0.03	Remaining Balance

Table 3.2. XRF Oxide analysis for CSA, wt. %.

SiO_2	Fe_2O_3	Al2O3	Na_2O	MgO	ZnO	MnO	CaO
46.35	18.80	20.85	0.85	13.15	0.31	0.23	0.62

The determination of the morphology and particle size of nano Al2O3 powder was conducted through the utilisation of a transmission electron microscope (TEM). Approximately 10 mg/L of alumina nanoparticles were introduced into an acetone solution and subjected to ultrasonic treatment for a duration of 4-5 minutes. **Fig. 3.3(a, b).** The TEM analysis of alumina particles is presented in **Fig. 3.3(a, b),** while the SEM analysis of CSA particulates is **Fig. 3.3(c, d).**

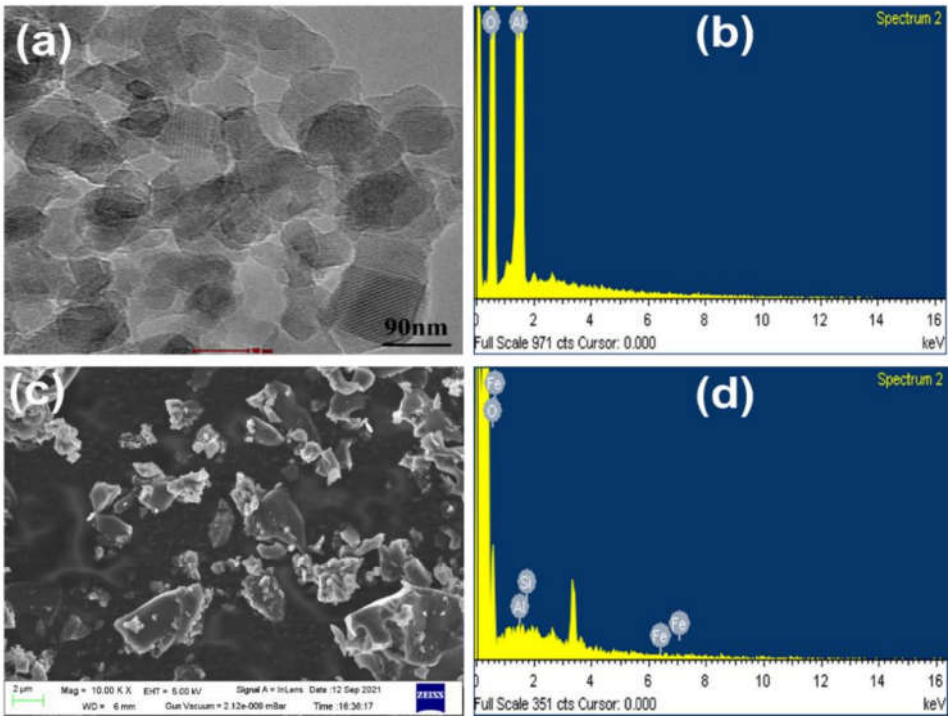

Fig. 3.3. (a, b) Nano-alumina powder TEM analysis and (c, d) SEM morphology of CSA particles.

Range of reinforcement materials, specifically alumina and CSA, was determined and documented in **Table 3.3** based on prior research efforts.

Table 3.3. Proportion of reinforcements

Sample	Nano size Al2O3 (wt. %)	Micro size CSA (wt. %)	AA7075 (wt. %)
N0	0%	0%	100%
N1	0.5%	1%	98.5%
N2	0.5%	2%	97.5%
N3	0.5%	3%	96.5%

3.1.2 Fabrication process

Aluminium hybrid metal matrix composites (HMMCs) were fabricated utilising the stir casting technique, as depicted in Figure 1. In this study, a combination of pure aluminium powder (m) and Al2O3 powder (nm) was utilised. The powders were compressed into a circular disk-shaped block and subsequently added to an injection moulding machine, as depicted in **Fig. 3.4 & Fig. 3.5.**

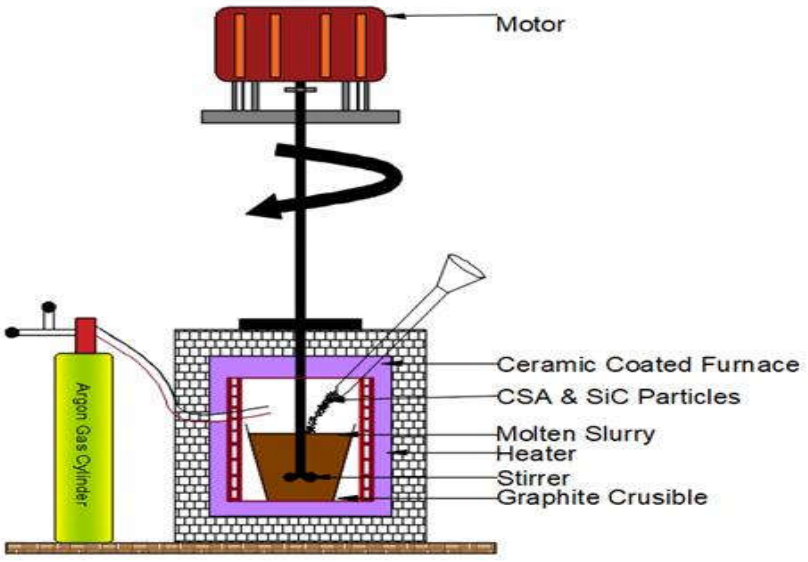

Fig. 3.4. Schematic diagram of stir casting setup

Fig. 3.5. Creating a powder using pure aluminium and nano-alumina

The aluminium (Al) matrix was subjected to a heating process until it reached its melting point. Subsequently, it was cooled down to the slurry stage and manually mixed using a two-step stir casting method. Upon subjecting the slurry to additional heat and employing a mechanical stirrer to agitate the matrix, the intended temperature is attained. The dispersion of particles throughout the matrix to achieve a uniform stirring effect is a primary advantage of the stir casting procedure in comparison to conventional stir casting. The concept of reinforcement is discussed in reference [281]. The optimal parameters for the stir casting process are presented in **Table 3.4**.

Table 3.4. Parameter of the stir casting process

Process Parameter	Selected Parameter
Mould preheats temperature	280^{o}C
Processing Temperature	950^{o}C
Preheat temperature of reinforcement	350^{o}C
Stirring speed	350 RPM
Stirring time	5 min
Blade angle	45^{o}
Position of stirer	upto 75% of depth

In order to remove the volatile substances that have been absorbed, the muffle furnace is employed to preheat the reinforcement for a duration of 2.5 hours. A graphite crucible is employed for the purpose of melting approximately 1.5 kg of pure Al 7075 alloy per individual sample. The two-stage casting process involves subjecting AA7075 to a heating phase until it reaches its melting point, followed by a subsequent cooling phase until it reaches a semisolid state. At this stage, preheated alumina and CSA particles are meticulously blended for a duration of 5-6 minutes. The molten slurry is subsequently subjected to a temperature of 950 °C, with varying weight percentages of reinforced particles. The weight percentages of samples N0, N1, N2, and N3 were determined based on existing literature and experimental research. The retention of both constants yielded negligible impact on the outcome; consequently, the proportion of both reinforcements was augmented over the course of the study. After the temperature of the melt reaches 950 °C, the liquid slurry undergoes agitation for a duration of 5-7 minutes. This is achieved by employing a four-blade mechanical stirrer that rotates at a speed ranging between 350-450 revolutions per minute. The purpose of this agitation is to guarantee a uniform dispersion of the reinforcement within the composite material.

3.2. Experimental details of AA7075/Al2O3$_{mp}$/CSA hybrid composites

3.2.1. Materials

A spectral analysis was conducted on Al 7075, and the composition is presented in **Table 3.1**. This study employs two particulate materials as reinforcements, namely primary reinforced particles (Al_2O_3) and secondary reinforced particles (CSA). Image shown in **Fig 3.6** depicts a scanning electron microscope (SEM) micrograph of Al_2O_3. The scanning electron microscopy (SEM) image of the CSA particles, is presented in the preceding section 3.1. The typical particle sizes of the Al2O3 and CSA powders were 25 μm and 70 μm, respectively.

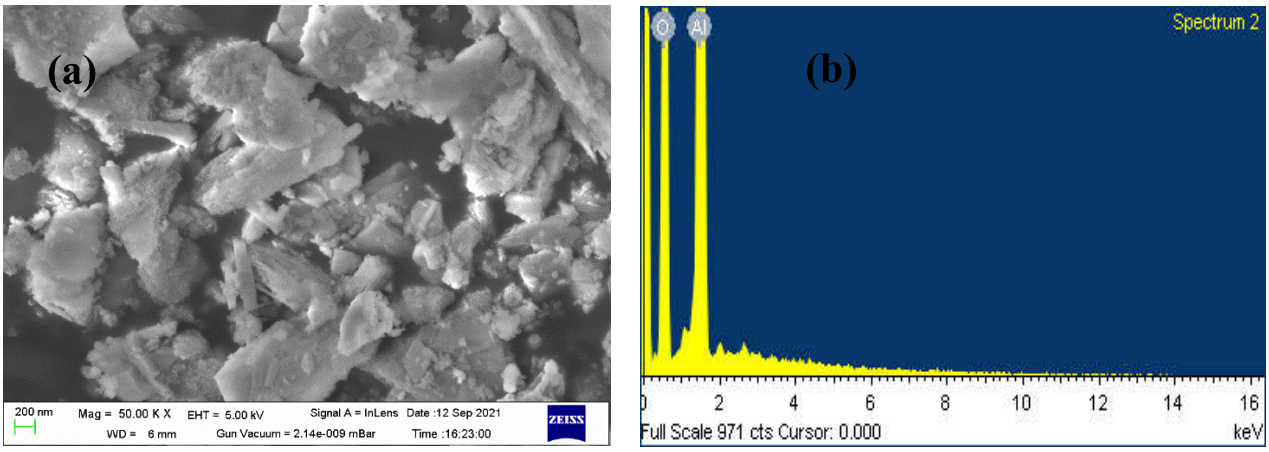

Fig. 3.6. (a) SEM morphology of Al_2O_3 particulates **(b)** Corresponding EDS of Al2O3 particulates

3.2.2 Fabrication Process

The two-step stir casting method is a cost-effective technique for the making of HAMC. The implementation of a two-step stirring process was evaluated as a potential means to enhance the efficiency and quality of casting products. In Fig. 3.4, the experimental setup for stir casting is shown. The present studies utilised the fabrication technique known as Rheocasting or Double stir casting technique. The AA7075 alloy was loaded into the graphite crucible, and the process of melting was conducted at a temperature of 750^{o}C. The temperature was maintained within the range of 750^{o}C to 800^{o}C for a duration of one hour. To minimise the presence of gases in the molten aluminium, C2Cl6 degassing tablets were utilised. The utilisation of molten metal agitation facilitated the incorporation of Magnesium, thereby enhancing the wettability characteristics and promoting the uniform dispersion of particles within the liquid medium. The Al2O3 and CSA particles were preheated at a temperature of 430^{o}C for a duration of 25 minutes in order to ensure their compatibility with the molten liquid, prevent moisture absorption, and avoid the presence of organic contaminants. Subsequently, these particles were introduced into the pool of liquid metal and agitated rapidly at a speed corresponding to the formation of vertices using a mechanical stirrer operating at a range of 300-350 revolutions per minute. The optimal parameters for the stir casting process are presented in **Table 3.5.**

Table 3.5. Process parameter for stir casting

Process Parameter	Selected Parameter
Mould preheats temperature	320^{o}C
Processing temperature	800^{o}C
Preheat temperature of reinforcement	430^{o}C
Stirring speed	350 RPM
Stirring time	10 min.
Blade angle	45^{o}
Position of stirrer	upto 75% of depth

The weight percentages of reinforcements were determined based on a comprehensive review of relevant literature, as documented in **Table 3.6.**

Table 3.6. The weight percentage of reinforcements

Sample	**Al2O3 (wt. %)**	**CSA (wt. %)**	**AA7075 (wt. %)**
Hc-0	0%	0%	100%
Hc-3	5%	3%	Remaining
Hc-6	5%	6%	Remaining
Hc-9	5%	9%	Remaining

The event persisted for a duration of ten minutes, during which two identical step sizes were employed. During the sequential operations, a stirring duration of 5 minutes was observed, which was subsequently succeeded by the formation of a semi-solid state. During the solidification process, the growth of multiple dendrites with numerous branches within the casting can lead to a decrease in its mechanical properties. The stirrer's optimal speed and stirring duration were implemented in accordance with prior scholarly works in order to eliminate the dendritic structure. The optimal parameters effectively divide the dendritic formation of the particulates during the casting process, ensuring their uniform dispersion. Following the removal of the solidified rectangular and cylindrical composites from the mould, the test samples underwent cutting using a wire EDM technique. Subsequently, the specimens were prepared in accordance with the guidelines outlined by ASTM standards to facilitate various testing procedures.

3.3. Characterization process

3.3.1 Microstructural Examination

The microscopic characteristics of the specimens were analysed using both microscopy with optics and SEM. The specimens composed of base alloy were subjected to examination using an optical microscope. In contrast, both the optical microscope and scanning electron microscopy which included energy-dispersive spectroscopy (EDS) were utilised for the analysis of the metal matrix composites (NMMCs). The failed specimens, characterised by irregular surfaces, were subjected to scanning for the purpose of analysis. The irregularity of the surfaces posed challenges in achieving proper focus when using an optical microscope. The optical microscope depicted in **Fig. 3.7** is the Neophot-21.

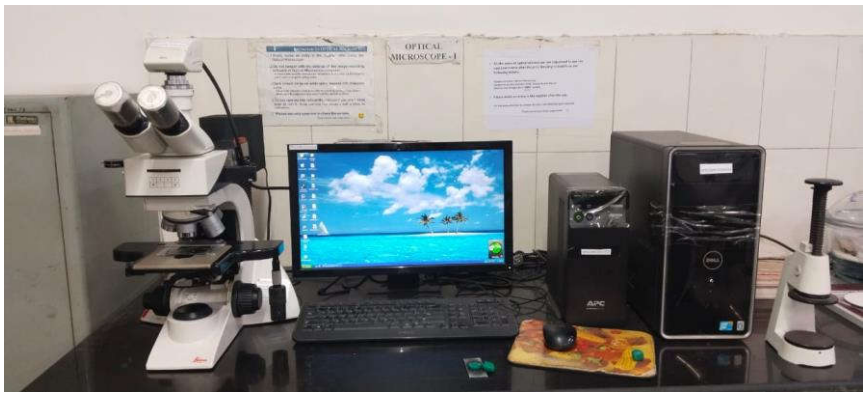

Fig. 3.7. Neophot-21 optical microscope

The optical system utilised in this study was the UIS (Universal Infinity System) with a reflected light illuminator of the tube. The magnification of the system was set to 1X, providing a super wide field of view with a numerical aperture of 26.5. This magnification range was compatible with eye pieces ranging from 50X to 2000X. The eye piece used in this study had a magnification of 10X and was equipped with cross lines and a neutral density filter to optimise light incidence.

Several different etchants were tested, and it was found that dilute Keller's etchant yielded the most favourable results. As a result, this particular etchant was selected for use in the experiment. Photomicrographs were captured for each specimen in order to examine their microscopic components and the dispersion of particles. The measurement of the distribution of Nano-Al2O3 particles was conducted using the following methodology.

The use of SEM was conducted to assess the dimensions and structure of the reinforcements. Additionally, a material and image analyser was utilised to examine the dispersion of Nano-Al2O3 particles at ten specific points on every sample. Subsequently, the mean value of these outcomes was computed. In this study, four distinct size ranges of reinforcement were selected, and the corresponding reinforcement distribution data were represented using a bar chart and a line graph. Additionally, an evaluation was conducted on the average aspect ratio and the distribution of the total average area of the particles. The composites' microstructure was analysed using a JSM-840A microscope with SEM. This particular microscope is equipped with a high-performance light element detector, which is a window-less detector capable of detecting elements with atomic numbers beginning from boron and higher. **Fig. 3.8.** illustrates a scanning electron microscope.

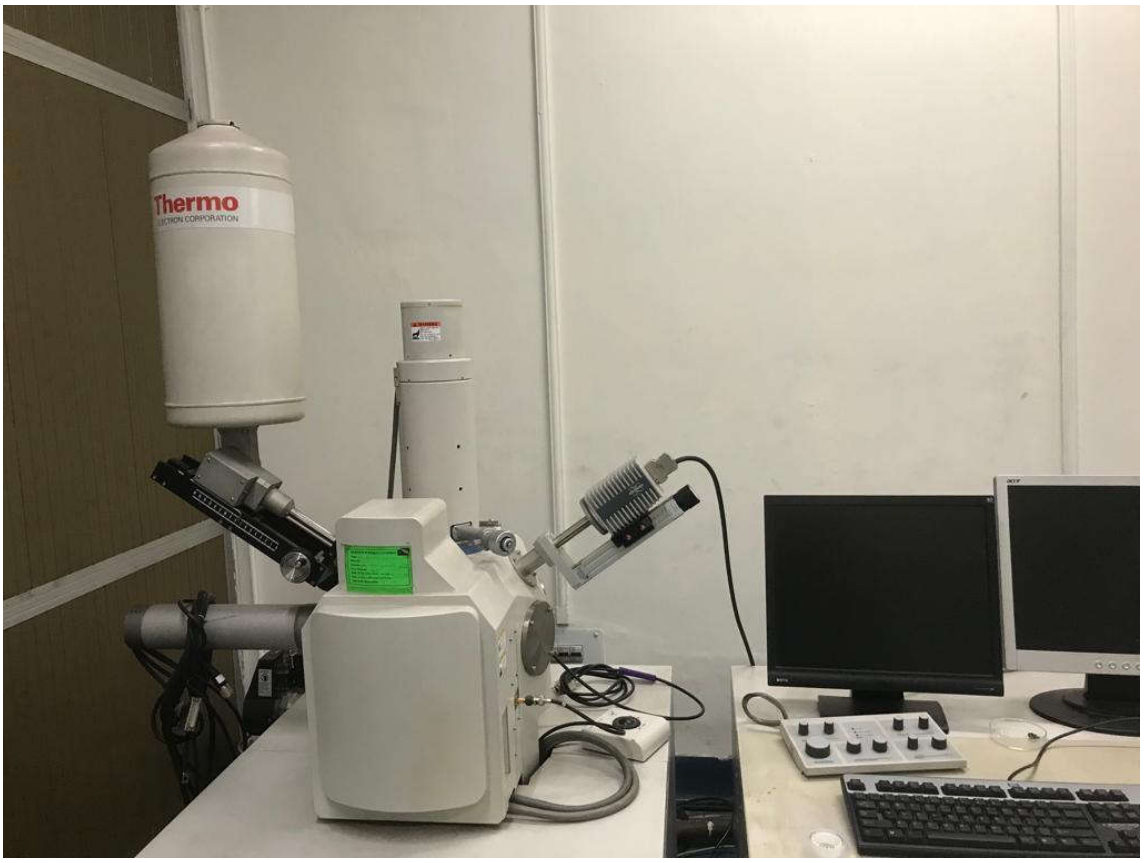

Fig. 3.8. JEOL Japan scanning electron microscope (SEM)

3.3.2 X-ray diffraction

The hybrid composite samples underwent analysis using a D8 Advanced X-ray diffractometer from Germany. Cobalt (Co) K radiation with a wavelength of 1.79 A was utilised, as depicted in **Fig. 3.9.**

Fig. 3.9. D8 Advanced, X-ray diffractometer, Germany

The XRD designs were acquired by conducting measurements within a 2θ range that extended from 20 to 120 degrees, with a step size of 0.02 degrees. The identification of multiple phases was accomplished by utilising X-Pert High score software to index the peaks, followed by the plotting of the indexing peaks (I vs. 2) using Origin 9.0 software.

3.3.3 Mechanical Characterization

3.3.3.1 Density and porosity:

The experimental density for various weight percentages of the reinforced particles was calculated using the displacement approach. Additionally, the rule of mixing (ROM) was used to calculate the hypothetical weight of HAMCs. Using the water displacement technique, the composite samples underwent an hour-long heating procedure in a furnace at a temperature of 125°C. Similarly, the weights of the composite samples were determined by utilising a highly accurate electronic weighing device. Subsequently, a polymeric gel is

applied to the sample surfaces in order to effectively seal any porosity present on the surface. The specimens were immersed in distilled water at a temperature of 28°C, and their masses were determined using a high-precision four-digit balance. The volume of the specimens was determined by utilising their weight. The density was calculated using the formula provided below:

$$\rho = \frac{Wp}{Ws} \quad (1)$$

where ρ denotes the specimen density, Wp stands for the weight of a preheated specimen, while Ws stands for the weight of a specimen suspended in water.

The following empirical equation was used to calculate the density of cast samples in terms of the volume percentage and density of the components:

$$\rho = V_f(\rho_{f-} \rho_m)\, \rho_m \quad (2)$$

where

V_f = Volume fraction of reinforcements

ρ_m = Density of matrix material

ρ_f = Density of reinforcement

The resulting samples' porosity is assessed by (Equation 3) using the derived theoretical and experimental density values.

$$Porosity(\%) = \frac{\rho_{theoretical} - \rho_{experimental}}{\rho_{theoretical}} X\ 100 \quad (3)$$

3.3.3.2 Micro Hardness Test

The microhardness of the specimens was evaluated using a Zwick/Roell Indentec Hardness Tester, which has a load range of 10 to 1000 grammes. The magnification range of the object lens varied from 10x to 40x. The indentation was captured using a 40X magnification, while the stress of 0.05 kg was applied for a duration of 10 seconds. The indenter utilised in this context was a cone-shaped tool made of diamond material. The experiment was conducted on the specimens at five distinct locations, and the mean value was recorded. The achievement of this task was facilitated through the utilisation of the samples that were subjected to microstructural analysis. The Micro Hardness Tester employed in the study is illustrated in **Fig. 3.10.**

Fig. 3.10. Zwick/Roell Indentec Hardness Tester

3.3.3.3 Tensile Test

The test was conducted using an Instron tension testing device. The machine was regulated using signal conditioners for stroke (LVDT), load, and two strain channels. The regulation was carried out by a digital controller based on a digital signal processor (DSP) with a resolution of 24 bits. Equipped with the requisite software and firmware. The extensometer used in the experiment had a travel distance of 0.5 mm and a gauge length of 12.5. The COD gauge, on the other hand, had a gauge length of 7 mm, a positive travel distance of 4 mm, and a negative travel distance of 1 mm. The transducers are equipped with an external shunt reference to facilitate straightforward calibration and incorporate electronic components to enable the implementation of a full bridge circuit. The furnace in question was identified as an ATS 3210 series model. The experiment was conducted using a 3-zone power pack with a power output of 4000 watts and an operating voltage of 230 volts. The

power pack had a maximum temperature capability of 1200 degrees Celsius. The ambient temperature recorded during the test was 27°C. Uniaxial loading was applied to the specimen until it reached the point of failure. The tensile tester currently being utilised exhibits two perspectives, as illustrated in **Fig. 3.11.**

Fig. 3.11. Uniaxial loading Tensile test

3.3.3.4 Thermal expansion coefficient test

The thermal expansion coefficients (TCE) of hybrid composites were determined by employing a thermal mechanical analyzer., as depicted in **Fig. 3.12.** TCE measurements were conducted under controlled conditions, specifically at a force magnitude, At a heating rate of 5 °C per minute, the temperature range considered spans from 30 to 250 °C.

Fig. 3.12. Thermal mechanical analyzer (TMA Q400 V7.4)

A thermocouple in proximity to the sample was employed to ascertain its temperature. The data was obtained by measuring the percentage of relative change in length (PRCL) against a temperature chart. Additionally, the experimental curves were numerically differentiated to determine the effective immediate CTE. The equation presented is employed to compute the immediate CTE with a specific temperature.

3.3.3.5 Thermal conductivity test

Thermal conductivity is defined as the quantification of the rate at which heat is conducted through a material of a specific thickness, in a direction perpendicular towards the surface of a specific area, due to a specific temperature gradient, while maintaining thermal equilibrium. The thermal conductivity measurement was performed under steady-state circumstances utilising an instrument that utilised the parallel heat-flow approach. In the framework of a state of equilibrium, the thermal conductivity of hybrid composites can be mathematically represented as K = (Qs/A)/(T/L), where Qs represents the rate of heat transfer per unit time, A denotes the area of the cross-section, and T indicates the temperature difference across a specified distance L.

The quick pulse approach is a method commonly employed to directly test the outside the axis temperature conductivity of composite materials. In the provided equation, the variable L is used to indicate the thickness of the sample. The symbol α is employed to denote the thermal diffusivity, while t1/2 is utilised to signify the period required to reach the second half of the optimum back surface temperatures. The conceptualization of this idea was originally ascribed to Parker & Jenkins (Parker et al., 1961). The surface of the sample will be subjected to a short exposure to radiant electromagnetic radiation, while the thermal diffuseness of the sample will be evaluated by monitoring the duration of heat propagation over the sample section.

3.3.3.6 Wear Test

The Ducom TR-201-M4 pin on a disc test machine, depicted in **Fig. 3.13.**, was employed to evaluate the dry sliding wear behaviour of various composite materials. Cylindrical specimens were utilised in order to carry out wear tests.

Fig. 3.13. Ducom TR- 201- M4 pin on the disc test machine

The specimens underwent a thorough polishing process at the sliding end, involving the use of abrasive paper with grades of 600, 1200, and 2000. Subsequently, a diamond polishing technique was employed, utilising 0.25 mm diamond paste. Prior to each test, the surface of the disc and the sliding end of the pin (sample) were appropriately cleaned using acetone. The disc was fabricated using EN-31 hardened steel, which possesses a hardness of 60 HRc.

The diameter of the track on the disc measured 50mm. The wear tests were carried out using specific test parameters, which included varying sliding speeds of 0.79, 0.94, and 1.04 m/sec, applied forces of 20, 30, and 40 N, and sliding distances of 1000, 1500, & 2000 m. The surfaces of the materials under investigation were analysed via SEM.

CHAPTER 4

RESULTS AND DISCUSSION

The current chapter presents the results of the effect of various stir-casting parameters on microstructural characterization, and mechanical and tribological properties. This chapter has been divided into two sections.

4.1 AA7075/Al2O3$_{np}$/CSA hybrid composites

4.1.1 Microstructural evaluation

The microstructural pictures of the composites are displayed in **Fig. 4.1(a-d).** The optical pictures show a homogeneous distribution of reinforcing particles that are distributed. Fig. Microsegregation (MgZn2) is uniformly distributed throughout the fine-grained composition, as shown in **Fig. 4.1(a).** As seen in **Fig.1.4(c, d).**, the levels of porosity show an increased trend with an increase in reinforcing content. The greatest porosity is readily seen in **Fig. 4.1(d).** of the research.

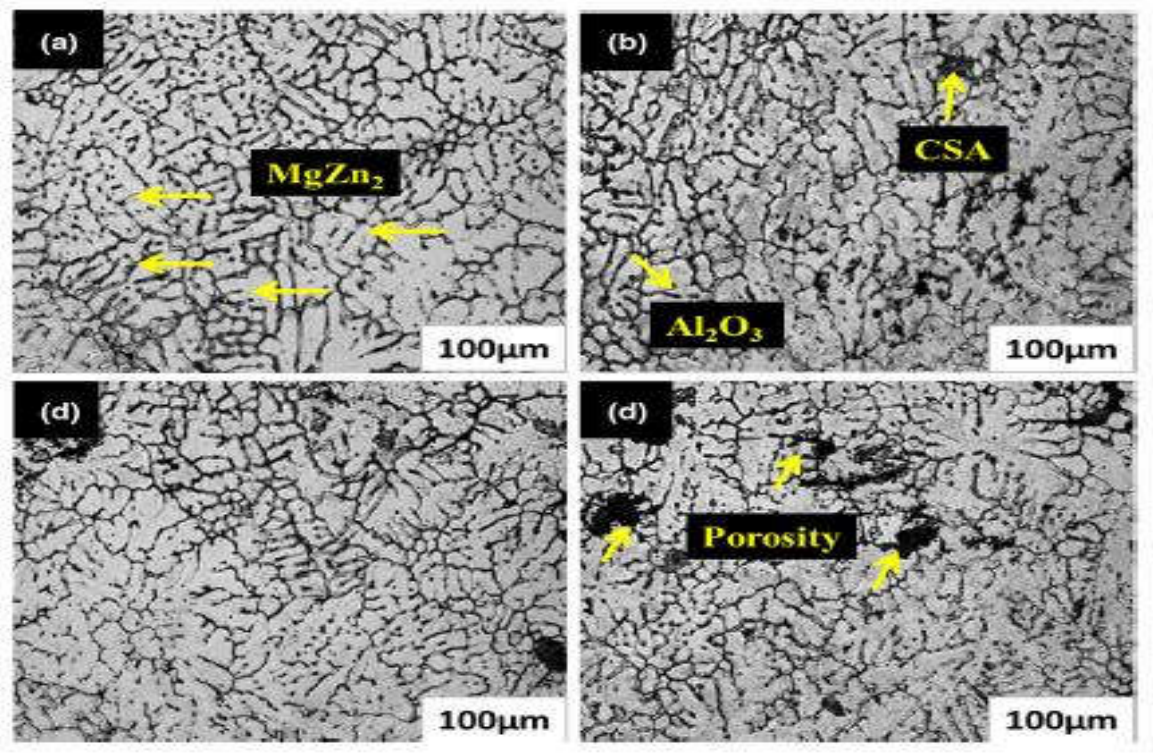

Fig. 4.1. (a) Base AA7075 alloy (N0), (b) HMMC (N1), (c) HMMC (N2), and (d) HMMC (N3) optical micrographs.

A high level of integration between the aluminium (Al), alumina (Al2O3), and carbon short fibres (CSA) in the composite material is shown by the uniform dispersion pattern of reinforced particles seen in the scanning electron microscope (SEM) images of hybrid metal matrix composites (HMMCs). The reinforced AA7075 alloy specimen photographed using scanning electron microscopy (SEM) is shown in **Fig. 4.2(a).** in a very obvious manner. **Fig. 4.2(b-d).** Al2Mg3Zn3, MgZn2, Al2CuMg, Al13Fe4, Al7Cu2Fe, Mg2Si, and Al2Cu are examples of intermediate phases that can develop during the solidification of the AA7075 alloy [195]. The uniform dispersion of reinforced Al2O3 and CSA particles is seen in **Fig. 4.2(b,c). 4.2(b, c).** As seen in **Fig. 4.2(d).** The porosity level is seen to rise as the weight % of reinforced particles is raised, according to section **Fig. 4.2(d).** of the research.

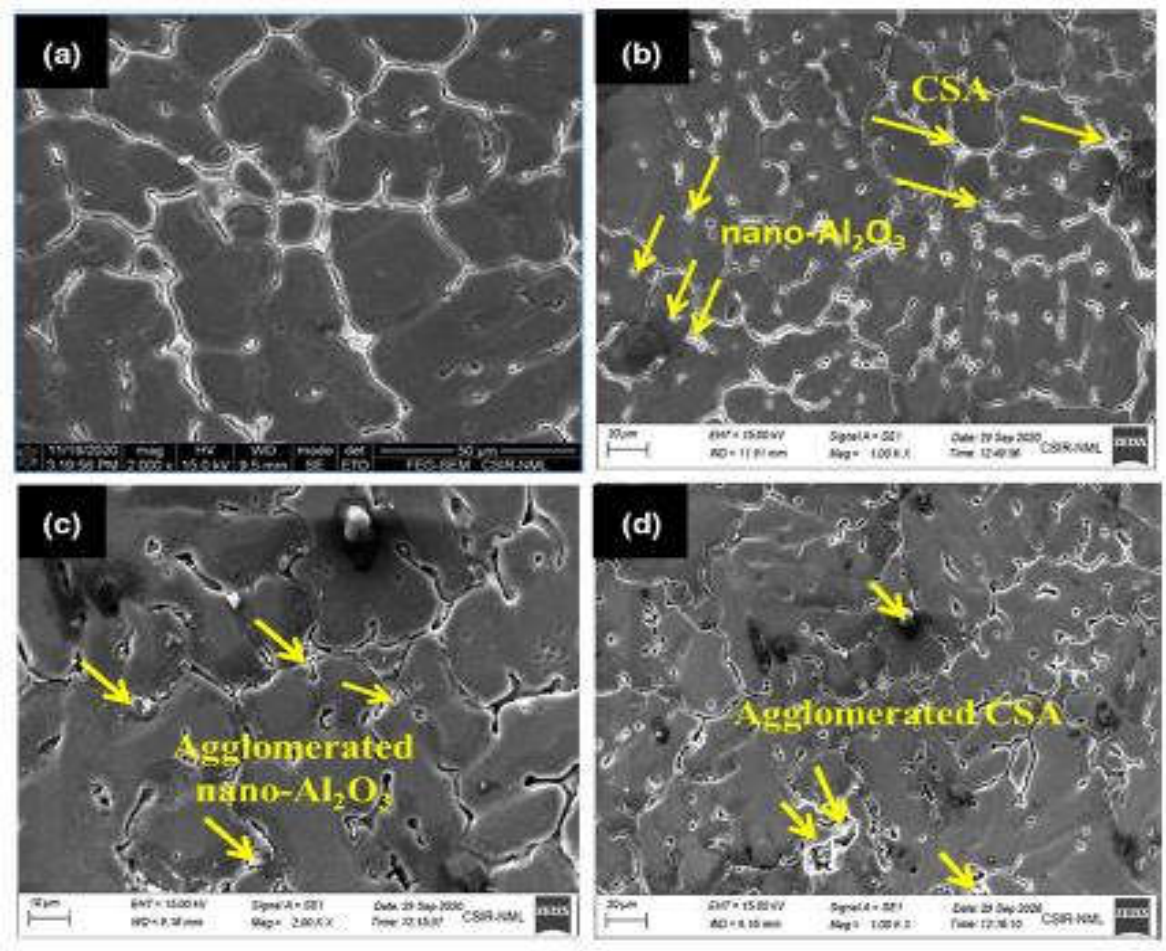

Fig. 4.2. (a) Base AA7075 alloy (N0), (b) HMMC (N1), (c) HMMC (N2), and (d) HMMC (N3) are shown in the following SEM photos.

Fig. 4.3. shows the images obtained by scanning electron microscopy (SEM) of the AA7075 alloy, coupled with the energy-dispersive X-ray spectroscopy (EDX) evaluation that goes with it. The example is **Fig. 4.3.(a).** has been strengthened. **Fig. 4.3(b-e).** is shown in detail.

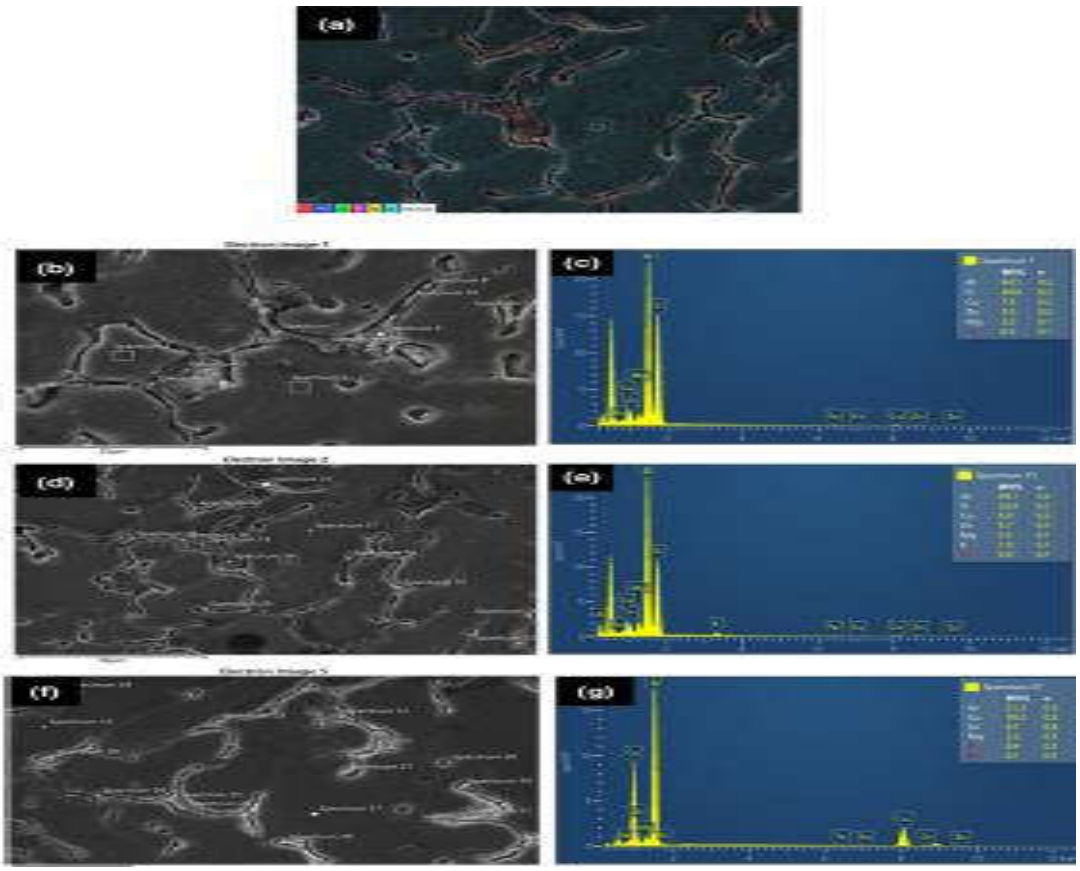

Fig. 4.3. (a) Base metal (N0), (b, c) HMMC (N1), (d, e) HMMC (N2), and (f, g) HMMC (N3) were all examined using SEM with EDX.

The particle phases reinforced with alumina (Al2O3) and coconut shell ash (CSA) in AA7075 were effectively generated and analysed in the current investigation. Energy-dispersive X-ray spectroscopy (EDX) and scanning electron microscopy (SEM) were used in the experiment. The presence of (Al, Al2O3, Si, Zn, and Cu) is clearly visible in the graph's principal peaks, confirming the presence of reinforced particles in the composite specimens. The presence of reinforced particles acts as a barrier, changing the direction of migration of dislocations between neighbouring grains and increasing the final tensile strength. In contrast to monolithic aluminium, composite samples with well distributed

reinforcement and little porosity exhibit multidirectional stresses due to the existence of grain refinement. The findings of the investigations performed on the samples using energy-dispersive X-ray spectroscopy (EDX) and scanning electron microscopy (SEM) are shown in Fig. 4.3. SEM pictures of the composite samples show consistent reinforcement dispersion, which points to a high-quality inclusion of hybrid Al/Al2O3/CSA metal matrix composites (MMCs). For homogeneous reinforcement dispersion inside the matrix, precise parameter selection for the stir casting process is essential. The distribution of reinforcement becomes more homogeneous as the temperature rises. The decision to use a high molten temperature in the process was made because the particles' melting point is higher than that of molten aluminium, which makes it easier to reduce clusters. With an increase in Al_2O_3 content, tiny clusters become more visible, mostly as a result of the reinforcements' thermal mismatch with the matrix. A liquid alloy's rate of solidification is slowed down by the presence of hard ceramics nearby, which promotes the growth of clusters. However, increasing the cross-sectional area (CSA) results in a decrease in the development of clusters since it is a malleable ceramic material.

The X-ray diffraction (XRD) profile. SiO2 and Al2O3 are present in substantial quantities in **Fig. 4.4.** The figure also suggests that CSA and Al2O3 are present in the hybrid composite. The lack of supplementary parts shows that the composites were cast successfully. The careful control of a number of casting process parameters, including as reaction time, reaction temperature, and melt stirring time, is necessary to achieve this result.

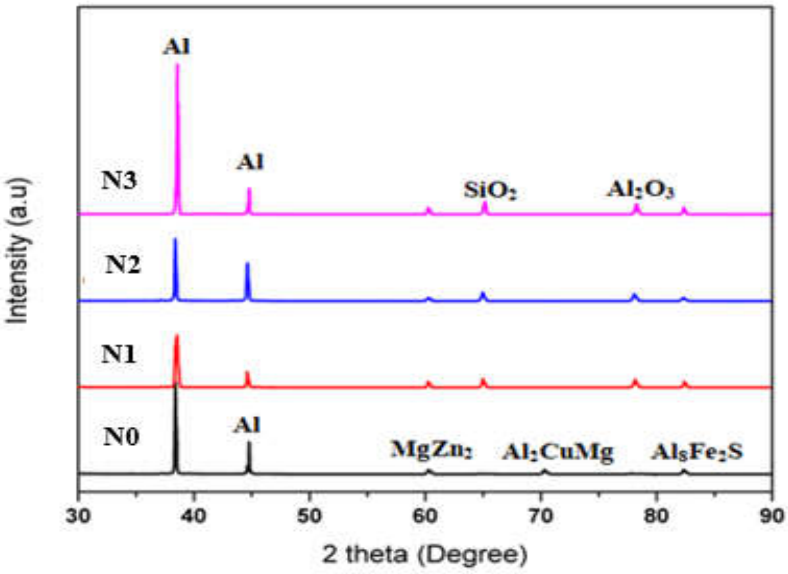

Fig. 4.4. XRD profile of developed hybrid composite

4.1.2 Evaluation of Mechanical behaviors

The mechanical characteristics of hybrid composites are improved by the inclusion of Al2O3 and CSA particles. **Fig. 4.5.** shows that the reinforcing materials CSA and Al2O3 improve the hardness of the AA7075/Al2O3/CSA hybrid metal matrix composites (HMMCs). Comparing the composite to the AA7075 alloy, the composite showed a much higher level of hardness. With the exception of pure AA7075, it was found that adding Al2O3 and SiO2 (CSA) particles to the matrix material increased the hardness of all samples. Al2O3 prevents persistent deformation after indentation by increasing the top surface's hardness.

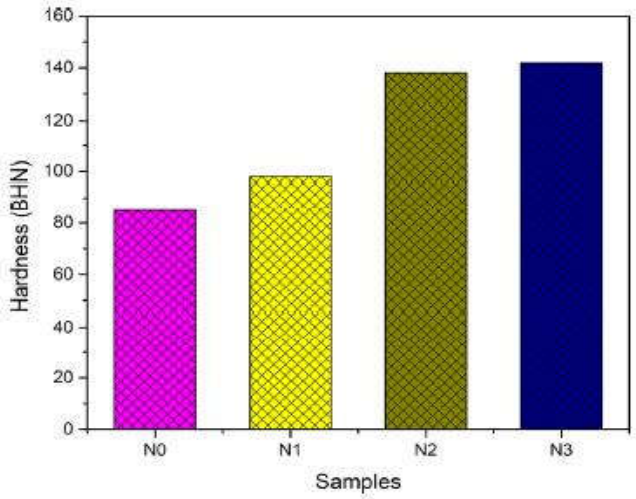

Fig. 4.5. Effect of the reinforcement's % composition on hardness

The hardness characteristics of hybrid metal matrix composites (HMMCs) are improved when ceramic particles are added to a metal matrix, which causes a change from ductility to brittleness. Increased non-uniformity and non-wettability issues are brought on by an increase in the weight % of reinforced particles, which ultimately results in increased molten metal viscosity and pouring challenges. The presence of evenly dispersed reinforced particles, the density of the reinforcement, the pace of solidification, and a decreased level of porosity were some of the major variables that influenced the hardness of the HMMCs (281). The resistance of the reinforced particles to being indented was assessed using the Brinell Hardness Number (BHN). For the N0, N1, N2, and N3 specimens, the ideal hardness levels were 85, 98, 138, and 142 BHN, respectively. Specimen N3 produced the best results. When hard ceramics are added to the matrix of aluminium, a malleable material, it changes state and becomes brittle, increasing its level of hardness. A larger amount of reinforcement causes the matrix to become less homogeneous and non-wettable, which raises the viscosity and makes pouring the composite material more difficult. The uniform distribution of reinforcement, the rate of solidification, the density of reinforcement particles, and the existence of minimum porosity are a few major parameters that influence the hardness of composites [282, 283].

All composite specimens that have been manufactured have been found to have lower impact strength than the AA7075 metal. A graphic representation of the average impact strength is shown in **Fig.4.6.**

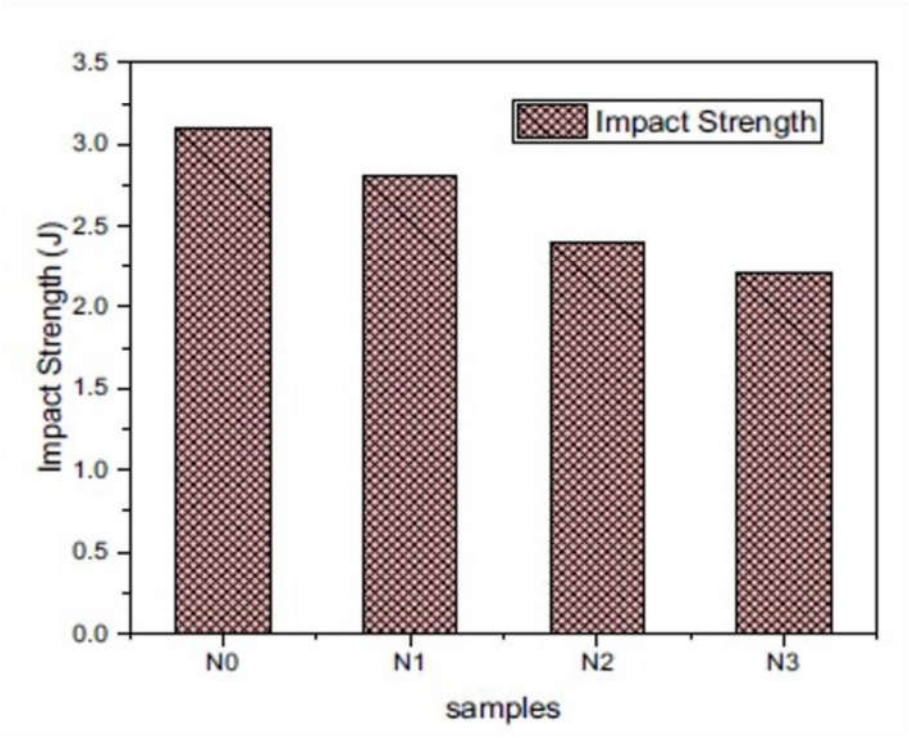

Fig. 4.6. Impact strength is affected by the reinforcement's % composition.

The Al-alloy exhibits noteworthy impact energy and ductility, resulting in durable deformation even at standard ambient temperature. The composite material's total impact strength is decreased by the presence of reinforced particles. Due to the hard ceramic particles' innate brittleness, stress concentration results. Clusters arise when there is an uneven distribution of reinforcement in the matrix material, which weakens the link between the matrix and the reinforced particles. The impact strength of Hybrid Metal Matrix Composites (HMMCs) is negatively impacted as a result of this phenomenon [284, 285]. A helpful statistic for determining how much energy reinforcing materials can endure and absorb is the impact strength value. Specimens N0, N1, N2, and N3 had ideal impact strength values of 3.1, 2.8, 2.4, and 2.21, respectively. **Fig. 4.6.** shows the value for the maximum impact strength for specimen N0, which is made of the AA7075 alloy. The pictures show fractographic analysis performed on an impact-fractured specimen using scanning electron microscopy (SEM). **Fig. 4.7.** Because there are more dimples than cleavage facets in specimen N0, it has higher impact strength ratings. The Al-alloy underwent a shift from a ductile to a brittle state as a result of the addition of second particles. **Fig. 4.7(a-d)** makes it easy to see how the fracture started and developed.

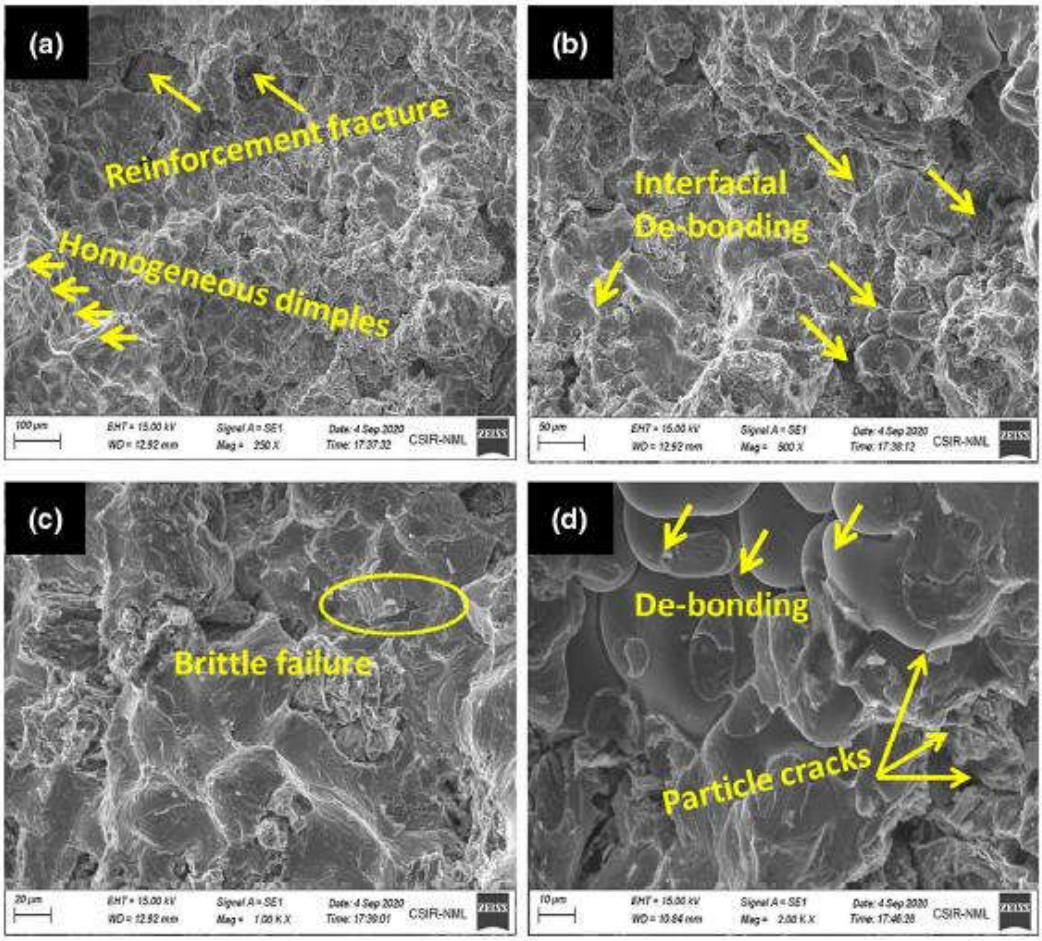

Fig. 4.7. After impact testing, SEM fracture surfaces of the casting: (a) Base metal (N0), (b) HMMC (N1), (c) HMMC (N2), and (d) HMMC (N3) are examples of materials.

In the aluminium matrix, the phenomena of fracture propagation occurs at the grain boundaries, where it causes the formation of facet structures inside the grains. There is evidence that stress concentration zones can emerge where reinforcing particles are present, resulting in an uneven fracture with inadequate energy absorption. Numerous sites inside the reinforcing particles exhibit the void nucleation phenomena. The growth of bigger voids results from a later alteration of the original crack forms. The review of the literature reveals an additional inverse link between impact strength and tensile strength. In particular, there is a direct correlation between tensile strength and impact strength. Brittleness and irregular hollows on the cracked surface might be blamed for this. In combination with Al2O3 particles, **Fig. 4.8.** shows the change in the average ultimate tensile strength (UTS) as a function of various CSA particles.

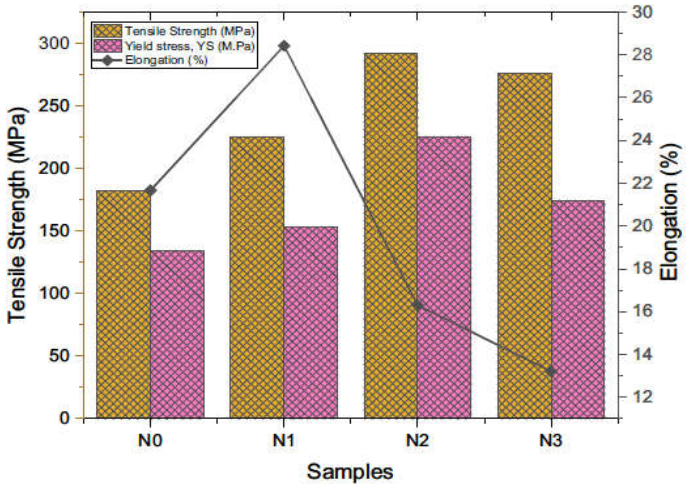

Fig. 4.8. Final tensile strength and % elongation are affected by the percentage composition of the reinforcement.

CSA content was added as a weighted proportion to the UTS results. The ultimate tensile strength (UTS) increases with increasing Al2O3 and SiO2 concentrations (CSA) because of mechanisms for stress transfer between the matrix substance and reinforcement particles. The existence of strong reinforcing particles, which serve as a barrier and stop cracks from propagating, explains the observed behaviour. The Orowan mechanism, also known as the crack propagation restriction, slows down the acceleration of dislocations in high modulus matrix composites (HMMCs) [286]. An improvement in ultimate tensile strength (UTS) may result from the considerable increase in dislocation density inside the aluminium matrix. Grain boundaries are enhanced as a result of the addition of CSA and Al2O3 to the aluminium matrix. A large increase in the existence of grain boundaries can be linked to the observed decrease in microcrack propagation, which increases the material's strength. The difference in the coefficient of thermal expansion between the matrix and reinforcement materials is one more explanation for the formation of geometrically necessary dislocations at the interface between the matrix and nano-reinforcement during the cooling process, which can increase strength. Through the preheating of Al2O3 with CSA particles, the interfacial tensile strength and homogenous distribution of reinforced particles in the Al matrix are improved in stir casting. Furthermore, preheating dispersed particles induces thermal stress, which lowers the ultimate tensile strength (UTS) in heterogeneous microstructures. A material's capacity to endure tensile forces may be indicated by the size of UTS. For samples N0, N1, N2, and N3, the corresponding mean ultimate tensile

strengths (UTS) values are 182, 225, 292, and 276 MPa. When compared to the AA7075 alloy, the N2 specimen showed the greatest value. Fig. 4.8. shows how yield strength and % elongation may vary. In terms of elongation, the N1 sample has the greatest value of 28.3%, while the N3 sample has the lowest value of 13%. As seen in **Fig. 4.9.**, tensile specimen fractures are often categorised as either ductile or brittle.

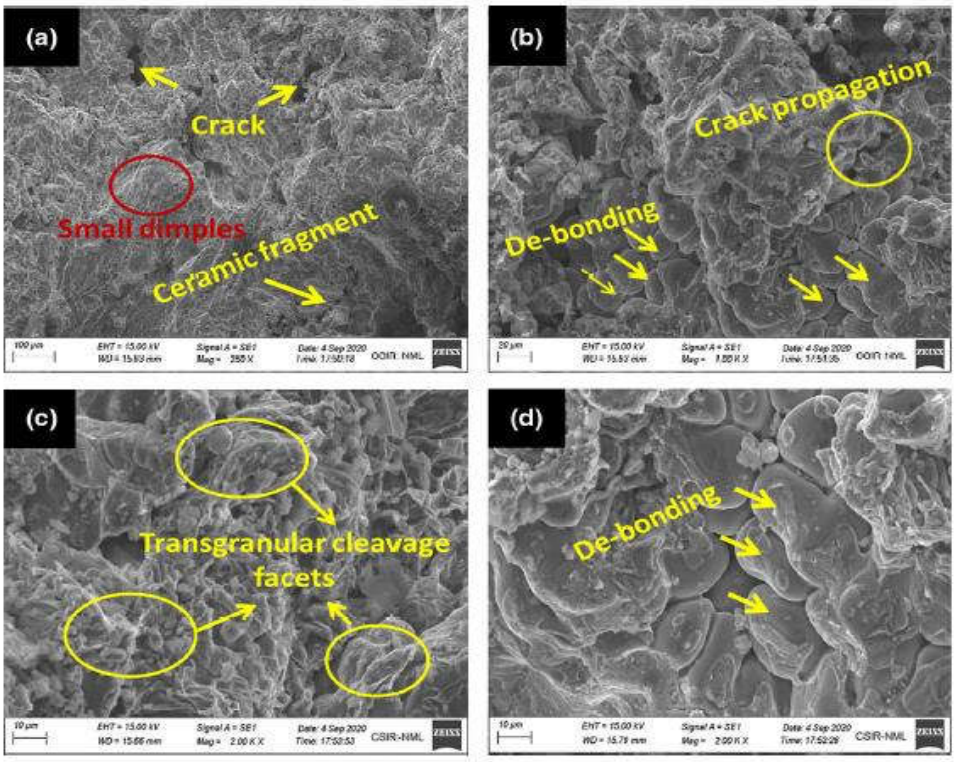

Fig. 4.9. Tensile test, the casting's SEM fracture surfaces: (a) Base metal (N0), (b) HMMC (N1), (c) HMMC (N2), and (d) HMMC (N3) are examples of materials.

The existence of non-uniform distributions of reinforced particles within the aluminium matrix and the production of secondary phases during the stir casting process are the main determinants of fracture behaviour. The existence of irregularly distributed second particles suggests that the brittle and stiff dispersion particle (Al2O3-CSA) and the ductile AA7075 alloy matrix have different strain capacities. FESEM images of stress fractures were used to analyse specimen failure behaviour, in particular micro-void coalescence and cleavage. In contrast to ductile fracture, which may be explained by the emergence of specimen necking, brittle fracture is characterised by a lesser degree of micro-void coalescence and plastic deformation, which is the cause of transgranular grain boundary movements. When a load is applied that is greater than the ultimate tensile strength (UTS), crack propagation

is shown to quicken. Both the agglomeration of grains and the creation of transgranular facets through micro-voids are thought to be responsible for this occurrence, which speeds up the cracking process [288].

The final compressive strength changes depending on whether CSA and nano-Al2O3 are present, as seen in **Fig. 4.10.**

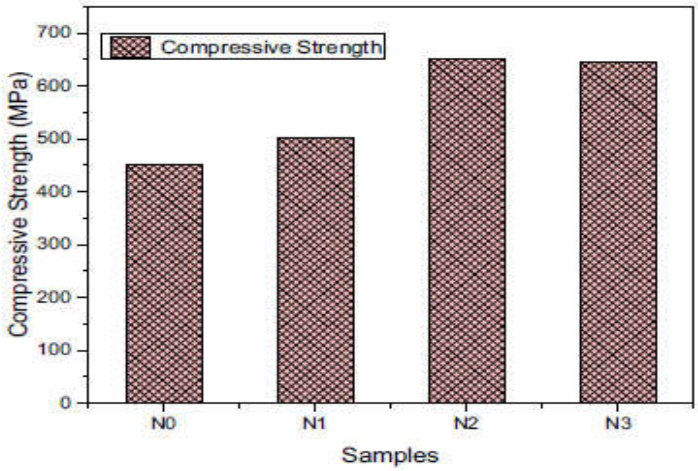

Fig. 4.10. Effect of reinforcing composition percentage on final compressive strength

In compared to the parent AA7075 alloy and the comparable results published by Embury [289], the ultimate compressive strength of all HMMCs samples has been enhanced. The considerable inclusion of calcium sulfoaluminate (CSA) and nano-sized aluminium oxide (Al2O3) particles is responsible for the hybrid aluminium composite's increased strength. The intentional procedure was continued until the matrix material could successfully accommodate the reinforced particles without experiencing any kind of distortion [290]. Due to the CSA and nano-Al2O3 enhanced particles' innate brittleness and hardness, matrix dispersion hardening takes place. As a secondary phase inside matrix alloys, the reinforced particles efficiently prevent the migration of dislocations and increase the overall strength of the hybrid composite. The compressive strength figures for the N0, N1, N2, and N3 specimens are, respectively, 450, 502, 650, and 645 MPa.

Fig. 4.11 shows how variations in the reinforcement affect flexural strength. The inclusion of reinforcement enhanced the flexural strength when compared to the basal aluminium alloy. The insertion of the reinforcement increased the specimens' strength and elastic modulus. This enhancement was made by restricting dislocation movement, which

eventually increased the flexural strength value. In contrast to the base Al-alloy, the composite specimens' flexural strength values show an increase.

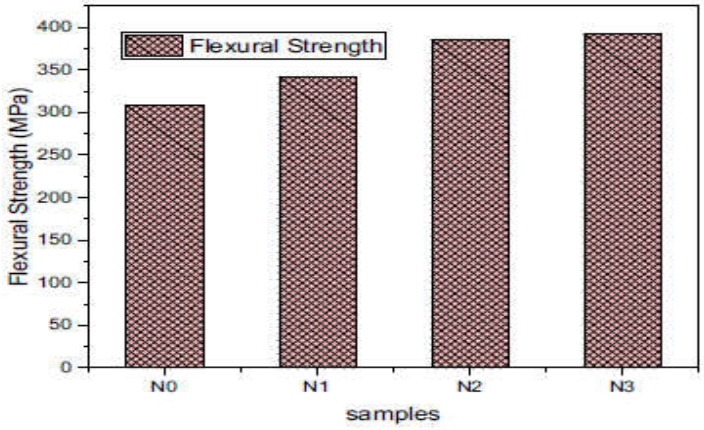

Fig. 4.11. Flexural strength is impacted by the reinforcement's % composition.

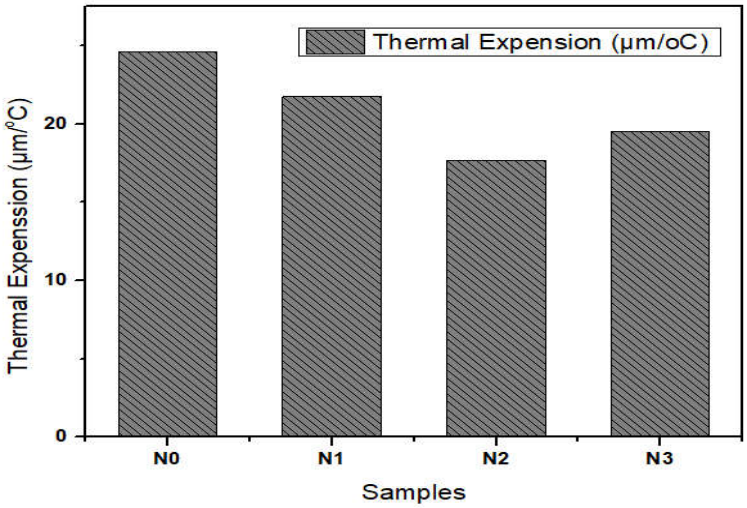

Fig. 4.12. Variation in each sample's thermal expansion coefficient at room temperature.

Fig. 4.12 and Fig. 4.13 demonstrate the link between the weight % of Al2O3 and CSA and the coefficient of thermal expansion in various samples.

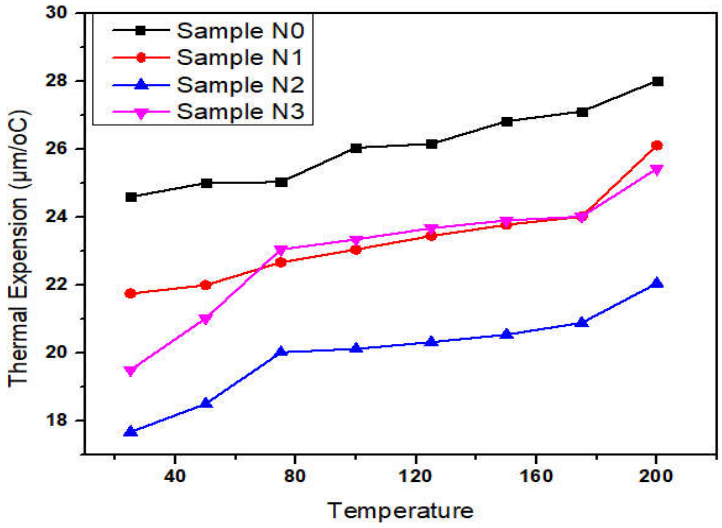

Fig. 4.13. Each sample's thermal expansion coefficient at various temperatures.

The results show that when exposed to temperature changes, hybrid composites display superior dimensional stability than the basic alloy. Particle size, the thermal expansion mismatch between the matrix and reinforcement, and interfacial interactions are some of the variables that affect the coefficient of thermal expansion of hybrid composites[291]. This analysis takes into account temperatures between 25 and 200 °C. The coefficient of thermal expansion (CTE) of the composite material under research has been seen to decrease with the addition of CSA particles and an equivalent amount of alumina. Compared to the AA7075 material, the hybrid composites have a lower coefficient of thermal expansion (CTE). Low coefficients of thermal expansion (CTE) ceramic materials include calcium aluminate (CSA) and aluminium oxide (Al2O3). The coefficients of thermal expansion (CTE) of the hybrid composite should be reduced as a result of incorporating these reinforcements into the base alloy matrix. Aluminium alloys' high coefficient of thermal expansion (CTE) causes dimensional instability as temperature rises [291]. Because of its quality, it cannot be used in final applications like electrical and electronic packaging. It is feasible to adjust the coefficient of thermal expansion (CTE) to meet the needs of various industrial applications by mixing reinforcements with AA 7075. Each sample was subjected to ten readings altogether.

Fig. 4.14. shows the thermal conductivity values of the basic alloy AA7075 and the CSA/Al2O3 composites at various temperatures while taking into account different CSA weight percentages. The number in **Fig. 4.14.** and the supplementary **Fig. 4.15.**

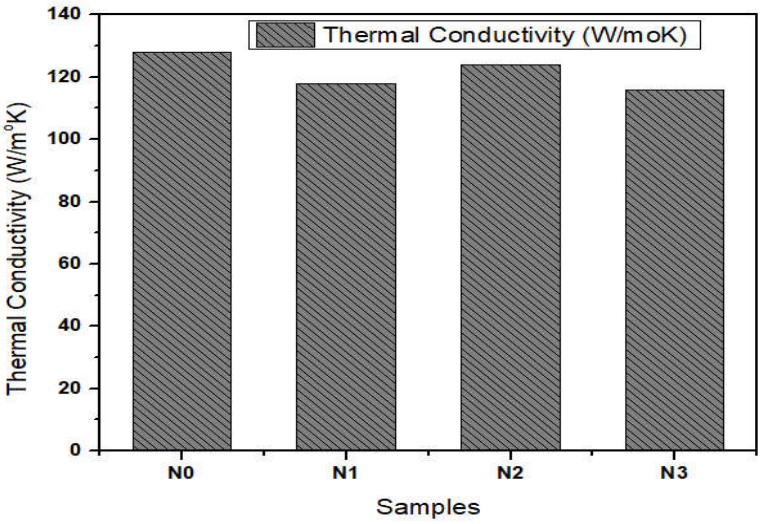

Fig. 4.14. Variation in each sample's thermal conductivity at room temperature

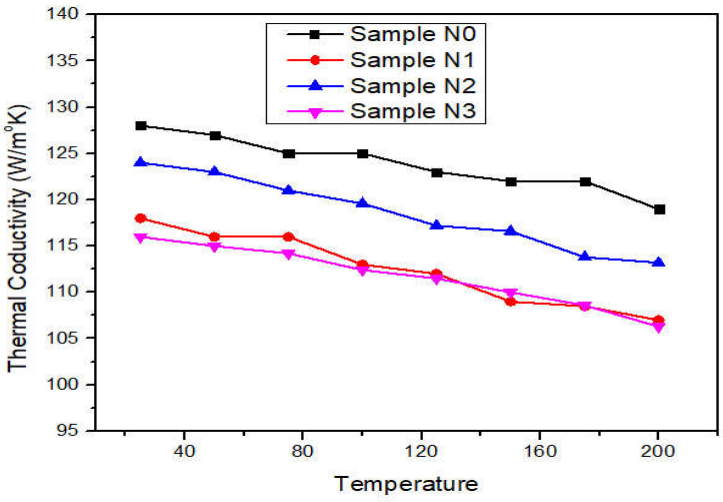

Fig. 4.15. Each sample's thermal conductivity varies as a function of temperature.

In comparison to the thermal conductivity of the base alloy, it was found that the thermal conductivity of hybrid composites was somewhat lower. The processing technique used, the warm conductivity & wettability characteristic of the reinforcing elements, the microstructure all have a major impact on the thermal conductivity of hybrid composites [292].

In this instance, it is shown that the thermal conductivity of both reinforced particles has significantly decreased. However, the produced composites show enhanced bonding between the matrix and reinforcing components, as well as a uniform distribution of the constituents. The production of dislocations at the grain boundary area can be caused by the existence of a thermal mismatch between the materials. At the interface between the reinforcement and matrix, these dislocations may cause phonon and electron scattering. In the current situation, it is shown that phonons and electrons both significantly contribute to improving a material's thermal conductivity. The critical energy transfer that takes place between photons and electrons at the contact is what allows for effective thermal conductivity. As the amount of cross-sectional area (CSA) rises, it is predicted that the density of dislocations would rise as well. The elastic strain field associated with the dislocation lines scatters phonons and electrons when dislocations are present [293]. The aforementioned elements significantly affect how much thermal conductivity hybrid composites have.

Fig. 4.16. shows the connection between second-phase particles and wear rate.

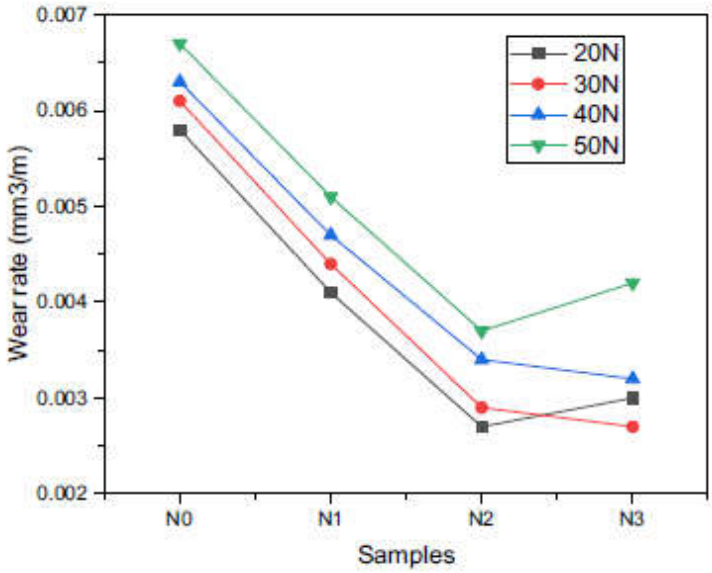

Fig. 4.16. Effect of reinforcement's % composition on wear rate under various loads.

Fig. 4.17. shows how the 2nd phase elements affect the fluctuation in the coefficient of friction.

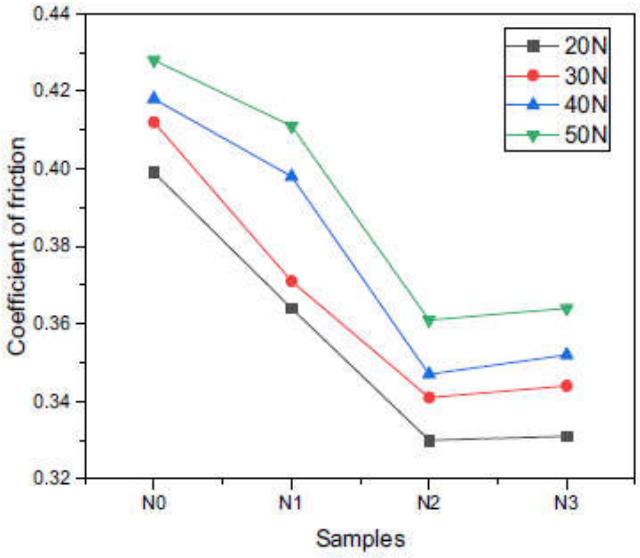

Fig. 4.17. Effect of the reinforcement's % composition on the friction coefficient under different loads.

In order to evaluate the resistance of the composite materials close to the sliding surface when exposed to fresh surfaces, the coefficient of friction and wear rate were determined. When there is less plastic deformation between the sliding material and the region of contact during sliding, the rate of wear is reduced. The existence of reinforced particles can be linked to the development of plastic deformation, which reduces the transfer of shear stress during sliding.

A new layer forms on the pin's surface as a result of the oxidation of metallic particles that occur during the sliding process. a translationally motion-formed stratum that exhibits deformation, delamination, and fracture. In order to prevent the dilution of contact surfaces, a fresh stratum is generated between mating surfaces [294, 295]. When compared to the base alloy, each composite specimen's wear rate consistently shows a reduction. The presence of CSA particles within the HMMCs lowers the coefficient of friction. The discharge of soft CSA particles acts as a solid lubricant during the wearing process, lowering the coefficient of friction. When pin surfaces roll or slide across the surface of the abrasive disc during rolling or sliding contact, a small-scale removal mechanism takes place, which results in the removal of material. The micro-cutting and micro-plowing processes are the main causes of abrasive wear. According to the results of the literature research, it has been shown that deformation occurs in circumstances with low levels of wear, principally because excessive wear and

micro-plowing conditions are present. The micro-cutting process is also responsible for deformation. The switch from micro-plowing to micro-cutting in HMMCs enhanced the wear resistance in the wear test against constant parameters such sliding distance, applied force, and sliding time. A modest amount of material displacement and a larger quantity of material removal occur in materials with strong wear characteristics. By using a micro-cutting mechanism, material is removed, resulting in the development of extremely small chips. On the other hand, the micro-plowing process causes material displacement, which results in the formation of a micro-edge.

Specimen N0, which is free of any reinforced particles, shows obvious indications of disintegration. The composite specimen that was created had improved wear resistance due to the addition of soft particles (CSA) and hard ceramic particles (Al2O3) to the aluminium matrix. A comparative study of specimen N2 with other composite specimens reveals that it has the least amount of wear.

Adhesion and delamination are the main wear processes seen in the basic alloys, as seen in **Fig. 4.18.**

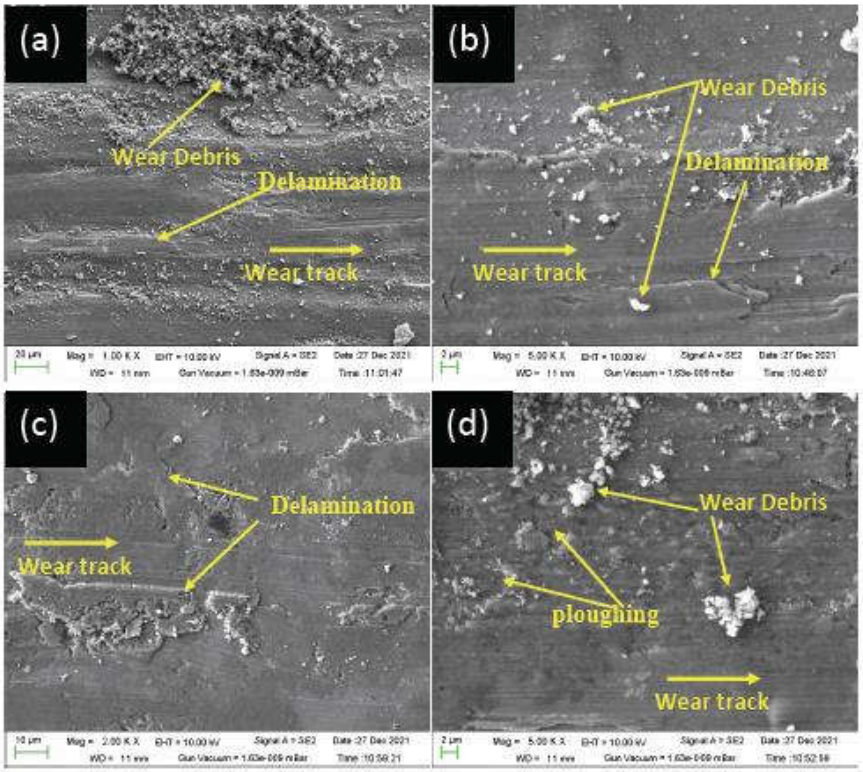

Fig. 4.18. Wear pattern of the (a) base alloy and (b-d) developed hybrid composite

There is proof that the land has been ploughed. It is possible to see a sizable plastic distortion in the direction of sliding, which denotes a greater level of wear. The prevalence of flake-shaped particles in the wear debris for N3 as seen in the scanning electron microscopy (SEM) picture suggests that delamination is the main cause of wear.

4.2 AA7075/Al2O3$_{np}$/CSA hybrid composites

4.2.1 Evaluation of Microstructure and XRD Analysis

Fig. 4.19(a–d) depicts the optical microstructure of the hybrid composite and base alloy samples.

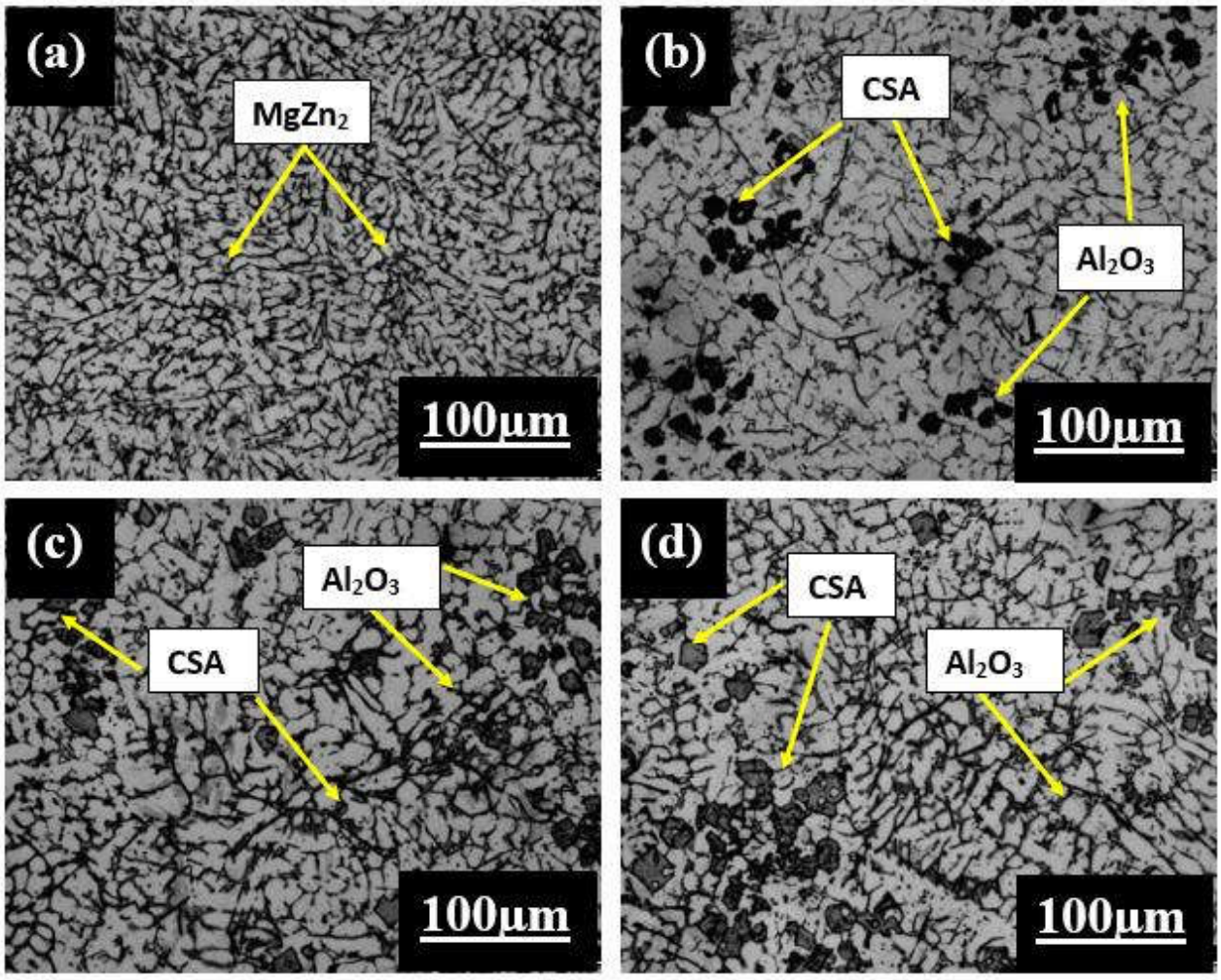

Fig. 4.19. The grain refinement for the dispersion of reinforcing particles is shown in optical metallographic pictures (a), (b), (c), and (d).

Evident uniform distributions of reinforced particles may be seen in the accompanying photos. Intermetallic phases including MgZn2, Al2CuMg, Al2Cu, Al7Cu2Fe, Mg2Si, Al13Fe4, and others have been seen to develop during the solidification of the 7075 aluminium alloy, according to earlier research [296]. A finely disseminated intermetallic phase, namely MgZn2, with a consistent distribution throughout the alloy matrix, is found in Sample M0 after analysis. Dislocations travel from one grain to the next while undergoing plastic deformation, crossing the boundaries separating distinct grains. When compared to the grain boundaries seen in the other samples, the grain boundaries of sample M0 show a much bigger size. Reinforcing chemicals like CSA and Al2O3 can be added to materials to improve their mechanical characteristics, which causes the creation of larger grain boundaries.

Fig. 4.19(b–d). shows the enlarged grain boundaries related to the strengthening of the particulate. Reinforcements operate as a barrier, preventing dislocations between neighbouring grains from moving in a certain direction and increasing the tensile strength. Due to the enhanced reinforcing distribution and decreased porosity in hybrid composite specimens, which results in the finer grain, multi-directional stresses are induced in composite samples as contrasted to the basic aluminium alloy.

The two-stage stir casting method must be used in order to achieve consistent CSA and Al2O3 particle dispersion inside the matrix. The CSA particles have a very low density as compared to Al2O3 and AA7075, which causes them to scatter throughout the molten material during the whole process. The CSA particles are manually incorporated into the semi-solid melt to extend their suspension. To achieve a state of homogeneity among the reinforced particles inside the matrix, it is crucial to choose the right conditions for ultrasonic stir casting.

Fig. 4.20. summarises the findings of the investigations performed on the as-cast samples using scanning electron microscopy (SEM) and energy dispersive X-ray spectroscopy (EDS). **Fig. 4.20(a-d).** The spreading of reinforcing elements inside the matrix is uniformly seen in the scanning electron microscope (SEM) pictures, indicating the high calibre of hybrid advanced materials composites (HAMCs).

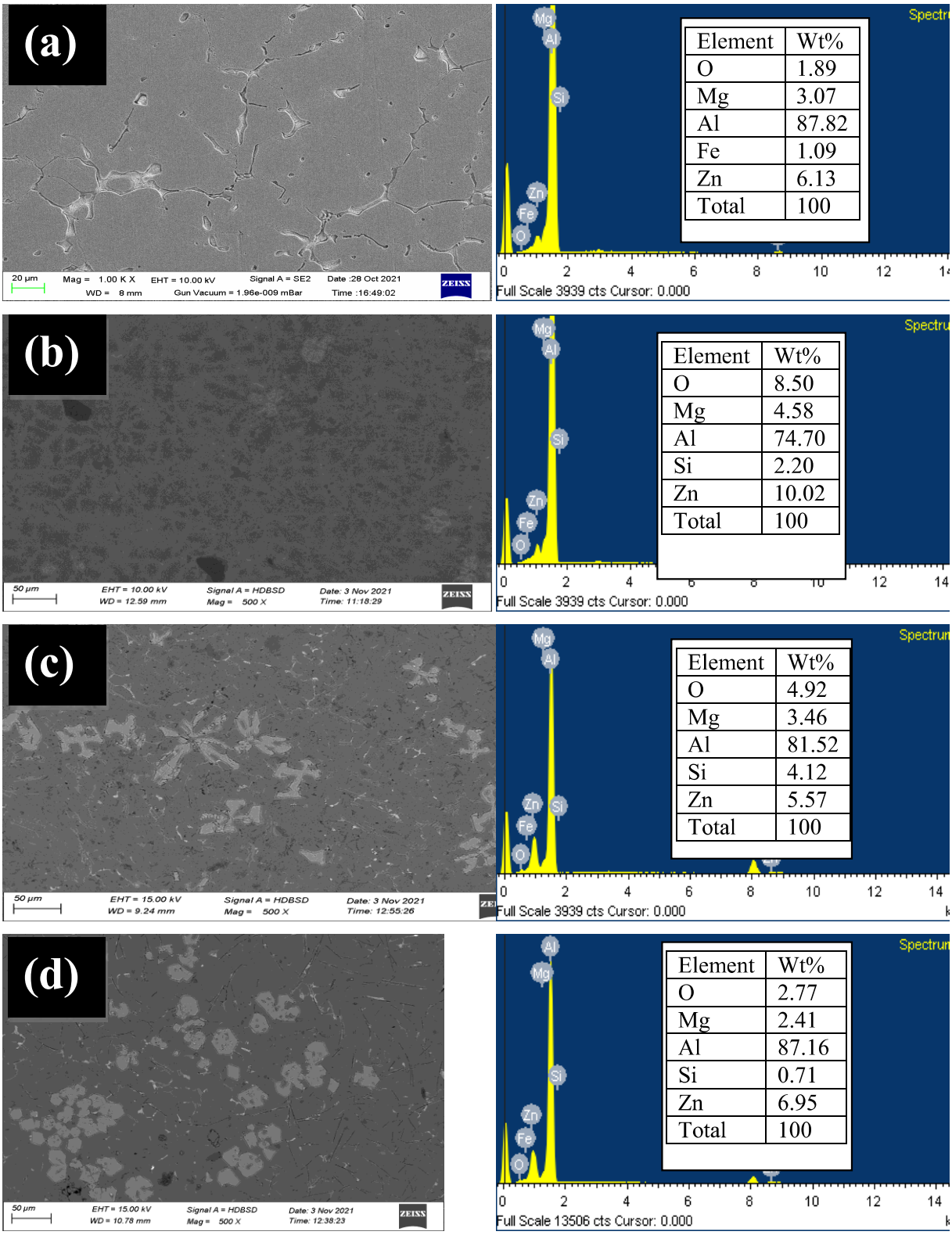

Fig. 4.20. SEM and EDS examination depicts the uniform dispersion reinforcing particles of (a) M-0, (b) M-1, (c) M-2, and (d) M-3.

The use of ultrasonic treatments causes a more uniform distribution of reinforcement throughout the matrix. The melting temperature of the reinforcements was more than that of the liquid aluminium alloy, thus a procedure was used that used a high molten temperature of 900°C to prevent cluster formation. Due to a thermal imbalance between the reinforcements and the matrix, the presence of high quantities of Al2O3 causes the creation of tiny clusters. Hard ceramics slow the solidification process down and make it easier for clusters to form when they are present near a liquid alloy. The difference in density between CSA and the aluminium matrix is one of the elements that help a cluster develop within the matrix. Cluster formation is reduced when ultrasonic treatment is used during the casting process. Additionally, CSA disposal offers a financially sensible and ecologically responsible way to improve environmental sustainability and cleanliness. In addition, the production process is more economically efficient.

Fig. 4.21. shows the fabricated specimen's X-ray diffraction (XRD) analysis. Multiple peaks are seen in the case of pure AA 7075 at various diffraction angles. Furthermore, it is shown that the peaks for the phases of Zn, Cu, and Mg overlap with the peaks for aluminium. The other elements have relatively low quantities, which are below the detection limit.

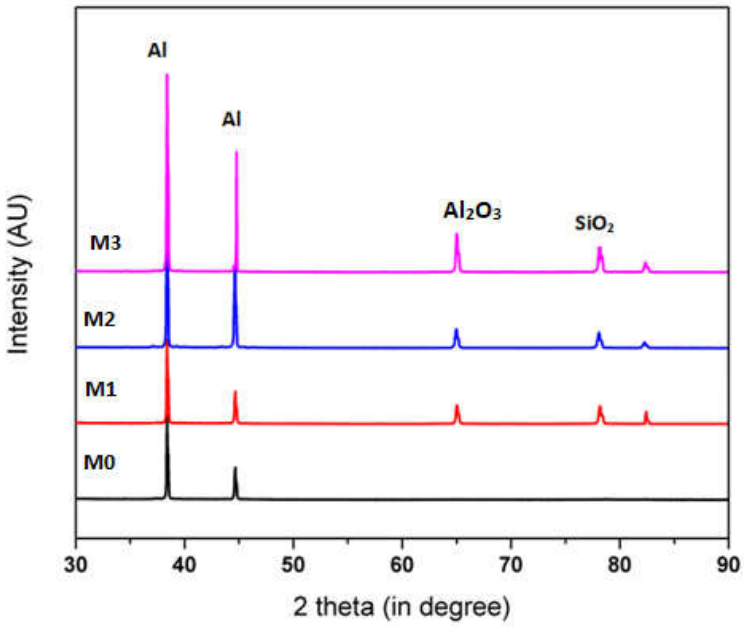

Fig. 4.21. Base alloy and manufactured composite specimen XRD analysis

It has been noted that there is a constant increase in the strength of Al2O3 peaks when the weight % of Al2O3 and CSA rises. The peaks connected to aluminium, on the other hand, showed diminished intensity and a modest shift towards greater two-theta angles. The lack of supplementary parts shows that the composites were cast successfully. The careful control of a number of casting process parameters, including reaction length or holding time, reaction temperature, melt stirring time, and ultrasonic treatment, is necessary to obtain this result.

4.2.2 Evaluation of Mechanical behaviors

The mechanical properties of metal matrix composites (MMCs) are influenced by the size and distribution of the reinforcements. It is crucial to investigate the relationship between the mechanisms for enhancing reinforcement and the distribution of reinforcement.

4.2.2.1 Density and Porosity

Fig. 4.22. shown in the study reveals density fluctuations. The experiment involves changing the reinforcement content's weight % at a value of **Fig. 4.22.**

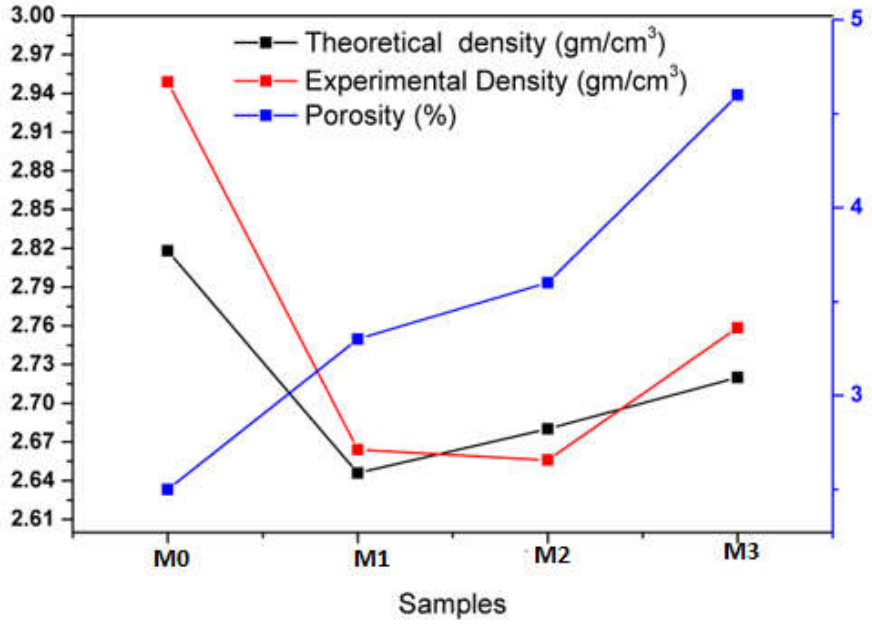

Fig. 4.22. Fluctuation in density when reinforced by a certain percentage.

According to published data, AA7075, Al2O3, and CSA have theoretical densities of 2.818 g/cc, 3.21 g/cc, and 0.48 g/cc, respectively. while calculating the theoretical density, Equation 1 is used, and while figuring out the experimental density, Equation 2.
The findings show that adding CSA content causes the density of the hybrid composite specimens to decrease. A similar outcome has been observed in the body of existing research, where the addition of rice husk ash causes a reduction in density and an increase in porosity in the composite material [297]. Due to the lower density, it is possible to hypothesise that the manufacture of lightweight aluminium hybrid composites might be done at a cost that is acceptable. Using Equation 3, it is possible to calculate the porosity of the composite material.

Sample M1 showed a drop in density of 17.8% when compared to the base alloy, sample M2 showed a loss of 18.3%, and sample M3 showed a decrease of 11.9%. The increase in porosity level and the growth of CSA particles were shown to be positively correlated. The dependability of this technology in the creation of hybrid composites is shown by the fact that the porosity shown in two-step ultrasonic stir casting is comparably lower than that seen in traditional stir casting. When a composite material's porosity is less than 4%, it is judged acceptable, claims a study [298]. At a weight of 9 units, it can be shown that based on the values in **Table 4.1.** The hybrid composite created for this investigation shows a tolerable maximum porosity of 4.6% for SiC.

4.2.2.2 Hardness

Fig. 4.23. shows the connection between increasing reinforcing particle density and increasing hardness. **Fig. 4.23.** When the reinforcement is increased, the hardness shows a rising tendency. The increased hardness is due to the matrix's increased fraction of reinforcing particles with higher difficulty [299]. The confined indentation zone gradually contains stiff silicon carbide particles, increasing the hardness. Dislocation movement is limited by the load-bearing capabilities of the Al2O3 particles implanted in the matrix. When reinforcement is used, the hardness value follows a similar rising trend, according to an earlier study [300].

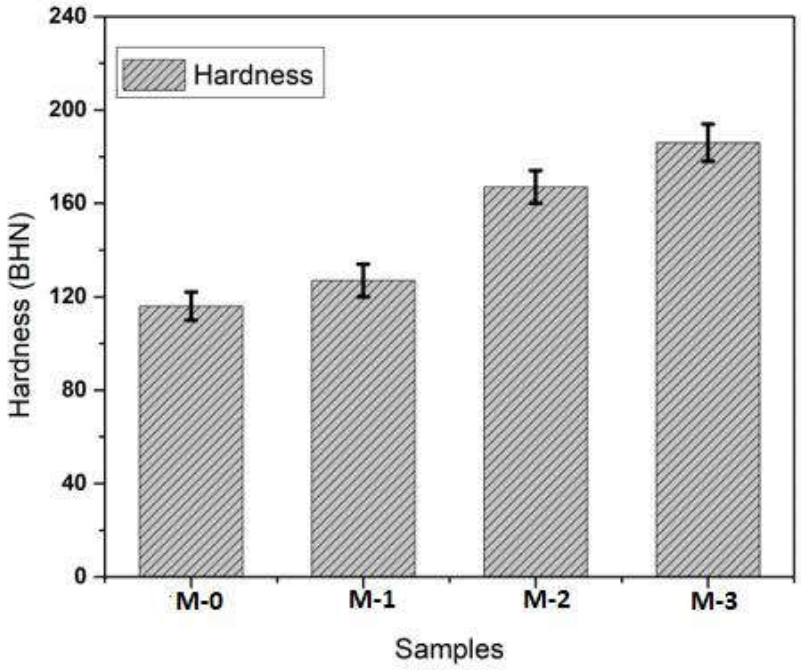

Fig. 4.23. Effects of reinforcing variation and hardness

The image in **Fig. 4.23.** The grain refining that takes place with greater Al2O3 and CSA reinforcement content levels is obviously shown. **Fig. 4.23.** The link between grain refining and the ensuing rise in hardness is governed by the Hall-Petch equation.

4.2.2.3 Tensile response

The ultimate tensile strength (UTS) of hybrid composites is noticeably improved when there are more ceramic particles present in the matrix. The better particle dispersion obtained throughout the manufacturing process is responsible for this improvement. The reason for the observed improvement is the strengthening effect brought on by the matrix bonding at the interface between the reinforcing particles. The M2 sample's maximum tensile strength was significantly increased by 35% as compared to the matrix. It was noted that the alloy AA7075's yield strength decreased in relation to its ultimate tensile strength when Al2O3 was added, following a similar trend. **Fig. 4.24.** demonstrates the relationship between engineering strain and stress. While the percentage elongation has been discovered to decrease, the weight ratios of Al2O3 and CSA in the composites have been seen to rise.

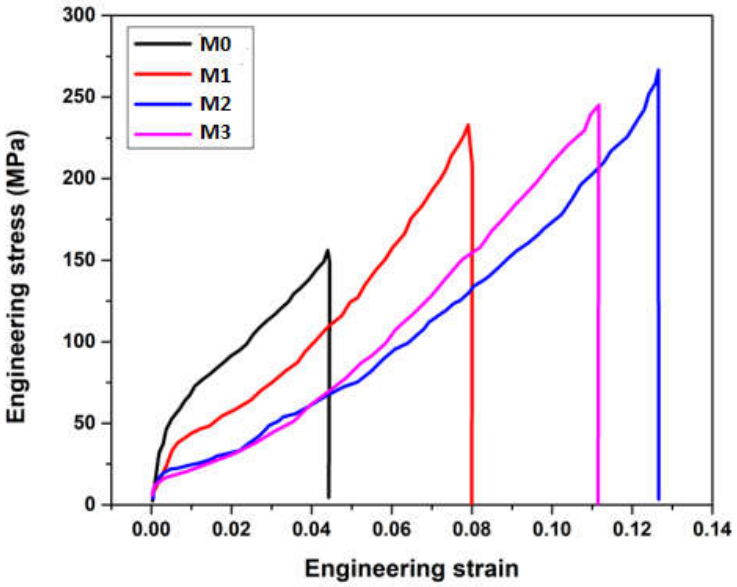

Fig. 4.24. Hybrid composite engineering stress-strain diagram

This implies that the composites' ductility has decreased. Hard Al2O3 and CSA are present in the hybrid composites, which increases brittleness and decreases ductility. A mixture of Al2O3 and CSA particles is distributed uniformly throughout the composite material. This uniform distribution was accomplished using the best stirring methods, and the improvement in ultimate tensile strength (UTS) is connected to it. See **Fig. 4.25.** shows the tensile properties of the created hybrid composites.

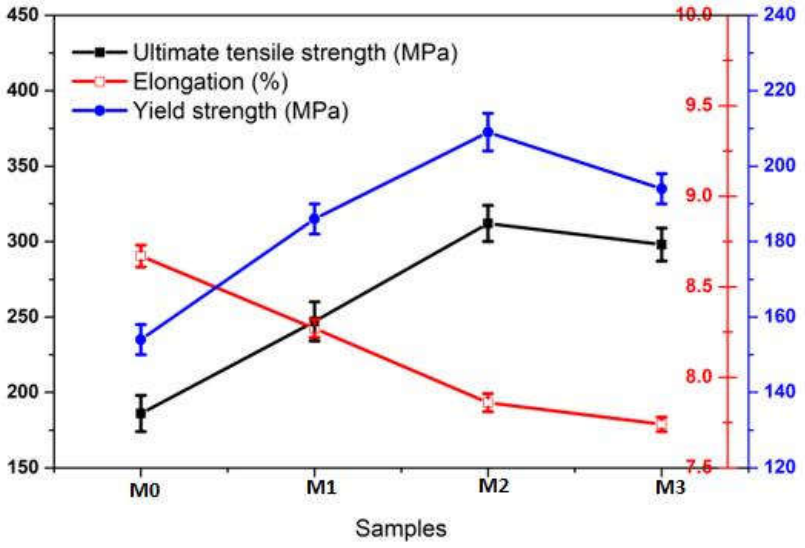

Fig. 4.25. Behaviour of the manufactured hybrid composites under tension.

Incorporating evenly distributed reinforcements helps hybrid composites meet the Orowan strengthening requirements [301] by limiting the mobility of dislocations and thus increasing their tensile strength. The tensile strength of the aluminium matrix improved similarly with the addition of Al2O3. In particular, the M3 sample's ultimate tensile strength (UTS) rose by around 32% in comparison to the base alloy matrix. The strengthening of interfacial connection between the components is responsible for this improvement [302]. The use of SiC and WC as reinforcements in composites has boosted ultimate tensile strength (UTS) and yield strength, according to the cited paper [303]. The development of volumetric strain around the reinforced particles is caused by the existence of a significant difference in the thermal expansion coefficients between the matrix and the reinforced particles. As a result, geometrically necessary dislocation (GND) loops arise. As a result of this event, the composites' strength was improved. The total tensile strength of the composite material is increased as a result of the presence of dislocations near Al2O3 particles, which inhibit the propagation of fractures under tensile loading conditions. Consistent findings from research on the mechanical characteristics and strengthening processes of AA5052/ZrB2 suggest that increasing the amount of ZrB2 particles increases strength [304]. With an increasing weight % of Al2O3 particles and a constant amount of CSA, the dislocation motions and resistance to fracture propagation showed an increased trend. As a result, the mechanical qualities were improved.

The various forms of failure that occur during the tensile test are analysed using the structural equation modelling factor graphs shown in **Fig. 4.26.** The ductile and brittle fracture processes in Metal Matrix Composites (MMCs) were studied by the researchers. The research's findings show that the AA7075Fig basal material has a large number of dendritic globules. According to **Fig. 4.26 (a).**, dendritic fractures have been seen in hybrid composites (305). **Fig. 4.26(b-d).** shows the dendritic microstructure of the hybrid composites reinforced with Al2O3 and CSA. The phenomena are illustrated in section **Fig. 4.26 (b-d).** functions as both a stress riser and a weak zone, finally resulting in the beginning of fractures [306]. The interaction between the ceramic particles and the alloy matrix interface, which operate as sites of stress concentration, promotes the spread of fractures along dendritic boundaries.

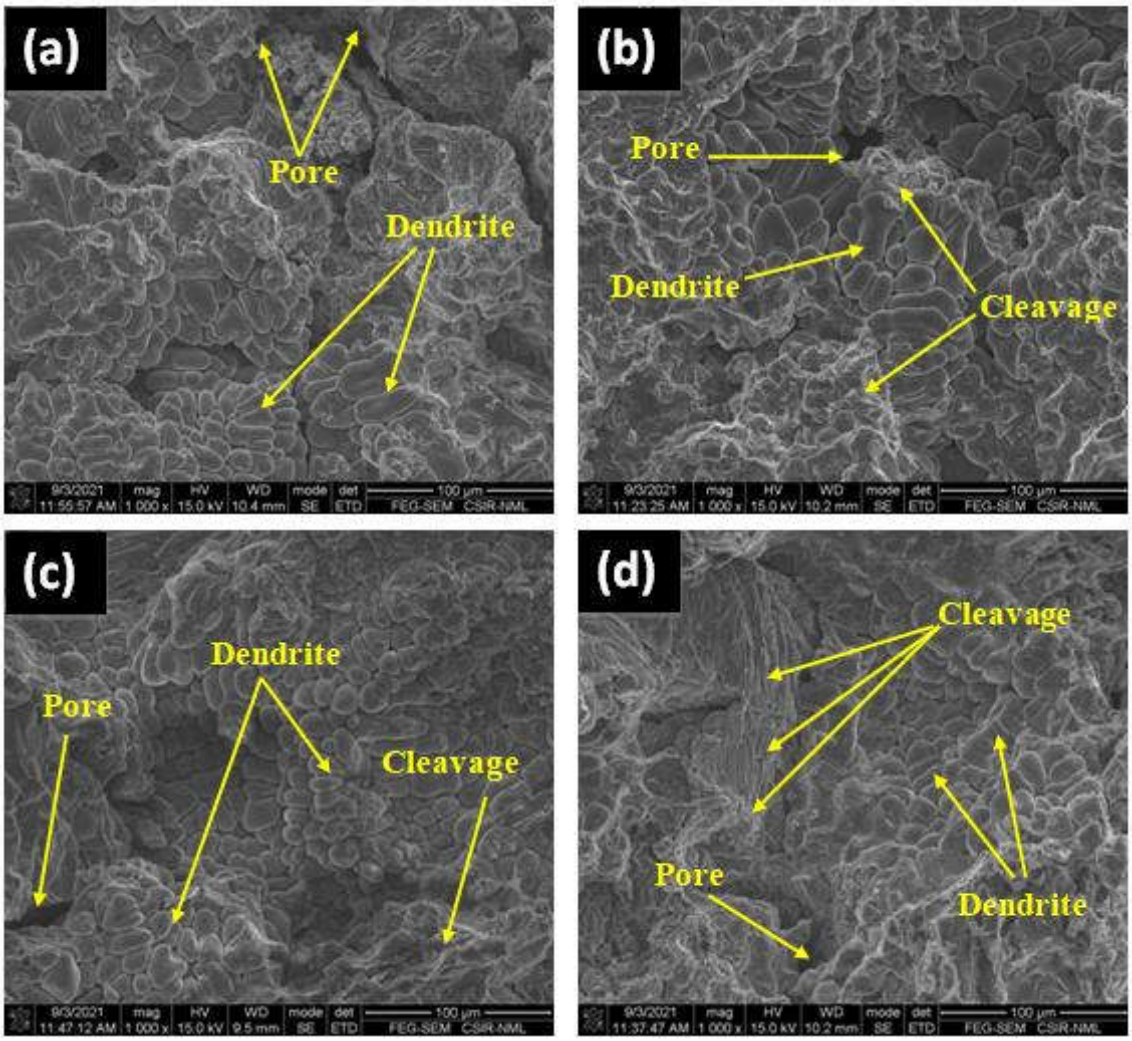

Fig. 4.26. The composite specimen's tensile specimens' fracture surface.

At the interfaces between ceramic particles and the soft alloy matrix material, microcracks are further produced, gradually displaying a dendritic structure. The failure of hybrid composites as a suitable alloy is supported by the observation of inter-dendritic stepwise dendrites and trans-granular cleavage facets on the fracture surface fractographs, as shown in **Fig. 4.26(b).** and **Fig 4.26(c).**, Figure. The results show that specimen M2, when compared to both the base alloy and specimen M3, had fewer microcracks and vacancies.

4.2.2.4 Coefficient of thermal expansion and thermal conductivity

The connection between the weight % of Al2O3 and CSA in each sample and the coefficient of thermal expansion over the temperature range of 25 to 200 °C is shown in **Fig. 4.27.**

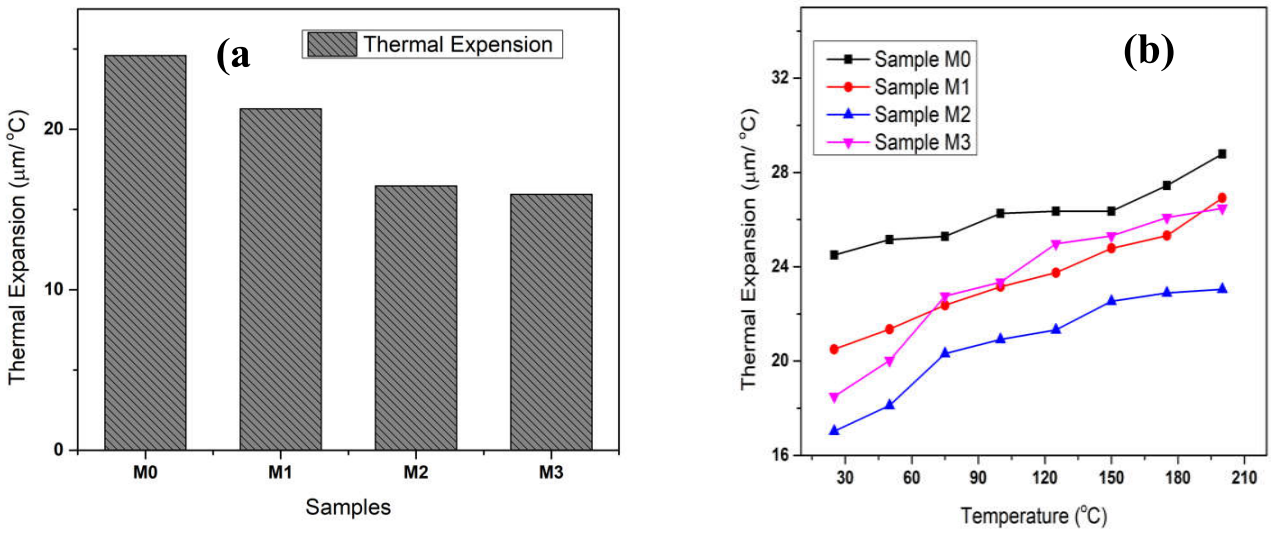

Fig. 4.27. A variation in each sample's thermal expansion coefficient at different temperatures (b) as compared to (a) room temperature

The coefficient of thermal expansion (CTE) of the composite material under consideration has been seen to decrease when a larger concentration of CSA particles is present together with an equivalent amount of alumina. In comparison to the AA7075 basic material, the hybrid composites' CTE value is reduced. Low coefficients of thermal expansion (CTE) are characteristic of ceramic materials like calcium aluminate (CSA) and aluminium oxide (Al2O3). The coefficients of thermal expansion (CTE) of the hybrid composite are expected to be reduced as a result of the addition of these reinforcements to the base alloy matrix. Aluminium alloys have a higher-than-average coefficient of thermal expansion (CTE), which makes them more susceptible to dimensional instability as temperature increases.

Considering various weight fractions of CSA, **Fig. 4.28.** shows the thermal conductivity of the base alloy AA7075 and /Al2O3/ CSA composites at various temperatures. **Fig. 4.28.** It was found that the heat conductivity of hybrid composites was significantly less than that of the basic alloy. The processing technique used, the thermal conductivity and wettability of the reinforcing elements, and the microstructure all have a major impact on the thermal conductivity of hybrid composites [24, 25].

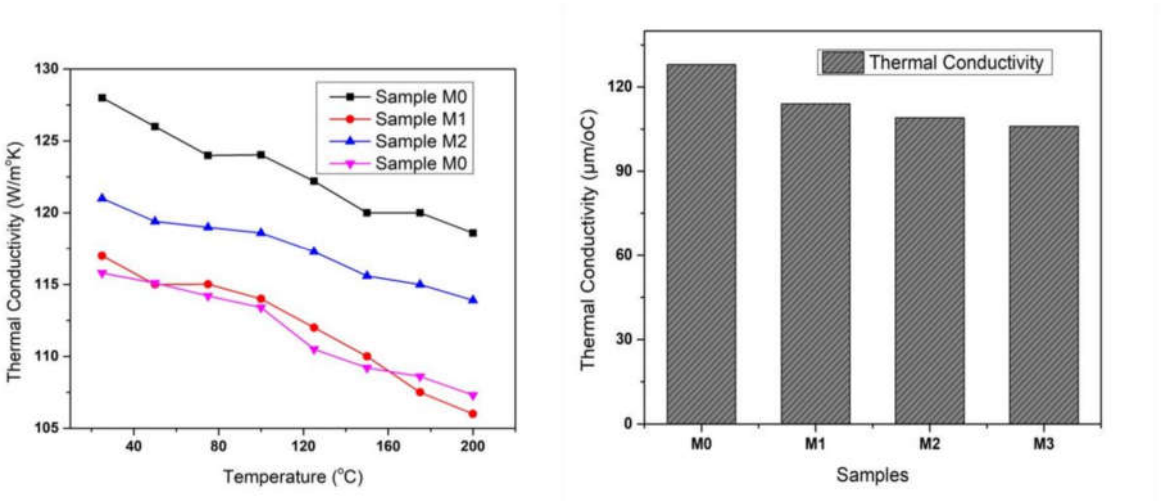

Fig. 4.28. Variation in each sample's thermal conductivity (a) at ambient temperature (b) at various temperatures

4.2.2.5 Tribological Behavior

Fig. 4.29. shows a graphical depiction of the wear rate variations for various reinforcement combinations.

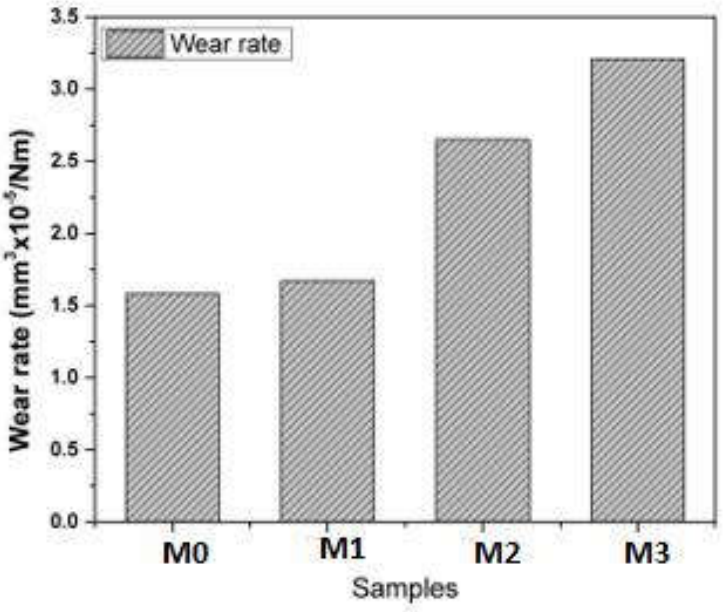

Fig. 4.29. Variation in the rate of wear for various combinations of reinforced particles.

Among all cast goods, the unreinforced AA7075 is determined to have the greatest wear rate, whereas sample M3 has the lowest wear rate. **Fig. 4.30(a-d).** shows the wear rate of

AA7075 and hybrid composites at various sliding distances under 10N and 20N loads. As the sliding distance grows, the wear rate shows an increasing trend that is predominantly caused by frictional forces between the in-contact surfaces.

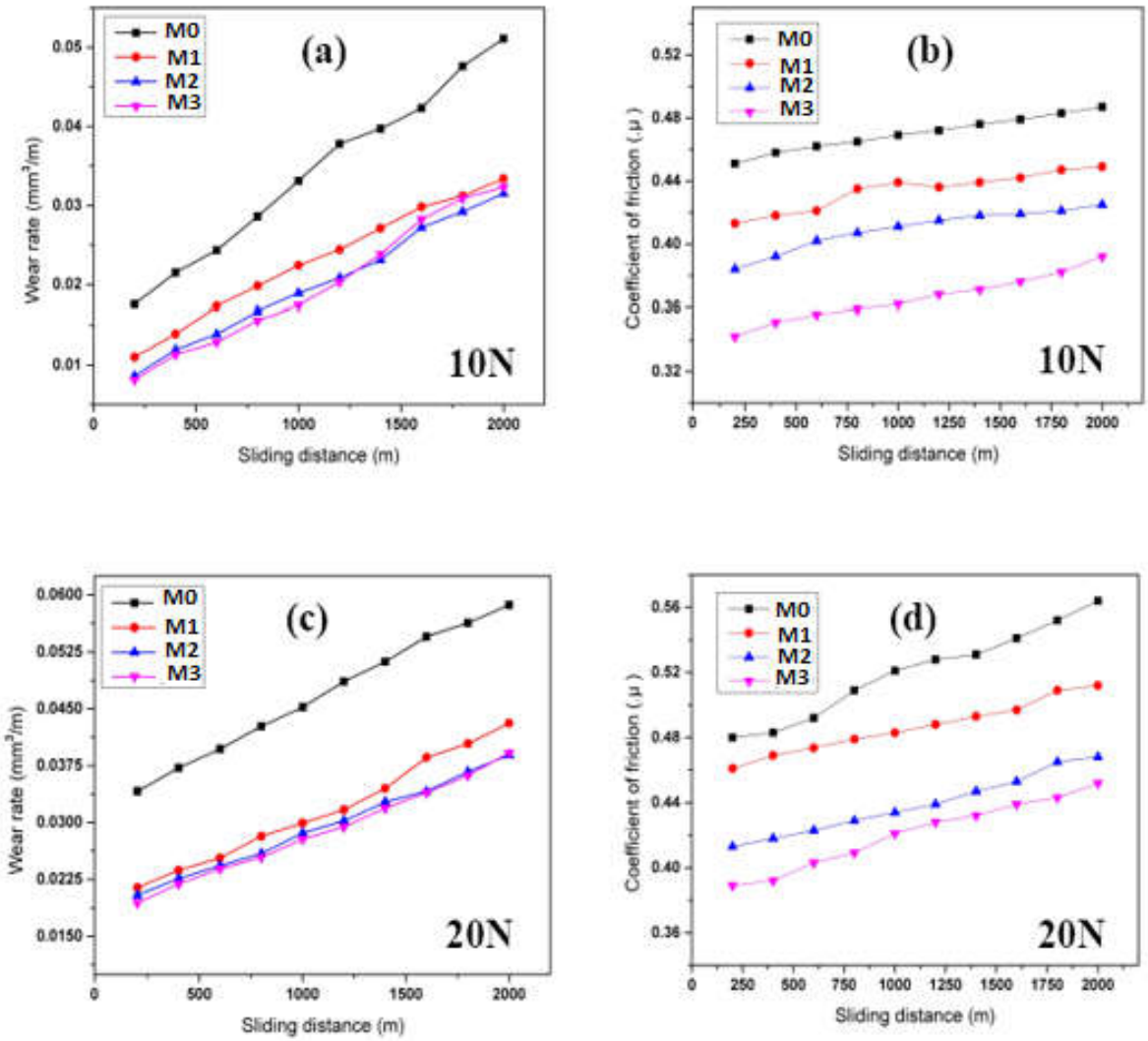

Fig. 4.30. (a-d) Variation in the wear rate and friction coefficient with sliding distance at loads of 10N and 20N

It has been shown that the temperature rise is inversely proportional to the separation between the contacting surfaces. This behaviour can be linked to frictional forces operating on the surfaces, which cause the pin material to soften and the contact point to subsequently be harmed. As a result, the monolithic alloy continues to wear as a result of this process [307]. In comparison to the base alloys, the wear resistance of the Al2O3 and CSA-reinforced hybrid composites showed a significant improvement, which can be mostly

attributed to the hardness improvement's large reduction in wear. Similar results were seen when SiC and fly ash were used to form a composite material, which was then stir cast into an AA2024 matrix [308].

Comparing specimens M1, M2, and M3 to specimens M0 reveals an increase in wear resistance, which may be attributed to a comparable rise in hardness brought on by a larger proportion of reinforcements. The load is the tribological parameter that has the greatest impact, as can be seen from the graphical trend [309]. Due to the amplified frictional forces, it has been discovered that material deterioration and temperature rise simultaneously with an increase in load. Similar trends were seen in the earlier investigation [310].

Both the composite surfaces and the metal contact surfaces are seen to develop oxide layers when the load is not very high. The tribological qualities are significantly influenced by the presence of oxide layers, which results in a major decrease in the coefficient of friction (COF) and the rate of wear. As the load is applied, the temperature at the interface of the contact surfaces rises proportionately, causing the oxide layers to gradually erode.

Layer development at contact surfaces is no longer prevented by the existence of oxide layers. As a result of the increased grain, which results from the development of frictional heat, the pin material softens [311]. This phenomenon happens as a result of wear, which causes the contact area to enlarge and the delimitation to shift as the applied stress rises. Fig. 4.30(c, d). shows the coefficient of friction (COF) at a maximum load of 20 N. The results are in section Fig. 4.30(c, d). show that the coefficient of friction (COF) decreases as the weight percentage (wt%) of silicon carbide (SiC) rises relative to the base alloy when there is a lubricating layer between self-mated couplings. According to reference [312], this effect leads to a more polished contact surface and a lower COF. The worn specimens' scanning electron microscopy (SEM) investigation revealed a variety of wear processes connected to various forms of reinforcement. According to **Fig. 4.31(a).**, adhesion and delamination are the main wear processes seen in the basic alloys. There is proof that the land has been ploughed. It is possible to see a sizable plastic distortion in the direction of sliding, which denotes a greater level of wear. **Fig. 4.31(b).** shows a similar shape for M1 in this case. **Fig. 4.31(b).** The adhesion and delamination processes demonstrate substantially reduced strength when the basic composition is contrasted. Additionally,

Figure X shows how decohesion damage manifests itself. In **Fig. 4.31(c).**, the behaviour is likewise related to surface damage. The main wear mechanism seen in the M2 is delamination wear.

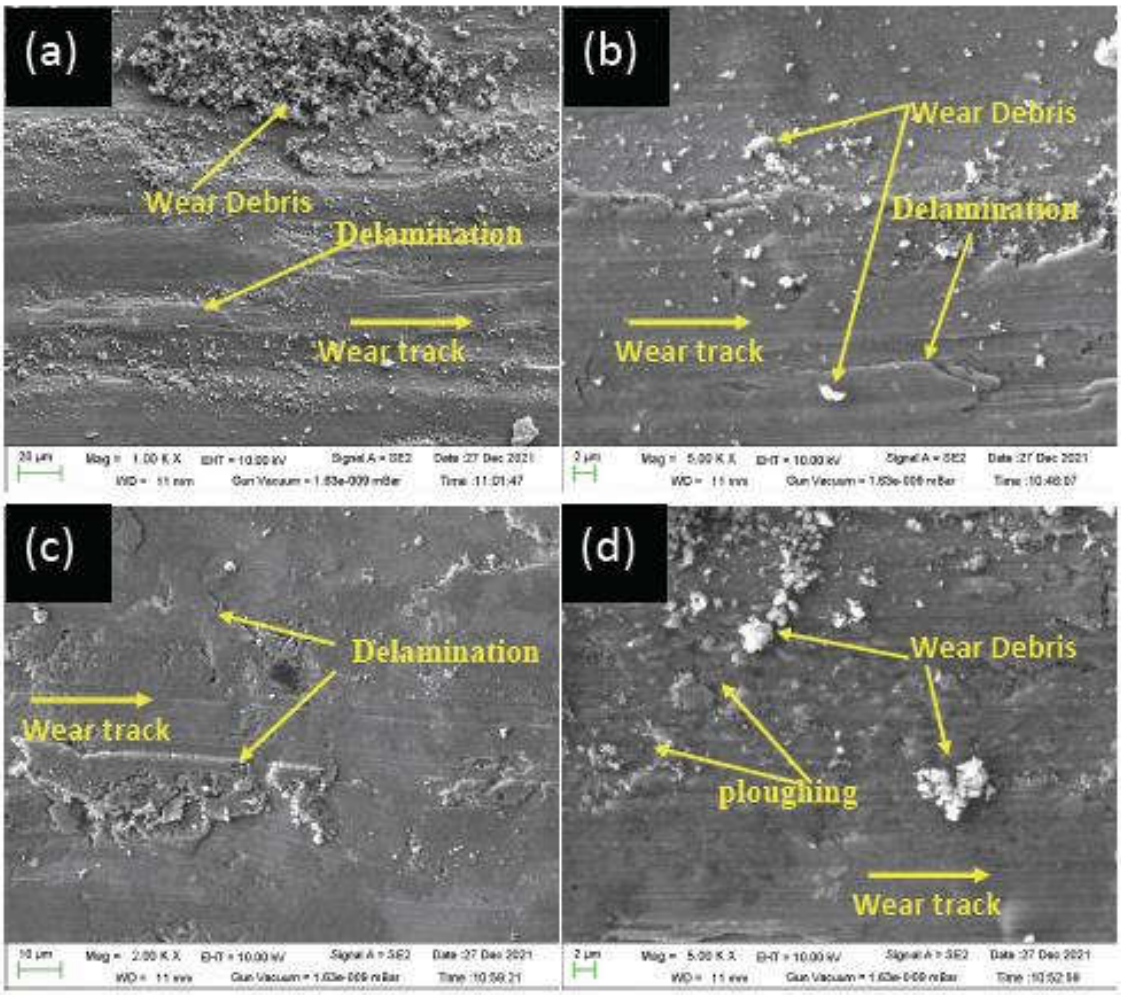

Fig. 4.31. (a-d) Developed composite's worn-surface morphology.

The prevalence of flake-shaped particles in the wear debris for M3 as seen in the scanning electron microscopy (SEM) picture suggests that delamination is the main cause of wear. The process of delamination is essentially nonexistent when there are higher concentrations of Al2O3, as seen in **Fig. 4.31(d).**, where ploughing is the predominant mechanism of abrasive wear. [49]. Previous research has shown that when the amount of reinforcing component rises, the wear mechanism changes from delamination wear to abrasive wear [313]. As a result of the presence of stiff ceramic particles, a noticeable reduction in plastic deformation is also seen.

CHAPTER 5
CONCLUSIONS AND FUTURE SCOPE

5.1. Conclusions

The following results were reached after the current study effort examined the effect of percentage reinforced particles Al2O3/CSA in AA7075 alloy:

- Al2O3 and CSA reinforced particles are uniformly distributed throughout the Al matrix, as shown in optical microscopy and SEM pictures. SEM with EDX analysis confirms the presence of reinforcements in the developed hybrid composite.
- By including Al2O3 and CSA reinforced particles in the Al matrix, hybrid composite's hardness is increased. The sample N3 with the highest hardness value (142 BHN) was With the inclusion of Al2O3 and CSA particles, the impact strength for each specimen of a hybrid composite decreases.
- The ultimate tensile strength of the hybrid composite increases with the addition of Al2O3 and CSA particles while dropping in the N3 specimen. With a 292MPa ultimate tensile strength, the N2 specimen tops the list. Transgranular facet, micro-void coalescence, dimples, and fractures were seen on surfaces that had undergone tensile and impact cracking.
- The CTE of the generated hybrid composites dropped while displaying improved dimensional stability as the CSA and alumina content rose.
- However, the poor thermal conductivity values of the reinforcements and the lack of effective electron-phonon coupling as a result of the electron and phonon scattering at the interface were the key reasons why the thermal conductivity was not enhanced.
- The fabrication of the hybrid composites exhibited considerably improved tribological behaviours because to the addition of Al2O3 and CSA. Comparing the composite specimen to the monolithic alloy, the wear rate was 51% lower.
- Higher Al2O3 concentrations make ploughing, the primary abrasive wear mechanism, readily apparent while almost eliminating the delamination process.

5.2. Future work

- ❖ According to this inquiry, the automotive and aerospace industries are using some of the proposed hybrid composite's possible applications as candidate materials.
- ❖ In the future, the researchers can expand on this study by doing in-depth research on the MMC's corrosion and fatigue behaviour.
- ❖ In this investigation, the composites' performance was assessed in their as-cast state.
- ❖ By redoing the experiments under mechanical working and heat-treated circumstances, future researchers can broaden the scope of this work.

REFERENCES

[1] K. Saidi and A. Omri, “Reducing CO2 emissions in OECD countries: Do renewable and nuclear energy matter?,” Prog. Nucl. Energy, vol. 126, p. 103425, 2020 [doi:10.1016/j.pnucene.2020.103425].

[2] J. J. Santin, C. H. Onder, J. Bernard, D. Isler, P. Kobler, F. Kolb, N. Weidmann, and L. Guzzella, “The World's Most Fuel-Efficient Vehicle: Design and Development of Pac Car II.” vdf Hochschulverlag AG, 2007.

[3] M. Kumar, Z. Shao, Z., Braun, C. and A. Bandivadekar, “Decarbonizing India’s Road Transport: A Meta-analysis of Road Transport Emissions Models”, 2022.

[4] M. Tisza and I. Czinege, “Comparative study of the application of steels and aluminium in lightweight production of automotive parts,” Int. J. Lightweight Mater. Manuf., vol. 1, no. 4, pp. 229-238, 2018 [doi:10.1016/j.ijlmm.2018.09.001].

[5] D. A. Baker and T. G. Rials, “Recent advances in low-cost carbon fiber manufacture from lignin,” J. Appl. Polym. Sci., vol. 130, no. 2, pp. 713-728, 2013 [doi:10.1002/app.39273].

[6] W. J. Joost, “Reducing vehicle weight and improving US energy efficiency using integrated computational materials engineering,” JOM, vol. 64, no. 9, pp. 1032-1038, 2012 [doi:10.1007/s11837-012-0424-z].

[7] D. Kumar, J., Jain, and N. N. Gosvami, “Macroscale to nanoscale tribology of magnesium-based alloys: A review,” Tribol. Lett., vol. 70, no. 1, p. 27, 2022 [doi:10.1007/s11249-022-01568-5].

[8] R. Hoogma, R. Kemp, J. Schot, and B. Truffer, Experimenting for Sustainable Transport. Taylor & Francis, 2002.

[9] W. S. Miller, L. Zhuang, J. Bottema, A. Wittebrood, P. De Smet, A. Haszler, and A.J.M.SA. Vieregge, vol. 280, no. 1, pp. 37-49, 2000 [doi:10.1016/S0921-5093(99)00653-X].

[10] R. Huang, M. Riddle, D. Graziano, J. Warren, S. Das, S. Nimbalkar, J. Cresko, and E. Masanet, 2016. “Energy and emissions saving potential of additive manufacturing: The case of lightweight aircraft components,” J. Cleaner Prod., vol. 135, pp. 1559-1570, 2016 [doi:10.1016/j.jclepro.2015.04.109].

[11] T. Dursun and C. Soutis, “Recent developments in advanced aircraft aluminium alloys,” Mater. Des. (1980–2015), vol. 56, pp. 862-871, 2014 [doi:10.1016/j.matdes.2013.12.002].

[12] A. S. Warren, “Developments and challenges for aluminium—A boeing perspective” in Mater. Forum, vol. 28, pp. 24-31, 2004.

[13] K. Nishino, “Development of fuel economy regulations and impact on automakers.” Mitsui Global Strategic Studies Institute [Monthly report], 2017.

[14] IHS, Light Vehicle Production from 2016 to 2024, by Major Market (in Million Units). Statista, 2017.

[15] A. Taub, E. De Moor, A. Luo, D. K. Matlock, J. G. Speer, U. and Vaidya, “Materials for automotive lightweighting,” Annu. Rev. Mater. Res., vol. 49, no. 1, pp. 327-359, 2019 [doi:10.1146/annurev-matsci-070218-010134].

[16] R. Lagneborg, “New steels and steel applications for vehicles,” Mater. Des., vol. 12, no. 1, pp. 3-14, 1991 [doi:10.1016/0261-3069(91)90086-J].

[17] M. J. Nunney, Light and Heavy Vehicle Technology. Routledge, 2007.

[18] S. Panthapulakkal, L. Raghunanan, M. Sain, B. KC, and J. Tjong, “Natural fiber and hybrid fiber thermoplastic composites: Advancements in lightweighting applications” in Green Composites. Woodhead Publishing, 2017, pp. 39-72.

[19] P. L. Kumar, A. Lombardi, G. Byczynski, S. N. Murty, B. S. Murty, and L. Bichler, “Recent advances in aluminium matrix composites reinforced with graphene-based nanomaterial: A critical review,” Prog. Mater. Sci., p. 100948, 2022.

[20] Y. Li, J. Liu, W. Huang, and S. Zhang, “Microstructure related analysis of tensile and fatigue properties for sand casting aluminium alloy cylinder head,” Eng. Fail. Anal., vol. 136, p. 106210, 2022 [doi:10.1016/j.engfailanal.2022.106210].

[21] P. Rohatgi, “Cast aluminium-matrix composites for automotive applications,” JOM, vol. 43, no. 4, pp. 10-15, 1991 [doi:10.1007/BF03220538].

[22] S. P. Rawal, “Metal-matrix composites for space applications,” JOM, vol. 53, no. 4, pp. 14-17, 2001 [doi:10.1007/s11837-001-0139-z].

[23] Q. Dai, J. Kelly, and A. Elgowainy, “Vehicle Materials: Material Composition of US Light-Duty Vehicles”. Chicago, USA: Energy Systems Division, Argonne National Labs, 2016, pp. 1-30.

[24] D. B. Miracle, “Metal matrix composites–from science to technological significance,” Compos. Sci. Technol., vol. 65, no. 15-16, pp. 2526-2540, 2005 [doi:10.1016/j.compscitech.2005.05.027].

[25] P. K. Krishnan, “Fabrication and application of aluminium metal matrix composites” in Adv. Manuf. Tech. Eng. Engineered Mater., pp. 133-151.

[26] M. Y. Zhou, L. B. Ren, L. L. Fan, Y. W. X. Zhang, T. H. Lu, G. F. Quan, and M. Gupta, “Progress in research on hybrid metal matrix composites,” J. Alloys Compd., vol. 838, p. 155274, 2020 [doi:10.1016/j.jallcom.2020.155274].

[27] A. Ramanathan, P. K. Krishnan, and R. Muraliraja, “A review on the production of metal matrix composites through stir casting–Furnace design, properties, challenges, and research opportunities,” J. Manuf. Processes, vol. 42, pp. 213-245, 2019 [doi:10.1016/j.jmapro.2019.04.017].

[28] L. Poovazhagan, K. Kalaichelvan, A. Rajadurai, and V. Senthilvelan, “Characterization of hybrid silicon carbide and boron carbide nanoparticles-reinforced aluminium alloy composites,” Procedia Eng., vol. 64, pp. 681-689, 2013 [doi:10.1016/j.proeng.2013.09.143].

[29] G. Moona, R. S. Walia, V. Rastogi, R. and Sharma, “Aluminium metal matrix composites: A retrospective investigation,” Indian J. Pure Appl. Phys. (IJPAP), vol. 56, no. 2, pp. 164-175, 2018.

[30] S. Singh, S. Gangwar, and S. Yadav, “A review on mechanical and tribological properties of micro/nano filled metal alloy composites,” Mater. Today Proc., vol. 4, no. 4, pp. 5583-5592, 2017 [doi:10.1016/j.matpr.2017.06.015].

[31] S. C. Yoo, D. Lee, S. W. Ryu, B. Kang, H. J. Ryu, and S. H. Hong, “Recent progress in low-dimensional nanomaterials filled multifunctional metal matrix nanocomposites,” Prog. Mater. Sci., vol. 132, p. 101034, 2023 [doi:10.1016/j.pmatsci.2022.101034].

[32] V. Khanna, V. Kumar, and S. A. Bansal, “Mechanical properties of aluminium-graphene/carbon nanotubes (CNTs) metal matrix composites: Advancement, opportunities

and perspective," Mater. Res. Bull., vol. 138, p. 111224, 2021 [doi:10.1016/j.materresbull.2021.111224].

[33] H. Sun, F. Saba, G. Fan, Z. Tan, and Z. Li, "Micro/nano-reinforcements in bimodal-grained matrix: A heterostructure strategy for toughening particulate reinforced metal matrix composites," Scr. Mater., vol. 217, p. 114774, 2022 [doi:10.1016/j.scriptamat.2022.114774].

[34] S. A. Sajjadi, M. T. Parizi, H. R. Ezatpour, and A. Sedghi, "Fabrication of A356 composite reinforced with micro and Nano Al2O3 particles by a developed compocasting method and study of its properties," J. Alloys Compd., vol. 511, no. 1, pp. 226-231, 2012 [doi:10.1016/j.jallcom.2011.08.105].

[35] V. Chak, H. Chattopadhyay, and T. L. Dora, "A review on fabrication methods, reinforcements and mechanical properties of aluminium matrix composites," J. Manuf. Processes, vol. 56, pp. 1059-1074, 2020 [doi:10.1016/j.jmapro.2020.05.042].

[36] A. K. Singh, S. Soni, and R. S.Rana, "A critical review on synthesis of aluminium metallic composites through stir casting: Challenges and opportunities," Adv. Eng. Mater., vol. 22, no. 10, p. 2000322, 2020 [doi:10.1002/adem.202000322].

[37] Q. Wang, "Evaluation of a new high temperature cast aluminium for cylinder head applications" in Proc. 122nd Metalcasting Congress, Fort Worth, TX, USA, 2018, pp. 3-5.

[38] K. P. Bloschock and A. Bar-Cohen, "Advanced thermal management technologies for defense electronics" in Def. Transform. Net-Centric Syst. SPIE, vol. 8405, pp. 157-168, 2012 [doi:10.1117/12.924349].

[39] Z. Baig, O. Mamat, and M. Mustapha, "Recent progress on the dispersion and the strengthening effect of carbon nanotubes and graphene-reinforced metal nanocomposites: A review," Crit. Rev. Solid State Mater. Sci., vol. 43, no. 1, pp. 1-46, 2018 [doi:10.1080/10408436.2016.1243089].

[40] A. Bahrami, N. Soltani, M. I Pech-Canul, and C. AGutiérrez, "Development of metal-matrix composites from industrial/agricultural waste materials and their derivatives," Crit. Rev. Environ. Sci. Technol., vol. 46, no. 2, pp. 143-208, 2016 [doi:10.1080/10643389.2015.1077067].

[41] D. Kumar, S. Angra, S. and S. Singh "Mechanical properties and wear behaviour of stir cast aluminium metal matrix composite: A review," Int. J. Eng., vol. 35, no. 4, pp. 794-801, 2022 [doi:10.5829/IJE.2022.35.04A.19].

[42] Available at: https://advance-composite.co.jp/en/combine-two-or-morematerials/.

[43] T. W. Clyne and P. J. Withers, An Introduction to Metal Matrix Composites. Cambridge University Press, 1995.

[44] J. D. Eshelby, “The determination of the elastic field of an ellipsoidal inclusion, and related problems,” Proc. R. Soc. Lond. A Math. Phys. Sci., vol. 241, no. 1226, pp. 376-396, 1957.

[45] A. J. Cyriac, Metal Matrix Composites: History, Status, Factors and Future. Oklahoma State University, 2011.

[46] D. B. Miracle, “Metal matrix composites–from science to technological significance,” Compos. Sci. Technol., vol. 65, no. 15-16, pp. 2526-2540, 2005 [doi:10.1016/j.compscitech.2005.05.027].

[47] D. B. Miracle and W. H. Hunt, Automotive Applications of Metal Matrix Composites. Aluminium Consultant Group Inc., 2004, pp. 1029-1032.

[48] C. Elanchezhian, B. V. Ramnath, G. Ramakrishnan, K. S. Raghavendra, M. Muralidharan, and V. Kishore, “Review on metal matrix composites for marine applications,” Mater. Today Proc., vol. 5, no. 1, pp. 1211-1218, 2018 [doi:10.1016/j.matpr.2017.11.203].

[49] M. P. Reddy, R. A. Shakoor, G. Parande, V. Manakari, F. Ubaid, A. M. A. Mohamed, and M. Gupta, “Enhanced performance of nano-sized SiC reinforced Al metal matrix nanocomposites synthesized through microwave sintering and hot extrusion techniques,” Prog. Nat. Sci. Mater. Int., vol. 27, no. 5, pp. 606-614, 2017 [doi:10.1016/j.pnsc.2017.08.015].

[50] A. Kumar, Kumar, R. C. Singh, and R. Chaudhary, “Recent progress in production of metal matrix composites by stir casting process: An overview,” Mater. Today Proc., vol. 21, pp. 1453-1457, 2020 [doi:10.1016/j.matpr.2019.10.079].

[51] S. V. Prasad and R. Asthana, “Aluminium metal-matrix composites for automotive applications: Tribological considerations,” Tribol. Lett., vol. 17, no. 3, pp. 445-453, 2004 [doi:10.1023/B:TRIL.0000044492.91991.f3].

[52] A. Heinz, A. Haszler, C. Keidel, S. Moldenhauer, R. Benedictus, and W. S. Miller, "Recent development in aluminium alloys for aerospace applications," Mater. Sci. Eng. A, vol. 280, no. 1, pp. 102-107, 2000 [doi:10.1016/S0921-5093(99)00674-7].

[53] M.K. Surappa, "Aluminium matrix composites: Challenges and opportunities," Sādhanā, vol. 28, no. 1-2, pp. 319-334, 2003 [doi:10.1007/BF02717141].

[54] J. Jayakumar, B. K. Raghunath, and T. H. Rao, "Recent development and challenges in synthesis of magnesium matrix nanocomposites—A review," Int. J. Latest Res. Sci. Technol., vol. 1, pp. 164-171, 2012.

[55] H. Z. Ye and X. Y. Liu, "Review of recent studies in magnesium matrix composites," J. Mater. Sci., vol. 39, no. 20, pp. 6153-6171, 2004 [doi:10.1023/B:JMSC.0000043583.47148.31].

[56] R. A. Saravanan and M. K. Surappa, Fabrication and characterisation of pure magnesium-30 vol.% SiCP particle composite." Materials Science and Engineering: A 276, vol. 1-2, 2000, pp. 108-116.

[57] S. N. Alam and H. Singh, "Development of copper-based metal matrix composites: An analysis by SEM, EDS and XRD," Microsc. Anal., vol. 28, no. 4, pp. 8-13, 2014.

[58] H. Singh, L. Kumar, and S. N. Alam, "Development of Cu reinforced SiC particulate composites." In IOP Conference Series, Mater. Sci. Eng. IOP Publishing, vol. 75, no. 1, p. 012007, 2015.

[59] M. Singh, D. P. Singh, Mondal, A. K. Jha, S. Das, and A. H. Yegneswaran, "Preparation and properties of cast aluminium alloy–sillimanite particle composite," Compos. A, vol. 32, no. 6, pp. 787-795, 2001 [doi:10.1016/S1359-835X(00)00187-1].

[60] B. Vijaya Ramnath, C. Elanchezhian, M. Jaivignesh, S. P. Rajesh, C. Parswajinan, and A. S. A. Ghias, "Evaluation of mechanical properties of aluminium alloy–alumina–boron carbide metal matrix composites," Mater. Des., vol. 58, pp. 332-338, 2014 [doi:10.1016/j.matdes.2014.01.068].

[61] P. S. Reddy, R. Kesavan, and B. Vijaya Ramnath,"Investigation of Mechanical Properties of Aluminium 6061-Silicon Carbide, Boron Carbide Metal Matrix Composite" Silicon, vol. 10, no. 2, pp. 495-502, 2018 [doi:10.1007/s12633-016-9479-8].

[62] P. Samal, P. R. Vundavilli, A. Meher, and M. M. Mahapatra, "Recent progress in aluminium metal matrix composites: A review on processing, mechanical and wear

properties," J. Manuf. Processes, vol. 59, pp. 131-152, 2020 [doi:10.1016/j.jmapro.2020.09.010].

[63] A. Macke, B. F. Schultz, and P. Rohatgi, "Metal matrix composites," Adv. Mater. Processes, vol. 170, no. 3, pp. 19-23, 2012.

[64] P. P. N. K. V. Rambabu, N. E. Prasad, V. V. Kutumbarao, and R. J. H. Wanhill, "Aluminium alloys for aerospace applications" in Aerospace Materials and Material Technologies, 2017, pp. 29-52 [doi:10.1007/978-981-10-2134-3_2].

[65] K. U. Kainer and B. L. Mordike, "Creep properties of powder metallurgically produced aluminium-glass composites" in Strength of Metals and Alloys. Pergamon, 1985, pp. 761-766 (ICSMA, p. 7).

[66] M. K. Sudarshan and M. K. Surappa, "Synthesis of fly ash particle reinforced A356 Al composites and their characterization," Mater. Sci. Eng. A, vol. 480, no. 1-2, pp. 117-124, 2008 [doi:10.1016/j.msea.2007.06.068].

[67] R. C. Shivamurthy and M. K. Surappa, "Tribological characteristics of A356 Al alloy–SiCP composite discs," Wear, vol. 271, no. 9-10, pp. 1946-1950, 2011 [doi:10.1016/j.wear.2011.01.075].

[68] S. Nagarajan, B. Dutta, and M. K. Surappa, "The effect of SiC particles on the size and morphology of eutectic silicon in cast A356/SiCp composites," Compos. Sci. Technol., vol. 59, no. 6, pp. 897-902, 1999 [doi:10.1016/S0266-3538(98)00131-6].

[69] R. N. Rao and S. Das, "Effect of matrix alloy and influence of SiC particle on the sliding wear characteristics of aluminium alloy composites," Mater. Des., vol. 31, no. 3, pp. 1200-1207, 2010 [doi:10.1016/j.matdes.2009.09.032].

[70] M. Kok, "Production and mechanical properties of Al2O3 particle-reinforced 2024 aluminium alloy composites," J. Mater. Process. Technol., vol. 161, no. 3, pp. 381-387, 2005 [doi:10.1016/j.jmatprotec.2004.07.068].

[71] S. Gopalakrishnan and N. Murugan, "Production and wear characterisation of AA 6061 matrix titanium carbide particulate reinforced composite by enhanced stir casting method," Compos. B Eng., vol. 43, no. 2, pp. 302-308, 2012 [doi:10.1016/j.compositesb.2011.08.049].

[72] M. Gupta, M. K. Surappa, and S. Qin, “Effect of interfacial characteristics on the failure-mechanism mode of a SiC reinforced A1 based metal-matrix composite,” J. Mater. Process. Technol., vol. 67, no. 1-3, pp. 94-99, 1997 [doi:10.1016/S0924-0136(96)02825-7].

[73] S. Sulaiman, Z. Marjom, M. I. S. Ismail, M. K. A. Ariffin, and N. Ashrafi, “Effect of modifier on mechanical properties of aluminium silicon carbide (Al-SiC) composites,” Procedia Eng., vol. 184, pp. 773-777, 2017 [doi:10.1016/j.proeng.2017.04.156].

[74] R. Soundararajan, A. Ramesh, S. Sivasankaran, and A. Sathishkumar, “Modeling and analysis of mechanical properties of aluminium alloy (A413) processed through squeeze casting route using artificial neural network model and statistical technique,” Adv. Mater. Sci. Eng., vol. 2015, 1-16, 2015 [doi:10.1155/2015/714762].

[75] T. Ram Prabhu, M. Murugan, B. P. Chiranth, R. K. Mishra, N. Rajini, P. Marimuthu, P. D. Babu, and G. Suganya, “Effects of dual-phase reinforcement particles (fly ash+ Al2O3) on the wear and tensile properties of the AA 7075 Al alloy based composites,” J. Inst. Eng. (India) S. D, vol. 100, no. 1, pp. 29-35, 2019 [doi:10.1007/s40033-019-00172-7].

[76] P. Vishwakarma, S. Soni, and P. M. Mishra, “Effect of reinforcement and volume fraction on mechanical behaviour of AA7075/B4C/fly-ash MMCp,” Int. J. Eng. Adv. Technol. 8, vol. 8958, p. 2249, 2019.

[77] P. C. S. Rao, T. Prasad, and M. Harish, “Evaluation of mechanical properties of Al 7075-ZrO2 metal matrix composite by using stir casting technique,” Int. J. Sci. Res. Eng. Technol., vol. 6, no. 4, pp. 377-381, 2017.

[78] A. Baradeswaran and A. E. Perumal, “Wear and mechanical characteristics of Al 7075/graphite composites,” Compos. B Eng., vol. 56, pp. 472-476, 2014 [doi:10.1016/j.compositesb.2013.08.073].

[79] S.A. Sajjadi, H. R. Ezatpour, and M. T Parizi, “Comparison of microstructure and mechanical properties of A356 aluminium alloy/Al2O3 composites fabricated by stir and compo-casting processes,” Mater. Des., vol. 34, pp. 106-111, 2012 [doi:10.1016/j.matdes.2011.07.037].

[80] G. Shankar, P. K. Jayashree, A. U. Kini, and S. S Sharma, Effect of Silicon Oxide (SiO2) Reinforced Particles on Ageing Behavior of AI-2024 Alloy, 2014, pp. 140-144.

[81] Ravichandran, M. and S. Dineshkumar, “Synthesis of Al-TiO2 composites through liquid powder metallurgy route,” SSRG-IJME, vol. 1, no. 1, pp. 12-15, 2014 [doi:10.14445/23488360/IJME-V1I1P103].

[82] N. Muralidharan, K. Chockalingam, K. Kalaiselvan, and N. Nithyavathy, “Investigation of ZrO2 reinforced aluminium metal matrix composites by liquid metallurgy route,” Adv. Mater. Process. Technol., pp. 1-15, 2022.

[83] S. Kundu, M. Hussain, V. Kumar, S. Kumar, and A. K. Das, “Direct metal laser sintering of TiN reinforced Ti6Al4V alloy based metal matrix composite: Fabrication and characterization,” Int. J. Adv. Manuf. Technol., vol. 97, no. 5-8, pp. 2635-2646, 2018 [doi:10.1007/s00170-018-2159-7].

[84] S. Kumar, J. H. Vignesh, and S. P. Joshua, “Investigating the effect of porosity on aluminium 7075 alloy reinforced with silicon nitride (Si3N4) metal matrix composites through STIR casting process,” Mater. Today Proc., vol. 39, pp. 414-419, 2021.

[85] D. G. Kvashnin, K. L. Firestein, Z. I. Popov, S. Corthay, P. B. Sorokin, D. V. Golberg, and D. V Shtansky, “Al− BN interaction in a high-strength lightweight Al/BN metal-matrix composite: Theoretical modelling and experimental verification,” J. Alloys Compd., vol. 782, pp. 875-880, 2019 [doi:10.1016/j.jallcom.2018.12.261].

[86] R. R. Veeravalli, R. Nallu, and S. M. M. Mohiuddin, “Mechanical and tribological properties of AA7075–TiC metal matrix composites under heat treated (T6) and cast conditions,” J. Mater. Res. Technol., vol. 5, no. 4, pp. 377-383, 2016 [doi:10.1016/j.jmrt.2016.03.011].

[87] B. Chen, K. Kondoh, J. S. Li, and M. J. P. B. E. Qian, “Extraordinary reinforcing effect of carbon nanotubes in aluminium matrix composites assisted by in-situ alumina nanoparticles” Compos. B Eng., vol. 183, p. 107691, 2020 [doi:10.1016/j.compositesb.2019.107691].

[88] A. Kumar, R. C. Singh, R. Chaudhary, and V. P. Singh, “Tribological studies and microstructural characterisation of SiC and fly ash particles based aluminium 2024 alloy composites prepared through stir casting route,” In IOP Conference Series, IOP Conf. Ser.: Mater. Sci. Eng. IOP Publishing, vol. 804, no. 1, p. 012025, 2020 [doi:10.1088/1757-899X/804/1/012025].

[89] A. K. Senapati, Senapati, P. C. Mishra, and B. C. Routara, “Use of waste fly ash in fabrication of aluminium alloy matrix composite,” Int. J. Eng. Technol., vol. 6, no. 2, pp. 905-912, 2014.

[90] N. Panwar and A. Chauhan, “Development of aluminium composites using Red mud as reinforcement-A review,” Recent Adv. Eng. Comp. Sci. (RAECS), vol. 2014, pp. 1-4, 2014.

[91] K. K. Reddy, Reddy, K.K., A. H. Shaik, V. K. R. Narahari, S. Pramanik, and S. Bhaumik, “Effect of reinforcements on graphite/titania/aluminium nanohybrid composites,” Proc. Inst. Mech. Eng. J, vol. 236, no. 2, pp. 217-224, 2022 [doi:10.1177/13506501211047741].

[92] S. Suresh, N. Shenbag, and V. Moorthi, “Aluminium-titanium diboride (Al-TiB2) metal matrix composites: Challenges and opportunities,” Procedia Eng., vol. 38, pp. 89-97, 2012 [doi:10.1016/j.proeng.2012.06.013].

[93] S. R. Biswal and S. Sahoo, “A comparative analysis on physical and mechanical properties of aluminium composites with Al2O3 and WS2 reinforcement” in Recent Advances in Mechanical Engineering: Select Proceedings of ICRAMERD. Singapore: Springer Nature Singapore, 2022, 2021, pp. 597-603.

[94] S. Das, T. K. Dan,,S. V. Prasad,. and P. K. Rohatgi, P.K., “Aluminium alloy—Rice husk ash particle composites,” J. Mater. Sci. Lett., vol. 5, no. 5, pp. 562-564, 1986 [doi:10.1007/BF01728691].

[95] P. B. Madakson, D. S. Yawas, and A. Apasi, “Characterization of coconut shell ash for potential utilization in metal matrix composites for automotive applications,” Int. J. Eng. Sci. Technol., vol. 4, no. 3, pp. 1190-1198, 2012.

[96] L. Weber and R. Tavangar, “Diamond-based metal matrix composites for thermal management made by liquid metal infiltration—Potential and limits” in Adv. Mater. Res., vol. 59, pp. 111-115. Trans Tech Publications Ltd, 2009.

[97] R. Dasgupta, “Aluminium alloy-based metal matrix composites: A potential material for wear resistant applications,” Int. Sch. Res. Not., vol. 2012, 1-14, 2012 [doi:10.5402/2012/594573].

[98] T. B. Rao, “Microstructural, mechanical, and wear properties characterization and strengthening mechanisms of Al7075/SiCnp composites processed through ultrasonic cavitation assisted stir-casting,” Mater. Sci. Eng. A, vol. 805, p. 140553, 2021 [doi:10.1016/j.msea.2020.140553].

[99] S. Lü, P. Xiao, D. Yuan, K. Hu, and S. Wu, “Preparation of Al matrix nanocomposites by diluting the composite granules containing Nano-SiCp under ultrasonic vibaration,” J. Mater. Sci. Technol., vol. 34, no. 9, pp. 1609-1617, 2018 [doi:10.1016/j.jmst.2018.01.003].

[100] Y. Yang, J. Lan, and X. Li, “Study on bulk aluminium matrix nanocomposite fabricated by ultrasonic dispersion of nanosized SiC particles in molten aluminium alloy,” Mater. Sci. Eng. A, vol. 380, no. 1-2, pp. 378-383, 2004 [doi:10.1016/j.msea.2004.03.073].

[101] D. Yuan, K. Hu, S. Lü, S. Wu, and Q. Gao, “Preparation and properties of Nano-SiCp/A356 composites synthesised with a new process,” Mater. Sci. Technol., vol. 34, no. 12, pp. 1415-1424, 2018 [doi:10.1080/02670836.2018.1458479].

[102] M. Razavi, A. R. Farajipour, M. Zakeri, M. R. Rahimipour, and A. K. Firouzbakht, “Production of Al2O3−SiC nano-composites by spark plasma sintering,” Bol. Soc. Española Ceram. Vidrio, vol. 56, no. 4, pp. 186-194, 2017 [doi:10.1016/j.bsecv.2017.01.002].

[103] Q. Han, R. Setchi, and S. L. Evans, “Synthesis and characterisation of advanced ball-milled Al-Al2O3 nanocomposites for selective laser melting,” Powder Technol., vol. 297, pp. 183-192, 2016 [doi:10.1016/j.powtec.2016.04.015].

[104] X. Zhang, S. Liang, H. Li, and J. Yang, “Mechanical and optical properties of transparent alumina obtained by rapid vacuum sintering,” Ceram. Int., vol. 43, no. 1, pp. 420-426, 2017 [doi:10.1016/j.ceramint.2016.09.175].

[105] M. Oghbaei and O. Mirzaee, “Microwave versus conventional sintering: A review of fundamentals, advantages and applications,” J. Alloys Compd., vol. 494, no. 1-2, pp. 175-189, 2010 [doi:10.1016/j.jallcom.2010.01.068].

[106] C. Zhou, X. Wu, T. L. Ngai, L. Li, S. Ngai, and Z. Chen, “Al alloy/Ti3SiC2 composites fabricated by pressureless infiltration with melt-spun Al alloy ribbons,” Ceram. Int., vol. 44, no. 6, pp. 6026-6032, 2018 [doi:10.1016/j.ceramint.2017.12.212].

[107] W. Yang, Q. Zhao, L. Xin, J. Qiao, J. Zou, P. Shao, Z. Yu, Q. Zhang, and G. Wu, “Microstructure and mechanical properties of graphene nanoplates reinforced pure Al matrix composites prepared by pressure infiltration method,” J. Alloys Compd., vol. 732, pp. 748-758, 2018 [doi:10.1016/j.jallcom.2017.10.283].

[108] K. Lichtenberg and K. A. Weidenmann, “Effect of reinforcement size and orientation on the thermal expansion behavior of metallic glass reinforced metal matrix

composites produced by gas pressure infiltration," Thermochim. Acta, vol. 654, pp. 85-92, 2017 [doi:10.1016/j.tca.2017.05.010].

[109] L. H. Qi, L.H., W. Q. Zheng, J. M. Zhou, and L. Y.Ju, "Effect of specific pressure on fabrication of 2D-Cf/Al composite by vacuum and pressure infiltration," Trans. Nonferrous Met. Soc. China, vol. 23, no. 7, pp. 1915-1921, 2013 [doi:10.1016/S1003-6326(13)62677-1].

[110] D. Han, H. Mei, S. Xiao, J. Xia, J. Gu, and L. Cheng, "Porous SiCnw/SiC ceramics with unidirectionally aligned channels produced by freeze-drying and chemical vapor infiltration," J. Eur. Ceram. Soc., vol. 37, no. 3, pp. 915-921, 2017 [doi:10.1016/j.jeurceramsoc.2016.10.015].

[111] J. Wannasin and M. C. Flemings, "Fabrication of metal matrix composites by a high-pressure centrifugal infiltration process," J. Mater. Process. Technol., vol. 169, no. 2, pp. 143-149, 2005 [doi:10.1016/j.jmatprotec.2005.03.004].

[112] J. Maj, M. Basista, W. Węglewski, K. Bochenek, A. Strojny-Nędza, K. Naplocha, T. Panzner, M. Tatarková, and F. Fiori, "Effect of microstructure on mechanical properties and residual stresses in interpenetrating aluminium–alumina composites fabricated by squeeze casting," Mater. Sci. Eng. A, vol. 715, pp. 154-162, 2018 [doi:10.1016/j.msea.2017.12.091].

[113] P. K. Rohatgi, D. Weiss, and N. Gupta, "Applications of fly ash in synthesizing low-cost MMCs for automotive and other applications," JOM, vol. 58, no. 11, pp. 71-76, 2006 [doi:10.1007/s11837-006-0232-4].

[114] T. K. Adelakin and O. M. Suárez, "Study of boride-reinforced aluminium matrix composites produced via centrifugal casting," Mater. Manuf. Processes, vol. 26, no. 2, pp. 338-345, 2011 [doi:10.1080/10426910903124829].

[115] S. Venkatesan and M. A. Anthony Xavior, "Tensile behavior of aluminium alloy (AA7050) metal matrix composite reinforced with graphene fabricated by stir and squeeze cast processes," Sci. Technol. Mater., vol. 30, no. 2, pp. 74-85, 2018 [doi:10.1016/j.stmat.2018.02.005].

[116] Y. Li, Q. L. Li, L. I. Dong, L. I. U. Wei, and G. G. Shu, "Fabrication and characterization of stir casting AA6061—31% B4C composite," Trans. Nonferrous Met. Soc. China, vol. 26, no. 9, pp. 2304-2312, 2016 [doi:10.1016/S1003-6326(16)64322-4].

[117] S. P. Kumarasamy, K. Vijayananth, T. Thankachan, and G. P. Muthukutti, “Investigations on mechanical and machinability behavior of aluminium/flyashcenosphere/Gr hybrid composites processed through compocasting,” J. Appl. Res. Technol., vol. 15, no. 5, pp. 430-441, 2017 [doi:10.1016/j.jart.2017.05.005].

[118] U. A. Curle and L. Ivanchev, “Wear of semi-solid rheocastSiCp/Al metal matrix composites,” Trans. Nonferrous Met. Soc. China, vol. 20, pp. s852-s856, 2010 [doi:10.1016/S1003-6326(10)60594-8].

[119] X. Liu, Y. Liu, D. Huang, Q. Han, and X. Wang, “Tailoring in-situ TiB2 particulates in aluminium matrix composites,” Mater. Sci. Eng. A, vol. 705, pp. 55-61, 2017 [doi:10.1016/j.msea.2017.08.047].

[120] K. Kaur and O. P. Pandey, “Microstructural characteristics of spray formed zircon sand reinforced LM13 composite,” J. Alloys Compd., vol. 503, no. 2, pp. 410-415, 2010 [doi:10.1016/j.jallcom.2010.04.249].

[121] M. M. Seleman and M. M. Z. El-Sayed, “Ahmed, and SabbahAtaya”. "Microstructure and mechanical properties of hot extruded 6016 aluminium alloy/graphite composites.", J. Mater. Sci. Technol., vol. 34, no. 9, pp. 1580-1591, 2018.

[122] H. Jafarian, J. Habibi-Livar, and S. H. Razavi, “Microstructure evolution and mechanical properties in ultrafine grained Al/TiC composite fabricated by accumulative roll bonding,” Compos. B Eng., vol. 77, pp. 84-92, 2015 [doi:10.1016/j.compositesb.2015.03.009].

[123] A. K. Bodukuri, K. Eswaraiah, K. Rajendar, and V. Sampath, “Fabrication of Al–SiC−B4C metal matrix composite by powder metallurgy technique and evaluating mechanical properties,” Perspect. Sci., vol. 8, pp. 428-431, 2016 [doi:10.1016/j.pisc.2016.04.096].

[124] A. E. Nassar and E. E. Nassar, “Properties of aluminium matrix nanocomposites prepared by powder metallurgy processing,” J. King Saud Univ. Eng. Sci., vol. 29, no. 3, pp. 295-299, 2017 [doi:10.1016/j.jksues.2015.11.001].

[125] Z. Yu, N. Zhang, Z. Chao, Y. Cao, Y. Sun, P. Shao, and G. Wu. "Effect of ball milling time on graphene nanosheets reinforced Al6063 composite fabricated by pressure infiltration method." Carbon 141 (2019): 25-39.

[126] H. K. Issa, A., Maleki, and A. Ghaei, “Development of an aluminium/amorphous Nano-SiO2 composite using powder metallurgy and hot extrusion processes,” Ceram. Int., vol. 43, no. 17, pp. 14582-14592, 2017 [doi:10.1016/j.ceramint.2017.06.057].

[127] H. Kwon, J. Mondal, K. A. AlOgab, V. Sammelselg, M. Takamichi, A. Kawaski, and M. Leparoux, “Graphene oxide-reinforced aluminium alloy matrix composite materials fabricated by powder metallurgy,” J. Alloys Compd., vol. 698, pp. 807-813, 2017 [doi:10.1016/j.jallcom.2016.12.179].

[128] M. Gürbüz, M. C. Şenel, and E. Koç, “The effect of sintering time, temperature, and graphene addition on the hardness and microstructure of aluminium composites,” J. Compos. Mater., vol. 52, no. 4, pp. 553-563, 2018 [doi:10.1177/0021998317740200].

[129] S. J. Niteesh Kumar, S. J., R. Keshavamurthy, M. R. Haseebuddin, and Praveennath G. Koppad, “Mechanical properties of aluminium-graphene composite synthesized by powder metallurgy and hot extrusion,” Trans. Indian Inst. Met., vol. 70, no. 3, pp. 605-613, 2017 [doi:10.1007/s12666-017-1070-5].

[130] R. Pérez-Bustamante, D. B. Morales, J. B. Martínez, I. E. Guel, and R. M. Sánchez “Microstructural and hardness behavior of graphene-nanoplatelets/aluminium composites synthesized by mechanical alloying,” J. Alloys Compd., vol. 615, pp. S578-S582, 2014 [doi:10.1016/j.jallcom.2014.01.225].

[131] B. T. Gibson, D. H. Lammlein, T. J. Prater, W. R. Longhurst, C. D. Cox, M. C. Ballun, K. J. Dharmaraj, G. E. Cook, and A. M. Strauss, “Friction stir welding: Process, automation, and control,” J. Manuf. Processes, vol. 16, no. 1, pp. 56-73, 2014 [doi:10.1016/j.jmapro.2013.04.002].

[132] F. Khodabakhshi, M. Nosko, and A. P. Gerlich “Effects of graphene nano-platelets (GNPs) on the microstructural characteristics and textural development of an Al-Mg alloy during friction-stir processing,” Surf. Coat. Technol., vol. 335, pp. 288-305, 2018 [doi:10.1016/j.surfcoat.2017.12.045].

[133] H. Rana and V. Badheka, “Influence of friction stir processing conditions on the manufacturing of Al-Mg-Zn-Cu alloy/boron carbide surface composite,” J. Mater. Process. Technol., vol. 255, pp. 795-807, 2018 [doi:10.1016/j.jmatprotec.2018.01.020].

[134] F. Khodabakhshi, S. M. Arab, P. Švec, and A. P. Gerlich, “Fabrication of a new Al-Mg/graphene nanocomposite by multi-pass friction-stir processing: Dispersion, microstructure, stability, and strengthening,” Mater. Char., vol. 132, pp. 92-107, 2017 [doi:10.1016/j.matchar.2017.08.009].

[135] A. Heidarzadeh, S. Mironov, R. Kaibyshev, G. Çam, A. Simar, A. Gerlich, F. Khodabakhshi, A. Mostafaei, D. P Field, J. D. Robson, and A. Deschamps, "Friction stir welding/processing of metals and alloys: A comprehensive review on microstructural evolution," Prog. Mater. Sci., vol. 117, p. 100752, 2021 [doi:10.1016/j.pmatsci.2020.100752].

[136] F. Khodabakhshi, A. P. Gerlich, and P. Švec "Fabrication of a high strength ultra-fine grained Al-Mg-SiC nanocomposite by multi-step friction-stir processing," Mater. Sci. Eng. A, vol. 698, pp. 313-325, 2017 [doi:10.1016/j.msea.2017.05.065].

[137] M. Orłowska, F. Pixner, A. Hütter, N. Enzinger, L. Olejnik, and M. Lewandowska, "Manufacturing of coarse and ultrafine-grained aluminium matrix composites reinforced with Al2O3 nanoparticles via friction stir processing," J. Manuf. Processes, vol. 80, pp. 359-373, 2022 [doi:10.1016/j.jmapro.2022.06.011].

[138] M. Khan, A. Rehman, T. Aziz, M. Shahzad, K. Naveed, and T. Subhani, "Effect of inter-cavity spacing in friction stir processed Al 5083 composites containing carbon nanotubes and boron carbide particles," J. Mater. Process. Technol., vol. 253, pp. 72-85, 2018 [doi:10.1016/j.jmatprotec.2017.11.002].

[139] I. Dinaharan, "Influence of ceramic particulate type on microstructure and tensile strength of aluminium matrix composites produced using friction stir processing," J. Asian Ceram. Soc., vol. 4, no. 2, pp. 209-218, 2016 [doi:10.1016/j.jascer.2016.04.002].

[140] I. Dinaharan, K. Kalaiselvan, and N. Murugan. "Influence of rice husk ash particles on microstructure and tensile behavior of AA6061 aluminium matrix composites produced using friction stir processing," Compos. Commun., vol. 3, pp. 42-46, 2017 [doi:10.1016/j.coco.2017.02.001].

[141] R. Maurya, B. Kumar, S. Ariharan, J. Ramkumar, and K. Balani "Effect of carbonaceous reinforcements on the mechanical and tribological properties of friction stir processed Al6061 alloy," Mater. Des., vol. 98, pp. 155-166, 2016 [doi:10.1016/j.matdes.2016.03.021].

[142] A. Hamdollahzadeh, M. Bahrami, M. Farahmand Nikoo, A. Yusefi, MK Besharati Givi, and N. Parvin, "Microstructure evolutions and mechanical properties of Nano-SiC-fortified AA7075 friction stir weldment: The role of second pass processing," J. Manuf. Processes, vol. 20, pp. 367-373, 2015 [doi:10.1016/j.jmapro.2015.06.017].

[143] H. G. Rana, V. J. Badheka, and A. Kumar, “Fabrication of Al7075/B4C surface composite by novel friction stir processing (FSP) and investigation on wear properties,” Procedia Technol., vol. 23, pp. 519-528, 2016 [doi:10.1016/j.protcy.2016.03.058].

[144] N. Yuvaraj, S. Aravindan, “Fabrication of Al5083/B4C surface composite by friction stir processing and its tribological characterization,” J. Mater. Res. Technol., vol. 4, no. 4, pp. 398-410, 2015 [doi:10.1016/j.jmrt.2015.02.006].

[145] S. Fouladi and M. Abbasi, “The effect of friction stir vibration welding process on characteristics of SiO2 incorporated joint,” J. Mater. Process. Technol., vol. 243, pp. 23-30, 2017 [doi:10.1016/j.jmatprotec.2016.12.005].

[146] G. Huang, W. Hou, and Y. Shen, “Evaluation of the microstructure and mechanical properties of WC particle reinforced aluminium matrix composites fabricated by friction stir processing,” Mater. Char., vol. 138, pp. 26-37, 2018 [doi:10.1016/j.matchar.2018.01.053].

[147] F. G. Vázquez, B. V. Arista, R. Muñiz, J. C. Ortiz, H. H. García, and J. Acevedo. “‘The role of friction stir processing (FSP) parameters on TiC reinforced surface Al7075-T651 aluminium alloy.’ soldagem&inspeção,” vol. 21, pp. 508-516, 2016.

[148] A. Thangarasu, N. Murugan, and I. Dinaharan “Production and wear characterization of AA6082-TiC surface composites by friction stir processing,” Procedia Eng., vol. 97, pp. 590-597, 2014 [doi:10.1016/j.proeng.2014.12.287].

[149] S. M. Arab, S. Karimi, S. A. J. Jahromi, S. Javadpour, and S. M. Zebarjad, “Fabrication of novel fiber reinforced aluminium composites by friction stir processing,” Mater. Sci. Eng. A, vol. 632, pp. 50-57, 2015 [doi:10.1016/j.msea.2015.02.032].

[150] M. Nazari, H. Eskandari, and F. Khodabakhshi, “Production and characterization of an advanced AA6061-graphene-TiB2 hybrid surface nanocomposite by multi-pass friction stir processing,” Surf. Coat. Technol., vol. 377, p. 124914, 2019 [doi:10.1016/j.surfcoat.2019.124914].

[151] K. Surekha, B. S. Murty, and K. Prasad Rao, “Effect of processing parameters on the corrosion behaviour of friction stir processed AA 2219 aluminium alloy,” Solid State Sci., vol. 11, no. 4, pp. 907-917, 2009 [doi:10.1016/j.solidstatesciences.2008.11.007].

[152] S. Shahraki, R. A. Behnagh, Y. Fotouhi, and H. Bisadi “Producing of AA5083/ZrO 2 nanocomposite by friction stir processing (FSP),” Metall. Mater. Trans. B, vol. 44, no. 6, pp. 1546-1553, 2013 [doi:10.1007/s11663-013-9914-9].

[153] N. Naghshehkesh, S.E. Mousavi, F. Karimzadeh, A. Ashrafi, M. Nosko, V. Trembošová, and B. Sadeghi "Effect of graphene oxide and friction stir processing on microstructure and mechanical properties of Al5083 matrix composite," Mater. Res. Express, vol. 6, no. 10, p. 106566, 2019 [doi:10.1088/2053-1591/ab3a6f].

[154] V. Kalyanamanohar, D. G. C. Gireesh et al., "Parameter optimization and evaluation of mechanical and thermal properties of nanographene reinforced Al 6060 surface composite using FSP" in AIP Conf. Proc. AIP Publishing LLC, vol. 1943, no. 1, p. 020052, 2018 [doi:10.1063/1.5029628].

[155] D. K. Lim, T. Shibayanagi, and A. P. Gerlich, "Synthesis of multi-walled CNT reinforced aluminium alloy composite via friction stir processing," Mater. Sci. Eng. A, vol. 507, no. 1-2, pp. 194-199, 2009 [doi:10.1016/j.msea.2008.11.067].

[156] S. Rathee, S. Maheshwari, A. N. Siddiquee, M. Srivastava, and S. K. Sharma "Process parameters optimization for enhanced microhardness of AA 6061/SiC surface composites fabricated via friction stir processing (FSP)," Mater. Today Proc., vol. 3, no. 10, pp. 4151-4156, 2016 [doi:10.1016/j.matpr.2016.11.089].

[157] M. H. Montazerian, M. Movahedi, and M. R. Jondi, "Effect of graphene and process parameters on mechanical performance and electrical resistance of aluminium to copper friction stir joint," Mater. Res. Express, vol. 6, no. 4, p. 046561, 2019 [doi:10.1088/2053-1591/aafe1a].

[158] H. Izadi and A. P. Gerlich, "Distribution and stability of carbon nanotubes during multi-pass friction stir processing of carbon nanotube/aluminium composites," Carbon, vol. 50, no. 12, pp. 4744-4749, 2012 [doi:10.1016/j.carbon.2012.06.012].

[159] D. Jayabalakrishnan and M. Balasubramanian, "Eccentric-weave FSW between Cu and AA 6061-T6 with reinforced graphene nanoparticles," Mater. Manuf. Processes, vol. 33, no. 3, pp. 333-342, 2018 [doi:10.1080/10426914.2017.1339323].

[160] P. K. Rohatgi, R. Asthana, and S. Das". "Solidification, structures, and properties of cast metal-ceramic particle composites.", Int. Met. Rev., vol. 31, no. 1, pp. 115-139, 1986.

[161] S. Gopalakrishnan and N. Murugan, "Production and wear characterisation of AA 6061 matrix titanium carbide particulate reinforced composite by enhanced stir casting method," Compos. B Eng., vol. 43, no. 2, pp. 302-308, 2012 [doi:10.1016/j.compositesb.2011.08.049].

[162] H. Kala, K. K. S. Mer, and S. Kumar "A review on mechanical and tribological behaviors of stir cast aluminium matrix composites," Procedia Mater. Sci., vol. 6, pp. 1951-1960, 2014 [doi:10.1016/j.mspro.2014.07.229].

[163] M. H. Rahman and H. M. M. A. Rashed, "Characterization of Silicon Carbide Reinforced Aluminum Matrix Composites" Procedia Eng., vol. 90, pp. 103-109, 2014 [doi:10.1016/j.proeng.2014.11.821].

[164] M. T. Sijo and K. R. Jayadevan, "Analysis of stir cast aluminium silicon carbide metal matrix composite: A comprehensive review," Procedia Technol., vol. 24, pp. 379-385, 2016 [doi:10.1016/j.protcy.2016.05.052].

[165] V. Bharath, M. Nagaral, V. Auradi, and S. A. Kori. "Preparation of 6061Al-Al 2 O 3 MMC's by Stir Casting and Evaluation of Mechanical and Wear Properties" Procedia Mater. Sci., vol. 6, pp. 1658-1667, 2014 [doi:10.1016/j.mspro.2014.07.151].

[166] K. Tee_L, L. Lu, and M. O. Lai, "In situ processing of Al–TiB2 composite by the stir-casting technique.", J. Mater. Process. Technol., vol. 89, pp. 513-519, 1999.

[167] J. Hashim, L. Looney, and M. S. J. Hashmi. "Metal matrix composites: Production by the stir casting method," J. Mater. Process. Technol., vol. 92-93, pp. 1-7, 1999 [doi:10.1016/S0924-0136(99)00118-1].

[168] J. J. Moses, I. Dinaharan, and S. J. Sekhar. "Prediction of influence of process parameters on tensile strength of AA6061/TiC aluminium matrix composites produced using stir casting," Trans. Nonferrous Met. Soc. China, vol. 26, no. 6, pp. 1498-1511, 2016 [doi:10.1016/S1003-6326(16)64256-5].

[169] B. P. Kumar and A. K. Birru, "Microstructure and mechanical properties of aluminium metal matrix composites with addition of bamboo leaf ash by stir casting method," Trans. Nonferrous Met. Soc. China, vol. 27, no. 12, pp. 2555-2572, 2017 [doi:10.1016/S1003-6326(17)60284-X].

[170] J. J. Moses, I. Dinaharan, and S. J. Sekhar, "Characterization of Silicon Carbide Particulate Reinforced AA6061 Aluminum Alloy Composites Produced via Stir Casting" Procedia Mater. Sci., vol. 5, pp. 106-112, 2014 [doi:10.1016/j.mspro.2014.07.247].

[171] K. V. Vishnu Prasad and K. R. Jayadevan, "Simulation of stirring in stir casting," Procedia Technol., vol. 24, pp. 356-363, 2016 [doi:10.1016/j.protcy.2016.05.048].

[172] A. T. Thomas, R. Parameshwaran, A. Muthukrishnan, and M. A. Kumaran, "Development of feeding & stirring mechanisms for stir casting of aluminium matrix composites," Procedia Mater. Sci., vol. 5, pp. 1182-1191, 2014 [doi:10.1016/j.mspro.2014.07.415].

[173] K. Mermerdaş, S. Manguri, D. E. Nassani, and S. M. Oleiwi, "Effect of aggregate properties on the mechanical and absorption characteristics of geopolymer mortar," Eng. Sci. Technol. An Int. J., Nov., vol. 20, no. 6, pp. 1642-1652, 2017 [doi:10.1016/j.jestch.2017.11.009].

[174] F. Chen, Z. Chen, F. Mao, T. Wang, and Z. Cao, "TiB2 reinforced aluminium based in situ composites fabricated by stir casting," Mater. Sci. Eng. A, vol. 625, pp. 357-368, 2015 [doi:10.1016/j.msea.2014.12.033].

[175] R. Singh and G. Singh, "Investigations of Al–SiC AMC prepared by vacuum moulding assisted stir casting," J. Manuf. Processes, vol. 19, pp. 142-147, 2015 [doi:10.1016/j.jmapro.2015.06.011].

[176] X. N. Zhang, L. Geng, and G. S. Wang, "Fabrication of Al-based hybrid composites reinforced with SiC whiskers and SiC nanoparticles by squeeze casting," J. Mater. Process. Technol., vol. 176, no. 1-3, pp. 146-151, 2006 [doi:10.1016/j.jmatprotec.2006.03.125].

[177] K. M. S. Manu, K. Sreeraj, T. P. D. Rajan, R. M. Shereema, B. C. Pai, and B. Arun, "Structure and properties of modified compocastmicrosilica reinforced aluminium matrix composite," Mater. Des., vol. 88, pp. 294-301, 2015 [doi:10.1016/j.matdes.2015.08.110].

[178] C. S. Goh, K. S. Soh, P. H. Oon, and B. W. Chua, "Effect of squeeze casting parameters on the mechanical properties of AZ91–Ca Mg alloys," Mater. Des., vol. 31, pp. S50-S53, 2010 [doi:10.1016/j.matdes.2009.11.039].

[179] C. Kannan and R. Ramanujam, "Comparative study on the mechanical and microstructural characterisation of AA 7075 Nano and hybrid nanocomposites produced by stir and squeeze casting," J. Adv. Res., vol. 8, no. 4, pp. 309-319, 2017 [doi:10.1016/j.jare.2017.02.005].

[180] G. Liu, Q. Wang, T. Liu, B. Ye, H. Jiang, and W. Ding, "Effect of T6 heat treatment on microstructure and mechanical property of 6101/A356 bimetal fabricated by squeeze casting," Mater. Sci. Eng. A, vol. 696, pp. 208-215, 2017 [doi:10.1016/j.msea.2017.04.072].

[181] M. Baghi, B. Niroumand, and R. Emadi, “Fabrication and characterization of squeeze cast A413-CSF composites,” J. Alloys Compd., vol. 710, pp. 29-36, 2017 [doi:10.1016/j.jallcom.2017.03.136].

[182] H. F. El-Labban, F. Hashem, M. Abdelaziz, and E. R. I. Mahmoud, “Preparation and characterization of squeeze cast-Al–Si piston alloy reinforced by Ni and Nano-Al2O3 particles,” J. King Saud Univ. Eng. Sci., vol. 28, no. 2, pp. 230-239, 2016 [doi:10.1016/j.jksues.2014.04.002].

[183] E. Hajjari, M. Divandari, and A. R. Mirhabibi, “The effect of applied pressure on fracture surface and tensile properties of nickel coated continuous carbon fiber reinforced aluminium composites fabricated by squeeze casting,” Mater. Des. (1980–2015), vol. 31, no. 5, pp. 2381-2386, 2010 [doi:10.1016/j.matdes.2009.11.067].

[184] W. Xu, X. Jin, W. Xiong, X. Zeng, and D. Shan, “Study on hot deformation behavior and workability of squeeze-cast 20 vol% SiCw/6061Al composites using processing map,” Mater. Char., vol. 135, pp. 154-166, 2018 [doi:10.1016/j.matchar.2017.11.026].

[185] C. Yang, Y. Zong, Z. Zheng, and D. Shan, “Experimental and theoretical investigation on the compressive behavior of aluminium borate whisker reinforced 2024Al composites,” Mater. Char., vol. 96, pp. 84-92, 2014 [doi:10.1016/j.matchar.2014.07.024].

[186] H. A. Alhashmy and M. Nganbe, “Laminate squeeze casting of carbon fiber reinforced aluminium matrix composites,” Mater. Des., vol. 67, pp. 154-158, 2015 [doi:10.1016/j.matdes.2014.11.034].

[187] R. Jojith, N. Radhika, and B. Saleh, “Metallographic, mechanical and reciprocating wear characterization and behavioural studies of untreated and T6 treated Al2O3/Al7Si0. 3Mg functional composite material,” Tribol. Int., vol. 174, p. 107693, 2022 [doi:10.1016/j.triboint.2022.107693].

[188] S. D. Kumar, M. Ravichandran, A. Jeevika, B. Stalin, C. Kailasanathan, and A. Karthick, “Effect of ZrB2 on microstructural, mechanical and corrosion behaviour of aluminium (AA7178) alloy matrix composite prepared by the stir casting route,” Ceram. Int., vol. 47, no. 9, pp. 12951-12962, 2021 [doi:10.1016/j.ceramint.2021.01.158].

[189] O. B. Bembalge and S. K. Panigrahi, “Development and strengthening mechanisms of bulk ultrafine grained AA6063/SiC composite sheets with varying reinforcement size ranging from Nano to micro domain,” J. Alloys Compd., vol. 766, pp. 355-372, 2018 [doi:10.1016/j.jallcom.2018.06.306].

[190] M. Sambathkumar, P. Navaneethakrishnan, K. S. K. S. Ponappa, and K. S. K. Sasikumar, "Mechanical and corrosion behavior of Al7075 (hybrid) metal matrix composites by two step stir casting process," Lat. Am. J. Solids Struct., vol. 14, no. 2, pp. 243-255, 2017 [doi:10.1590/1679-78253132].

[191] N. Radhika and K. S. Sai Charan, "Experimental analysis on three body abrasive wear behaviour of stir cast Al LM 25/TiC metal matrix composite," Trans. Indian Inst. Met., vol. 70, no. 9, pp. 2233-2240, 2017 [doi:10.1007/s12666-017-1061-6].

[192] A. Kumar, R. C. Singh, and Rajiv Chaudhary, "Investigation of Nano-Al2O3 and micro-coconut shell Ash (CSA) reinforced AA7075 hybrid metal–matrix composite using two-stage stir casting," Arab. J. Sci. Eng., vol. 47, no. 12, pp. 15559-15573, 2022 [doi:10.1007/s13369-022-06728-2].

[193] Y. Pazhouhanfar and B. Eghbali, "Microstructural characterization and mechanical properties of TiB2 reinforced Al6061 matrix composites produced using stir casting process," Mater. Sci. Eng. A, vol. 710, pp. 172-180, 2018 [doi:10.1016/j.msea.2017.10.087].

[194] N. Srivastava and G. P. Chaudhari, "Strengthening in Al alloy nano composites fabricated by ultrasound assisted solidification technique," Mater. Sci. Eng. A, vol. 651, pp. 241-247, 2016 [doi:10.1016/j.msea.2015.10.118].

[195] A. Kumar, R. C. Singh, and Rajiv Chaudhary, "Investigation of microstructure and several quality characteristics of AA7075/Al2O3/Coconut shell ash hybrid nano composite prepared through ultrasonic assisted stir-casting," J. Mater. Eng. Perform., pp. 1-16, 2022 [doi:10.1007/s11665-022-07780-7].

[196] K. Amouri, S. Kazemi, A. Momeni, and M. Kazazi, "Microstructure and mechanical properties of Al-nano/micro SiC composites produced by stir casting technique" Mater. Sci. Eng. A, vol. 674, pp. 569-578, 2016 [doi:10.1016/j.msea.2016.08.027].

[197] S. Ganguly and A. K. Mondal, "Influence of SiC nanoparticles addition on microstructure and creep behavior of squeeze-cast AZ91-Ca-Sb magnesium alloy," Mater. Sci. Eng. A, vol. 718, pp. 377-389, 2018 [doi:10.1016/j.msea.2018.01.131].

[198] H. Uozumi, K. Kobayashi, K. Nakanishi, T. Matsunaga, K. Shinozaki, H Sakamoto, T. Tsukada, C. Masuda, and M. Yoshida "Fabrication process of carbon nanotube/light

metal matrix composites by squeeze casting," Mater. Sci. Eng. A, vol. 495, no. 1-2, pp. 282-287, 2008 [doi:10.1016/j.msea.2007.11.088].

[199] N. Valibeygloo, R. A. Khosroshahi, and R. T. Mousavian. "Microstructural and mechanical properties of Al-4.5 wt% Cu reinforced with alumina nanoparticles by stir casting method," Int. J. Miner. Metall. Mater., vol. 20, no. 10, pp. 978-985, 2013 [doi:10.1007/s12613-013-0824-2].

[200] M. Akbari and H. R. Karbalaei, "Baharvandi, and O. Mirzaee". "Nano-sized aluminium oxide reinforced commercial casting A356 alloy matrix: Evaluation of hardness, wear resistance and compressive strength focusing on particle distribution in aluminium matrix.", Compos. B Eng., vol. 52, pp. 262-268, 2013.

[201] B.S. Yigezu, M. M. Mahapatra, and P. K. Jha, Influence of Reinforcement Type on Microstructure, Hardness, and Tensile Properties of an Aluminium Alloy Metal Matrix Composite, 2013.

[202] D. R. Kongshaug, J. B. Ferguson, B. F. Schultz, and P. K. Rohatgi, "Reactive stir mixing of Al–Mg/Al 2 O 3np metal matrix nanocomposites: Effects of Mg and reinforcement concentration and method of reinforcement incorporation," J. Mater. Sci., vol. 49, no. 5, pp. 2106-2116, 2014 [doi:10.1007/s10853-013-7903-7].

[203] H. Su, W. Gao, Z. Feng, and Z. Lu, "Processing, microstructure and tensile properties of nanosized Al2O3 particle reinforced aluminium matrix composites," Mater. Des. (1980–2015), vol. 36, pp. 590-596, 2012 [doi:10.1016/j.matdes.2011.11.064].

[204] J. Lakshmipathy and B. Kulendran, "Reciprocating wear behavior of 7075Al/SiC in comparison with 6061Al/Al2O3 composites," Int. J. Refract. Met. Hard Mater., vol. 46, pp. 137-144, 2014 [doi:10.1016/j.ijrmhm.2014.06.007].

[205] K. Sekar, K. Allesu, and M. A. Joseph, "Effect of T6 heat treatment in the microstructure and mechanical properties of A356 reinforced with Nano Al2O3 particles by combination effect of stir and squeeze casting," Procedia Mater. Sci., vol. 5, pp. 444-453, 2014 [doi:10.1016/j.mspro.2014.07.287].

[206] M. Akbari and O. Karbalaei, "Mirzaee, and H. R. Baharvandi," Fabr. Study Mech. Prop. Fract. Behav. Nanometric Al2O3 particle-reinforced A356 composites focusing on the parameters of vortex method." Materials & Design 46, pp. 199-205, 2013.

[207] G. B. Kumar, C. S. P. Rao, N. Selvaraj, and M. S. Bhagyashekar, "Studies on Al6061-SiC and Al7075-Al2O3 metal matrix composites," J. Miner. Mater. Char. Eng., vol. 9, no. 1, pp. 43-55, 2010.

[208] S. Tahamtan, M. Emamy, and A. Halvaee, "Effects of reinforcing particle size and interface bonding strength on tensile properties and fracture behavior of Al-A206/alumina micro/nanocomposites," J. Compos. Mater., vol. 48, no. 27, pp. 3331-3346, 2014 [doi:10.1177/0021998313509860].

[209] H. R. Ezatpour, M. T. Parizi, S. A. Sajjadi, G. R. Ebrahimi, and A. Chaichi, "Microstructure, mechanical analysis and optimal selection of 7075 aluminum alloy based composite reinforced with alumina nanoparticles" Mater. Chem. Phys., vol. 178, pp. 119-127, 2016 [doi:10.1016/j.matchemphys.2016.04.078].

[210] R. S. Rana and R. Purohit, "Development and analysis of Al-matrix nanocomposites fabricated by ultrasonic assisted squeeze casting process," Mater. Today Proc., vol. 2, no. 4-5, pp. 3697-3703, 2015.

[211] V. Balaji, N. Sateesh, and M. M. Hussain, "Manufacture of aluminium metal matrix composite (Al7075-SiC) by stir casting technique," Mater. Today Proc., vol. 2, no. 4-5, pp. 3403-3408, 2015 [doi:10.1016/j.matpr.2015.07.315].

[212] P. Dong, H. Zhao, F. Chen, and J. Li, "Microstructures and properties of A356–10% SiC particle composite castings at different solidification pressures," Trans. Nonferrous Met. Soc. China, vol. 23, no. 8, pp. 2222-2228, 2013 [doi:10.1016/S1003-6326(13)62721-1].

[213] P. Gurusamy, B. Prabu, and R. Paskaramoorthy "Influence of processing temperatures on mechanical properties and microstructure of squeeze cast aluminium alloy composites," Mater. Manuf. Processes, vol. 30, no. 3, pp. 367-373, 2015 [doi:10.1080/10426914.2014.973587].

[214] H. Xu, J. Yan, Z. Xu, B. Zhang, and S. Yang. "Interface structure changes during vibration liquid phase bonding of SiCp/A356 composites in air," Compos. A, vol. 37, no. 9, pp. 1458-1463, 2006 [doi:10.1016/j.compositesa.2005.06.017].

[215] I. Sahin and A. Akdogan Eker, "Analysis of microstructures and mechanical properties of particle reinforced AlSi7Mg2 matrix composite materials," J. Mater. Eng. Perform., vol. 20, no. 6, pp. 1090-1096, 2011 [doi:10.1007/s11665-010-9738-6].

[216] A. Mazahery and Mohsen O. Shabani, “Nanosized silicon carbide reinforced commercial casting aluminium alloy matrix: Experimental and novel modeling evaluation,” Powder Technol., vol. 217, pp. 558-565, 2012 [doi:10.1016/j.powtec.2011.11.020].

[217] M. Vanarotti, P. Shrishail, B. R. Sridhar, K. Venkateswarlu, and S. A. Kori, “Study of mechanical properties & residual stresses on post wear samples of A356-SiC metal matrix composites,” Procedia Mater. Sci., vol. 5, pp. 873-882, 2014 [doi:10.1016/j.mspro.2014.07.374].

[218] S. M. Seyed Reihani, “Processing of squeeze cast Al6061-30vol% SiC composites and their characterization” Mater. Des., vol. 27, no. 3, pp. 216-222, 2006 [doi:10.1016/j.matdes.2004.10.016].

[219] G. V. Kumar, C. S. P. Rao, and N. Selvaraj, “Mechanical and dry sliding wear behavior of Al7075 alloy-reinforced with SiC particles,” J. Compos. Mater., vol. 46, no. 10, pp. 1201-1209, 2012 [doi:10.1177/0021998311414948].

[220] S. Gargatte, R. R. Upadhye, V. S. Dandagi, S. R. Desai, and B. S. Waghamode “Preparation & characterization of Al-5083 alloy composites,” J. Miner. Mater. Char. Eng., vol. 1, no. 01, p. 8-14, 2013.

[221] A. Sakthivel, R. Palaninathan, R. Velmurugan, and P. R. Rao, “Production and mechanical properties of SiC p particle-reinforced 2618 aluminium alloy composites,” J. Mater. Sci., vol. 43, no. 22, pp. 7047-7056, 2008 [doi:10.1007/s10853-008-3033-z].

[222] R. S. Rana, “Characterization of mechanical properties and microstructure of aluminium alloy-SiC composites,” Mater. Today Proc., vol. 2, no. 4-5, pp. 1149-1156, 2015 [doi:10.1016/j.matpr.2015.07.026].

[223] G. G. Sozhamannan, P. S Balasivanandha, and V.S. K. Venkatagalapathy, "Effect of processing paramters on metal matrix composites: stir casting process.", J. Surf. Engineered Mater. Adv. Technol., vol. 2012, 2012.

[224] A. Mazahery and Mohsen O. Shabani, “Application of the extrusion to increase the binding between the ceramic particles and the metal matrix: Enhancement of mechanical and tribological properties,” J. Mater. Sci. Technol., vol. 29, no. 5, pp. 423-428, 2013 [doi:10.1016/j.jmst.2013.03.016].

[225] A. Mazahery, M. Alizadeh, and M. O. Shabani “Study of tribological and mechanical properties of A356–Nano SiC composites,” Trans. Indian Inst. Met., vol. 65, no. 4, pp. 393-398, 2012 [doi:10.1007/s12666-012-0143-8].

[226] R. Harichandran and N. Selvakumar, “Effect of Nano/micro B 4 C particles on the mechanical properties of aluminium metal matrix composites fabricated by ultrasonic cavitation-assisted solidification process,” Arch. Civ. Mech. Eng., vol. 16, no. 1, pp. 147-158, 2016 [doi:10.1016/j.acme.2015.07.001].

[227] A. Mazahery, M. O. Shabani, M. R. Rahimipour, A. A. Tofigh, and M. Razavi, “Effect of coated B4C reinforcement on mechanical properties of squeeze cast A356 composites,” Kovove Mater., vol. 50, no. 2, pp. 107-113, 2012 [doi:10.4149/km_2012_2_107].

[228] A. Mazahery and Mohsen O. Shabani, “Existence of good bonding between coated B4C reinforcement and al matrix via semisolid techniques: Enhancement of wear resistance and mechanical properties,” Tribol. Trans., vol. 56, no. 3, pp. 342-348, 2013 [doi:10.1080/10402004.2012.752552].

[229] A. Mazahery and M. O. Shabani, “Sol–gel coated B4C particles reinforced 2024 Al matrix composites,” Proc. Inst. Mech. Eng. L, vol. 226, no. 2, pp. 159-169, 2012 [doi:10.1177/1464420711428996].

[230] A. Mazahery, M. O. Shabani, E. Salahi, M. R. Rahimipour, A. A. Tofigh, and M. Razavi, “Hardness and tensile strength study on Al356–B4C composites,” Mater. Sci. Technol., vol. 28, no. 5, pp. 634-638, 2012 [doi:10.1179/1743284710Y.0000000010].

[231] A. Mazahery and Mohsen O. Shabani, “Existence of good bonding between coated B4C reinforcement and al matrix via semisolid techniques: Enhancement of wear resistance and mechanical properties,” Tribol. Trans., vol. 56, no. 3, pp. 342-348, 2013 [doi:10.1080/10402004.2012.752552].

[232] A. Mazahery and Mohsen O. Ostad Shabani, “Mechanical properties of squeeze-cast A356 composites reinforced with B 4 C particulates,” J. Mater. Eng. Perform., vol. 21, no. 2, pp. 247-252, 2012 [doi:10.1007/s11665-011-9867-6].

[233] A. Mazahery, M. Alizadeh, and M. O. Shaban, “Wear of Al–Si alloys matrix reinforced with sol–gel coated particles,” Mater. Technol., vol. 27, no. 2, pp. 180-185, 2012 [doi:10.1179/175355511X13178856214678].

[234] Y.H. Seo and C.-G. Kang, “The effect of applied pressure on particle-dispersion characteristics and mechanical properties in melt-stirring squeeze-cast SiCp/Al composites,” J. Mater. Process. Technol., vol. 55, no. 3-4, pp. 370-379, 1995 [doi:10.1016/0924-0136(95)02033-0].

[235] V. Dao, S. Zhao, W. Lin, and C. Zhang "Effect of process parameters on microstructure and mechanical properties in AlSi9Mg connecting-rod fabricated by semi-solid squeeze casting," Mater. Sci. Eng. A, vol. 558, pp. 95-102, 2012 [doi:10.1016/j.msea.2012.07.084].

[236] P. Vijian and V. P. Arunachalam, "Modelling and multi objective optimization of LM24 aluminium alloy squeeze cast process parameters using genetic algorithm," J. Mater. Process. Technol., vol. 186, no. 1-3, pp. 82-86, 2007 [doi:10.1016/j.jmatprotec.2006.12.019].

[237] P. Senthil and K. S. Amirthagadeswaran, "Optimization of squeeze casting parameters for non symmetrical AC2A aluminium alloy castings through Taguchi method," J. Mech. Sci. Technol., vol. 26, no. 4, pp. 1141-1147, 2012 [doi:10.1007/s12206-012-0215-z].

[238] H. Goyal, N. Mandal, H. Roy, S. K. Mitra, and B. Mondal, "Multi response optimization for processing Al–SiCp composites: An approach towards enhancement of mechanical properties," Trans. Indian Inst. Met., vol. 68, no. 3, pp. 453-463, 2015 [doi:10.1007/s12666-014-0476-6].

[239] W. G. Hai Su, W. Gao, H. Zhang, H. Liu, J. Lu, and Z. Lu "Optimization of stirring parameters through numerical simulation for the preparation of aluminium matrix composite by stir casting process," J. Manuf. Sci. Eng., vol. 132, no. 6, 2010. [https://doi.org/10.1115/1.4002851]

[240] M. Dhanashekar and V. S. S. Kumar, "Squeeze casting of aluminium metal matrix composites-an overview," Procedia Eng., vol. 97, pp. 412-420, 2014 [doi:10.1016/j.proeng.2014.12.265].

[241] A. Maleki, B. Niroumand, and A. Shafyei, "Effects of squeeze casting parameters on density, macrostructure and hardness of LM13 alloy," Mater. Sci. Eng. A, vol. 428, no. 1-2, pp. 135-140, 2006 [doi:10.1016/j.msea.2006.04.099].

[242] M. S. Yong and A. J. Clegg, "Process optimisation for a squeeze cast magnesium alloy metal matrix composite," J. Mater. Process. Technol., vol. 168, no. 2, pp. 262-269, 2005 [doi:10.1016/j.jmatprotec.2005.01.012].

[243] R. Umunakwe, O. C. Okoye, U. S. Nwigwe, A. Oyetunji, and I. J. Umunakwe, "Effects of stirring time and particles preheating on porosity, mechanical properties and

microstructure of periwinkle shell-aluminium metal matrix composite (PPS-ALMMC),” Ann. Fac. Eng. Hunedoara, vol. 15, no. 3, p. 133, 2017.

[244] J. Hashim, L. Looney, and M. S. J. Hashmi, “Metal matrix composites: Production by the stir casting method,” J. Mater. Process. Technol., vol. 92-93, pp. 1-7, 1999 [doi:10.1016/S0924-0136(99)00118-1].

[245] C. S. Jawalkar, Ajay Singh Verma, and N. M. Suri, “Fabrication of aluminium metal matrix composites with particulate reinforcement: A review,” Mater. Today Proc., vol. 4, no. 2, pp. 2927-2936, 2017 [https://doi.org/10.1016/j.matpr.2017.02.174].

[246] J. Hashim, “The production of cast metal matrix composite by a modified stir casting method,” Jurnalteknologi, 2001: 9â-20 [doi:10.11113/jt.v35.588].

[247] A. Kumar, A. Nirala, V. P. Singh, B. K. Sahoo, R. C. Singh, R. Chaudhary, A. K. Dewangan, G. K. Gaurav, J. J. Klemeš, and X. Liu “The utilisation of coconut shell ash in production of hybrid composite: Microstructural characterisation and performance analysis,” J. Cleaner Prod., vol. 398, p. 136494, 2023 [doi:10.1016/j.jclepro.2023.136494].

[248] Light Metals, n.d. Available at: http://www.temponik.com/Material.

[249] “Aluminium matrix composite (AMC) pushrods 2018”. Available at: http://solutions.3m.com/3MContentRetrievalAPI/BlobServlet?lmd=1149596328000&assetType=MMM_Image&locale=en_US&blobAttribute=ImageFile&fallback=true&univid=1114293769330&placeId=62603&version=current.

[250] Aluminium Composite Panel, Manufacturer | ALUCOWORLD n.d. Available at: http://www.alucoworld.com.

[251] “Metal Matrix Composite Ceramics – Advanced Ceramics n.d.” Available at: https://ceramics. Available at: http://ferrotec.com/products/metal-matrix.

[252] “Metal Matrix Composite (MMC),”, n.d. Available at: https://www.ceramtec.com/ceramicmaterials/metal-matrix-composites.

[253] E. X. Suprem, “Metal Matrix Composites (MMCs) – Materion n.d.” Available at: https://materion, Com/products/metal-matrix-composites/supremex.

[254] Elementum, “3D Aluminium MMC materials set n.d.” Available at: https://www.elementum3d, Com/aluminium-mmc.

[255] “M Cubed Technologies, A world leader in ceramics and Metal Matrix Composites n.d.” Available at: http://www.mmmt.com/materials/metal-matrix-composites.html.

[256] “Gamma Alloys – Nanotechnology inside every aluminium bar! n.d.” http:. Available at: http://gammaalloys.com/reinforced-lightweight-alloys/#mmc.

[257] A. M. Razzaq, D. L. A. A. Majid, and M. R. Ishak “A brief research review for improvement methods the wettability between ceramic reinforcement particulate and aluminium matrix composites.” In IOP Conference Series, Mater. Sci. Eng. IOP Publishing, vol. 203, no. 1, p. 012002, 2017.

[258] J. M. Mistry and P. P. Gohil, “Research review of diversified reinforcement on aluminium metal matrix composites: Fabrication processes and mechanical characterization,” Sci. Eng. Compos. Mater., vol. 25, no. 4, pp. 633-647, 2018 [doi:10.1515/secm-2016-0278].

[259] B. Thakur, S. Barve, and P. Pesode “Investigation on mechanical properties of AZ31B magnesium alloy manufactured by stir casting process,” J. Mech. Behav. Biomed. Mater., vol. 138, p. 105641, 2023 [doi:10.1016/j.jmbbm.2022.105641].

[260] G. Rajan, A. K. Godasu, and S. Mula, “Effect of friction stir processing on microstructural evolution and mechanical properties of nanosized SiC reinforced AA5083 nanocomposites developed by stir casting,” Mater. Today Commun., vol. 35, p. 105912, 2023 [doi:10.1016/j.mtcomm.2023.105912].

[261] V.G. SP, “Effect of ultrasonic treatment during stir casting on mechanical properties of AA6063-SiC composites,” Mater. Chem. Phys., vol. 294, p. 126977, 2023 [doi:10.1016/j.matchemphys.2022.126977].

[262] D. Kumar and L. Thakur, “Influence of hybrid reinforcements on the mechanical properties and morphology of AZ91 magnesium alloy composites synthesized by ultrasonic-assisted stir casting,” Mater. Today Commun., vol. 35, p. 105937, 2023 [doi:10.1016/j.mtcomm.2023.105937].

[263] S. Ranjan and P. K. Jha, “Investigation on the thermodynamic stability of phases evolved in Al-based hybrid metal matrix composite fabricated using in-situ stir casting route,” J. Manuf. Processes, vol. 95, pp. 14-26, 2023 [doi:10.1016/j.jmapro.2023.03.084].

[264] D. Makwana and B. Pramod, “Dry sliding wear and heat flux mapping of closed-cell Mg-2Zn-2Ca foam fabricated by stir casting route,” Mater. Lett., vol. 330, p. 133379, 2023 [doi:10.1016/j.matlet.2022.133379].

[265] S. Memar, M. Azadi, “An evaluation on microstructure, wear, and compression behavior of Al2O3/brass matrix nanocomposites fabricated by stir casting method,” Mater. Today Commun., vol. 34, p. 105130, 2023 [doi:10.1016/j.mtcomm.2022.105130].

[266] P. Kumaravelu and J. Kandasamy, “Controlling the mechanical failures of stir-cast Mg-AZ91D alloy using dicalcium silicate reinforcement,” Eng. Fail. Anal., vol. 146, p. 107139, 2023 [doi:10.1016/j.engfailanal.2023.107139].

[267] D. Kumar, S. Singh, and S. Angra “Dry sliding wear and microstructural behavior of stir-cast al6061-based composite reinforced with cerium oxide and graphene nanoplatelets,” Wear, vol. 516-517, p. 204615, 2023 [doi:10.1016/j.wear.2022.204615].

[268] C. Kumar, S. Sarkar, G. Mukhopadhyay, P. C. Chakraborti, I. Sen, and S. Roy. “Systematic study of the effect of K2TiF6 flux content on the microstructure and mechanical properties of Al–B4C composites,” Mater. Sci. Eng. A, vol. 871, p. 144913, 2023 [doi:10.1016/j.msea.2023.144913].

[269] C. K. Dhinakarraj, N. Senthilkumar, K. Palanikumar, and B. Deepanraj, “Experimental interrogations on morphologies and mechanical delineation of silicon nitride fortified Mg-Al-Zn alloy composites,” Mater. Today Commun., vol. 35, p. 105731, 2023 [doi:10.1016/j.mtcomm.2023.105731].

[270] B. Saleh, A. Ma, R. Fathi, N. Radhika, G. Yang, and J. Jiang “Optimized mechanical properties of magnesium matrix composites using RSM and ANN,” Mater. Sci. Eng. B, vol. 290, p. 116303, 2023 [doi:10.1016/j.mseb.2023.116303].

[271] V. Chenrayan, V. Vaishnav, K. Shahapurkar, C. Manivannan, V. Tirth, I. M. Alarifi, M. A. Alamir, C. I. Pruncu, and L. Lamberti, “Tribological performance of TiB2-graphene Al 7075 hybrid composite processed through squeeze casting: At room and high temperature,” Tribol. Int., vol. 185, p. 108486, 2023 [doi:10.1016/j.triboint.2023.108486].

[272] R. Vicente, K. Cesca, A. F. V. Silva, D. Oliveira, C. J. Andrade, and A. Ambrosi “Hierarchical membrane by centrifugal casting and effects of incorporating activated carbon as pore-former,” J. Eur. Ceram. Soc., vol. 43, no. 8, pp. 3447-3453, 2023 [doi:10.1016/j.jeurceramsoc.2023.02.040].

[273] H. Ismail, M. N. Z. Zakri, A. Ahmad, and H. Mohamad “Effect of sintering temperature on the phase, microstructural, physical, mechanical, and in vitro biomineralisation properties of porous wollastonite ceramics fabricated using the gel

casting method," Ceram. Int., vol. 49, no. 9, 14166-14176, 2023 [doi:10.1016/j.ceramint.2023.01.003].

[274] F. Guan, W. Jiang, Z. Zhang, J. Wang, G. Li, and Z. Fan, "Interfacial microstructure, mechanical properties and strengthening mechanism of Mg/Al bimetallic composites produced by a novel compound casting with the addition of Gd," Mater. Char., vol. 200, p. 112898, 2023 [doi:10.1016/j.matchar.2023.112898].

[275] S. Chakravarty, R. Sikder, P. Haldar, T. Nandi, and G. Sutradhar, "Experimental investigation on feasibility of industrial waste to resource conversion for cupola slag," Results Eng., vol. 17, p. 100962, 2023 [doi:10.1016/j.rineng.2023.100962].

[276] B. Chen, X. Sun, D. Liu, H. Tian, and J. Gao, "A novel method combining VAT photopolymerization and casting for the fabrication of biodegradable Zn–1Mg scaffolds with triply periodic minimal surface," J. Mech. Behav. Biomed. Mater., vol. 141, p. 105763, 2023 [doi:10.1016/j.jmbbm.2023.105763].

[277] Y. Zhang, J. Yu, J. Guo, G. He, Y. Zhao, Q. Lu, J. Wu, X. Shu, X. Lin, and Q. Chen, "Improving osteogenic and antibacterial properties of porous titanium scaffolds by facile flow-casting of bioactive glass-Ag@MSN coatings," Surf. Coat. Technol., vol. 459, p. 129400, 2023 [doi:10.1016/j.surfcoat.2023.129400].

[278] C. Ye, Y. Zhao, Y. Li, X. Zhao, M. Li, J. Shi, and X. Liu,"Structure, impedance and conduction mechanisms of tape-casting (Na0. 5TiO2, 2023 (Bi, 44Nd0. 01Sr0. 02Ca0)" Ceram. Int., vol. 49 no. 02 pp. 14571-80 [https://doi.org/10.1016/j.ceramint.2023.01.047].

[279] S. J. Huang, M. Subramani, K. Borodianskiy, P. N. Immanuel, and C. C. Chiang, "Effect of equal channel angular pressing on the mechanical properties of homogenized hybrid AZ61 magnesium composites," Mater. Today Commun., vol. 34, p. 104974, 2023 [doi:10.1016/j.mtcomm.2022.104974].

[280] K. Senthilraj and G. Rajamurugan, "Influence of Al2TiO5 particles on AA6061 composites fabricated by bottom pouring stir casting technique," Mater. Lett., vol. 338, p. 134085, 2023 [doi:10.1016/j.matlet.2023.134085].

[281] V. R. Rao, N. Ramanaiah, and M. M. M. Sarcar, "Tribological properties of Aluminium Metal Matrix Composites (AA7075 Reinforced with Titanium Carbide (TiC) Particles)" Int. J. Adv. Sci. Technol., vol. 88, pp. 13-26, 2016 [doi:10.14257/ijast.2016.88.02].

[282] P. K. Yadav, G. Dixit, S. Dixit, V. P. Singh, S. K. Patel, R. Purohit, and B. Kuriachen “Effect of eutectic silicon and silicon carbide particles on high stress scratching wear of aluminium composite for various testing parameters,” Wear, vol. 482-483, p. 203921, 2021 [doi:10.1016/j.wear.2021.203921].

[283] A. Baradeswaran and A. E. Perumal, “Wear and mechanical characteristics of Al 7075/graphite composites,” Compos. B Eng., vol. 56, pp. 472-476, 2014 [doi:10.1016/j.compositesb.2013.08.073].

[284] A. Bhandakkar, R. C. Prasad, and S. M. Sastry, “Fracture toughness of AA2024 aluminium fly ash metal matrix composites,” Int. J. Compos. Mater., vol. 4, no. 2, pp. 108-124, 2014.

[285] R. Manikandan, and, and T. V. Arjunan, “Studies on micro structural characteristics, mechanical and tribological behaviours of boron carbide and cow dung ash reinforced aluminium (Al 7075) hybrid metal matrix composite” Compos. B Eng., vol. 183, p. 107668, 2020 [doi:10.1016/j.compositesb.2019.107668].

[286] M. K. Surappa, S. V. Prasad, and P. K. Rohatgi, “Wear and abrasion of cast Al-alumina particle composites,” Wear, vol. 77, no. 3, pp. 295-302, 1982 [doi:10.1016/0043-1648(82)90055-2].

[287] S. Ozden, R. Ekici, and F. Nair “Investigation of impact behaviour of aluminium based SiC particle reinforced metal–matrix composites,” Compos. A, vol. 38, no. 2, pp. 484-494, 2007 [doi:10.1016/j.compositesa.2006.02.026].

[288] Y. Sahin, "Preparation and some properties of SiC particle reinforced aluminium alloy composites." *Materials & design* vol.24, no. 8 pp. 671-679 2003 [https://doi.org/10.1016/S0261-3069(03)00156-0].

[289] J. D. Embury, “Plastic flow in dispersion hardened materials,” Metall. Trans. A, vol. 16, no. 12, pp. 2191-2200, 1985 [doi:10.1007/BF02670418].

[290] D. L. McDanels, “Analysis of stress–strain, fracture, and ductility behavior of aluminium matrix composites containing discontinuous silicon carbide reinforcement,” Metall. Trans. A, vol. 16, no. 6, pp. 1105-1115, 1985 [doi:10.1007/BF02811679].

[291] H. Hatta, T. Takei, and M. Taya “Effects of dispersed microvoids on thermal expansion behavior of composite materials,” Mater. Sci. Eng. A, vol. 285, no. 1-2, pp. 99-110, 2000 [doi:10.1016/S0921-5093(00)00721-8].

[292] K. Chu, X. Wang, Y. Li, D. Huang, Z. Geng, X. Zhao, H. Liu, and H. Zhang, "Thermal properties of graphene/metal composites with aligned graphene," Mater. Des., vol. 140, pp. 85-94, 2018 [doi:10.1016/j.matdes.2017.11.048].

[293] P. G. Koppad, H. R. A. Ram, and K. T. Kashyap "On shear-lag and thermal mismatch model in multiwalled carbon nanotube/copper matrix nanocomposites," J. Alloys Compd., vol. 549, pp. 82-87, 2013 [doi:10.1016/j.jallcom.2012.09.073].

[294] P. K. Yadav, G. Dixit, S. Dixit, V. P. Singh, S. K. Patel, R. Purohit, and B. Kuriachen, "Effect of eutectic silicon and silicon carbide particles on high stress scratching wear of aluminium composite for various testing parameters," Wear, vol. 482-483, p. 203921, 2021 [doi:10.1016/j.wear.2021.203921].

[295] A. Ureña, J. Rams, M. Campo, and M. Sanchez, "Effect of reinforcement coatings on the dry sliding wear behaviour of aluminium/SiC particles/carbon fibres hybrid composites," Wear, vol. 266, no. 11-12, pp. 1128-1136, 2009 [doi:10.1016/j.wear.2009.03.016].

[296] S. Sardar, S. K. Karmakar, and D. Das "High stress abrasive wear characteristics of Al 7075 alloy and 7075/Al2O3 composite," Measurement, vol. 127, pp. 42-62, 2018 [doi:10.1016/j.measurement.2018.05.090].

[297] K. K. Alaneme and T. M. Adewale, "Influence of rice husk ash–silicon carbide weight ratios on the mechanical behaviour of Al-Mg-Si alloy matrix hybrid composites," Tribol. Ind., vol. 35, no. 2, p. 163, 2013.

[298] K. K. Alaneme, B. O. Ademilua, and M. O. Bodunrin, "Mechanical properties and corrosion behaviour of aluminium hybrid composites reinforced with silicon carbide and bamboo leaf ash," Tribol. Ind., vol. 35, no. 1, p. 25, 2013.

[299] A. A. Hamid, P. K. Ghosh, S. Jain, and S. Ray, "The influence of porosity and particles content on dry sliding wear of cast in situ Al(Ti)–Al2O3(TiO2) composite" Wear, vol. 265, no. 1-2, pp. 14-26, 2008 [doi:10.1016/j.wear.2007.08.018].

[300] G. V. Kumar, C. S. P. Rao, and N. Selvaraj, "Mechanical and dry sliding wear behavior of Al7075 alloy-reinforced with SiC particles," J. Compos. Mater., vol. 46, no. 10, pp. 1201-1209, 2012 [doi:10.1177/0021998311414948].

[301] Z. Zhang and D. L. Chen, "Contribution of Orowan strengthening effect in particulate-reinforced metal matrix nanocomposites," Mater. Sci. Eng. A, vol. 483-484, pp. 148-152, 2008 [doi:10.1016/j.msea.2006.10.184].

[302] R. Deaquino-Lara, N. Soltani, A. Bahrami, E. Gutiérrez-Castañeda, E. García-Sánchez, and M. A. L. Hernandez-Rodríguez, “Tribological characterization of Al7075–graphite composites fabricated by mechanical alloying and hot extrusion,” Mater. Des., vol. 67, pp. 224-231, 2015 [doi:10.1016/j.matdes.2014.11.045].

[303] C. Fenghong, C. Chang, W. Zhenyu, T. Muthuramalingam, and G. Anbuchezhiyan, “Effects of silicon carbide and tungsten carbide in aluminium metal matrix composites,” Silicon, vol. 11, no. 6, pp. 2625-2632, 2019 [doi:10.1007/s12633-018-0051-6].

[304] N. Kumar, G. Gautam, R. K. Gautam, A. Mohan, and S. Mohan “A study on mechanical properties and strengthening mechanisms of AA5052/ZrB2 in situ composites,” J. Eng. Mater. Technol., vol. 139, no. 1, p. 011002, 2017 [doi:10.1115/1.4034692].

[305] A. Pineau, A. Benzerga, and T. Pardoe, “Failure of metals I: Brittle and ductile fracture” Acta Mater., vol. 107, pp. 424-483, 2016 [doi:10.1016/j.actamat.2015.12.034].

[306] J. Li, S. Lü, S. Wu, and Q. Gao, “Effects of ultrasonic vibration on microstructure and mechanical properties of nano-sized SiC particles reinforced Al-5Cu composites,” Ultrason. Sonochem., vol. 42, pp. 814-822, 2018 [doi:10.1016/j.ultsonch.2017.12.038].

[307] A. Baradeswaran, A. Elayaperumal, and R. F. Issac “A statistical analysis of optimization of wear behaviour of Al-Al2O3 composites using Taguchi technique,” Procedia Eng., vol. 64, pp. 973-982, 2013 [doi:10.1016/j.proeng.2013.09.174].

[308] R. N. Rao, and S. Das. "Effect of matrix alloy and influence of SiC particle on the sliding wear characteristics of aluminium alloy composites." *Materials & Design* vol. 31, no. 3 pp. 1200-1207, 2010. [https://doi.org/10.1016/j.matdes.2009.09.032].

[309] N. Selvakumar and S. C. Vettivel, “Thermal, electrical and wear behavior of sintered Cu–W nanocomposite,” Mater. Des. (1980–2015), vol. 46, pp. 16-25, 2013 [doi:10.1016/j.matdes.2012.09.055].

[310] A. Baradeswaran, A. Elayaperumal, and R. F. Issac, “A statistical analysis of optimization of wear behaviour of Al-Al2O3 composites using Taguchi technique,” Procedia Eng., vol. 64, pp. 973-982, 2013 [doi:10.1016/j.proeng.2013.09.174].

[311] H. Ma. F. Zhao, M. Li, P. Wang, Y. Fu, G. Wang, and X. Liu “Construction of hollow binary oxide heterostructures by Ostwald ripening for superior photoelectrochemical removal of reactive brilliant blue KNR dye,” Adv. Powder Mater., vol. 2, no. 3, p. 100117, 2023 [doi:10.1016/j.apmate.2023.100117].

[312] A. Baradeswaran, S. C. Vettivel, A. E. Perumal, N. Selvakumar, and R. F. Issac "Experimental investigation on mechanical behaviour, modelling and optimization of wear parameters of B4C and graphite reinforced aluminium hybrid composites," Mater. Des., vol. 63, pp. 620-632, 2014 [doi:10.1016/j.matdes.2014.06.054].

[313] B. Venkataraman and G. Sundararajan, "Correlation between the characteristics of the mechanically mixed layer and wear behaviour of aluminium, Al-7075 alloy and Al-MMCs," Wear, vol. 245, no. 1-2, pp. 22-38, 2000 [doi:10.1016/S0043-1648(00)00463-4].

LIST OF PUBLICATION

Publications

SCI Journals: 7

Published: 4

1. **Kumar, Ashish**, R. C. Singh, and Rajiv Chaudhary. " Investigation of Microstructure and Several Quality Characteristics of AA7075/Al2O3/Coconut Shell Ash Hybrid Nano Composite Prepared through Ultrasonic Assisted Stir-Casting." Journal of Materials Engineering and Performance (2022). **Impact Factor- 2.9**.
2. **Kumar, Ashish**, R. C. Singh, and Rajiv Chaudhary. "Investigation of Nano-Al2O3 and Micro-coconut Shell Ash (CSA) Reinforced AA7075 Hybrid Metal–Matrix Composite using Two-Stage Stir Casting." Arabian Journal for Science and Engineering 47, no. 12 (2022):15559-15573. **Impact Factor- 2.3**.
3. **Kumar, Ashish**, Akhileshwar Nirala, V. P. Singh, Biraj Kumar Sahoo, R. C. Singh, Rajiv Chaudhary, Ashok K. Dewangan, Gajendra Kumar Gaurav, Jiří Jaromír Klemeš, and Xinghui Liu. "The utilisation of coconut shell ash in production of hybrid composite: Microstructuralcharacterisation and performance analysis." Journal of Cleaner Production 398 (2023):136494**. Impact Factor- 11.1**
4. **Kumar Ashish**, V.P. Singh, Akhileshwar Nirala , R.C. Singh , Rajiv Chaudhary , Abdel-Hamid I. Mourad , B. K. Sahoo , Deepak Kumar. “Influence of Tool Rotational Speed on Mechanical and Corrosion Behaviour of Friction Stir Processed AZ31/Al2O3 Nanocomposite Journal of Magnesium and Alloys”, Journal of Magnesium and Alloys, **Impact Factor- 17.6**

Communicated in SCI Journals

1. Kumar Ashish, V.P. Singh, B. K. Sahoo R.C. Singh , Rajiv Chaudhary , Deepak Kumar.. “Enhancing Microstructural and Tribological Characteristics of Al-Zn-Mg-

Cu Alloy Through Micro/Nano Al2O3 Reinforcement", Tribology International, **Impact Factor -6.2** TRIBINT-D-23-02476R2 Under review.

2. Kumar Ashish, V.P. Singh, R.C. Singh , Rajiv Chaudhary , Abdel-Hamid I. Mourad , Deepak Kumar.. "A Review of Aluminum Metal Matrix Composites: Fabrication Route, Reinforcements, Microstructural, Mechanical and corrosion Properties", Journal of Materials Science *:* Manuscript Number: JMSC-D-23-06454. **Impact Factor -4.5** Under review.
3. Kumar Ashish, V.P. Singh, Akash malik, B. K. Sahoo, R.C. Singh , Rajiv Chaudhary. "The utilization of agricultural and industrial waste in the synthesis of AA7075-based novel lightweight composite", Journal of Materials Science, Manuscript Number: JMSC-D-23-06598. **Impact Factor -4.5** Under review.

International Conferences:

1. Research paper entitled & quot; Tribological studies and microstructural characterisatio of SiC and fly ash particles based aluminium 2024 alloy composites prepared through **stir** casting route" presented at 8 th International Symposium on Fusion of Science & Technology (ISFT-2020), held at J.C. Bose University of Science & Technology, YMCA, Faridabad, India from January 6-10, 2020.
2. Research paper entitled & quot; Recent progress in production of metal matrix composites by stir casting process: An overview" presented in International conference on mechanical and Energy Technology (ICMET-2019) at Galgotias college of Engineering and Technology on 07-08 November, 2019.
3. Research paper entitled & quot; Investigation of Microstructural, Hardness and Tensile Response of Stir Cast AA7075 Composite" communicated in International conference on mechanical and Energy Technology (ICMET-2023) at Galgotias college of Engineering and Technology on 07-08 December, 2023.
4. Research paper entitled & quot; Investigation of Thermal Behaviors of as-cast Hybrid Composites Using Alumina and Coconut shell ash as Reinforcements" communicated in International Symposium on Fusion of Science &

Technology (ISFT-2024), held at J.C. Bose University of Science & Technology, YMCA, Faridabad, India from January 8 13,2024.

Arabian Journal for Science and Engineering (2022) 47:15559–15573
https://doi.org/10.1007/s13369-022-06728-2

RESEARCH ARTICLE-MECHANICAL ENGINEERING

Investigation of Nano-Al_2O_3 and Micro-coconut Shell Ash (CSA) Reinforced AA7075 Hybrid Metal–Matrix Composite Using Two-Stage Stir Casting

Ashish Kumar[1,2] · R. C. Singh[1] · Rajiv Chaudhary[1]

Received: 10 August 2021 / Accepted: 17 February 2022 / Published online: 11 March 2022

Abstract
The present work is focused on the influences of reinforced particles on mechanical, microstructural, and tribological performances of AA7075 hybrid metal–matrix composites (HMMCs). Al_2O_3 and coconut shell ash (CSA) were reinforced using two-stage stir casting by varying the wt% (0–5) of reinforcement. Microstructural analysis and various phase identifications were examined with the help of scanning electron microscope (SEM) equipped with EDX and optical microscope. Various mechanical testing such as tensile, hardness, 3-point bend test, and tribological behaviors were carried out to know the HMMCs properties. Microstructural images revealed a homogeneous distribution of reinforced particles in the metal–matrix and EDX confirmed the presence of dispersed reinforcements (Al_2O_3 and CSA) in the HMMCs. It was seen that mechanical properties and tribological behavior have been increased after addition of Al_2O_3 and CSA reinforced particles whereas slightly decreased in impact strength. Transgranular cleavage facets, micro-void coalescence, dimples, and crack were shown in SEM images of fractured specimens during impact and tensile testing.

Keywords AA7075 · Al_2O_3 · Coconut shell ash (CSA) · Stir casting · Microstructure · Mechanical properties · Flexural test

1 Introduction

Al-alloys have its own inherent properties such as good mechanical strength, low density, and excellent corrosion resistance, and it leads to a widespread application in automobile and aerospace industries [1]. Particularly AA7075 alloy is a cold-finished wrought product having zinc as a primary alloying element. It has the highest tensile strength among all Al-screw machine alloys. AA7075 alloy is used for the highly stressed structural components including aircraft fitting, shafts, gear, and a variety of other commercial aircraft, transportations, and equipment [2]. Generally, the Al-alloys strength can be enhanced in various means, including: (i) by the addition of insoluble second particles to form hybrid metal–matrix composite (HMMCs) [3], (ii) by the precipitation hardening method [4], (iii) by the surface coatings method, (iv) by the cryogenic treatments method, etc. [5]. Among the above-mentioned processes, HMMCs contain much concentration in improving the tribological and mechanical properties of aluminum. A metal composite is generally made up of two or more than two insoluble phase particles. Comparing the base constituents material, HMCs have better properties in various aspects. Since it is easily fabricable, low density, and superior engineering properties, aluminum and its alloys are preferably chosen to be as the matrix material in majority conditions [6]. Typically, the Al-MMCs are processed under (i) Liquid-state (pressurized die casting, stir casting, infiltration process), (ii) solid-state (diffusion bonding, physical-vapor deposition (PVD), and powder metallurgy (PM)), and (iii) in situ dispensation. Researchers suggested that the stir casting is the helpful and most effective route among these mentioned procedures. Prior to the production of HMMCs, several crucial set of parameters such as stirring time and speed, melting temperature, holding or dwell time, stirring position, die preheating, and insoluble second particles can be deliberated. The properties of developed composite are decided by the optimum selection of mentioned parameters [7–13].

✉ Ashish Kumar
ashuatcoer@gmail.com

1 Department of Mechanical Engineering, Delhi Technological University, Delhi 110042, India

2 Department of Mechanical Engineering, Galgotias College of Engineering and Technology, Greater Noida 201306, India

JMEPEG
https://doi.org/10.1007/s11665-022-07780-7

1059-9495/$19.00

TECHNICAL ARTICLE

Investigation of Microstructure and Several Quality Characteristics of AA7075/Al_2O_3/Coconut Shell Ash Hybrid Nano Composite Prepared through Ultrasonic Assisted Stir-Casting

Ashish Kumar, R.C. Singh, and Rajiv Chaudhary

Submitted: 17 June 2022 / Revised: 29 November 2022 / Accepted: 4 December 2022

The present study focuses on the investigation of mechanical, thermal, and corrosion behaviors of cast hybrid nano-metal matrix composites of AA7075 with Al_2O_3 and coconut shell ash (CSA) nano- and micro-sized particulates, respectively, as reinforcements. Using an ultrasonic assisted stir-casting technique, the hybrid composites were fabricated using 2, 4, and 6% by weight of CSA and 0.5% by weight of Al_2O_3 in equal proportions. SEM, EDS, XRD, porosity, tensile, damping, dislocation density, coefficient of thermal expansion, and polarization tests were used to characterize four different combinations. The findings indicated that the nano- and micro-sized particulates were spread evenly in the matrix. The dislocation density, which is caused by a thermal mismatch between the matrix and the reinforced particles, as well as composite porosity, have been found to have a significant impact on the damping behaviors of hybrid composites. Also, the thermal expansion coefficient of HMMCs decreased with the addition of Al_2O_3 and CSA. The corrosion resistance was gradually increased by increasing the weight percentage of reinforcement in the AA7075 matrix.

Keywords corrosion, damping characteristics, dislocation density, hybrid composite, nano-reinforcement, thermal property

1. Introduction

Hybrid metal matrix composites (HMMCs) were developed to improve the performance of composites that were previously restricted to single reinforcement. In a hybrid metal matrix, two or more synthetic ceramics are added to a metal matrix. Carbides, oxides, and borides could be used as ceramic particles to reinforce the aluminum matrix (Ref 1-3). The most widely employed reinforcing materials are alumina (Ref 4), silicon carbide (Ref 5), boron carbide (Ref 6), and graphite (Ref 7), among others. Moreover, aluminum oxide and graphite particles made from these are more affordable. The desirable properties, like the flexible coefficient of thermal expansion and the solid lubricating characteristic, render these reinforcement particle forms suitable for producing components such as engine bearings, cylinder liners, pistons, and piston rings (Ref 8-12). The present scenario in the fabrication of hybrid composite is reinforcing agriculture waste (secondary reinforcement) with synthetic ceramic (primary reinforcement) (Ref 9). The broad applicability of such hybrid composites has attracted the attention of researchers who have designed and conducted experiments to develop superior and cost-efficient MMCs. Several good attempts have been made at producing MMCs from industrial wastes like graphite (Ref 7), fly ash (Ref 6), red mud (Ref 13), and the ashes of agricultural wastes like bagasse ash (Ref 14), coconut shell ash (Ref 15), corn cob (Ref 16), basalt fibers (Ref 17), coconut shell char (Ref 18), maize stalk (Ref 19), and rice husk ash (Ref 20). The advantages of including CSA are ease of access, low cost, low density, and lower pollution (Ref 21). According to the literature review, AMCs with CSA play a significant role in the progress of HMMCs due to their improved mechanical behaviors and widespread applications in a variety of fields. However, reinforcing natural ceramic is insufficient to improve the composite's quality characteristics. As a result, it's been combined with synthetic ceramic to increase mechanical, corrosion, and tribological properties.

In current scenario, nano-sized reinforcing particulates are being utilized in the metal matrix nanocomposite (MMnC). The use of nanoscale reinforced particulates at matrix interfaces provides a larger surface area, which results in improved composite properties like fatigue life, mechanical strength, and creep resistance at high temperatures without any loss of ductility (Ref 15, 22-25). The sizes, shapes, distribution of particulates, thermal stability, and hardening mechanism of nano-reinforcement materials have a significant impact on the final characteristics of MMnCs (Ref 23). The most difficult issue in the stir-casting method for processing MMnCs is achieving uniform reinforcement dispersion. The significant variability in densities between nanoparticles and molten

Ashish Kumar, Department of Mechanical Engineering, Delhi Technological University, New Delhi, Delhi 110042, India; and Galgotias College of Engineering and Technology, Greater Noida 201306, India; and **R.C. Singh** and **Rajiv Chaudhary**, Department of Mechanical Engineering, Delhi Technological University, New Delhi, Delhi 110042, India. Contact e-mail: ashuatcoer@gmail.com.

Journal of Materials Engineering and Performance

Published online: 27 December 2022

Journal of Cleaner Production 398 (2023) 136494

Contents lists available at ScienceDirect

Journal of Cleaner Production

journal homepage: www.elsevier.com/locate/jclepro

The utilisation of coconut shell ash in production of hybrid composite: Microstructural characterisation and performance analysis

Ashish Kumar [a,b,**], Akhileshwar Nirala [b], V.P. Singh [c,d], Biraj Kumar Sahoo [e], R.C. Singh [a], Rajiv Chaudhary [a], Ashok K. Dewangan [f], Gajendra Kumar Gaurav [h,&,*], Jiří Jaromír Klemeš [g], Xinghui Liu [h,i,***]

[a] Department of Mechanical Engineering, Delhi Technological University, Delhi, 110042, India
[b] Galgotias College of Engineering and Technology, Greater Noida, 201306, India
[c] Department of Mechanical Engineering, IES College of Technology, Bhopal, 462044, India
[d] Department of Mechanical Engineering, NIT Mizoram, Aizawl, 796012, India
[e] Materials Engineering Division, CSIR- National Metallurgical Laboratory (NML), Jamshedpur, 831007, India
[f] Department of Mechanical Engineering, National Institute of Technology, Delhi, 110036, India
[g] Sustainable Process Integration Laboratory, SPIL, NETME Centre, Faculty of Mechanical Engineering, Brno University of Technology, VUT Brno, Technická 2896/2, 61669, Brno, Czech Republic
[h] School of Physics and Electronic Information, Yan'an University, Yan'an, 716000, China
[i] Department of Materials Physics, Saveetha School of Engineering, Saveetha Institute of Medical and Technical Sciences (SIMTS), Thandalam, Chennai, 602105, Tamilnadu, India

ARTICLE INFO

Handling Editor: Cecilia Maria Villas Bôas de Almeida

Keywords:
Coconut shell ash
Cleaner approach
Hybrid composite
Nanoindentation
Microstructural evaluation
Ultrasonic-stir casting

ABSTRACT

Agriculture waste-reinforced hybrid metal matrix composites (HMMCs) have developed as a potentially green, productive, economical, and ideal replacement for particle-reinforced composites. A number of industries, including aerospace, automotive, and packaging, have demonstrated a keen interest in the development of new and innovative composites in a sustainable manner, is bio-waste particulate reinforced composite. The effect of reinforcements is investigated in the current research work, which employs the ultrasonic stir casting method with SiC (ranging from 3 to 9% by weight) and coconut shell ash (5% by weight in equal proportion) as reinforcement along with the aluminium matrix. With the two-stage ultrasonic stir casting process, the distribution of reinforcement in the aluminium matrix is ensured to be uniform. The microstructure evolution, mechanical and tribological behaviours were also evaluated to ascertain the integrity of fabricated composites. The XRD analysis confirms the reinforcements and oxide layer formed on the specimen surface. Currently, the fabricated composite improves monolithic alloy in terms of hardness and tensile strength approximately by 60% and 66%, respectively, while reducing wear rate by 51%. The nanoindentation investigation implies that the composites that have been developed have improved nanomechanical properties. Overall, using CSA along with SiC in HMMCs could be a potential product to reduce the usage of synthetic fiber and application design for economical products.

1. Introduction

The rapid development of the economy causes substantial enrichment of organic solid waste, including agricultural, industrial, forestry, and municipal solid waste (Dong et al., 2022). Because of the substantial contamination produced by the inappropriate treatment of organic solid waste, researchers have been looking for new ways to replace traditional rapidly deteriorating and burningin order to address environmental issues (Bahrami et al., 2016). This waste utilisation would not only be cost-effective, but it may also result in foreign exchange earnings and pollution reduction. As a result, current researchers are focused on recycling waste material by transforming it into green material for usage

* Corresponding author. School of Physics and Electronic Information, Yan'an University, Yan'an, 716000, China.
** Corresponding author. Department of Mechanical Engineering, Delhi Technological University, Delhi, 110042, India.
*** Corresponding author. School of Physics and Electronic Information, Yan'an University, Yan'an, 716000, China.
E-mail addresses: ashuiacoer@gmail.com (A. Kumar), gaurav@fme.vutbr.cz (G.K. Gaurav), liuxinghui119@gmail.com (X. Liu).

https://doi.org/10.1016/j.jclepro.2023.136494
Received 7 December 2022; Received in revised form 13 February 2023; Accepted 17 February 2023
Available online 23 February 2023
0959-6526/

ARTICLE IN PRESS
JID: JMAA [m5+;August 1, 2023;20:44]
Available online at www.sciencedirect.com
ScienceDirect
Journal of Magnesium and Alloys xxx (xxxx) xxx
www.elsevier.com/locate/jma

Influence of tool rotational speed on mechanical and corrosion behaviour of friction stir processed AZ31/Al_2O_3 nanocomposite

Ashish Kumar[a,b,*], V.P. Singh[c,d,*], Akhileshwar Nirala[b], R.C. Singh[a], Rajiv Chaudhary[a], Abdel-Hamid I. Mourad[e], B.K. Sahoo[f], Deepak Kumar[g,*]

[a] Department of Mechanical Engineering, Delhi Technological University, Delhi 110042, India
[b] Department of Mechanical Engineering Galgotias College of Engineering and Technology, Greater Noida 201310, India
[c] Department of Mechanical Engineering, National Institute of Technology Mizoram, Aizawl 796012, India
[d] Department of Mechanical Engineering, IES College of Technology Bhopal, 462044, India
[e] Mechanical and Aerospace Engineering Department, College of Engineering, United Arab Emirates University, Al-Ain 15551, United Arab Emirates
[f] Materials Engineering Division, CSIR - National Metallurgical Laboratory (NML) Jamshedpur, 831007, India
[g] Department of Mechanical Engineering, Carnegie Mellon University, Pittsburgh, PA 15213, USA

Received 28 December 2022; received in revised form 12 June 2023; accepted 23 June 2023
Available online xxx

Abstract

Nano-sized reinforcements improved the mechanical characteristics efficiently by promoting more implicit particle hardening mechanisms compared to micron-sized reinforcements. Nano-sized particles lessen the critical particle solidification velocity for swamp and thus offers better dispersal. In the present investigation, the friction stir processing (FSP) is utilized to produce AZ31/Al_2O_3 nanocomposites at various tool rotation speeds (i.e., 900, 1200, and 1500 rpm) with an optimized 1.5% volume alumina (Al_2O_3) reinforcement ratio. The mechanical and corrosion behavior of AZ31/Al_2O_3-developed nanocomposites was investigated and compared with that of the AZ31 base alloy. The AZ31 alloy experienced a comprehensive dynamic recrystallization during FSP, causing substantial grain refinement. Grain-size strengthening is the primary factor contributed to the enhancement in the strength of the fabricated nanocomposite. Tensile strength and yield strength values were lower than those for the base metal matrix, although an upward trend in both values has been observed with an increase in tool rotation speed. An 19.72% increase in hardness along with superior corrosion resistance was achieved compared to the base alloy at a tool rotational speed of 1500 rpm. The corrosion currents (Jcorr) of all samples dropped with increase in the rotational speed, in contrast to the corrosion potentials (Ecorr), which increased. The values of Jcorr of AZ31/Al_2O_3 were 42.3%, 56.8%, and 65.5% lower than those of AZ31 alloy at the chosen rotating speeds of 900, 1200, and 1500 rpm, respectively. The corrosion behavior of friction stir processed nanocomposites have been addressed in this manuscript which has not been given sufficient attention in the existing literature. Further, this work offers an effective choice for the quality assurance of the FSP process of AZ31/Al_2O_3 nanocomposites. The obtained results are relevant to the development of lightweight automobile and aerospace structures and components.

Keywords: Friction stir processing; AZ31 alloy; Al_2O_3; Nanocomposite; Mechanical properties; Corrosion resistance.

1. Introduction

Magnesium (Mg) and its alloys have drawn a lot of interest for several industries, including automotive, aerospace, and electronics, in the last few decades [1]. Due to their numerous attractive attributes, such as lightweight and good specific strength, these alloys are in higher demand [2,3]. The AZ31 is most frequently used alloys in the AZ-series, and around 70% of Mg cast products are made from this alloy [4,5]. Numerous researchers have investigated various materials, including carbon nanotubes (CNTs) [6], alumina (Al_2O_3) [7,8], graphene nanoplatelets [9], silicon carbide (SiC) [10], zirconium oxide (ZrO_2) [11], and yttrium oxide (Y_2O_3) [12], as reinforcement

* Corresponding authors.
E-mail address: deepakku@andrew.cmu.edu (D. Kumar).

https://doi.org/10.1016/j.jma.2023.06.012

Materials Today: Proceedings 21 (2020) 1453–1457

Contents lists available at ScienceDirect

Materials Today: Proceedings

journal homepage: www.elsevier.com/locate/matpr

Recent progress in production of metal matrix composites by stir casting process: An overview

Ashish Kumar [a,b,*], R.C. Singh [a], Rajiv Chaudhary [a]

[a] Department of Mechanical Engineering, Delhi Technological University, Delhi 110042, India
[b] Department of Mechanical Engineering, Galgotias College of Engineering and Technology, Greater Noida 201306, India

ARTICLE INFO

Article history:
Received 26 August 2019
Received in revised form 15 October 2019
Accepted 15 October 2019
Available online 13 November 2019

Keywords:
Stir casting
Aluminium metal matrix composites
Reinforcement
Mechanical properties
Future potential

ABSTRACT

The need of light weighted materials has led to the use of composites like aluminium (Al) metal matrix composites (AMMCs) for advanced material performance. These days the AMMCs have been considered as the most potential candidate for structural and functional applications. AMMCs composite materials are used in marine, defence, automotive, aerospace, and heat prone areas. Stir casting method is prominent technique for developing metal matrix composites (MMCs) due to its easiness and production at reasonable price with bulk manufacturing competency. This review article contains substantial aspects of stir casting route like; mechanical properties, effect of various reinforcement, various challenges and future research potential in the development of composites.

Selection and peer-review under responsibility of the scientific committee of the International Conference on Mechanical and Energy Technologies.

1. Introduction

The hybrid composite materials are the blend of two or more metal or non-metal which are soluble or insoluble to each other, and possesses numerous properties which show advance to any of the individual base materials. Specific strength of hybrid composite materials is much higher than other materials, such as steel. In the automotive industries, weight reduction is the primary goal which promotes to replace the ordinary components with MMCs [1]. Several ranges of secondary particle materials are available and the innovative casting technologies are paying attention on mass production of various MMCs. The various hybrid composite materials are generally categorized into two types the reinforcement particle and matrix materials used for manufacturing. As per the matrix material composites; it is categorized as Polymer Matrix Composites (PMCs), Metal Matrix Composites (MMCs), Carbon Matrix composites, and Ceramic Matrix Composites (CMCs). Among all, MMCs has benefits as compare to other composites materials due to its high temperatures resistance capability, oxidation, electrical and thermal conductivities, and improved mechanical properties [2–4]. Amongst the existing matrix constituents (Al, Cu, Mg, Fe, and Ti) for production of MMCs, Mg and Al are the very common in terms of their availability and application. Amongst the various existing matrix materials, Al alloys are extensively used for MMCs production. Certain attractive properties of Al are light weight, availability, cheaper and easy to process with several methods with higher strength to mass ratio and better corrosion resistance [2]. Fig. 1 represents the schematic set up of stir casting process.

The reinforcement particles can be in the form of fibre, particulates, interpenetrating or layer type. As per the reinforcement material utility, composite materials can be categorized into fibre, flake, laminar, particulate and filled reinforced composite. Among all reinforce material composites, and particulate reinforced composites are easily available, reasonable and ease to diffuse into matrix and form comparatively homogeneous distribution in the metal matrix. The assortment of these reinforce particles are grounded on the utility and applications of the hybrid composite [5,6]. Aluminium matrix is generally reinforced with SiC or Al_2O_3 or B_4C or WC, are one of the frequently used MMCs which develop enhanced mechanical properties with comparatively lesser fabrication cost [7]. Fig. 2 represent the several reinforcement and matrix materials that can be utilized for the development of MMCs.

Stir casting methods interpretation for approximately 67% by MMCs vol. % development [8], and so an extensively evaluation

* Corresponding author at: Department of Mechanical Engineering, Delhi Technological University, Delhi 110042, India.
E-mail address: ashuatcoer@gmail.com (A. Kumar).

https://doi.org/10.1016/j.matpr.2019.10.079
2214-7853/
Selection and peer-review under responsibility of the scientific committee of the International Conference on Mechanical and Energy Technologies.

IOP Conf. Series: Materials Science and Engineering **804** (2020) 012025 doi:10.1088/1757-899X/804/1/012025

Tribological studies and Microstructural characterisation of SiC and Fly Ash Particles Based Aluminium 2024 alloy Composites Prepared through Stir Casting Route

Ashish Kumar[1,2*], R.C. Singh[1], Rajiv Chaudhary[1], Virendra Pratap Singh[3]

[1]Dept. of Mechanical Engg, Delhi Technological University, Delhi-110042,
[2]Dept. of Mechanical Engg, Galgotias College of Engg. & Tech. Gr. Noida-201307,
[3]Dept. of Mechanical Engg, NIT Mizoram, Mizoram-796012, India
Email Id: ashuatcoer@gmail.com

Abstract. Aluminium and its alloys have excellent characteristics such as low density, high ductility and appropriate strength. In the marine, automotive and high-speed train sector, they find extensive applications. The volume percentage of metal matrix and reinforcement material and also the method of manufacturing the composites are the vital factors in making composite product. Composites of a metal matrix (MMCs), such as SiC and Al strengthened fly ash particles, are most widely used because of their excellent high hardness, high strength, corrosion resistance, stiffness and wear properties. The high strength and rigidity of AA 2024 alloys are well known. The high specific strength of such alloys with suitable reinforcement gives better yield properties and finds various applications at a reasonable cost. This article includes the study on mechanical and microstructural behaviour of AA 2024 metal matrix composites by reinforcing SiC and fly ash particles.

Keywords: Stir Casting, Metal Matrix Composites, Fly Ash, Silicon Carbide (SiC), Microstructure, Hardness

1. Introduction

Now a days the traditional heavy materials components have been replaced by modern lightweight composite materials which are economical, high specific strength used in various applications. The stiffness, strength and hardness of composite materials are highly dependent on the type of reinforcement and percentage volume in the base matrix. In the modern era throughout the globe, different structural and vehicle manufacturers are concentrating on innovative wear resistance component and replace the cast iron by aluminium based composite material in various uses [1-2, 15-17]. Composites materials based on Al as base matrix and reinforced by various secondary particles like; B_4C, SiC and fly ash had been done by various scientists and researchers. It is found that the Al-based composites have low wear rate, high thermal conductivity as per requirement, low density and higher heat capacity potential comparing with traditional steel [3-5]. The effect of 20 vol. % SiC reinforced AA359 aluminium amalgams has shown higher wear resistance in an arid sliding environment [6].

The production of green components has been used to accumulative responsiveness environment worldwide. Fly ash generally obtained from the pulverized coal burning at various coals based thermal power plants, the waste by-product of shows a very low density, therefore, very useful in producing high strength and low weight hybrid metal composites. Reprocessing Fly Ash saves energy and comparatively cheaper. Several researches have established and shown that Al-Fly Ash hybrid composites can enhance the rigidity, tensile strength, shock-absorbing capacity, and wear resistance but at the same decreasing the density of base matrix alloy [7, 8]. Fly Ash comprises mostly of Al_2O_3, SiO_2, Fe_2O_3, and oxides such as P, Mg, and Ca, comprises less volume fraction of particles like; mullite, hematite and crystalline quartz [9].